

Evaluation of load capacity of concrete railway slab spans with defects

Maciej Maksymowicz

February 2008

Civil Engineering Department
University of Minho
4800-058 Guimarães, Portugal

Acknowledgments

This research has been carried out at the Department of Civil Engineering at the University of Minho between 2004 and 2007 and founded by the Integrated Project “Sustainable Bridges – Assessment for Future Traffic Demands and Longer Lives”, contract No TIP3-CT-2003-001653, a part of 6th Framework Programme of European Union, for which I thank very much.

I would like to thank my supervisor Professor Paulo J. S. Cruz from University of Minho for the opportunity to conduct this Thesis, all necessary conditions of working and for a lot of freedom in my research. Thanks are also due to my co-supervisor Professor Jan Bień from Wrocław University of Technology in Poland for his advice, sharing his experience with, continuous encouragement, careful guidance and fruitful cooperation. Moreover I would like also to thank both of them for the proof-reading of this Thesis and all their comments and suggestions.

Professor Kazimierz Rykaluk from Wrocław University of Technology helped me face the problems related to my duties from the Sustainable Bridges project. Thank you very much for all your advices, recommended literature and the time spent for nice and fruitful consultations.

Thanks to the Portuguese Railway Administration (REFER) especially expressed to the director of special structures José Carlos Clemente for the access to railway bridge structures. I thank also the staff of REFER: Ana Isabel Silva and Hugo Patrício for the material

necessary to write this these. I express my acknowledgement also to Teles Nunes and his bridge inspectors' team for nicely spent time during the bridge visual inspections.

I thank Zygmunt Kubiak from the Polish Railway Administration (PKP) for information and materials used during preparation of this Thesis. Special thanks are destined to Jerzy Czastkiewicz for the photographic documentation of damaged bridges.

I also thank Professors Manuel Filipe Santos and Paulo Cortez from University of Minho for additional publications on the Neural Network Technology used in this Thesis.

Last time I was in luck to work with friendly and helpful people in Gifford (England) where I received a strong support related to a proofreading of this Thesis. I would like to thank my teacher of English Lorna Erginel and my colleagues: William Spencer, Adrian Shawcross and particularly Mark Meyts for a special effort. I warmly thank also other people not mentioned here by name. Moreover, having an access to the Gifford's library, I was given an opportunity to study innumerable amount of publications related to this Thesis for which I thank Gifford very much as well.

A warm "thank you!" is dedicated to all of my friends for creating a pleasant working environment and providing a lot of laughter during many coffee breaks.

However, my greatest appreciation is to my loving wife Dagmara. Without her support, the time of this study would have been for me too difficult. Thank you for putting up with me especially as things got hectic and time consuming towards the end of the Thesis.

February 2008

Maciej Maksymowicz

Abstract

This study presents a complete methodology for the load capacity assessment of existing damaged railway slab spans made of reinforced concrete.

The databases of the Polish (PKP) and Portuguese (REFER) railway infrastructure administrations are analysed. Furthermore, a study on the reports of international scientific projects i.e. “Sustainable Bridges” and “SAMCO” have lead to a conclusion that from among existing railway bridge stock, simply supported spans are the most common form of construction. Moreover, the spans carrying single tracks dominate in this group. The statistical information based on these sources has been presented in this study.

Based on the Author’s observations, consultations with bridge inspectors as well as the literature study, a uniform and multi-level classification system of bridge defects has been presented. This system reflects all the defects that may occur during a bridges service life. Their influence on the load capacity is emphasized. To evaluate the load capacity of damaged structure information on defect parameters is essential. For this reason the Author presented a survey of testing methods to be applied in bridge condition appraisal. To explain the nature of defects in terms of their causes, the taxonomy of degradation mechanisms, leading to these defects, is presented as well.

The defects considered in this study have also been presented in terms of their modelling using of various geometry models. The conception of a numerical defect modelling by means

of three parameters (i.e. intensity, location and extent) is included. Conclusions following from the statistical survey on the railway bridge stock have induced the Author to analyse the possibility of application of a simplified geometry model of a span – simply supported beam. In order to compare results of the load capacity assessment several numerical analyses have been performed. The range of application of the simplified span model has been established by means of a 5% threshold of difference between results obtained by the considered models. To perform effective analyses of the load capacity of an existing span, the Author created and presented his own program called “Damage Assessment Graphic Analyser” (DAGA). By means of a built-in graphic editor this program allows visualizations in a three dimensional space of a span with defects in the concrete and reinforcing steel, i.e. losses of material and material parameters modifications. This tool automatically performs the static-strength analysis and results, presented as envelopes of cross-section load capacity (for designed as well as current condition – with defects) and bending moments for various load classes. Using the DAGA program a set of parametric analyses (static-strength) has been carried out. Their results have been collected in a knowledge base to be implemented in an expert tool, called ANALisys of CONcrete DAMages (ANACONDA) based on the hybrid network technology with analytical and neural components incorporated, designed by the Author. At the end of this Thesis the conclusions and directions of further investigation can be found.

Resumo

A presente tese apresenta uma metodologia avançada para a análise / avaliação da capacidade resistente de pontes ferroviárias com tabuleiro em laje de betão.

A análise das bases de dados das administrações ferroviárias polaca (PKP) e portuguesa (REFER), para além do estudo de relatórios recentes de projectos científicos internacionais, tais como exemplo os projectos " *Sustainable Bridges*" e "SAMCO", permitiram concluir que das pontes ferroviárias existentes a maioria corresponde a soluções simplesmente apoiadas. Entre estas as pontes com via única são claramente o tipo dominante. Neste estudo é apresentada toda a informação estatística dos dados coligidos nessas fontes.

Tendo por base as observações do autor, as consultas aos inspectores de pontes, assim como o estudo exaustivo da literatura existente, foi apresentado um sistema de classificação uniforme e multi-nível das anomalias mais comuns em pontes. Este sistema reproduz as anomalias que ocorrem durante o período de vida útil de uma ponte. A influência destas anomalias na capacidade resistente é devidamente abordada. A resposta a este problema tem sido objecto de grande atenção pela comunidade técnica e científica, devido aos desenvolvimentos ocorridos nos métodos experimentais de apoio às inspecções e ao aprofundamento do conhecimento da classificação dos mecanismos de degradação.

As anomalias acima mencionadas foram apresentadas, em termos da sua modelação, através de vários modelos geométricos. Para o efeito a modelação numérica de qualquer anomalia é

efectuada tendo por base três parâmetros – intensidade, localização e extensão. As conclusões retiradas da análise estatística das pontes ferroviárias existentes induziram o autor a desenvolver um sistema de análise da possibilidade de aplicação de um modelo geométrico, simplificado, para a modelação do efeito das anomalias neste tipo de pontes. O campo de aplicação do modelo simplificado foi estabelecido como válido para as situações correspondentes a 5% de diferença entre os resultados obtidos pelos modelos em questão.

Para efectuar as análises da capacidade resistente das pontes em questão, o autor desenvolveu um programa de cálculo automático designado "*DAGA – Damage Assessment Graphic Analyser*" (DAGA). Através da inserção de um editor gráfico o programa permite a visualização 3D das anomalias existentes no betão e armaduras (perda de materiais e modificação das propriedades dos materiais). Esta ferramenta permite a análise e visualização das envolventes da capacidade resistente para diversos casos de carga e para diversos cenários de anomalias.

Mediante a utilização programa DAGA foram efectuados estudos paramétricos (comportamento estático) e os seus resultados foram coligidos numa base de dados a ser posteriormente usada modelos de inteligência artificial. Para o efeito desenvolveu, ainda, um programa de cálculo designado por "*ANACONDA – ANALisys of CON crete DAMages*" baseada na tecnologia de redes híbridas com componentes analíticas e neuronais incorporadas.

Finalmente, são apresentadas as principais conclusões e a recomendação de futuras linhas de investigação neste campo.

Streszczenie

Niniejsze opracowanie prezentuje kompleksowe podejście do oceny nośności istniejących płytowych przęseł kolejowych wykonanych z betonu zbrojonego z uwzględnieniem uszkodzeń konstrukcji.

Zaprezentowano dane statystyczne dotyczące istniejących obiektów mostowych w oparciu o analizy baz danych polskiej (PKP) i portugalskiej (REFER) administracji infrastruktury kolejowej jak również o raporty międzynarodowych projektów naukowych, tj. „Sustainable Bridges” oraz „SAMCO”. Z dostępnych danych wynika, iż konstrukcje o przęsłach swobodnie podpartych stanowią największą populację kolejowych obiektów mostowych, a spośród nich dominującą grupą są obiekty usytuowane w ciągu linii jednotorowych.

Na podstawie własnych obserwacji, konsultacji z inspektorami mostowymi a także studiów literaturowych Autor pracy przedstawił wielopoziomowy, jednolity system klasyfikacji uszkodzeń jako całościowy wachlarz występujących defektów analizowanego typu konstrukcji ze szczególnym uwzględnieniem ich wpływu na nośność. Zagadnienie uszkodzeń wpływających na nośność analizowanego typu przęseł zostało wzbogacone o przegląd dostępnych metod badawczych umożliwiających ich identyfikację oraz ocenę kondycji analizowanej konstrukcji. Również charakterystyka mechanizmów degradacji jako geneza powstałych uszkodzeń została zawarta w pracy jako rozwinięcie tego tematu.

Opisane uszkodzenia znalazły odzwierciedlenie w sposobie ich modelowania przy użyciu różnych modeli geometrii przęsła. W pracy została przedstawiona koncepcja numerycznego opisu uszkodzeń za pomocą trzech parametrów, tj. intensywności, lokalizacji oraz rozległości. Wnioski płynące z dostępnych danych statystycznych odnośnie istniejących obiektów mostowych skłoniły Autora pracy do przeprowadzenia analizy możliwości stosowania uproszczonego modelu obliczeniowego konstrukcji z uszkodzeniami. Przeprowadzono szereg symulacji mających na celu porównanie nośności obliczonej za pomocą wyjściowego oraz uproszczonego modelu geometrii przęsła. Zakres stosowalności tego modelu wyodrębniono 5% progiem różnicy w otrzymanych wynikach z analizowanych modeli geometrii.

W celu przeprowadzenia efektywnej analizy nośności uszkodzonych żelbetowych płytowych przęseł kolejowych Autor opracował program komputerowy Damage Assessment Graphic Analyser (DAGA). Program wraz z wbudowanym edytorem graficznym umożliwia wizualizację w przestrzeni trójwymiarowej analizowanego obiektu mostowego wraz z uszkodzeniami betonu i zbrojenia, tj. ubytki materiału oraz modyfikacje cech materiałowych. Program automatycznie przeprowadza analizę statyczną i wytrzymałościową, a wyniki analiz przedstawia w formie wykresów obwiedni nośności przy zginaniu (dla stanu zaprojektowanego i aktualnego – z uszkodzeniami) oraz obwiedni momentów zginających dla poszczególnych klas obciążeń.

Za pomocą programu DAGA przeprowadzono szereg analiz parametrycznych (statyczno – wytrzymałościowych), których wyniki zgromadzono w tzw. bazie wiedzy do wykorzystania w ramach technologii narzędzi ekspertowych. Autor opracował odrębny program komputerowy ANALysis of CONcrete DAMages (ANACONDA) bazujący na technologii sieci hybrydowych przy wykorzystaniu komponentów analitycznych oraz neuronowych.

Niniejsze opracowanie zamyka podsumowanie i wskazanie kierunków dalszych badań.

Contents

Chapter 1. Introduction.....	1
1.1 Background and motivations.....	1
1.2 Objectives.....	3
1.3 Outline of the Thesis	4
1.4 Notations and symbols	5
1.4.1 Roman – Upper Case.....	5
1.4.2 Roman – Lower Case	6
1.4.3 Greek – Upper Case	7
1.4.4 Greek – Lower Case.....	7
1.4.5 Abbreviations	8
1.5 Term definitions	9
Chapter 2. Railway bridge span survey	11
2.1 Introduction	11
2.2 Bridge types.....	12
2.3 Bridge age profile.....	14
2.4 Bridge span profile.....	15
2.5 Cross section forms of RC slab spans	17

2.6 Track constructions	20
Chapter 3. Classification of defects	23
3.1 Introduction	23
3.1.1 Methods based on the “cause” criterion	24
3.1.2 Methods based on the “effect” criterion	25
3.1.3 Methods based on the “cause-effect” criterion	27
3.1.4 Methods based on combination of criteria	27
3.1.5 Other methods	30
3.1.6 Critical review	31
3.2 General conception and criteria of defect classification	32
3.3 Types of defects	33
3.3.1 Contamination	34
3.3.2 Deformation	35
3.3.3 Deterioration	36
3.3.4 Discontinuity	37
3.3.5 Displacement	38
3.3.6 Loss of material	39
3.4 Hierarchical system of defect classification	40
Chapter 4. Testing methods	43
4.1 Test locations	43
4.2 Non-destructive testing	44
4.2.1 Mechanical vibrations	44
4.2.2 Electromagnetic and optical methods	48
4.2.3 Electrical methods	55
4.3 Minor destructive methods	59
4.3.1 Samples	59
4.3.2 Near-surface strength tests	60
4.3.3 Phenolphthalein and Rainbow-Test	62
4.3.4 Chloride Test	63
4.4 Basic methods	64
4.4.1 Direct measurement	64
4.4.2 Rebound (Schmidt) hammer	65
4.4.3 Tapping	67

4.5 Visual inspection	67
4.6 Load testing	68
4.7 Application of testing methods	69
Chapter 5. Mechanisms of degradation	71
5.1 Introduction	71
5.2 General conception of classification	73
5.3 Chemical degradation mechanisms	74
5.3.1 Alkali-Aggregate Reaction (AAR).....	74
5.3.2 Carbonation	76
5.3.3 Corrosion.....	77
5.3.4 Crystallisation.....	79
5.3.5 Leaching	79
5.3.6 Oil and fat influence	81
5.3.7 Salt and acid actions	81
5.4 Physical mechanisms.....	83
5.4.1 Creep	83
5.4.2 Fatigue.....	83
5.4.3 Fire	85
5.4.4 Freeze-thaw	87
5.4.5 Modification of foundation conditions.....	89
5.4.6 Overloading.....	89
5.4.7 Shrinkage.....	90
5.4.8 Vandalism.....	91
5.4.9 Weathering	92
5.5 Biological degradation mechanisms.....	92
5.5.1 Accumulation of dirt or rubbish	92
5.5.2 Living organisms activity	93
5.6 Other methods of classification.....	94
5.7 Effects of degradation mechanisms.....	95
Chapter 6. Numerical modelling of slab spans with defects.....	97
6.1 Introduction	97
6.2 Geometry models	99
6.3 Coordinates system	100

6.4 Defect intensity	101
6.4.1 Loss of concrete	101
6.4.2 Loss of reinforcement.....	102
6.4.3 Concrete Strength reduction.....	103
6.4.4 Elastic modulus reduction in concrete	104
6.4.5 Strength reduction in reinforcement.....	105
6.4.6 Elastic modulus reduction in reinforcement.....	105
6.5 Defect extent	106
6.6 Defect location	107
6.7 Analysis of the simplified model efficiency	109
6.7.1 Introduction	109
6.7.2 Geometry.....	109
6.7.3 Material	110
6.7.4 Loads	110
6.7.5 Analysis of structures without defects	111
6.7.6 Analysis of structures with defects.....	112
Chapter 7. Analysis of damaged structures by means of DAGA program.....	119
7.1 Introduction	119
7.1.1 Computer devices.....	119
7.1.2 Technologies	121
7.1.3 Graphic tools for assessment of defects	122
7.1.4 Defect analysis	124
7.2 Architecture of the DAGA program.....	125
7.3 Geometry.....	128
7.4 Loads	129
7.4.1 Dead load.....	129
7.4.2 Moving load	129
7.5 Material parameters.....	130
7.6 Reinforcement	130
7.7 Defects.....	131
7.8 Procedure of load capacity assessment	134
7.8.1 Limit states	134
7.8.2 Analysis.....	134

7.9 Results of the analysis	137
7.10 Defect modelling based on photos	138
Chapter 8. Neural network technology for the load capacity assessment.....	141
8.1 Introduction	141
8.1.1 General motivations	141
8.1.2 Basic principles on Neural Network Technology	142
8.1.3 Historical outline	146
8.1.4 Application of Neural Network Technology in civil engineering.....	148
8.1.5 Application of Neural Network Technology in bridge engineering	150
8.2 General functional scheme of ANACONDA program	152
8.3 Neural components (composition, training and testing)	154
8.3.1 Neural component N_1	154
8.3.2 Neural component N_2	161
8.4 Functional components	168
8.4.1 Functional component F_1	168
8.4.2 Functional component F_2	169
8.4.3 Functional component F_3	169
8.4.4 Functional component F_4	170
8.4.5 Functional components F_5, F_6 and F_7	170
8.4.6 Functional component F_8	171
Chapter 9. Conclusions	173
9.1 General conclusions	173
9.2 Bridge survey	173
9.3 Taxonomy of defects	174
9.3.1 Classification of defects	174
9.3.2 Testing methods	174
9.3.3 Mechanisms of degradation	174
9.4 Defect modelling	175
9.5 Load capacity assessment.....	175
9.5.1 Program DAGA.....	176
9.5.2 Program ANACONDA	176
9.6 Further developments.....	177

References	179
Appendix A. Parametric analysis of load capacity of cross-section for RC slab spans with defects.....	189
A.1. Introduction	189
A.2. Analysis.....	190
A.3. Conclusions	202
Appendix B. User’s Manual of DAGA program	203
B.1. Interface.....	204
B.2. Geometry of the span	205
B.3. Reinforcement	206
B.3.1. Longitudinal reinforcement.....	206
B.3.2. Stirrups	207
B.4. Material properties	208
B.5. Loads	209
B.5.1. Dead load.....	209
B.5.2. Live load.....	209
B.6. Discretisation.....	211
B.6.1. Longitudinal reinforcement.....	211
B.6.2. Stirrups	211
B.6.3. Concrete	212
B.7. Modelling of defects.....	212
B.7.1. Loss of reinforcement.....	212
B.7.2. Loss of concrete	213
B.7.3. Loss of bond concrete-reinforcement.....	214
B.7.4. Strength modification.....	214
B.7.5. Defect modelling based on photos	215
B.8. Display	215
Appendix C. User’s manual of ANACONDA program.....	217
C.1. Geometry.....	217
C.2. Loads	218
C.3. Defects.....	219
C.4. Analysis and results.....	220

Chapter 1

Introduction

1.1 Background and motivations

Bridges are constructed primarily to carry communication routes, such as railways, over an obstacle like road, river etc. In terms of railway and roadway infrastructure, bridges play a crucial role for the surface transport. From an economic point of view and general industrial development, bridges make the communication much easier and faster.

Though the first bridge structures had been built in the ancient times, their intensive development started at the end of the XIX century. According to the railway bridge survey of the Sustainable Bridges project (Sustainable Bridges 2005) only 4% of the European concrete railway bridge infrastructure is older than 100 years and the majority (55%) of the railway bridge stock was built after the 2nd World War. The war activities caused a huge devastation of civil engineering infrastructure, especially in terms of the surface communication. Many countries affected by the war were forced to rebuild their bridge stock. In Poland, the highest number of newly constructed bridges was observed between 1956 and 1980 (Bień et al. 1997). Countries not afflicted with the war activities such as Portugal noted bridge stock development as a steady process (REFER 2005). Despite a great number of newly constructed bridges per year their relative participation in the whole existing bridge population does not exceed 1.0% (Bień 2002). The presented facts clearly illustrate that old bridges are the dominating part of the whole existing railway bridge population.

During bridge service life many degradation mechanisms occur resulting in various defect types causing bridge condition reduction related mainly to the lack of suitable maintenance. Bridge condition needs to be assessed in order to give the bridge administration a basis to make a rational decision on the further service of the considered structure as well as to allocate their financial resources. Bridge condition is commonly understood as a general measure representing their technical condition (values of bridge technical parameters, e.g. geometry, material characteristics, etc.) and serviceability (e.g. load capacity, clearance, maximum speed, etc). Bridge management systems take into account various condition components, but the load capacity is its main measure, e.g. Inventory System PONTIS (Branco & de Brito 2004). In the Sufficiency Rating of the National Bridge Inventory (NBI) of Alabama State (USA) the Structural Adequacy and Safety Factor contributes at the level of 55% (weighted percentage) against the Serviceability and Functional Obsolescence (30%) and the Essentiality for Public Use (15%), which explains the importance of the load capacity (Grimes et al. 2001). Assessment of load capacity gives a basis for replacement, structural repair, upgrading, load restriction, closure of considered bridge structure (Woodward et al. 2001).

The need for assessment of old bridges is currently a crucial problem for various bridge administrations that tend to consider this fact. This tendency can be observed regarding qualitative evolution of the global bridge budgets in Switzerland, where a ratio between new bridges and the actions related to maintenance, repair, rehabilitation and replacement is decreasing (Branco & de Brito 2004). Bridge repair or demolition, service load reduction or even closing traffic is a common problem to face for each railway infrastructure administration and the problem has a special meaning if its budget is limited.

Proper education of the future bridge engineers to be able to deal with existing bridge structures is another problem. Nowadays technical universities are teaching students to be engineers in terms of new bridge designing. On the one hand universities provide their students a great support in terms of mathematics, static, strength of material and also computer aided design on the other hand their graduates are not prepared to perform the analyses of damaged bridge structures. Usually this knowledge is partly available for graduates working on the particular topics in the framework of their further researchers, i.e. PhD studies.

The load capacity assessment requires advanced testing methods for bridge condition evaluation. To date a large amount of publication on this topic has been produced. A connection between advanced testing techniques, and load capacity assessment taking into

account defects occurred seem to be a powerful possibility of dealing with the existing bridge infrastructure. The problem is significantly important, because the bridge documentation is usually not complete or sometimes does not even exist. Moreover, even if the bridge documentation is available, there is no guaranty that the conformity between this documentation and existing construction is ensured.

The load capacity analysis requires suitable computer tools to be applied. Currently the software market offers a great number of computer applications to analyse bridge structures providing more sophisticated methodology of analysis, i.e. Finite Element Methods for example LUSAS, ROBOT, COSMOS, SAP etc. Regarding the design of new structures the programs offered are sufficient, but in terms of assessment of existing bridges some additional elements need to be provided. On the one hand these programs offer some tools for defect analysis, but on the other hand the components provided are difficult to apply and require their users to be trained. The effective analysis of damaged bridge structure requires a simple application of the results from visual inspections (also using the elements of photogrammetry), graphic modelling of damaged construction and structural analysis with visualization of data provided as well as results obtained. To date there is no computer programs meeting these requirements.

1.2 Objectives

The objective of this Thesis is to propose a complete methodology for evaluation of load capacity of railway reinforced (RC) concrete slab spans with defects. This study has been divided into the following sub-tasks:

- The survey of railway RC spans to justify the selection of construction type to be considered;
- Taxonomy of defects occurred to the considered structures enriched by the classification of their causes (i.e. degradation mechanisms) as well as testing method to identify them;
- Conception of defect modelling by means of various geometry models and establishing the range of application for the considered geometry model;
- Analysis of the load capacity of considered structures with defects by means of a computer tools with a graphic editor for defect modelling, using the analytical procedure as well as Neural Network Technology (NNT).

1.3 Outline of the Thesis

The presented Thesis is composed of 9 Chapters and 3 Appendices.

In Chapter 1 a general introduction and the objectives of this study are presented.

Chapter 2 presents the type constructions under consideration against the available statistical information in terms of cross section forms, static schema systems, track constructions, age profile etc. The presented results are based on the study of data bases of Polish (PKP) and Portuguese (REFER) railway infrastructure administrations and also refer to the reports of two international scientific projects, i.e. “Sustainable Bridges” (www.sustainablebridges.net) and “SAMCO” (www.samco.org).

Chapter 3 deals with defects which occur to considered span constructions. Based on the existing solutions and presenting their disadvantages the Author introduced a uniform and multi-level classification system for defects. The special attention is focused on defects which exert an influence on the load capacity of a span.

In Chapter 4 a description of testing methods for defect identification as well as bridge geometry measurement is provided. Also a relationship between considered defect types and available testing methods is developed.

In Chapter 5 a classification system for degradation mechanisms is presented. For each mechanism a description is given along, including the associated defects, as well as existing mitigating solutions to the problem.

Chapter 6 introduces the concept of defect modelling by means of three parameters, i.e. intensity, extent and location. The Author presents the procedure of application of these parameters for various geometry model classes. The conclusions extracted from the statistical information (presented in Chapter 2) lead the Author to analyse the possibility of application of a simplified geometry model – simply supported beam. In this part of the study a set of efficiency analyses of this model are presented and discussed.

Chapter 7 presents a methodology of load capacity assessment by means of the Author’s computer program “Damage Assessment Graphic Analyser” (DAGA). The main features of this tool, as well as the possibilities of the load capacity assessment are presented.

By means of the program DAGA a large amount of the parametric analyses, i.e. static-strength, of damaged structures has been carried out. The results with the input parameters have been stored in a knowledge base to apply within an expert tool. Chapter 8 presents the

possibilities of the load capacity assessment by means of software utilising hybrid network technology including neural and analytical components. For these purposes another Author's program, called ANACONDA, has been presented.

Chapter 9 includes conclusions drawn from this study and suggestions for further directions of investigation.

There are three Appendices attached to this study. Appendix A includes the results of the parametric analysis to be applied in the expert tool ANACONDA as a knowledge base. Appendix B presents the user's manual of the DAGA program. Appendix C includes the user's manual of the ANACONDA program.

1.4 Notations and symbols

In order to keep common understanding of all the symbols used in this work and avoid any ambiguity the Author presents the following their definitions.

1.4.1 Roman – Upper Case

A_b	Cross section area of the ballast;
$A_{s,b}$	Cross section area of the bottom layer of reinforcement;
$A_{s,t}$	Cross section area of the top layer of reinforcement;
A_{corr}	Cross section area of the corroded rebar;
B	Slab width;
B_b	Ballast width;
B_s	Sleeper width;
B_{sw}	Side walk width;
E^1	1D model of bridge geometry;
E^2	2D model of bridge geometry;
E^3	3D model of bridge geometry;
E_c	Elastic modulus of the concrete;
E_d	Defect extent;
$E_{s,b}$	Elastic modulus of the bottom layer of reinforcement;
$E_{s,t}$	Elastic modulus of the top layer of reinforcement;

F_{ij}^c	Internal force in concrete at layer “j” of cross section “i”;
F_{ij}^s	Internal force in reinforcement at layer “j” of cross section “i”;
F_m	Functional component number “m” of the expert tool ANACONDA;
H	Slab height;
H_b	Ballast thickness;
H_r	Rail height;
H_{sw}	Side walk height;
I_d	Defect intensity;
L	Slab length;
L_a	Length of reinforcement anchorage;
L_d	Defect location;
L_t	Theoretical span length;
M	Bending moment;
M_{max}	Maximal value of bending moment;
$M_{max,g}$	Maximal value of bending moment caused by dead load;
$M_{max,p}$	Maximal value of bending moment caused by moving load;
M_R	Load capacity of cross-section;
M_{Res}	Load capacity reserve of considered cross section;
N_m	Neural component number “m” of the expert tool ANACONDA;
P	Concentrated moving load intensity;
R_c	Compressive strength of concrete;
$R_{s,b}$	Strength of the bottom layer of reinforcement;
$R_{s,t}$	Strength of the top layer of reinforcement.

1.4.2 Roman – Lower Case

$a_{s,b}$	Location in cross section of the bottom layer of reinforcement;
$a_{s,t}$	Location in cross section of the top layer of reinforcement;

e_d	Occurrence function used in defect modelling;
f	Deflection;
f_a	Activation function of a neuron;
f_d	Substitute function for the defect intensity function I_d and for the defect occurrence function e_d ;
g	Linear weight of total dead load;
g_t	Linear weight of rail track;
i	Number of the current cross section;
j	Number of the current layer of cross section;
m	Number of layers of analysed cross section;
n	Number of virtual cross sections;
n_B	Number of the longitudinal bar elements across the span length;
n_L	Number of the transversal bar elements along the span length;
q	Uniform moving load intensity;
v	Predicted velocity of trains;
x	Axis of the global coordinate system parallel to the span axis;
y	Axis of the global coordinate system parallel to the span width;
y_{bt}	Location of the ballast on the side walk;
z	Axis of the global coordinate system parallel to the span height.

1.4.3 Greek – Upper Case

$\Delta\varepsilon_{im}$ Stress modification in layer “ m ” of cross-section “ i ”.

1.4.4 Greek – Lower Case

α Load class coefficient;

ε_{ij} Strain at layer “ j ” of cross section “ i ”;

γ Load safety coefficient for the moving load;

γ_1 Load safety coefficient for constructional parts;

γ_2	Load safety coefficient for non-constructural parts;
γ_b	Weight by volume of the ballast;
γ_c	Weight by volume of the concrete;
ρ	Reinforcement ratio;
σ_{ji}^c	Stress in concrete at layer “j” of cross section “i”;
σ_{ji}^s	Stress in reinforcement at layer “j” of cross section “i”;
ξ	Normalised coordinate, parallel to the “x” axis of the global coordinate system used also for the cross-section location;
ψ	Normalised coordinate, parallel to the “y” axis of the global coordinate system;
ζ	Normalised coordinate, parallel to the “z” axis of the global coordinate system.

1.4.5 Abbreviations

1D	One-dimensional;
2D	Two-dimensional;
3D	Three-dimensional;
BMS	Bridge Management System;
<i>DAF</i>	Dynamic Amplification Factor;
<i>DAF_b</i>	Dynamic Amplification Factor taking the ballast thickness into consideration;
<i>DAF_v</i>	Dynamic Amplification Factor taking the predicted train velocity <i>v</i> into consideration;
DAGA	Computer program “ <i>Damage Assessment Graphic Analyser</i> ” for load capacity assessment of damaged railway RC slab spans;
FEM	Finite element method;
LC	Load capacity;
NDT	Non-Destructive Tests;
NNT	Neural Network Technology;
PKP	Polskie Koleje Państwowe – Polish Railway Administration;

REFER	Rede Ferroviária Nacional, E.P – Portuguese Railway Infrastructure Administration;
RC	Reinforced concrete;
SLS	Serviceability Limit States;
ULS	Ultimate Limit States.

1.5 Term definitions

To keep the common understanding of the terms being used in this work and avoid any ambiguity the following basic definitions have been introduced:

Bridge	Engineering construction built to carry communication route (i.e. road, railroad or path) over a gorge, valley, road, railway track, river, body of water, or any other physical obstacle;
Bridge condition	General measure presenting bridge technical condition and bridge serviceability;
Bridge serviceability	Measure of differences between current and designed values of bridge service parameters, e.g. load capacity, clearance, maximum speed, etc.;
Bridge technical condition	Measure of differences between current and designed values of bridge technical parameters, e.g. geometry, material characteristics, etc.;
Contamination	Appearance of any type of a dirtiness or not designed plant vegetation;
Critical zone	The zone of the slab, where the maximal value of bending moment exceeds the value of the load capacity of cross section;
Current bridge condition	Bridge condition taking current defects into consideration;
Defect	Effect diminishing bridge technical condition and/or bridge serviceability, sometimes defined as <i>damage</i> ;

Deformation	Geometry changes incompatible with the project, with changes of mutual distances of structure element points;
Degradation causes	Factors or conditions conducive to initiation as well as development of <i>degradation mechanisms</i> during operation of the bridge;
Degradation mechanism	The process causing defect(s) to construction;
Deterioration	Physical and/or chemical changes of structural features against designed values;
Discontinuity	Inconsistent with a project break of material continuity;
Discretisation	Model precision level applied in DAGA program;
Displacement	Displacement of a structure or its part incompatible with the project but without changes of distances of the structure element points, also restrictions in designed displacement capabilities;
Load capacity of cross section	The biggest value of bending moment, which can be safely (and according to the code requirements) transmitted by the analysed cross section of the element;
Load capacity of span	Maximum acceptable class of service load, which can be safely applied for the construction;
Load capacity reserve	Value M_{Res} expressed by the difference $M_R - M_{max}$ for every cross section, where the value M_R represents the actual load capacity of cross section and M_{max} – the biggest value of bending moment; the load capacity is analysed according to the current code;
Loss of material	Decrease of designed amount of structure material;
Non-Destructive Tests (NDT)	Techniques of testing without any interference in integrity of tested structure;
Parameter	Variable (dimension, defect type, material properties etc.) exerting an influence on structure behaviour;
Reinforcement ratio	The ratio between cross-sectional area of reinforcement and total area of considered cross-section.

Chapter 2

Railway bridge span survey

2.1 Introduction

This chapter presents existing European railway bridge constructions focusing on their types and also span profiles based on the available statistical information. The presented results are based on the reports of two European projects: “Sustainable Bridges - Assessment for Future Traffic Demands and Longer Lives” (Sustainable Bridges 2005) and “Structural Assessment Monitoring and Control, SAMCO” (2003) and also refers to the particular queries to the bridge inventory data bases of the Portuguese Railway Administration (REFER 2003) and the Polish Railway Company (PKP) presented by Bień et al. (1997). In the framework of the “Sustainable Bridges” project an investigation on the railway bridge inventory was carried out. The idea was to give a background to the work in the various Work Packages of this project. The following countries took part in this task: Austria, Belgium, Czech Republic, Denmark, Finland, Germany, Hungary, Ireland, Italy, Poland, Portugal, Slovakia, Spain, Sweden and Switzerland. The SAMCO network consists of 20 European principal partners coming from private enterprises, industry, research and development as well as from regional and city governments. This network covers all the relevant fields of structural assessment, monitoring and control as a part of the bridge management. In the framework of the SAMCO project questionnaires about bridge types were sent to the various institutions, directorates, companies and consultants, who managed about 45,000 railway and roadway bridges in total.

2.2 Bridge types

According to the results of the investigation performed within the Sustainable Bridges project on the existing railway bridge infrastructure (almost 220,000 constructions), masonry structures form the biggest group (40.7%) of structures. Concrete bridges are the next (22.7%) with domination of the 39,214 (78.5%) reinforced concrete (RC) structures. The percentage distribution in regards to the applied material type is presented in Fig. 2-1.

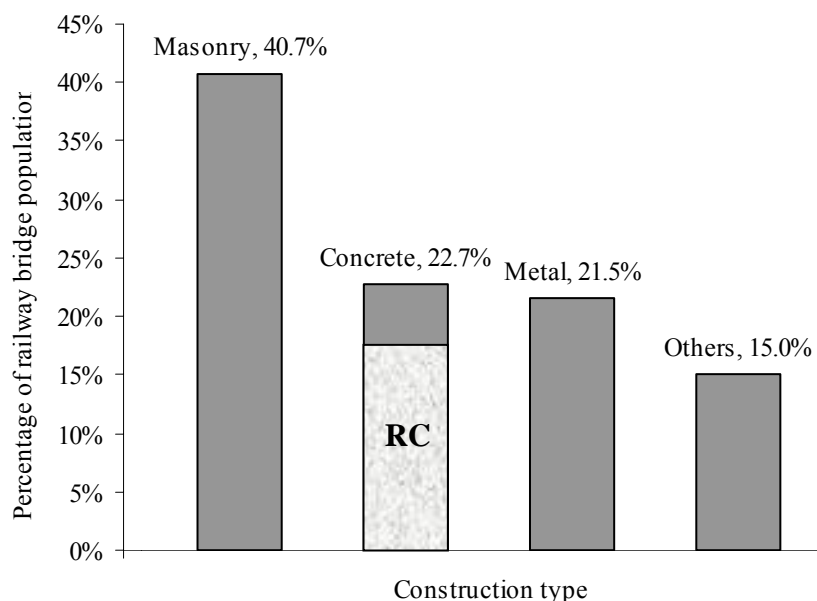


Fig. 2-1 Railway bridge types (Sustainable Bridges 2005)

According to the investigation performed within the SAMCO project concrete bridges are the biggest group (80%) of the analysed bridge population with 37% of RC structures. Railway and roadway bridges have been taken into consideration and this fact can explain the difference between results obtained from these two projects regarding the bridge types. In Table 2-1 distribution of various bridge types is presented.

Table 2-1 Bridge types (SAMCO 2003)

BRIDGES	NUMBER	PERCENTAGE
Reinforced concrete	16,481	37%
Pre-stressed concrete	17,281	40%
Post-tensioned concrete	225	1%
Un-reinforced concrete	940	2%
Composite	1,271	3%
Steel	3,887	9%
Timber	792	2%
Stone	1,376	3%
Others	1,154	3%

In Poland the existing railway bridge infrastructure (under the responsibility of the Polish Railway Administration PKP, i.e. bridges, viaducts and footbridges) consists of 7,902 structures (Bień et al. 1997) and bridges with concrete girders form the biggest group (almost 37%) of bridges with a domination of RC concrete slab spans (67.8%).

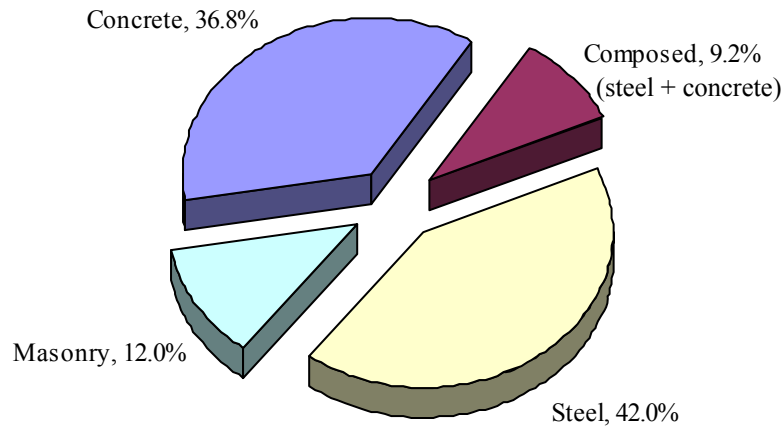


Fig. 2-2 Material of main girders of railway bridges in Poland (Bień et al. 1997)

The Portuguese railway administration (REFER) has under its responsibility 8,754 bridge structures and culverts (REFER 2005). In this group 2,858 constructions are defined as bridge structures and 2,162 as railway bridges.

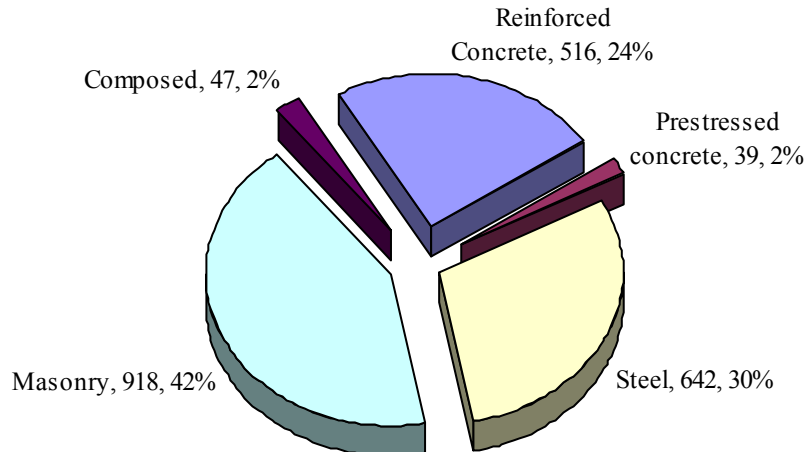


Fig. 2-3 Material of main girders of railway bridges in Portugal (REFER 2005)

The masonry structures are the biggest group among the Portuguese railway bridges (918 pieces, 42%). Railway bridge structures made of RC are situated at the second place 516 (24%) constructions. In this group 273 bridges (53%) are situated along single lines, where traffic in both directions can share the same track. In this group 418 bridges (81%) have been designed as single span constructions. The data related to the type of span cross section is unfortunately unavailable, but from the information collected by the Author of this Thesis their population is significant too.

2.3 Bridge age profile

Only 25% of European RC railway bridges are less than 20 years old. Bridges of 20-50 years old constitute the biggest group of RC railway bridge structures (55%), see Fig. 2-4.

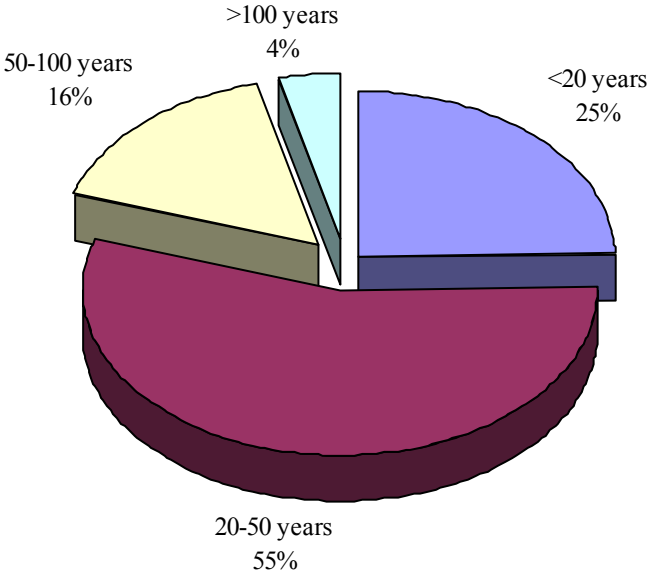


Fig. 2-4 Age profile of railway RC bridges in Europe (Sustainable Bridges 2005)

In Fig. 2-5 the age profile of the Polish railway concrete slab spans is presented (Bień et al. 1997). The first constructions of this type were constructed at the end of the 19th century, but the most intensive development took place after the 2nd World War. Almost 45% of them are over 100 years old and only 15% - less than 40 years old.

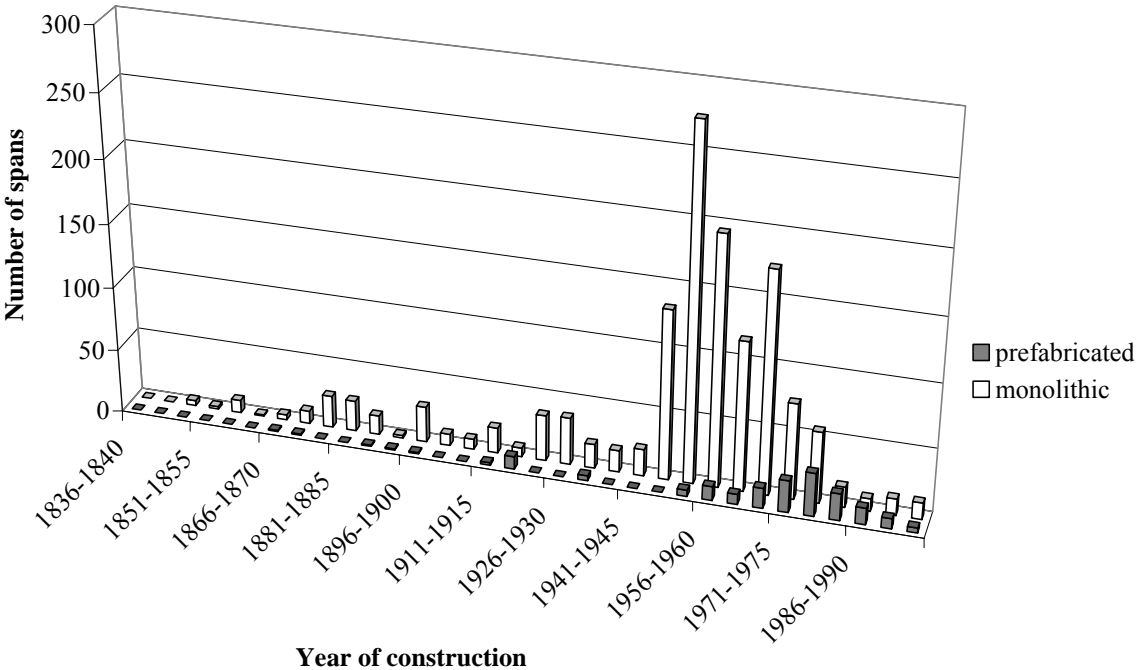


Fig. 2-5 Age profile of railway RC slab spans in Poland (Bień et al. 1997)

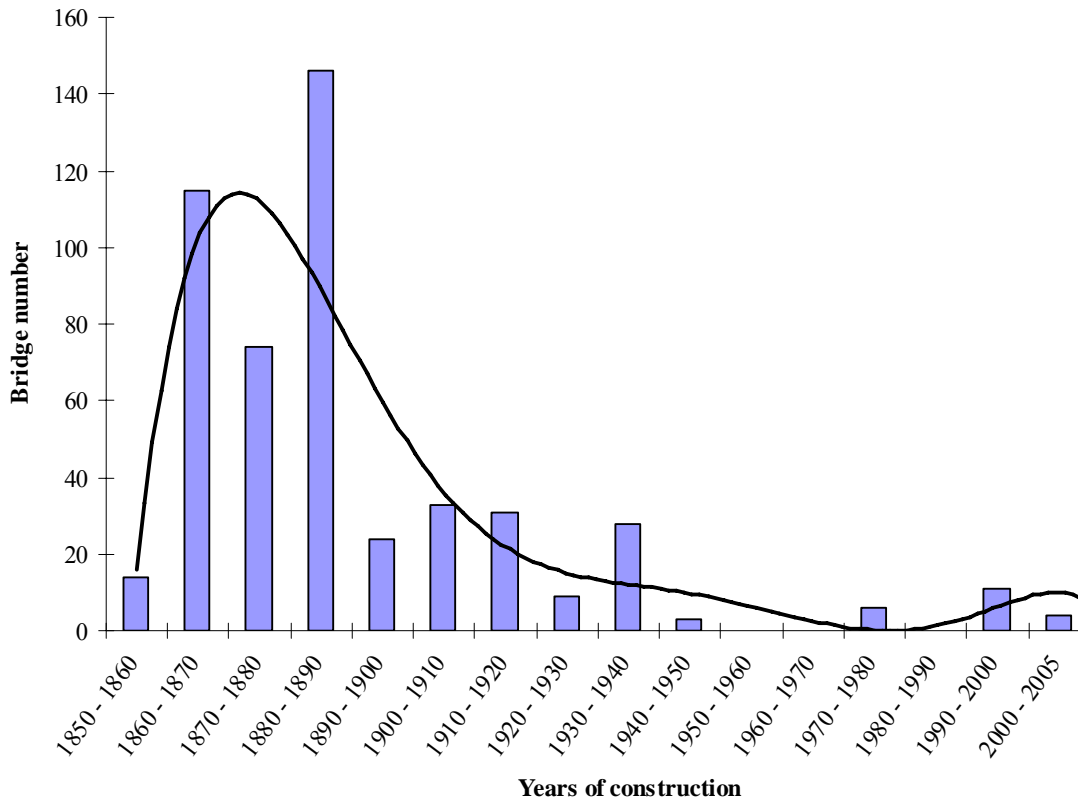


Fig. 2-6 Age profile of railway bridges with RC spans in Portugal (REFER 2003)

In Fig. 2-6 the distribution of railway RC bridges in Portugal in regards to their age profile as a histogram is presented. The maximum of the exposed trend line is located at the end of 19th century. The presented results probably also include the bridge supports, made mainly of masonry, which can explain this curiosity.

2.4 Bridge span profile

The results of research performed within SAMCO project are presented in Table 2-2 as the span profile of roadway and railway bridges. Almost 80% of the European bridges are small structures and only 4% of them are classified as large bridges.

Table 2-2 Bridge span profile (SAMCO 2003)

BRIDGES	NUMBER	PERCENTAGE
Large (more than 5 span or total length over 500 m)	1635	4%
Medium	7844	17%
Small (1-2 span and total length less than 40 m)	36532	79%

Similar results have been obtained by researchers from the Sustainable Bridges project. In Fig. 2-7 the span profile of railway reinforced concrete bridges is presented. The short-span bridges, defined as $L < 10\text{m}$, are the dominating railway RC bridge population and only 4% can be defined as bridge structures with more than 40 meter of span length.

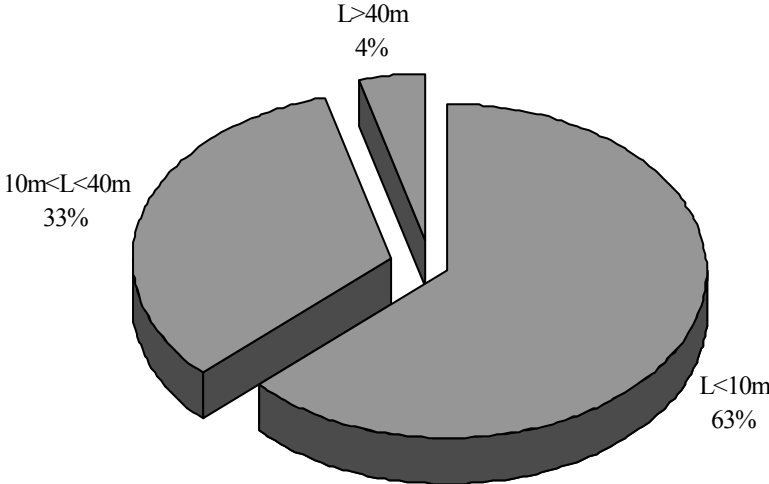


Fig. 2-7 Span profile of railway RC bridges in Europe (WP1 2005)

The distribution of the Portuguese railway RC bridges confirms the results obtained within the Sustainable Bridges project. The railway RC bridges with 3-14m of span represent the biggest group in the Portuguese railway network. In Fig. 2-8 the frequency of the single span is presented in the form of histogram. The exposed trend line underlines the span distribution of the Portuguese bridges. The maximum of this distribution is situated at the point of 5-7 meters of the span length, but the extent of the bridge group with longer spans (the range of 7-20meters) clearly shows that this population is also large.

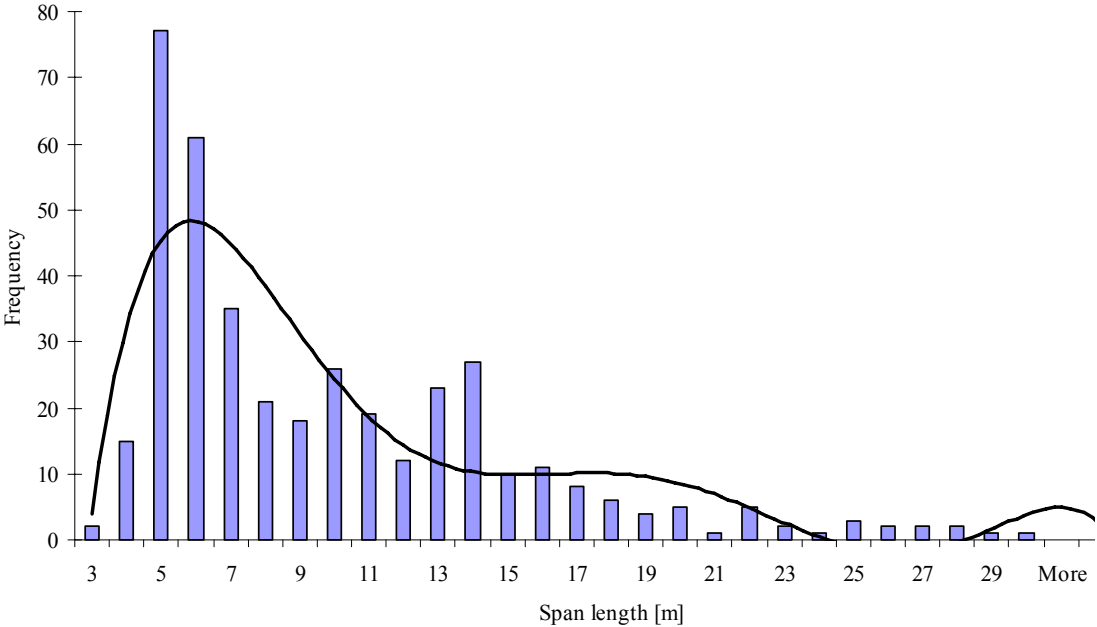


Fig. 2-8 Span profile of railway RC bridges in Portugal (REFER 2003)

Concerning the bridge age profile, the presented results based on various knowledge sources are similar and the conclusion that short-span bridges are the dominating group can be drawn.

2.5 Cross section forms of RC slab spans

According to the publication of Madaj & Wołowicki (1997) the slab span is one of the common types of reinforced concrete railway bridges. This kind of structure has the following advantages:

- Low construction height;
- Facility of supports' distribution;
- Simple formwork with small circuit moistening;
- Facility of reinforcement construction;
- Easy cementation, consolidation and curing of the fresh concrete;
- Elimination of the classical deck construction (slab, stringers and floor beams) and bracings;
- High rigidity (flexural and torsional) of the slab girder, which ensures good transmission of non symmetrical as well as dynamic loads;
- Constant slab stiffness increases durability of track construction and span insulation;
- Smooth bottom of the span surface allows much easier ventilation and avoids potential degradation mechanisms (Fig. 2-9).

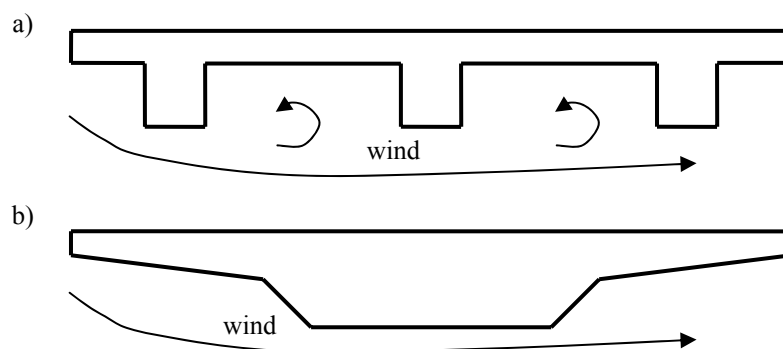


Fig. 2-9 Comparison of slab-girder span (a) with slab span (b) in respect to ventilation at the bottom face

The form of span regarding its bottom face is strictly related to the risk of degradation occurrence. The percentage area of the bottom surface of the slab is relatively smaller in comparison to the slab-girder span, which means the smaller area exposed to the attack of aggressive environment. An example of a girder-slab span and a slab span is presented in Fig. 2-13. The mentioned area of the bottom face of slab-girder span may be even 100% (or more – depending on the construction height) greater than the bottom face of the slab span.

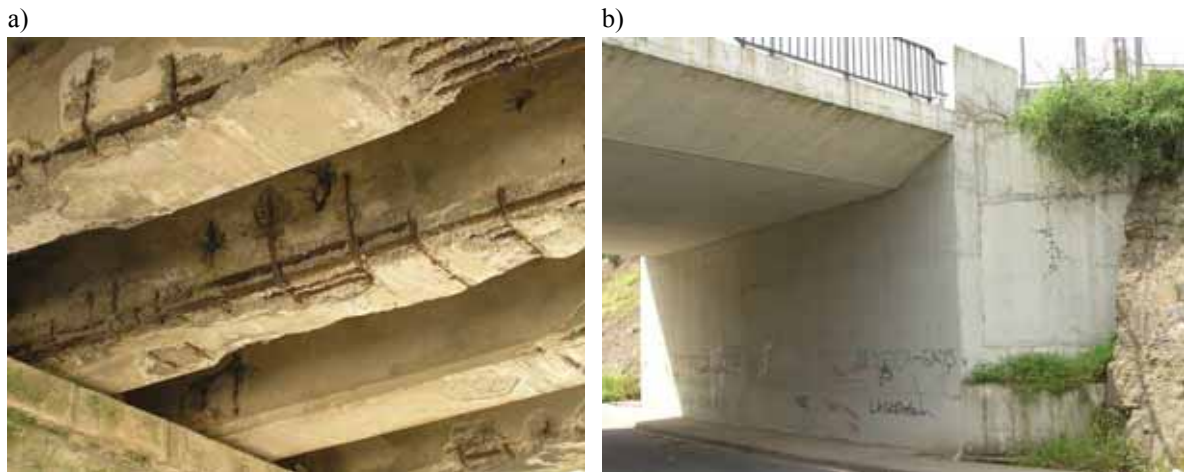


Fig. 2-10 Comparison of slab-girder span (a) and slab span (b) in respect to areas of the risk of degradation occurrence (photographed by the Author)

On the other hand the slab deadweight and material excess in its neutral surface are disadvantages of this kind of solutions. In Fig. 2-11 the most popular slab spans, in terms of their forms of cross-section, have been presented. They are:

- Rectangular (Fig. 2-11a);
- With extended brackets (Fig. 2-11b);
- With curved bottom face (Fig. 2-11c);
- With edge beams (Fig. 2-11d).

Concerning this kind of spans, especially with the rectangular cross section (Fig. 2-11a and Fig. 2-12), the participation of the dead load on the total bending moment reaches 40-50%.

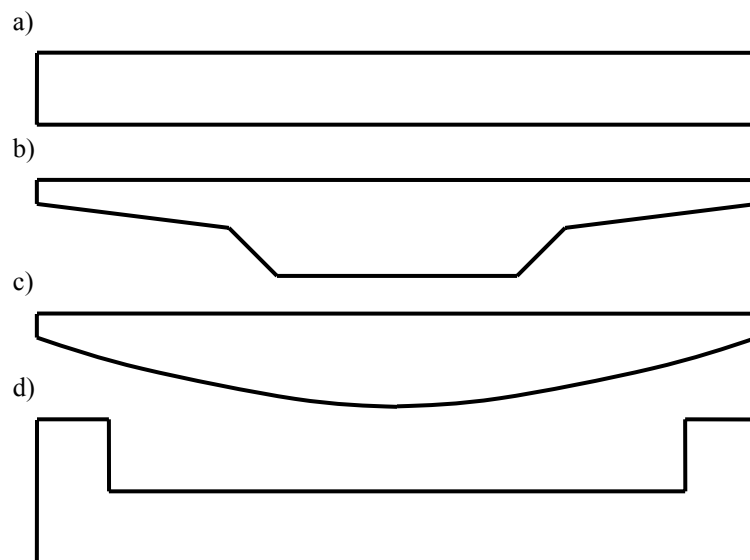


Fig. 2-11 Basic forms of cross sections of RC slab spans

Moreover such heavy span requires special conditions regarding its bearing and supports. From the economic point of view this fact makes this type of construction more expensive.

To reduce deadweight of the span and increase material effort a modified solution of slab span (the cross section with extended brackets) can be used.



Fig. 2-12 Example of slab span with rectangular cross section (photographed by the Author)

In Fig. 2-11b and Fig. 2-13 examples of the slab spans with extended brackets are presented. In this case the dead load related to the weight of the span may be reduced by 10-15%.



Fig. 2-13 Example of slab span with extended brackets (photograph courtesy of Jerzy Czastkiewicz, PKP)

Application of voids parallel to the axis of the span is another solution for reduction of deadweight, but it makes the construction process difficult, laborious and time consuming.

Another solution is cross section with curvilinear outline of the bottom face (Fig. 2-11c) or rectangular cross section with edge beams (Fig. 2-11d and Fig. 2-14), which allows a reduction of the construction depth. This solution is especially useful in case of the crossing of two railway lines, where the clearance of the bottom line is significantly limited.



Fig. 2-14 Example of slab span with rectangular cross section and edge beams (photographed by the Author)

2.6 Track constructions

Track construction has a substantial meaning regarding the intensity of dead load, dynamic amplification factor DAF for moving loads and their distribution through the horizontal layers of span. The considered span constructions can be divided into the tracks with and without ballast and solutions with ballast (see an example in Fig. 2-15) are the absolutely dominating group.

Regarding the load intensity the ballast weight is a significant part of the dead load and its intensity varies between 20 and 30% of the total dead load.



Fig. 2-15 Example of railway track with ballast (photographed by the Author)

The ballast thickness H_b influences the DAF value which can be evaluated by means of the function of the span length and the ballast thickness. While H_b causes higher value of the dead

load, the DAF value is reduced (for H_b). See the equation (B-1) in Appendix B for more information. The distribution of the DAF value in the mentioned function of the span length L and ballast thickness H_b is presented in Fig. 2-16.

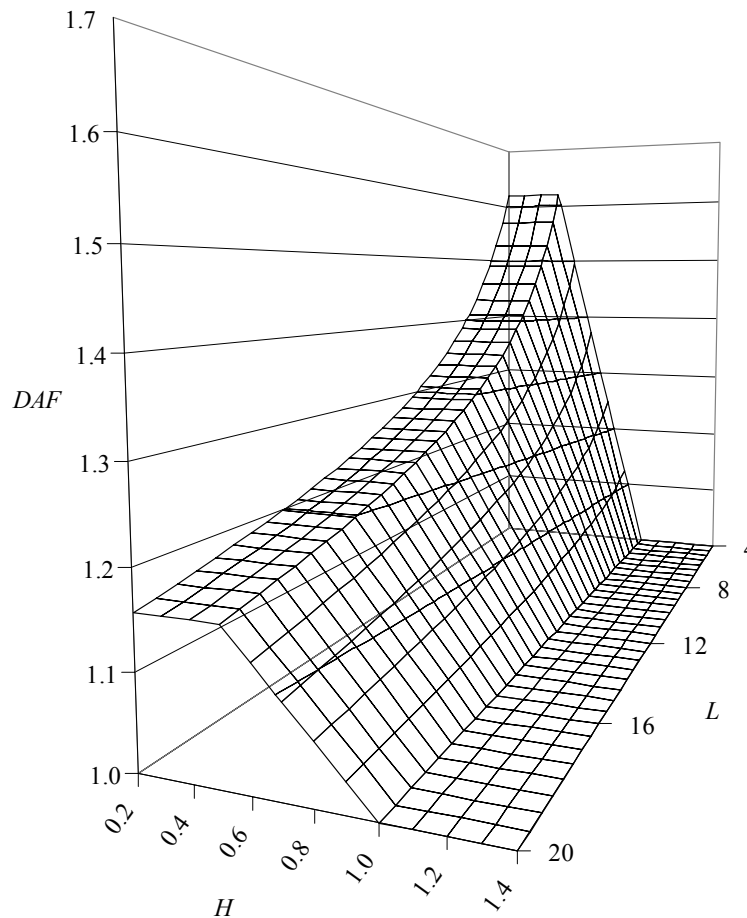


Fig. 2-16 DAF values in function of span length L [m] and ballast thickness H_b [m] according to PN-85/S-10030

The presence of the ballast causes the change of the moving load (especially from the train axles) character from the concentrated into the uniform interaction. The angle of 45 degrees is a commonly accepted value for the load transmission.

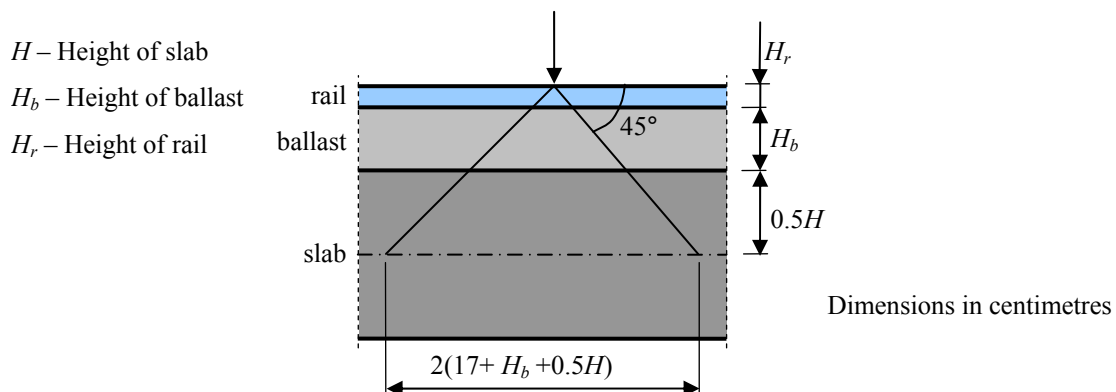


Fig. 2-17 Simplified longitudinal distribution of load

In case of the typical span with 80 cm of the slab height and 30 cm of the ballast thickness (see Fig. 2-17) the participation of the track elements in area of load distribution in the

longitudinal direction of the span reaches about 50%. This influence is even greater regarding the transversal direction of the span because of the presence of rail sleepers, see Fig. 2-18.

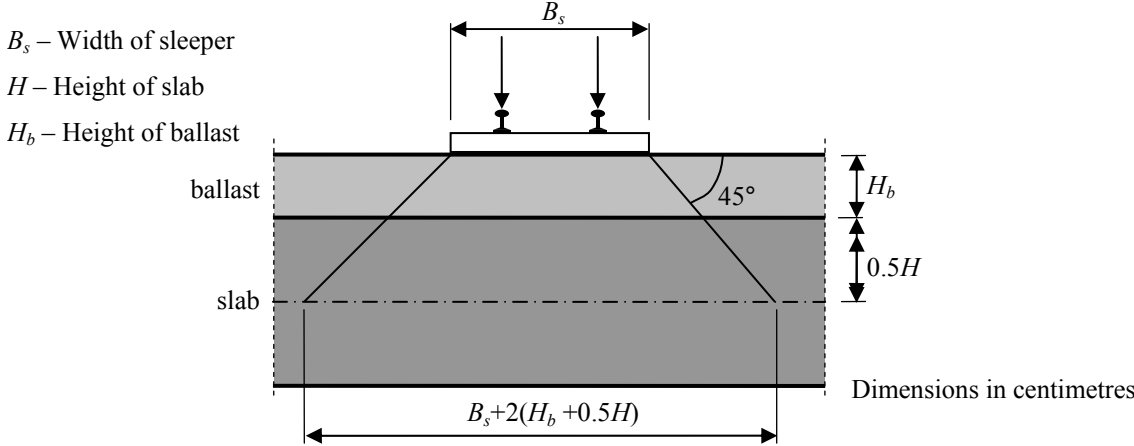


Fig. 2-18 Simplified transverse distribution of load

Chapter 3

Classification of defects

3.1 Introduction

The proper evaluation of load capacity of damaged RC railway bridges requires a consistent methodology of defects classification, identification and modelling. The problem is even more significant, when the assessment procedure is carried out by more than one person. Some inconsistencies at this level may cause severe misunderstandings leading to incorrectly performed analysis.

In the available literature various ways of defects classifying can be found. The criteria used at the creation level of the bridge defect classification can be distinguished into the three following groups:

- *Cause criterion* – related to the cause of the defect;
- *Effect criterion* – regarding the degradation mechanisms effects;
- *Cause–effect criterion* – connecting the cause with the effect as a basis of their classification.

Various researchers applied various classification criteria. Some of them used more than one criterion which makes such solution inconsistent and not clear. In the following sections several classifying way will be presented and discussed. Also a critical review of solutions found will be presented.

3.1.1 Methods based on the “cause” criterion

Domsa (1996) proposed a classification of defects under the aspect of their origin specifying the requirements of the quality control:

- Building material (corresponding choice and considering the selected material);
- Design (the solving of the structure system such as to correspond to the conception and solution of ensemble; the solving and dimensioning of the construction elements considering the execution possibilities and the technologies that will be used.);
- Erection, mounting (the achievement according to the requirements of the design of the laying out, placement, and mounting of the structure elements, of the assemblies, setting up the reinforcements, concrete pouring up, and so on.);
- Chance causes (the precaution of some possible floods, earthquakes, emanation of gas, etc., defects in equipment’s operation and taking the adequate measures of preventing the deterioration of constructions.);
- Exploitation (the immediate remedy of any faults of the constructions).

Defects classified in Concrete Society (2000) are distinguished into the following groups:

- defects related to construction phase (i.e. plastic shrinkage cracks; plastic settlement cracks; early thermal contraction cracks; crazing; long-term drying shrinkage cracks);
- load-induced cracking and structural design inadequacies (i.e. overloading; cracks induced by temperature changes; impact damage; abrasion, erosion and cavitation; deformations);
- environmental effects (weathering of structures; biological growth; bacteriological attack; staining; lime leaching; freeze-thaw damage; fire damage);
- deterioration related to aggregate properties (aggregate swelling and shrinkage; aggregate softening; alkali-silica reaction; chlorides; sulphides);
- chemical attack (i.e. sulphates; chlorides; physical salt weathering; acids; other substances);
- reinforcement corrosion.

3.1.2 Methods based on the “effect” criterion

Bień (2002) presented a three-level uniform system of defects prescribed for all types of bridge structures (concrete, steel and masonry). On the top level, seven basic defect types can be found: deformations, material destruction, loss of discontinuity, losses of material, defects of protection, displacements and contaminations. This classification system is mainly based on the “effect” criterion, however, some inconsistencies can be found.

In case of *deformations*, this defect type is distinguished into the permanent (for example caused by accident with traffic) and temporary (i.e. excessive deflection caused by moving load) deformations. These defects are distinguished by the “cause-effect” criterion.

Concerning *contamination*, this type is divided into *dirtiness* and *plant vegetation*. *Dirtiness* is distinguished by the *cause-effect* criterion: *dirtiness caused by natural environment* and *dirtiness caused by human activity*. A reference to defect causes can be observed.

Defect attribution to the particular construction type (concrete, masonry or steel) takes place below the top accuracy level. For some construction types this solution seems to be not suitable. For example *torsion of element* can be prescribed for the steel construction; *absorbability increase* can be identified in the concrete as well as in the masonry constructions. Separation of this system in terms of the construction type (material) would make this classification more transparent.

Defects of protection are defined as partial or total dysfunction of a protection coat. The protection coat cannot be treated as a construction element designed for stress transmitting. For this cause *strength reduction* of the protective coat is not justified to be listed there.

Branco & de Brito (2004) presented a system of defects classified into the following nine groups with a location and functional nature of defect as a criterion of the classification: Superstructure Global Behaviour; Foundation / Abutments / Embankments; Concrete Elements; Reinforcement / Cables; Bearings; Joints; Wearing Surface (Asphalt) / Watertightness; Water Drainage; Secondary Elements. In terms of this Thesis only some of them are to be analysed. In Table 3-1 a fragment of this classification is presented.

Though this research presents a significant contribution to the classification of defects some findings can be listed here. The presented classification is based mainly on the “effect” criterion, but some defects are suggesting a degradation mechanism rather than its final effect, for example scour, settlement or embankment erosion.

Table 3-1 Defects of concrete bridges, fragment (Branco & de Brito 2004)

Superstructure Global Behaviour	
Permanent deformation	Column tilting
Relative displacement	Vibration
Foundation / Abutments / Embankments	
Scour	Embankment slippage
Settlement	Heavy vegetation growth / burrows
Rotation	Obstruction of the waterway by debris
Settlement / failure of the approach slab	Silting
Embankment erosion	
Concrete Elements	
Corrosion stain	Concrete crushing
Efflorescence / moisture stain	Map cracking
Concretion / swelling	Longitudinal crack
Wear / scaling / disintegration	Transverse crack
Voids / porous area / honeycombing / aggregate nest	Diagonal crack
Stratification / segregation	Crack over / under a bar
Delamination / spalling	
Reinforcement / Cables	
Exposed bar (loss of cover)	Broken bar
Exposed duct (loss of cover)	Broken strand / wire
Exposed strand / wire (loss of cover)	Deficiently grouted duct
Corroded bar	Faulty sealing of prestressed anchorage
Bar with reduced cross section	Corroded anchorage

Another element worthy to be mentioned is inconsequence in the level of accuracy of defect description. For example map cracking, longitudinal crack, transverse crack, diagonal crack and crack over/under a bar are listed as separated items, whereas each of them represents the same type of defect, i.e. discontinuity. Each of them differs from the others its direction and the relative location with respect to the reinforcement. On the other hand a delamination / spalling is listed as a single damage. Delamination is a kind of discontinuity and spalling should be considered as a loss of material. Both of these defects should be listed as the separated items. Defects such as exposed bar, duct and strand / wire were also called loss of cover. This defect is definitely related to the concrete damage and does not necessarily mean that the steel covered has been damaged. In the Author's opinion these defects should be attributed to the defects of concrete.

Definition of each defect must be clear and unambiguous. The corrosion of reinforcement is usually related to the reduction of the cross sectional area of rebar. The defects called corroded bar as well as bar with reduced cross section seem to mean the same defect.

3.1.3 Methods based on the “cause-effect” criterion

Currie & Robery (1994) distinguishing defects by their causes created system focused on cracks occurred. This classification would be suitable to apply in degradation mechanisms classification.

Table 3-2 Types of cracking in reinforced concrete (Currie & Robery 1994)

After hardening					Before hardening
Physical	Chemical	Environmental	Structural	Mix design	Support
Shrinkage of aggregates	Corrosion of reinforcing bars	Freeze-thaw cycling	Accidental loading	Early frost damage	Formwork movement
Drying shrinkage of concrete	Alkali aggregate reaction	Seasonal temperature variations	Creep	Plastic settlement	Sub-grade movement
Crazing	Carbonation shrinkage	Thermal gradient during hydration	Under-design or change in loading		

It is difficult to check what the cause of a considered defect was. This fault makes this approach useless in the purposes of this Thesis.

3.1.4 Methods based on combination of criteria

In Swedish Bridge Inspection Manual (1996) defects are loosely listed without any hierarchical system of classifying. Each of them has its own description and almost everyone is illustrated by photo. The following types can be found there: leaching; weathering; spalling; corrosion; embrittlement; cracking; flexural cracking; tension cracking (distinguished into shrinkage, temperature and settlement cracks); shear cracking; combined flexural and shear cracking; fracture; crushing; loosening; deformation; misalignment; movement; scratch; dent; leakage; scour; casting defect and loss. All the mentioned criteria of defect classification can be found here.

Concerning the *cause criterion* the following examples can be found: *corrosion* (related to the reaction between metals and their surroundings, causing conversion to the corrosion products) and *casting defect* (caused by faulty placing of concrete). In case of the *effect criterion* (regarding the degradation mechanisms effects) – there are: deformation (loss by an element

its original shape), misalignment (loss by an element of its correct position or adjustments) or *leakage* (loss by an element/material of its watertightness). Some examples related to the *cause-effect criterion* can also be found such as *shrinkage cracks* and *spalling* (when concrete splits off in sheets or becomes stratified as a result of internal forces). Using different types of criteria makes this classification ambiguous.

Horváth & Popa (1996) proposed the following general defects grouping:

- physic-mechanical degradations;
- chemical degradations;
- faults of structural and constructive order;
- faults of functional and architectural order.

In the first and second case the terms mixing “defect-degradation” suggests application of the “cause-effect” criterion. In case of the next groups the “cause” criterion seems to be applied.

Žnidarič & Peruš (2000) divided defects into: displacements and deformations; concrete; reinforcing and prestressing steel. This approach presents a common problem of defining criteria of defect classification at its creation level.

Table 3-3 Classification of defects presented by Žnidarič & Peruš (2000)

Displacements and deformations		Concrete	Reinforcing and prestressing steel
Substructure	Superstructure		
Lateral movement	Vertical deflection	Poor workmanship: peeling, stratification, honeycomb, voids	Corrosion of stirrups
Tilt, rotation, out-of-plumb	Unsmooth approach, bump	Plastic shrinkage and settlement cracks, crazing	Corrosion of main reinforcement, reduction of steel area in the section
Differential settlement		Strength lower than required	Duct deficiencies
Scoured area beneath pier/abutment		Depth of cover less than required	Corrosion of prestressing tendons
		Carbonation front	
		Chloride penetration	
		Cracking caused by direct loading, imposed deformation and restraint	
		Mechanical defects, erosion, collision	
		Efflorescence, exudation, popouts	
		Leakage through concrete, at cracks, joints	
		Wet surface	
		Freezing and thawing	
		Freezing in presence of de-icing salts, scaling	
		Cover defects caused by corrosion	
		Spalling caused by corrosion of reinforcement	
		Open joint between segments	

All of the criterion types can be found. For example, vertical deflection of the superstructure, concrete strength lower than required can be attributed to defect group distinguished by the *effect* criterion. Freezing and thawing as well as corrosion of stirrups represent the defects distinguished by the *cause* criterion. Finally cracking of concrete caused by direct loading or concrete cover defects caused by reinforcement corrosion are distinguished by the *cause-effect* criterion.

In FIB Bulletin (2003) defects have been divided into the following bridge part groups: riverbanks, riverbed, embankments; substructure; superstructure; concrete; reinforcement; bearings; expansion joints; pavement with waterproofing membrane; curbs; safety barriers; joint sealing; protective devices; drainage systems. For each of these groups a list of prescribed defects is attached. The main problem is lack of clear defect definitions.

According to the definitions presented in this publication the term *deterioration* (as a frequently listed defect for concrete, bearings, expansion joints, curbs, safety barriers etc.) is defined as “*process that adversely affects the structural performance (...)*”. On the other hand the term *defect* is defined as “*unfavourable change in the condition of a structure that can affect structural performance*”. The term collision: “*process-change*” can make the defect identification ambiguous.

An example of the next inadequacy is placing terms like: superstructure, reinforcement and safety barriers at the same accuracy description level. The reinforcement and safety barriers are the parts of this superstructure. A multi-level classification system would resolve this problem. Moreover the safety barriers (and also curbs, drainage systems, etc.) are non-structural bridge components. Separation the structural bridge elements from the non-structural would make this classification more transparent.

Another term conflict is in case of the deformation defect. This type is prescribed for bearings, curbs and safety barriers. Deformations are distinguished into the transverse and the vertical displacement. For bearing there are also rotations. The conflict “*deformation-displacement*” appears. Moreover the deformation defect type is not prescribed for the superstructure.

The lack of clear definitions appears also in case of prescribed defects for substructure and superstructure as well. An excessive vertical displacement is the only one available defect of superstructure. The vertical displacement seems to be impossible to occur, but lack of deflections in the list of defects for this construction group suggests an occurred mistake. Regarding substructures instead of displacements there are movements (lateral) of substructure.

The criterion of defect classification is the next inadequacy of the analysed publication. In this work all of mentioned criterions before have been found. The following examples of defects distinguished by the *cause criterion* have been found: erosion of embankments, differential settlements of substructure, corrosion of main reinforcement. In case of the *effect criterion* (regarding the degradation mechanisms effects) – there are: lateral movements of the substructure, honeycomb of concrete, deformations of curbs. The *cause–effect criterion* is represented by: delamination of concrete due to impact load, malfunction of the bearings due to dirt, mechanical defects of protective devices due to impact load. The selection of the suitable criterion is necessary, but mixing different kinds of these criterions is not acceptable.

3.1.5 Other methods

Monks (1981) summarised defects of concrete taking into account blemishes at its surface.

Table 3-4 Classification of concrete surface defects according to Monks (1981)

COLOUR VARIATIONS		PHYSICAL IRREGULARITIES	
Technical term	Appearance	Technical term	Appearance
Inherent colour variation	Differences related to colour of constituents	Misalignment	Step, undulation or other departure from intended shape
Aggregate transparency	Mottled with dark areas similar in size and shape to coarse aggregate	Blow-holes	Individual, usually rounded cavities usually less than 10 mm
Negative aggregate transparency	Mottled with light areas corresponding to coarse aggr.	Aggregate bridging	Irregular cavities
Hydration discoloration	Variation in tone due to differences in water content	Honeycombing	Coarse, stony surface
Dark discoloration and glazing	Very dark, specular and impermeable areas	Grout loss	Sand-textured areas lacking cement paste
Segregation discoloration	Speckled or flecked	Scouring	Eroded areas with exposed stone or sand particles
Contamination	Discoloration from contaminants in concrete mix	Scaling	Loss of thin layer of hardened mortar
Staining	Discoloration not related to the constituents of the mix	Spalling	Loss of piece of hardened concrete
Oil discoloration	Cream or brown colour showing sand or aggregate too	Form scabbing	Form material or barrier coating adhering to concrete
Retardation	Weak, sand-coloured matrix which may not have hardened	Plastic cracking	Crack, usually discontinuous, in or near top surface
Dusting	Light-coloured powdery surface which may weather to expose the aggregate	Stress cracking	Crack often long and uniform in width
Drying discoloration	Variation in tone, visible only some time after striking	Map cracking (crazing)	Network of fine cracks dividing surface into areas 10 to 50 mm across
Lime bloom (efflorescence)	Chalky white powder or deposit		

Defects are distinguished by the colour variations (variations of colour or tone) and the physical irregularities (i.e. in texture or planeness) and presented with their technical names, brief descriptions and probable causes, see Table 3-4. When concrete is not to be exposed to view, blemishes are seldom significant; colour variations resulting from surface effects are of no consequence, and minor physical irregularities can usually be ignored.

In terms of the load capacity assessment, the classification system should not include defects occurring at the concrete surface only. The presented defects can be treated in terms of the durability of the structure only or at least the aesthetics of the construction.

Folic & Ivanov (1996) presented two other classification systems. In the first defects are distinguished as follows:

- danger degree related to the further possibility of bridge operation (minor, great and critical);
- manner of defect appearance (i.e. defect predicable and visible according to rules);
- possibilities of defect repair (i.e. defect whose repairs are technically impossible or economically unjustified).

The second system is divided into the following groups:

- technical properties;
- cause of defect occurrence (internal properties or external influences);
- speed of defect occurrence (gradual or haste);
- defect consequences for further service (minor, considerable and critical);
- defect range (partial and complete);
- time of defect occurrence and service life (during construction, service or imposing structural rejection).

These defect classification systems involve all the criteria of defect classifying.

3.1.6 Critical review

Defects may be caused by more than one cause, usually difficult to explain. It is why the “cause” criterion does not guarantee suitable basis for the unambiguous classification. Moreover in bridge condition assessment, the causes of defect do not play so important role as final effects of degradation mechanisms. Cause of defects, modelling of degradation

mechanisms and future condition forecasting is more related to the bridge durability assessment. This Thesis deals with bridge condition evaluation in the current point of time.

The criterion "cause-effect" is closer to the objectives of this Thesis, but the description of defect presented in this way is more complicated because of the relation to defect causes and effects. In terms of the load capacity assessment, where effects of degradation mechanisms plays crucial role, description of defects is too complex and difficult to apply.

The "effect" criterion is the most justified. A multi-level classification system of defects, presented in the next part of this chapter, allows for their precise modelling. According to the literature review the solution presented by the Author is similar to approaches proposed by Bień (2002) and Branco & de Brito (2004). Though these solutions contain some inconsistencies, they will be considered as a start point in this chapter basing on the "effect" criterion of defect classification.

3.2 General conception and criteria of defect classification

The proposed solutions have been presented as a hierarchical defect system based on the examples of defect descriptions found in the available literature as well as the Author's observations from the bridge visual inspections. This system distinguishes four levels of the description accuracy (Fig. 3-1) to allow describing defects with required information accuracy.

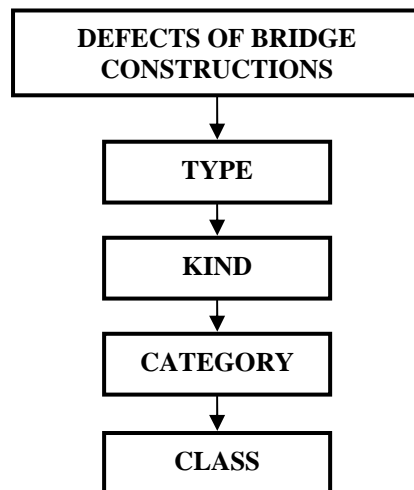


Fig. 3-1 Levels of accuracy of description in the classification of defects

At the top level of the proposed classification there are six defect types: contamination, deformation, deterioration, discontinuity, displacement and loss of material. Their definition will be presented in the next section. The second level of this classification (kind of defect) system is prescribed for the RC concrete components (i.e. concrete, reinforcement and protection). The lower levels have been created for more detailed descriptions of defects

according to their particular characteristics. This system, modified according to the particular characteristics of the other construction materials, is suitable also for masonry and steel bridges; see the Sustainable Bridges reports (Bień et. al 2004, Sustainable Bridges 2007).

The presented system allows for the numerical describing of all identified defects of construction. The main objectives of presented solutions are listed as follows:

- Introduction of uniform classification and identification system of all types of defects of RC railway bridges;
- Possibility of description of any combination of defects;
- Creation of methods of defect identification and classification to apply to the various types of geometry models of constructions;
- Formation of defect classification system enabling the creation of numerical models of defects, which can be used by expert tools supporting evaluation of technical condition of the bridges.

Moreover time of intensive European integration require from bridge engineering a unification of existing systems into the one common methodology.

3.3 Types of defects

At the top level of the proposed classification system of RC railway slab span defects there are six basic defect types:

- Contamination – Dirtiness or not designed plant vegetation;
- Deformation – Geometry changes incompatible with the project, with changes of mutual distances of structure element points;
- Deterioration – Physical and/or chemical changes of structural features against designed values;
- Discontinuity – Inconsistent with a project break of material continuity;
- Displacement – Change (or restriction) of location of a structure or its part incompatible with the project but without its deformation;
- Loss of material – Decrease of designed amount of structure material.

3.3.1 Contamination

In case of concrete and protection the contamination is distinguished into the inorganic (aggressive and neutral) and the organic (penetrating and superficial) defect classes. An example of leaching effect is presented in Fig. 3-2. Products of this degradation can be observed also on the supports. Contamination classes are distinguishable at the chemical analysis level.



Fig. 3-2 Example of contamination of concrete (photographed by the Author)

Another example of contamination defect is presented in Fig. 3-3. The neutral steel corrosion products (the rust) are flowing down making the concrete slab surface stained.



Fig. 3-3 Example of neutral contamination of concrete (photographed by the Author)

Contaminations in terms of the load capacity assessment play the secondary role as an indicator of possible internal defects or material destruction for a further testing. For example the stained concrete surface indicates the corrosion of rebars which may mean some loss of

material. Many bridges, especially closely situated to the places where people live, are “decorated” with various “paintings”, commonly called “graffiti”. This defect, considered as a neutral inorganic contamination of concrete, does not influence the load capacity, but the aesthetics of the bridge is affected. It is very difficult to struggle with this phenomenon, especially when these defects occur at night. Fig. 3-4 presents an example of a reinforced concrete railway span with this type of defect. To control this phenomenon some local authorities allows young people to paint some part of bridges, i.e. supports.



Fig. 3-4 Example of neutral inorganic contamination (photograph courtesy of Jerzy Czastkiewicz, PKP)

3.3.2 Deformation

This defect type is prescribed for the concrete and the protection components of RC concrete and is distinguished into the following categories: deflection (caused by bending forces), slip (caused by shearing forces) and swell (related to the spatial increase of the volume).



Fig. 3-5 Example of deformation: deflection (photograph courtesy of Zygmunt Kubiak, PKP)

In Fig. 3-5 an example of deformation (with exposed span deflection f) of railway slab span is presented. Probably this defect occurred as a consequence of construction errors. The considered span structures and their high rigidities as well as relatively short span lengths make this defect only theoretical case. Even if deformation has occurred, it is usually caused by construction errors. For this reason this defect has been excluded from the further research.

3.3.3 Deterioration

This defect type has been distinguished regarding the reinforced concrete components.

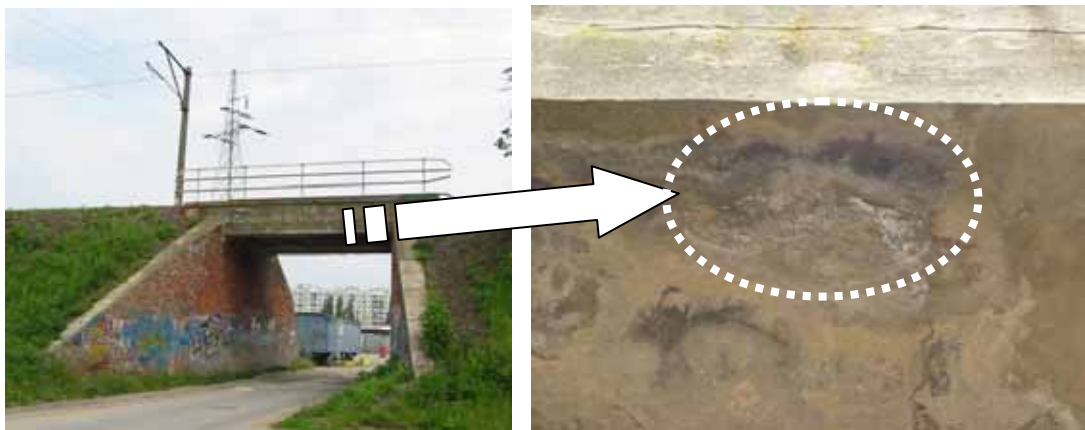


Fig. 3-6 Example of concrete deterioration: permeability increase (photographed by the Author)

For the concrete and protection (kind) several class defects have been attributed and distinguished by the categories (modification of chemical and physical features). Defect classes of reinforcement are considered as a single (modification of physical features) category. In Fig. 3-6 an example of concrete deterioration (permeability increase) is presented.

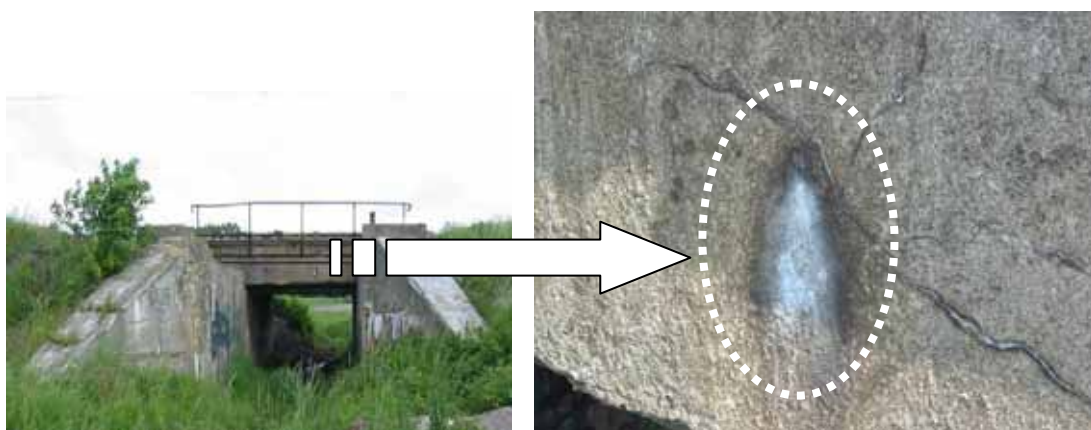


Fig. 3-7 Example of concrete deterioration (permeability increase) with coexisting with contamination and discontinuity defects (photographed by the Author)

A common situation during bridge service-life is the coexistence of various defects. In Fig. 3-7 an example of concrete permeability increase accompanied by cracks and contamination is presented. The proposed uniform multi-level defect classification system allows describing

any defect combinations. This defect type has a special meaning in terms of the load capacity assessment. The strength parameters of concrete and reinforcing steel such as strength as well as elastic modulus reduction are the most important features regarding the deterioration. Other classes of this defect can be considered as indicator of other property modifications.

For instance calcium hydroxide reduction of concrete can be translated to the strength reduction. The pH factor reduction in concrete is a suitable indicator of corrosion likelihood.

3.3.4 Discontinuity

Discontinuity has been divided into the following defect categories: crack (discontinuity of material perpendicular to the element surface covering a part of the cross-section), fracture (discontinuity of material perpendicular to the element surface occurred at the whole cross-section, dividing it into separate parts) and delamination (discontinuity of material parallel to the element surface). This defect type has been attributed to concrete (crack and delamination only), protection and reinforcement (crack and fracture only). Discontinuity is distinguished by relation to the main force direction in structure element: irregular, longitudinal, perpendicular and skew. An example of the longitudinal crack is presented in Fig. 3-8. Concerning the considered span structures bending is the main internal interaction.

Perpendicular cracks in concrete occur in the tensile zone. For this reason this defect is important regarding the corrosion risk only. In case of the irregular cracks such as crazing, it can be translated into the concrete strength reduction. Delamination of concrete can be considered as loss of material.

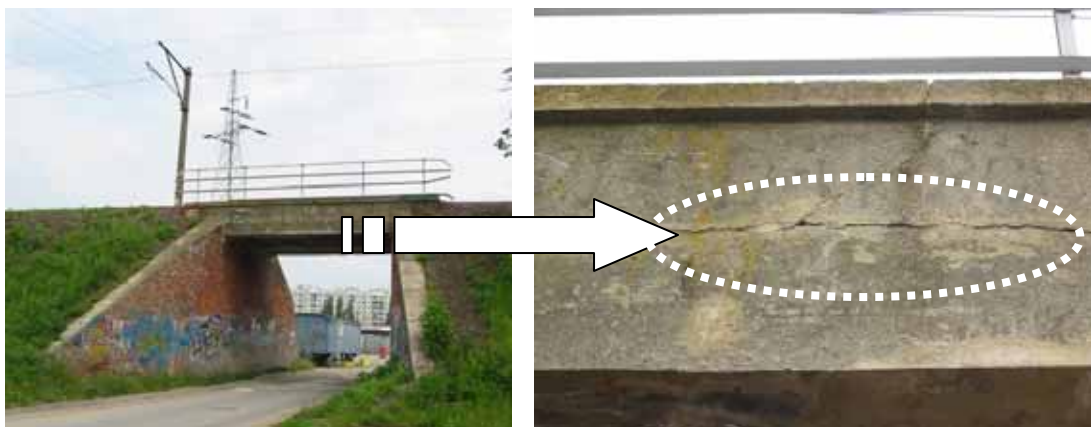


Fig. 3-8 Example of discontinuity: longitudinal crack in concrete (photographed by the Author)

Fracture of concrete has been considered as a theoretical case only. This discontinuity category occurred to concrete slab spans was not observed by the Author and no comment on this defect category was found in the available literature as well. Sometimes discontinuities

occur in reinforcement. In case of fracture this defect can be interpreted as loss of material of 100% intensity. In Fig. 3-9 an example of the fracture of stirrup is presented.



Fig. 3-9 Example of discontinuity: fracture of the stirrup (photograph courtesy of Jerzy Czastkiewicz, PKP)

3.3.5 Displacement

This defect type (Fig. 3-10 and Fig. 3-11) is prescribed for concrete component only. At the deeper level displacement is distinguished into the following categories: excessive and limited. In both cases the rotation and translation has been considered.

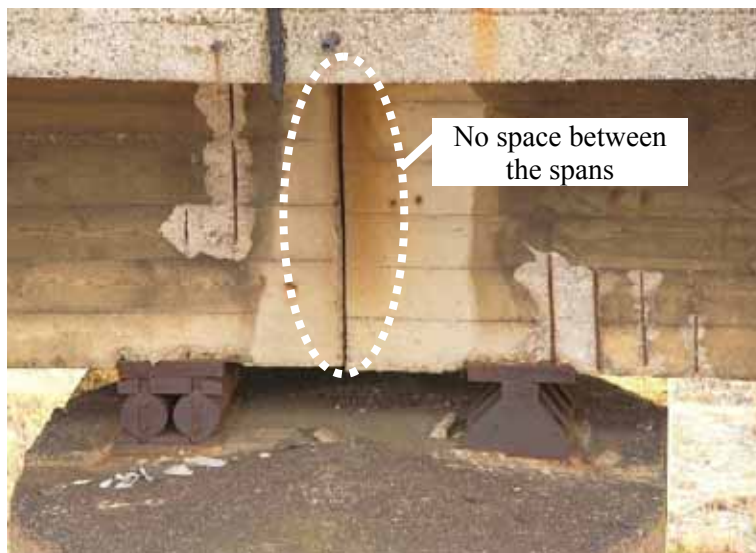


Fig. 3-10 Example of limited displacement: translation (photograph courtesy of Jerzy Czastkiewicz, PKP)

Both defects are accompanied by other defects like loss of concrete and stirrups (Fig. 3-10) and penetrating organic contamination (Fig. 3-11). Coexistence of various defects is a typical situation during bridge service life.

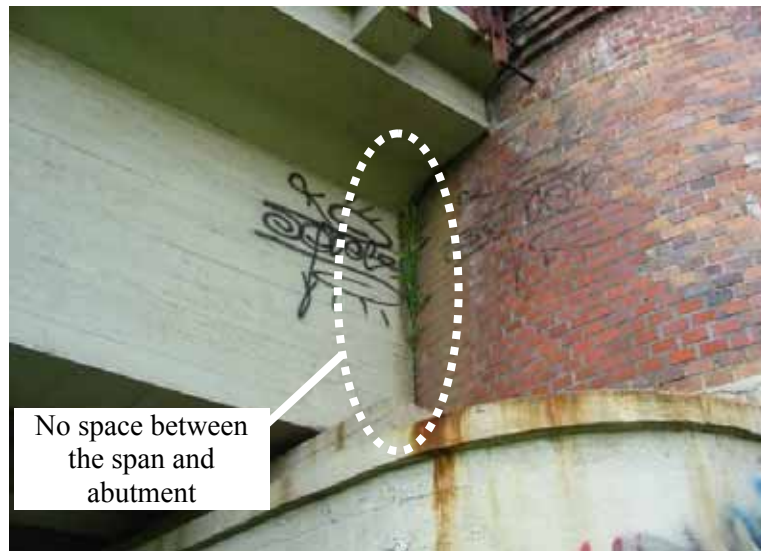


Fig. 3-11 Example of limited displacement (translation) defects coexisting with contaminations – penetrating organic and neutral inorganic (photographed by the Author)

3.3.6 Loss of material

Loss of material has been prescribed for all of the RC components (concrete, protection and reinforcement). At the lower level (category of defect) of this system only concrete and reinforcement are divided into the more detailed defect categories like honeycomb, spalling and split (concrete) and also superficial and pitting loss of reinforcement. Fig. 3-12 presents a common situation during the bridge service life. At the same place the following defects occurred: loss of concrete, loss of reinforcement, deterioration of concrete and even superficial organic contamination of concrete.



Fig. 3-12 Example of loss of concrete and protection (photograph courtesy of Jerzy Czastkiewicz, PKP)

The developed defect classification allows a precise identification. In Fig. 3-13 another example of loss of concrete with symptoms of reinforcement corrosion is presented.



Fig. 3-13 Example of loss of concrete (photographed by the Author)

3.4 Hierarchical system of defect classification

The four-level hierarchical classification of defects of RC railway slab spans is presented in Table 3-5. This system can be applied for each geometrical model. Its multilevel structure allows adjusting defect identification precision to structure modelling accuracy requirement. Defects directly influencing the load capacity have been bolded and their cells shaded. Some positions have been considered as indicators of other defects (for instance pH reduction as increased reinforcement corrosion risk or irregular crack pattern – effect of Alkali-Aggregate Reaction resulting in concrete strength reduction) and marked (only bolded font) as well.

Table 3-5 Hierarchical system of defect classification, continued on the next page

TYPE	KIND	CATEGORY	CLASS
Contamination	Concrete	Inorganic	Aggressive
			Neutral
		Organic	Penetrating
			Superficial
	Protection	Inorganic	Aggressive
			Neutral
		Organic	Penetrating
			Superficial
Reinforcement	Inorganic	Penetrating	
		Superficial	
Deformation	Concrete	Deflection	
		Slip	
		Swell	
	Protection	Deflection	
		Slip	
		Swell	

Table 3-5 Hierarchical system of defect classification, continuation

TYPE	KIND	CATEGORY	CLASS
Deterioration	Concrete	Modification of chemical features	Calcium hydroxide reduction
			pH factor reduction
			Salt concentration increase
		Modification of physical features	Absorbability increase
			Elastic modulus reduction
			Embrittlement increase
			Frost-resistance reduction
			Permeability increase
	Porosity increase		
	Strength reduction		
	Protection	Modification of chemical features	Calcium hydroxide reduction
			pH factor reduction
			Salt concentration increase
		Modification of physical features	Adhesion reduction
Embrittlement increase			
Fading			
Frost-resistance reduction			
Permeability increase			
Porosity increase			
Reinforcement	Modification of physical features	Loss of bond	
		Strength reduction	
Discontinuity	Concrete	Crack	Irregular
			Longitudinal
			Perpendicular
			Skew
	Protection	Delamination	Crack
			Delamination
			Fracture
			Crack
Reinforcement	Fracture	Fracture	
		Fracture	
Displacement	Concrete	Excessive	Rotation
			Translation
		Limited	Rotation
			Translation
Loss of material	Concrete	Honeycomb	
		Pop-out	
		Scaling	
		Spalling	
	Protection		
	Reinforcement	Superficial	Pitting
Pitting			

Concerning contamination they have been excluded from the further investigation as a factor related to the durability. Even corroded (contaminated) reinforcement, with likely its loss of material, cannot be considered, because the material loss has been already taken into account

as another defect type. Also deformation has been excluded as theoretical cases. Displacements are related to the static system changes. Basing on the opinion of bridge inspectors and Author's observations, this defect, as a non-occurring, can be excluded from consideration as well. In case of discontinuity only reinforcement has been considered. In the numerical analysis this defect can be treated as a material loss. Discontinuities of concrete influence the durability of the structure. Occurred cracks increase the degradation rate. On the other hand these defects may indicate the areas of concrete where the risk of reinforcement corrosion is higher. Discontinuities, also with reinforcement corrosion, may cause losses of bond between concrete and steel. All of defects prescribed to the protection cannot be considered, because the protection of concrete is not designed as a construction part, though is integral part of concrete. Table 3-6 presents a relationship between various defect types and the following components of the bridge condition: load capacity, durability and aesthetics.

Table 3-6 Influence of various defect types on bridge condition components

DAMAGE TYPE	LOAD CAPACITY	DURABILITY	AESTHETICS
Contamination	-	□	☒
Deformation	-	-	☒
Deterioration	☒	☒	□
Discontinuity	☒	☒	☒
Displacement	□	-	☒
Loss of material	☒	☒	☒

Notation: □ - limited influence; ☒ - strong influence

The influence of defects on bridge condition components has various intensities. **Load capacity** of the construction can be reduced mainly by deterioration (i.e. strength reduction), discontinuities (cracks in the concrete as a result of the alkali-aggregate reactions and translated to concrete strength) and loss of material. Deformation and displacement can reduce load capacity, but for the considered span constructions these defect type have only theoretical meaning confirmed by the bridge inspectors. In case of **durability**, bridge condition component depends mainly on the appearance of deterioration, discontinuity and loss of material. The influence of the contamination has the secondary meaning. The **aesthetics** changes usually indicate occurred defects like contamination, deformation, discontinuity, displacement and loss of material. Sometimes the deterioration occurs as a visible defect.

Chapter 4

Testing methods

The objective of testing programme is to obtain information on the structure's condition which is needed to take remedial steps.

4.1 Test locations

To obtain required information on the material properties various, tests should be performed. Their location is essential. For example the concrete situated closer to the top of a pour is weaker than the concrete close to the bottom. According to the report of Concrete Society (2000) the difference may be of the order 25%. This is due to the effects of bleed and settlement resulting in a higher water/cement ratio in the upper part of a pour. In thick sections there may be a difference in strengths and other properties close to and remote from the surface due to the different temperature rise during the early period of hydration. Regarding elements subjected to bending, the concrete in the top layers may be subjected to greater compression. Even if the lower layers have higher strength their value will be not reached before the top layer reaches its maximal capacity. For this reason the concrete strength distribution can be neglected if the strength of the top layer is considered.

The condition appraisal if the concrete bridge requires identification of structural defects and ongoing potential degradation mechanisms as well. In literature there are various techniques of testing for defects identification applicable in concrete bridge structures. These methods can be divided into the four groups presented in Fig. 4-1.

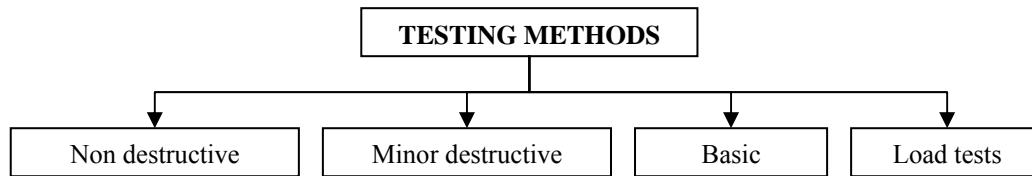


Fig. 4-1 Basic types of testing methods applicable in concrete bridge structures

In the following sections a brief description of the available testing method will be presented. In Table 4-2 a relationship between defect types and available testing methods can be found.

4.2 Non-destructive testing

Numerous non-destructive testing (NDT) methods allow assessing the current bridge condition, i.e. obtaining indirect measurements of the integrity of concrete and the state of reinforcement, without destroying the structure. These techniques allow detecting and identifying the most of common defects like: deterioration, discontinuity, loss of material, deformation and displacement. In this section a brief description of possibilities of defect identification is presented. According to report of Concrete Society (2000) it is important to recognise that the results of such measurements are dependent on several factors, and calibration with the concrete under investigation is recommended. Where more than one technique is available for evaluating a property or performance characteristic, techniques can be used in combination to reduce uncertainty.

4.2.1 Mechanical vibrations

4.2.1.1 Acoustic emission

This method refers to the transient elastic waves generation during the energy release from localized sources within a structure during its loading. The source of these emissions is closely associated with the plastic deformation and the initiation and extension of cracks in a structure under stress. As a structure is loaded, its particular points may be strained beyond their elastic limit and crushing or microcracking may occur. During loading the emission rate and signal level increase slowly and consistently until failure approaches (80-90% of ultimate) and then there is a rapid increase (Appraisal of existing structures 1996). Concrete may recover some aspects of its pre-cracked internal structure, and reloading over a particular stress range may again generate emissions (British Standard 1986). This technique is based on the detection and conversion of these high frequency elastic waves to electrical signals. The emission is generally not in the audible range and may be monitored by transducers connected to recording equipment (British Standard 1986).



Fig. 4-2 Acoustic emission transducer

An example of acoustic emission (AE) equipment is presented in Fig. 4-2. The main advantage of this method is the possibility of crack detection (FIB 2003). It may also be used to identify the location of crack initiation and propagation by means of multiple detectors (British Standard 1986). Location within a 3D zone of concrete is possible with a 3D array of sensors, while simple arrays provide a zonal, linear or planar location, achieved by measuring the time arrival of emissions at different sensors. AE monitoring increases the sensitivity and safety of load testing since emission commences at the early onset of damage. A proprietary technique has recently been developed for detecting early stages of rebar corrosion (Highways Agency 2006).

4.2.1.2 Impact-echo

This is a method for the evaluation of concrete structures, based on the use of impact-generated stress waves that propagate through a structure and are reflected by internal flaws and external surfaces. Surface displacements caused by the arrival of reflected waves at the impact surface are recorded by a transducer. These are processed to display their amplitude and frequency, and may be saved for post-processing (Highways Agency 2006). The typical equipment is presented in Fig. 4-3 and consists of hand-held transducers (a), a set of spherical impactors (b) and data acquisition and analysis system (c).

This method allows detecting cracks and measuring their depths (Nowak 1990, Ryall 2001) which has a special meaning in terms of the reinforcement corrosion risk. Other discontinuities such as delaminations in concrete around reinforcing bars (Nowak 1990, Ryall 2001, Moczko 2004) and between concrete and other surfacing material (Nowak 1990) can be detected by this method as well. Voids that present a large target size may also be detected. The accuracy of void detection may be expressed in terms of the minimum lateral target size

of voids that may be detected. The quality of results varies according to the impactor diameter, which influences the input frequency – a smaller impactor gives a higher input frequency, higher resolution, but shallower depth penetration. Water filled voids are not detected (Highways Agency 2006).



Fig. 4-3 Impact-Echo Test System provided by James Instruments Inc.

The Impact-Echo method can be applied in the geometrical parameter measurement. The main application of this technique takes place in the thickness measurement of any concrete elements available from one side only (Moczko 2004, Highways Agency 2006). The thickness of concrete slabs may be obtained to an accuracy of 3% (Highways Agency 2006). By means of this method it is possible to detect the presence and depth to reinforcement (Highways Agency 2006).

Despite of presented advantages this technique is not perfect. According to the report of Highways Agency (2006) this testing method requires prior information on construction details (i.e. radar survey, drawings etc.) to facilitate interpretation of results. Congested reinforcement is likely to make measurements unreliable. In most situations, cracks are visible on the surface and can be measured with greater certainty by simple methods.

4.2.1.3 Ultrasonic pulse velocity

Ultrasonic pulse velocity (UPV) methods are used to gain information about a material or structure by injecting a pulse and recording the response. This technique measures the transmit time of sound waves passing from an emitter transducer through the concrete to a receiver transducer placed on the surface of a body of concrete. Ultrasonic pulses can be

received on opposite, adjacent or the same face by receivers. The pulse velocity can be calculated if the length of the path taken by the pulse is known.

The velocity of ultrasonic pulses travelling in a solid medium depends upon the density, dynamic Poisson's ratio and elastic properties of the medium. These pulses round voids. The transmission of such pulses can provide information on the integrity of RC structures.

The typical UPV equipment, presented in Fig. 4-4, includes two transducers (a) – emitter and the receiver. Both are connected to a control box (b). The display (c) indicates the transit time of the ultrasonic pulse between the transmitting and receiving transducers.

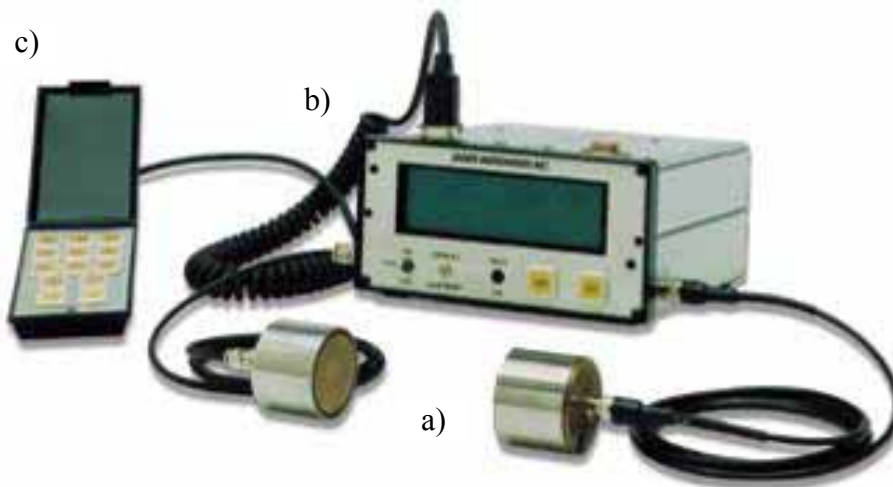


Fig. 4-4 V-Meter Mark II of Qualitest company

This method allows detecting cracks (Ryall 2001, Wibreg 1995, Highways Agency 2006), delaminations in concrete (Wibreg 1995), strength of concrete (Bridge Inspection Manual 1996), frost splitting due to water in voids (Bridge Inspection Manual 1996) and also extent of deterioration and concrete uniformity (British Standard 1986, Wibreg 1995). This technique allows also estimating the depth of fire or chemical attack (British Standard 1986). By means of the extracted cores direct measurements of UPV across the diameter at intervals along the axis of the specimen can be used to detect variations with depth and also to calibrate the instrument and provide an estimate of in situ strength (Appraisal of existing structures 1996, Concrete Society 2000). Another advantage of this technique is that it allows investigating the structure by tomography which can build up a 3D image of the internal structure. This technique may be appropriate for detailed investigation of an area of known defects (Highways Agency 2006). The slope of a plot of the transducer spacing vs. time gives the ultrasonic pulse velocity through the cover zone and can give some indication of the following, as shown in Fig. 4-5 according to Concrete Society (2000).

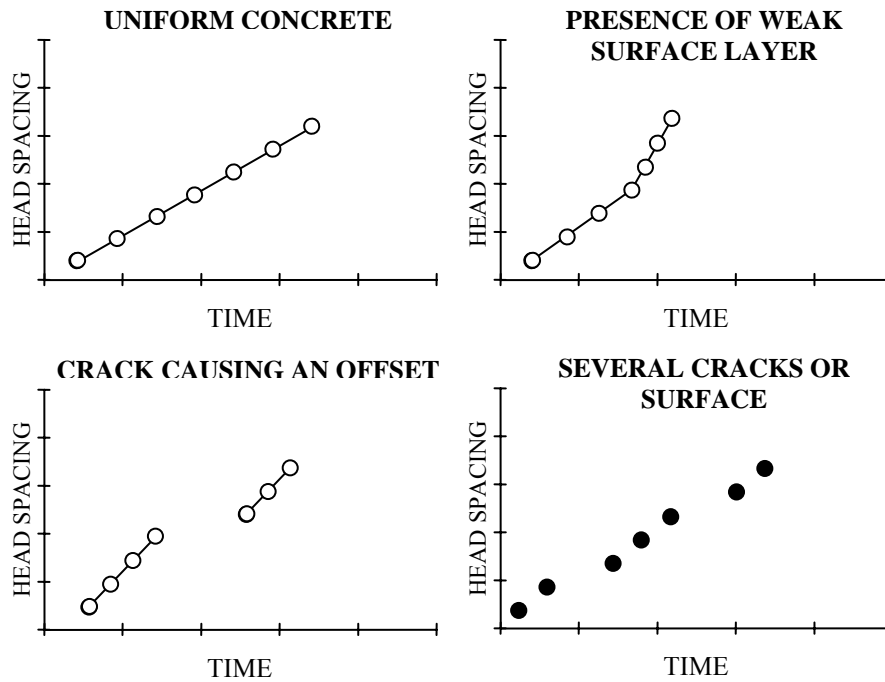


Fig. 4-5 Interpretation of indirect UPV measurement (Concrete Society 2000)

This method has some disadvantages:

- Additional information obtained from other methods, such as radar or impact-echo, are required to plan investigation and interpret results (Highways Agency 2006);
- Measured values may be affected by surface texture, moisture content, temperature, stress, congested reinforcement and also specimen size (British Standard 1986, Appraisal of existing structures 1996, Highways Agency 2006);
- Material properties such as type of cement, type and size of aggregate and age of concrete influence the results as well (Concrete Society 2000);
- It is suitable for use only by experienced users (Appraisal of existing structures 1996, Highways Agency 2006).

4.2.2 Electromagnetic and optical methods

4.2.2.1 Covermeter

This device is able to locate reinforcement in terms of its depth, distribution and direction within concrete (British Standard 1986, Appraisal of existing structures 1996, Concrete Society 2000, Diggist 2000, King & Dakin 2001, Highways Agency 2006). Though in some cases covermeters may indicate both bar size and location, generally in order to accurately measure cover, it is necessary to know the bar diameter and vice versa (British Standard 1986, Diggist 2000, King & Dakin 2001). Bars of different diameter give a different response and if reliable drawings are not available, the concrete at selected location should be broken out to

expose the reinforcement so that the actual bar size can be measured (Concrete Society 2000) or can be measured by means of the radiography. This technique is based upon measurement of the change of an electromagnetic field caused by steel embedded in the concrete. To check reinforcement locations, the search head (Fig. 4-6, a) is moved slowly across the surface of the concrete generating an electromagnetic field. This field becomes distorted when passed over a metal object and produces a local change in the field strength.



Fig. 4-6 Cover-meter produced by Elcometer Inspection Equipment

The readout is observed until a minimum is reached and the position of the head is noted. The information is processed to give details (to be displayed Fig. 4-6, b) of the concrete cover. The signal received will increase with increasing bar size and decrease with increasing bar distance (cover). Covermeter surveys need to be correlated with other information from the investigation, including defect mapping, carbonation depths and chloride profiles (Diggist 2000). More information about this technique principles can be found in British Standard (1986), Perkins (1997), Concrete Society (2000) and King & Dakin (2001).

This technique may be used to find reinforcement location as a preliminary to other testing methods in which reinforcement should be avoided, e.g. coring, UPV or near to surface methods. This measurement is essential before any structure is drilled (British Standard 1986, Highways Agency 2006). A site accuracy of estimated cover of ± 5 mm within the working range of the instrument may be expected (British Standard 1986). Most modern equipment has digital readout and some systems have an audible output applied as the search head approaches the position of a reinforcing bar (Concrete Society 2000). Some covermeters are capable of recording data for post-survey download and they can also incorporate software that allows for data logging and reinforcement imaging (Diggist 2000, King & Dakin 2001).

The covermeter is easy to operate but has several disadvantages. In heavily reinforced structures or members with cover thicker than 60mm it may not be possible to obtain reliable results (British Standard 1986, Appraisal of existing structures 1996, Concrete Society 2000). The user must be aware that if there are two or more bars within detection range then the

instrument will receive a greater signal and inevitably indicate a cover that is shallower than the true cover (King & Dakin 2001). Deep reinforcement can be only detected by frequent measurement within drilled holes if damage is to be avoided (Highways Agency 2006). The effect of bar size is important if this is less than 10 mm or greater than 32 mm (British Standard 1986). The results of investigation with covermeter can be affected by particles of magnetite presented in concrete aggregate (British Standard 1986, Appraisal of existing structures 1996, Diggest 2000). The performance of the equipment may be influenced by temperature variations (British Standard 1986, Appraisal of existing structures 1996) especially by the negative temperatures (Diggest 2000). The standard electro-magnetic covermeter does not identify non-magnetic reinforcement, such as stainless steel, but appropriate equipment is being developed (Concrete Society 2000).

4.2.2.2 Impulse Radar

This method uses electromagnetic wave propagation. Transmitting and receiving antennae combined in a single head are passed over the investigated surface at a controlled speed in a series of traverses. The transmitter emits a continuous series of high-frequency electromagnetic pulses of radio energy and the receiver detects reflections from material boundaries and features with different electrical properties such as reinforcement or defects. The reflected energy is recorded as a pattern on paper, on a television monitor or as a digital signal.



Fig. 4-7 Equipment of Ground Penetrating Radar technology

The travel time of radio pulses depends on the layer thickness or depth to embedded features. Also velocity of wave propagation can be affected by variations in moisture and salinity.

The typical equipment consists of radar antenna (transmitter and receiver combined in a single head) and control unit (Fig. 4-7). More information on this technique can be found in (Concrete Society 2000, King & Dakin 2001, Highways Agency 2006, Mathews 1998, British Standard 1986, Diggest 2000, Appraisal of existing structures 1996). This technique can be applied to obtain some information related to geometry as well as defects occurred. Regarding the geometry parameters Impulse Radar can be used to estimate element thickness (British Standard 1986, Appraisal of existing structures 1996, Mathews 1998, Concrete Society 2000, King & Dakin 2001).

This measurement, however well suited, requires velocity and “time-zero” calibration to achieve absolute indications of thickness (Mathews 1998). Also location and reinforcement cover orientation and spacing can be investigated by means of this method (British Standard 1986, Appraisal of existing structures 1996, Mathews 1998, Concrete Society 2000, King & Dakin 2001, Highways Agency 2006). In case of cover depth estimation ‘time-zero’ calibration is necessary (Mathews 1998).

Regarding defects mainly discontinuities are available such as delamination and cracks as well as voids in concrete (Concrete Society 2000, King & Dakin 2001, Highways Agency 2006, Mathews 1998, British Standard 1986, Diggest 2000, Appraisal of existing structures 1996). The presence of moisture in cracks and delaminations as well as shallow voids makes its detection easier. Air-filled voids may need to be at least 20 mm deep to be detectable. Delaminated thin layer may be identified, but it is generally not possible to measure their thickness (Mathews 1998).

By means of this technique some symptoms of degradation mechanisms can be identified. Impulse Radar has been applied to identify zone of moisture penetration, reinforcement corrosion and chloride contamination (Mathews 1998, King & Dakin 2001).

The method requires contact with the concrete surface and allows large areas to be surveyed relatively quickly (Appraisal of existing structures 1996, King & Dakin 2001) especially on an extensive structure with very restricted access (Highways Agency 2006). In favourable circumstances, radar can also provide some broad indications on a number of other parameters (information on density, delamination or the presence of chlorides and moisture) (Diggest 2000). The technique can be very powerful and works best in simple planar construction e.g. slabs (Appraisal of existing structures 1996).

The equipment (for which training and specialist software required) is expensive and interpretation of the data collected must be undertaken by a skilled specialist since many

factors contribute to the results. Processing off site is recommended with consequent delay to results (Appraisal of existing structures 1996, Perkins 1997, Concrete Society 2000, King & Dakin 2001, Highways Agency 2006).

Congested reinforcement makes the analysis more difficult. Though some attempts have been made to develop techniques to identify second layers of rebars, these have not been applied except on local areas. Radar is unlikely to be able to resolve more than two layers of rebars. Closely spaced bars (less than 10 cm) reduce signal penetration and individual bars are unlikely to be detected. Problems may be encountered with square twisted bars because of their scattering characteristics (Highways Agency 2006, Mathews 1998).

4.2.2.3 Laser Distance Meter

This device has not been developed to identify defects. It can be used to identify the structure in terms of its geometry, i.e. span width, length etc. The information obtained by this device can be taken into consideration during load capacity assessment.



Fig. 4-8 Laser Distance Meters developed by Loyola Enterprises

In Fig. 4-8 the hand-held laser meters provided by Loyola Enterprises for distance measurements of length, squares and volumes are presented. Shortcut keys for addition, subtraction, area and volume calculation make measuring fast and very reliable. Due to its small and ergonomic size this device fits into every pocket. In order to take measurement the user needs to point the laser beam at the target, press the DIST-key and read the measured value, even in the dark. The presented meters are characterized by parameters depending on the particular models. Their typical measuring accuracy varies between 1.5 and 2.0 mm and the range of measurement is from 0.05 to 200 m.

4.2.2.4 Radiography

This technique is common in medicine but also for example in weld inspection. Radiography enables a photograph to be taken showing details of the inside of a concrete member. It is

used to determine the location and size of reinforcement, to check for the existence of voids and area of poor compaction in concrete where other NDT methods are not suitable. The system, presented in Fig. 4-9, is composed of a radiation source, the concrete element being examined and the image collector. Two types of radiation can be used: gamma rays (applicable for member thicknesses of up to 500 mm) and high energy X-rays (appropriate for thicker elements up to 1600 mm). Imaging of voids and embedded metal are produced on a suitable film placed behind the concrete member, whilst the beam of rays (gamma or X) is directed at the front face of concrete element. The presence of high or low density areas (caused by reinforcement or voids respectively) produces respectively light and dark areas on the film. The image can be produced in real-time on a screen. More information can be found in references (British Standard 1986, Perkins 1997, Concrete Society 2000, King & Dakin 2001, FIB 2003, Highways Agency 2006).

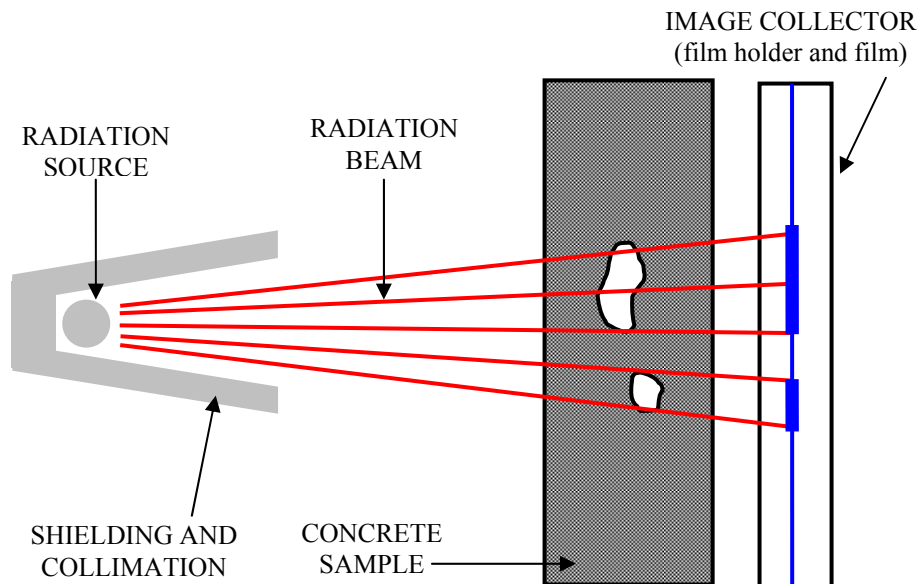


Fig. 4-9 Layout of typical radiography system for concrete (Concrete Society 2000)

Radiography is a NDT method applicable for locating reinforcement especially beyond the range of covermeters (British Standard 1986, Concrete Society 2000, King & Dakin 2001). This technique can be also used for corrosion identification (Highways Agency 2006). Loss of material can be seen on the sides of reinforcing bars, or an approximation of the loss of section on top or bottom of the bars can be obtained from the different shading of the image (Highways Agency 2006). The location and sizing of reinforcing bars may be determined by photogrammetric analysis of the radiograph (British Standard 1986). This method can be used locating areas of voids in concrete (British Standard 1986, Concrete Society 2000, Highways Agency 2006). Radiography may be used whilst a bridge remains open to traffic (Highways Agency 2006).

Due to Health & Safety issue in using gamma rays and high-energy X rays, the use of this method is confined to investigations which justify the cost of the special precautions which have to be taken (British Standard 1986, Perkins 1997, Concrete Society 2000, FIB 2003, Highways Agency 2006). This type of work is only performed by radiographers with experience (British Standard 1986, Concrete Society 2000, King & Dakin 2001).

4.2.2.5 Thermography

This method is based on heat transfer properties of material. Basically, anomalies in concrete (i.e. voids, discontinuities, porosity etc.) conductor heat less than good quality concrete. Variability of heat transfer cause small localised differences in surface temperature. By means of the infra-red devices (i.e. scanner, camera, temperature measuring gun, thermal imager etc.) images of temperature differentials can be obtained for analysis. In Fig. 4-10 an example of the thermal camera provided by Ashtead Technology is presented.



Fig. 4-10 Thermal Camera, model Flir 695 provided by Ashtead Technology

This camera offers both thermal and visual imaging. By means of a drop-down list of common materials to be inspected this device can be adjusted to particular needs of the user. The technique gives a 2D assessment of areas of defect. Thermographic investigation uses often natural source of heat such as the sun. The survey may be carried out during a day, when defective areas tend to have a warmer surface as the velocity of heat transition is slower. At night the heat, stored during a day, flows from the structure to the colder environment (i.e. air) which allows performing the investigation also at night. In this case defective areas are cooler as less heat is conducted from the concrete. More information can be found in (British

Standard 1986, Appraisal of existing structures 1996, Concrete Society 2000, Highways Agency 2006).

This method can be applied for the following tasks:

- Delaminations in concrete (British Standard 1986, Bridge Inspection Manual 1996, Nowak 1990) and around reinforcing bars and other surfacing material (Ryall 2001);
- Debonding (Helmerich & Niederleithinger 2005);
- Loss of material like cavities and hollows (British Standard 1986, Appraisal of existing structures 1996, Bridge Inspection Manual 1996, Helmerich & Niederleithinger 2005, Highways Agency 2006);
- Frost splitting due to water in voids (Ryall 2001);
- Thickness measurement of thin layers (Helmerich & Niederleithinger 2005),
- Distribution of humidity (British Standard 1986, Appraisal of existing structures 1996, Helmerich & Niederleithinger 2005);
- Depth and size of inhomogeneities (Helmerich & Niederleithinger 2005);
- Access to the only one surface exposed required (British Standard 1986);
- No needs of the safety precautions as for radiography (British Standard 1986).

This method is sensitive to differences in surface roughness. Rough surfaces have a higher emissivity than smooth areas (Concrete Society 2000) which affects readings. Precautions have to be taken to avoid interference from extraneous heat sources (British Standard 1986).

4.2.3 Electrical methods

4.2.3.1 Electrical potential

This method is based on the measurement of the electrical potential of the reinforcement relative to a reference half-cell placed on the concrete surface. The result can be interpreted as the likelihood of corrosion activity. The results are plotted on potential contour maps enabling localized zones of corrosion risk to be identified. Usually the greatest corrosion risk is associated with areas in which the potential gradient is steep. The typical equipment (see Fig. 4-11) consists of a half-cell reference electrode (a) and a high-impedance voltmeter (b). The half-cell is a tube with a porous end with a metal rod in a saturated solution of its own salts e.g. copper in copper sulphate or silver in silver chloride.

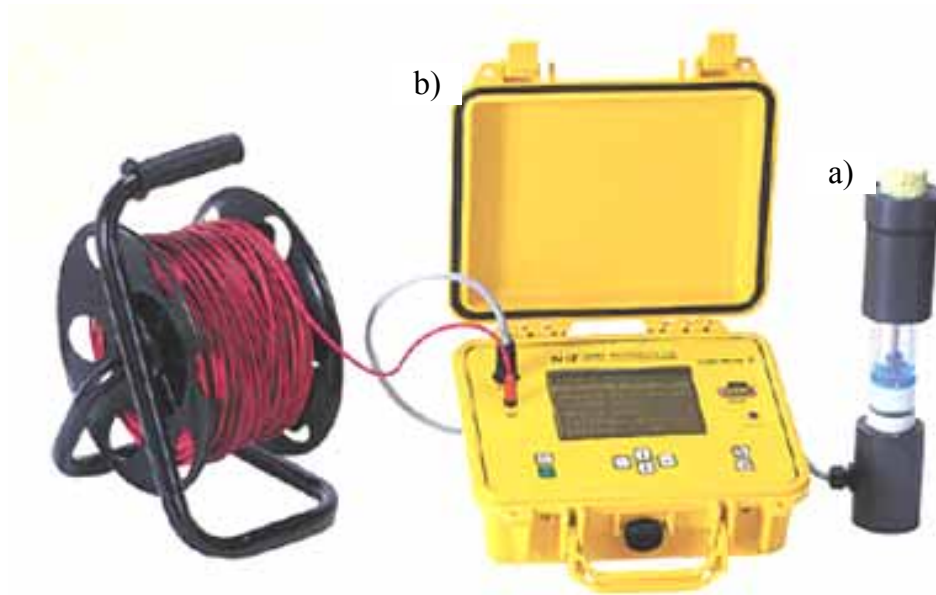


Fig. 4-11 System for corrosion potential analysis of probable corrosion produced by the James Instruments Inc.

By means of terminals the voltmeter is connected to the reinforcement and to the half-cell reference electrode. The concrete functions as an electrolyte. Electrical contact with reinforcement requires drilling a small hole and surface to be sprayed by water. This technique can give the following readings:

- For potentials less negative than -200mV the probability of corrosion is less than 0.1;
- For readings between -200mV and -350mV , the probability of corrosion is about 0.5;
- For readings numerically greater than -350mV , the probability of corrosion is greater than 0.5.

More information on this technique can be found in (British Standard 1986, Appraisal of existing structures 1996, Bridge Inspection Manual 1996, Perkins 1997, Ściślewski 1999, Concrete Society 2000, Diggest 2000 and Ryall 2001).

This technique requires interpretation of the results to be done by an experienced operator who is aware of various limitations. For example, in case of significant carbonation results can be shifted in a $+200\text{ mV}$ (Concrete Society 2000).

This method is sensitive to weather conditions which may significantly influence the measurements (Appraisal of existing structures 1996). Protective or decorative coatings applied to the concrete may affect the results as well (British Standard 1986). High negative readings may be indicative of oxygen starvation with little reinforcing bar corrosion, particularly if the concrete is saturated. If the concrete is very dry the potential may be less negative (Concrete Society 2000).

4.2.3.2 Resistivity of concrete cover

The principle of the method is based on measurements of the ability of electrical corrosion currents to flow through concrete. This technique is used to investigate areas of greatest corrosion risk identified by means of the electrical potential mapping described before. The measurement can be performed by means of either 2-probe or 4-probe (Wenner) methods. In case of the Wenner method metal electrodes are inserted in a straight line on or below the concrete surface at equal spacings (Fig. 4-12). A current is passed through the outer electrodes while the voltage difference between the inner electrodes is measured.

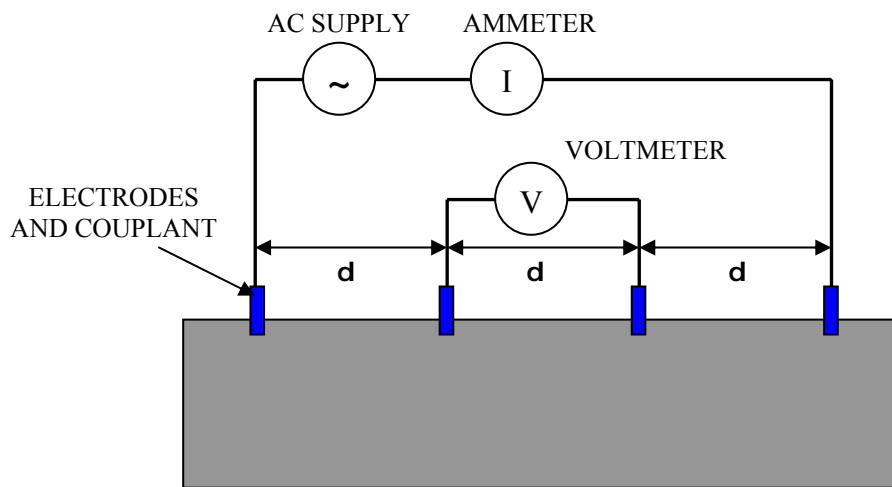


Fig. 4-12 Typical layout of resistivity test array (Concrete Society 2000)

The measurements obtained give an indication of the risk of corrosion (see Table 4-1).

Table 4-1 Relationship between resistivity and corrosion rate according to (Concrete Society 2000)

Resistivity (kΩcm)	Likely corrosion rate
< 3	Very high
5 – 10	High
10 – 20	Low
> 20	Negligible

More information on this method can be found in (British Standard 1986, Appraisal of existing structures 1996, Concrete Society 2000, Diggist 2000).

Obtained results can be affected by moisture, salt content and temperature as well as reinforcement located close to the surface and poor coupling between the probes and the concrete surface (British Standard 1986, Concrete Society 2000).

4.2.3.3 Potential and resistance mapping merged method

This method, based on the electrical potential and concrete resistivity measurement applied by Łakomy (2004), allows identifying areas of internal defects caused by reinforcement corrosion. Distribution of electrical potential with its gradients is the basic criterion of corrosion risk assessment. The electrical resistivity distribution in concrete cover is considered as a comparative criterion.

According to Łakomy (2004) it is possible to distinguish three characteristic area types:

- Type 1 – area where both parameters (electrical potential and resistivity) represent low values, which means 0.95 appearance of corrosion. Additional testing (carbonization, chlorides, cover measurement etc.) can explain the causes of the corrosion;
- Type 2 – area of high considered parameters – 0.90 probability that corrosion is not taking place. Additional testing can be applied as a controlling measurements;
- Type 3 – area of low value of the basic parameter (electrical potential). In this case the 50% probability of corrosion should be considered to be 0.50. The results of the additional testing may eliminate these areas from the further condition appraisal.

4.2.3.4 Galvanostatic pulse

A short, 50 μA current pulse is applied to the reinforcement from a counter electrode placed on the concrete surface together with a reference electrode.



Fig. 4-13 Galva Pulse instrument manufactured by Germann Instruments

This current causes change of the reinforcement potential which is monitored by the counter electrode. The result can be plotted as contour maps showing polarization resistance gradients

(Concrete Society 2000). Though this method is a rapid non-destructive polarization technique suitable for evaluation of reinforcement corrosion, its complexity and available equipment makes this method useful mainly in laboratory (Łakomy 2004).

4.3 Minor destructive methods

Minor-destructive testing (MDT) methods involve some degree of damage to structure assessed. These methods can identify the following defects: deterioration, discontinuity and loss of material. A brief description of these methods is presented in this section.

4.3.1 Samples

4.3.1.1 Coring

These methods extract concrete specimens in order to measure depth of carbonation and pH factor of carbonated concrete combining chemical procedures (Ryall 2001). Extracted concrete specimens can be subjected to various tests such evaluation of concrete strength (Bridge Inspection Manual 1996, Ryall 2001), of frost resistance (Ryall 2001), permeability (Ryall 2001) or chemical analyses such as chloride and sulphate contents (Ściślewski 1999).



Fig. 4-14 Hand held coring machine, model MK Diamond MK-2000P, provided by ToolFetch company

Visual inspection of extracted concrete probes can identify internal loss of material such as voids and cracks. As cores are usually drilled to a depth of at least 100mm they are likely to pass through reinforcement. Though coring allows accurate measurement of cover, type and size of reinforcement there is risk of damaging the reinforcement. Remedial actions to repair defects make this technique expensive (Appraisal of existing structures 1996). An example of hand held coring machine is presented in Fig. 4-14. Cores are extremely useful as they provide a means of determining the strength of the in situ concrete. They can be used for

visual and petrographic analysis and can be sectioned or drilled to provide samples for chemical analysis. Samples from cores can be used to determine of chloride content.

4.3.1.2 Dust samples

Dust samples are frequently obtained from structures using a hand-held rotary percussive drill with a bit with a diameter of 10, 12 or 20 mm. It may be necessary to drill a close pattern of holes to obtain sufficient material for analysis. The drill dust can be recovered using a plastic shroud around the bit or an angled plastic tube with a sample bag on the end. Dust samples are dissolved in acid at the laboratory and can be tested for chloride, sulphate or cement content by chemical means or iron-specific electrodes.

4.3.1.3 Lump samples

Lump samples can be easily obtained from corners or edges using a hammer and chisel. They have the advantage that they can be obtained without special equipment but the range of tests for which they can be used is limited. Lump samples can be used for visual and petrographic examination, chemical testing and, if they are large enough, for drilling to obtain dust samples. They are rarely big enough to permit sub-samples to be taken for strength determination except possibly by point load testing techniques. However, the samples may have been cracked during sampling and so the strengths would probably be unrepresentative.

4.3.1.4 Reinforcement samples

The presented NDT methods in Section 4.2 allow engineers to analyse the reinforcement in terms of its geometry (cover, diameter, location etc.) and some defects such as loss of material, discontinuities, etc. The complex assessment of load capacity requires also strength parameters to be provided to the analysis. It is particularly important when the documentation of the analysed bridge does not exist. Unfortunately no NDT method is available to evaluate reinforcement strength. The extracting of steel samples from existing structure remains the only solution to determine reinforcement strength. The decision about reinforcement extracting (causing usually reduction of load capacity) cannot be taken rashly. Development of laboratory techniques allows for analysis of the chemical composition of extracted steel (swarf) and identifying its grade. It should be noted that identification of the chemical composition of steel is not sufficient to evaluate its strength (Wójtowicz 2004).

4.3.2 Near-surface strength tests

Various near-to-surface test methods can be used to assess the concrete strength in situ. For all these tests, there is no unique relationship between the measured parameter and strength.

Information suggesting any such relationship that might be provided with the equipment should be treated with caution as its use could lead to errors in assessment of compressive strength. In this section some of them are presented.

4.3.2.1 Pull-off

This approach has been developed to measure in-situ tensile strength of concrete by applying a direct tensile force (Concrete Society 2000, Ryall 2001, Moczko 2004). A circular steel disc is glued to the concrete surface. The force required to pull this disc is measured. Dampness can affect the bond achieved. Results are relevant only if the tensile failure is through the concrete, not the adhesive. Results may be correlated to strength properties measured on standard specimens (British Standard 1986). In Fig. 4-15 an example of the typical equipment is presented. If necessary the partial coring may be used in order to eliminate surface skin effects (British Standard 1986). This permits the strength to be measured at a greater depth. The choice of the test location can be based on the results of the visual inspections or by the results of the concrete surface hardness test.



Fig. 4-15 Pull-off tester produced by Proceq CN Ltd

The results of the hammer sounding may indicate area in which spalling occurs. In these areas pull-off tests have no use at all (FIB 2003).

4.3.2.2 Pull-out

This method allows the compressive strength of concrete to be measured (British Standard 1986, Concrete Society 2000, Moczko 2004) and only one exposed surface is required. A 6 mm diameter expanding wedge anchor bolt with a wedge anchor (see the typical equipment in Fig. 4-16) is inserted into a drilled hole. The bolt is loaded in tension by means of a reaction stand which includes torquemeter acting on a greased nut.



Fig. 4-16 Pull-out equipment

The force required to pull out the bolt causing a conical fracture is measured. This force is then correlated with the compressive strength of concrete (FIB 2003).

4.3.3 Phenolphthalein and Rainbow-Test

Carbonation effects can be assessed by means of a solution of **phenolphthalein** indicator in ethyl alcohol. This test is most commonly used which turns a purple-red colour on uncarbonated surfaces (pH above 10) and appears colourless in contact with concrete which has lower pH, i.e. which has carbonated.

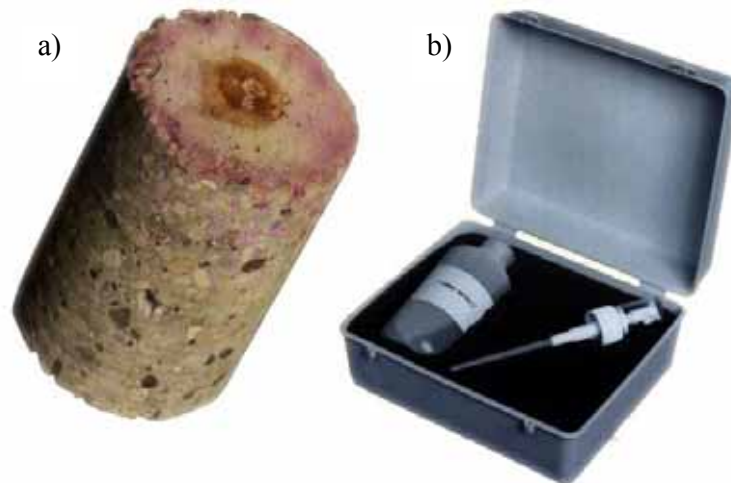


Fig. 4-17 Concrete sample (a) and equipment of the phenolphthalein test – Carbo Detect (b) provided by James Instruments Inc.

By means of extracted concrete specimens the carbonation depth can be measured (Perkins 1997). In Fig. 4-17 an example of drilled concrete sample and equipment for phenolphthalein test, provided by James Instruments Inc., is presented. A purple-red colour indicates higher value of pH factor. Alternatively, the powder from drill holes can be sprayed or allowed to

fall on indicator-impregnated paper (Appraisal of existing structures 1996, Concrete Society 2000). If the colour change to pink does not occur rapidly, it means that the identification of carbonated layer is not clear and it is then necessary to confirm these indications by petrography (Diggest 2000). The change in pH occurs only a few millimetres ahead of the line indicated by the test. This method provides a good indication of the location of depassivation front (Concrete Society 2000). However, the sensitivity of this method for only selected pH values is its disadvantage. It does not allow determining pH distribution (Moczko 2004).

To face this problem another method, called **Rainbow-Test**, can be applied. This technique offers determining the pH distribution on the basis of colour distribution of the analysed concrete surface previously sprayed by the special chemical substance.



Fig. 4-18 Rainbow Test – colours of sprayed concrete against its pH value (German Instruments 2003)

The value pH=11 refers to the purple colour. The transition from purple colour to green corresponds to pH=9 and signifies the corrosion risk (Moczko 2004). In Fig. 4-18 a colour-scale against the pH values of analysed concrete sample is presented (German Instruments 2003).

4.3.4 Chloride Test

This technique allows measuring of chloride content in concrete both in situ and in laboratory. The size of the equipment is such that it can be carried in an attaché case (see an example in Fig. 4-19). A sample of powder is drilled out and dissolved in an acid solution, after which measurement and evaluation can be carried out directly (Bridge Inspection Manual 1996). An electrochemical reaction of the chloride ions with the prepared acid solution takes place. A special device converts the voltage generated by the chloride concentration and shows the chloride concentration on a LCD display. Test results, after the sample has been obtained, can be determined and read in a few minutes. This test can be performed by staff without specialist experience and for most practical purposes its results are generally of sufficient accuracy to evaluate the chloride content (Appraisal of existing structures 1996). In case of structures exposed to chlorides and it is necessary to establish chloride penetration profiles at selected locations on a structure (Diggest 2000).



Fig. 4-19 The CL 2000 Chloride Test System produced by NDT James Instruments Inc.

Chloride contents should be measured at some small increments about 1 cm to establish its profile. In case of the absence of reliable results 0.4% weight of chloride to weight of cement may be considered as a chloride threshold below which the corrosion risk of reinforcement is low.

4.4 Basic methods

4.4.1 Direct measurement

This testing is based on the simplest measurement of structure without advanced technology and can be used for defect identification as well as structural geometry. In Fig. 4-20 an example of a magnifying glass is presented.



Fig. 4-20 Magnifying Glass by e-Tay Industrial Co., Ltd

The measurement is qualitative rather than quantitative and may indicate whether a defect (for example crack, symptom of reinforcement corrosion – loss of material, etc.) has occurred or not. This tool is especially useful in crack identification.

To complete this testing a crack width ruler can be applied (see an example in Fig. 4-21).



Fig. 4-21 Crack width ruler produced by Elcometer

Bigger defects can be measured by a specialty steel tape. Lengths can reach 10.0 meters. Its stiffness allows the user to handle in one hand and take a measurement in the vertical direction. In Fig. 4-22 an example of this tool is presented.



Fig. 4-22 Specialty steel tape provided by The Perfect Measuring Tape Co

Defects need to be located in terms of the global structure geometry. Basic geometry parameters such as span length, width etc. should be determined as well. To do this a measuring tape can be applied (Fig. 4-23). Various producers provide tapes of various lengths.



Fig. 4-23 Measuring tape provided by The Perfect Measuring Tape Co

4.4.2 Rebound (Schmidt) hammer

This test is based on the principle that the rebound of elastic mass depends upon the hardness of the surface which it strikes, which is an indication of concrete strength. The results may be

correlated (i.e. by calibrating against core tests) with its other properties such as compressive strength (Perkins 1997, Ryall 2001).



Fig. 4-24 Rebound Hammer, Manual Model W-M-350 produced by Qualitest company

This test is easy to carry out. Light abrasion of the surface is required over an area about 60mm in diameter at each test location. In Fig. 4-24 an example of rebound hammer is presented. This device is composed of a mass which slides on a plunger housed within a metal cylinder. At the start, the plunger is fully extended and the mass is attached to the end of the plunger remote from the concrete surface inside the cylinder housing. The end of the plunger is placed against the concrete surface and the housing is moved towards the concrete. This causes the plunger to retract into the housing and extend a spring connected to the mass and the housing.

When the plunger is almost fully retracted, the self-release catch is activated and the mass, under the action of the force from the spring, accelerated along the plunger in the direction of the concrete surface. The mass strikes an enlarged section of the plunger and rebounds. The rebound distance is measured on a sliding scale. More information can be found in the report of Concrete Society (2000).

This technique is subject to some inaccuracies. The results can be influenced by moisture of the surface, cement type and mix characteristics. Rough surfaces cannot be tested as they do not give reliable results (British Standard 1986, Perkins 1997). The measurements can be affected also by human error, so care must be taken when considering results from different users. The correlation between rebound hammer reading and strength needs to be determined for the actual concrete under investigation. This technique is related only to a depth of up to 30 mm and its results can be influenced by carbonation of the concrete surface causing its localized hardening (British Standard 1986, Appraisal of existing structures 1996) and indirectly resulting in the increasing the concrete strength (Ryall 2001). For this reason carbonation tests are recommended to be performed as well (Ściślewski 1999). The impact is

applied on the surface of small area making the readings susceptible to local variations. To obtain a representative result at least nine readings should be taken in each location (Appraisal of existing structures 1996).

4.4.3 Tapping

This is one of the simplest methods of bridge testing, which allows detecting discontinuity (crack, delamination) or reduction of adhesion of protection (Bridge Inspection Manual 1996). This method allows also detecting internal loss of material such as cavities.

4.5 Visual inspection

Visual inspection, as a preliminary step of bridge assessment, involves gathering of data from existing bridge via regular visual control based on various standards. Results of inspection are saved in the records (bridge book, sheets and digital files as well) for further analysis. This type of bridge examination gives a basis for taking decision on the use of some particular testing methods such as NDT techniques. The information derived from the investigation will enable the residual capacity of a structure or element to be assessed and will enable an appropriate repair strategy to be selected (Concrete Society 2000). In Fig. 4-25 an example of a visual inspection of a railway bridge is presented.



Fig. 4-25 Typical visual inspection performed by bridge inspectors from REFER (photographed by the Author)

Visual inspection plays a significant part of the diagnosis and assessment process. This test may be quickly performed without specialist equipment. Its low cost (although it can escalate depending on site conditions and equipment used) makes this method common (Highways Agency 2006). This method allows cracks detection (Nowak 1990, Bridge Inspection Manual 1996), reinforcement losses as a corrosion effects (Nowak 1990), losses of concrete,

deteriorations, deformations, displacements and contaminations. Visual inspection is the most common method, but it identifies deterioration once it has reached an advance stage. Moreover the concrete interior, including reinforcement and voids, cannot be examined directly.

4.6 Load testing

The load testing of bridges can be of great benefit to engineers in aiding their understanding of the behaviour of bridges at both serviceability and the ultimate limit states under the action of live load (Ryall 2001). Identification of defects by means of the load tests is difficult. From the theoretical point of view all of defects causing modifications of the construction stiffness can be considered. Such modifications influence the results of the static and dynamic load tests. Loss of material must be significant before it modifies the stiffness to appoint where it is measured by test. The results of the study performed by Maeck et al. (2002) indicate that it is possible to localize defect. An example of a load test is presented in Fig. 4-26.



Fig. 4-26 Typical load test of railway RC bridge (photograph courtesy of prof. Jan Bień, WUT)

4.7 Application of testing methods

In Table 4-2 the application range of the testing methods applied for identification of the basic defect types is presented. Four groups of the available testing methods are distinguished: non-destructive, minor-destructive, basic methods and load tests.

Table 4-2 Testing methods to identify defects exerting the influence on load capacity of considered span types

Defects Testing methods	Deterioration						Discont.		Loss of material	
	Concrete				Reinforc.		Concrete	Reinforcement	Concrete	Reinforcement
	Calcium hydroxide red.	pH factor reduction	Salt concentration incr.	Elastic modulus red.	Strength reduction	Loss of bond				
Non destructive testing										
Mechanical vibrations										
Acoustic emission							<input checked="" type="checkbox"/>			<input type="checkbox"/>
Impact-echo							<input checked="" type="checkbox"/>		<input type="checkbox"/>	
Ultrasonic pulse velocity				<input checked="" type="checkbox"/>	<input checked="" type="checkbox"/>		<input checked="" type="checkbox"/>			
Electromagnetic methods										
Cover-meter			<input checked="" type="checkbox"/>							<input type="checkbox"/>
Impulse Radar			<input checked="" type="checkbox"/>				<input checked="" type="checkbox"/>		<input checked="" type="checkbox"/>	<input type="checkbox"/>
Radiography									<input checked="" type="checkbox"/>	<input checked="" type="checkbox"/>
Thermography						<input checked="" type="checkbox"/>	<input checked="" type="checkbox"/>		<input checked="" type="checkbox"/>	
Electrical methods										
Electrical potential			<input checked="" type="checkbox"/>							<input type="checkbox"/>
Resistivity of concrete cover										<input type="checkbox"/>
Potent. and resist. mapping method										<input type="checkbox"/>
Galvanostatic pulse										<input checked="" type="checkbox"/>
Impulse Radar										
Minor destructive methods										
Sampling	<input checked="" type="checkbox"/>	<input checked="" type="checkbox"/>	<input checked="" type="checkbox"/>	<input checked="" type="checkbox"/>	<input checked="" type="checkbox"/>	<input checked="" type="checkbox"/>	<input type="checkbox"/>		<input type="checkbox"/>	
Pull-off					<input checked="" type="checkbox"/>					
Pull-out					<input checked="" type="checkbox"/>					
Phenolphthalein		<input checked="" type="checkbox"/>								
Rainbow-Test		<input checked="" type="checkbox"/>								
Rapid Chloride Test			<input checked="" type="checkbox"/>							
Basic methods										
Direct measurement							<input checked="" type="checkbox"/>	<input type="checkbox"/>	<input checked="" type="checkbox"/>	<input checked="" type="checkbox"/>
Rebound (Schmidt) hammer				<input checked="" type="checkbox"/>	<input checked="" type="checkbox"/>					
Tapping							<input type="checkbox"/>		<input type="checkbox"/>	
Visual inspection						<input type="checkbox"/>	<input checked="" type="checkbox"/>		<input checked="" type="checkbox"/>	<input checked="" type="checkbox"/>
Load tests										
Static and dynamic tests				<input type="checkbox"/>			<input type="checkbox"/>	<input type="checkbox"/>	<input type="checkbox"/>	<input type="checkbox"/>

Notation: - limited usefulness; - wide usefulness

The solution presented in this section is similar to a methodology described in Branco & de Brito (2004). These researchers proposed an idea of the correlation matrices between defects and testing methods. In the matrix, in the intersection of each line (representing a defect) and each column (representing a diagnostic method), a coefficient representing the knowledge-based correlation degree between defect and technique has been introduced. The criteria adopted for that coefficient are:

- 0 – No correlation: no relation whatsoever (direct or indirect) between defect and the diagnostic method;
- 1 – Low correlation: the diagnostic method may be useful as a second choice to a high correlation method when the latter cannot be performed or yields inconclusive results; it may also be useful to obtain secondary information on the extent or cause of the defect;
- 2 – High correlation: the diagnostic method is, in principle, essential to the inspection of the defect; it provides necessary information on the extent, degree, and cause of the defect; it may be replaced by a low correlation method if, for some reason (lack of equipment, workmanship, time, etc.), it cannot be performed; its use does not invalidate the use of other methods if more detailed information is thought to be necessary.

The correlation matrix is based on the defect classification presented by Branco & de Brito (2004) and discussed in Section 3.1. The presented disadvantages of this classification explain the Author's solutions applied.

Chapter 5

Mechanisms of degradation

5.1 Introduction

Defects in RC structures occur as result of various degradation mechanisms. As it has been mentioned in Chapter 3, a single defect may be caused by more than one cause (i.e. degradation mechanism). Assessing of existing RC bridge structures requires a correct defect identification as well as suitable understanding of the nature of degradation mechanisms, which is particularly important in terms of prevention of defects in the future. To date many publications have been produced dealing with degradation mechanisms. Most of them present non-uniform solutions in terms of level of their description. In some publications the following mechanisms (listed together) may be found: sulphates with seawater attack (Lauer 1991); alkali-aggregate reaction with corrosion in the salt environment (Fagerlund 1997); chlorides with atmospheric influences (Ściślewski 1999). The degradation mechanisms such as seawater attack or atmospheric influences are complex, i.e. composed of a number of separate mechanisms. For example the atmospheric influences can be presented as a combination of for carbonation, freeze-thaw or others. Each of them may be considered separately. Incomplete content of the mechanisms is another point highlighted by the literature study. The solutions proposed by various researchers are often concentrated on the particular aspects only. For example Lauer (1991) deals with chemical phenomena only, whereas other publication is related to the mechanisms resulting in cracks (Mitzel et al. 1982).

Table 5-1 Information on degradation mechanisms found in literature

Degradation mechanism Publication	Chemical									Biological	Physical								
	Acids reactions	Alkali-Aggregate Reactions	Carbonation	Chlorides penetration	Corrosion of reinforcement	Creation of composed salts	Leaching	Oil and fat influence	Sulphates reactions		Creep	Fatigue of material	Fire	Freeze-thaw	Overloading	Scour of foundation	Shrinkage	Vandalism	Weathering
Galloway et al. (1979)												✓							
Mitzel et al. (1982)											✓		✓		✓	✓	✓		
Moss (1982)												✓							
Davies & Austen (1987)												✓							
Bijen (1989)	✓	✓	✓		✓				✓										
Wallace & Whitehead (1989)																		✓	
Lauer (1991)		✓			✓				✓										
Department of Transport (1993)		✓	✓	✓	✓		✓												
Design Manual (1993)												✓							
Cheetham (1994)																		✓	
Neville (1995)													✓						
Appraisal of existing structures (1996)			✓										✓						
Al-Serori et al. (1996)													✓						
Fagerlund (1997)	✓	✓	✓	✓	✓		✓		✓					✓					
Hobbs (1998)			✓	✓										✓					
Lambert & Macdonald (1998)			✓	✓	✓									✓			✓		
Ściślewski (1999)	✓		✓	✓	✓	✓	✓	✓	✓										
Concrete Society (2000)	✓	✓	✓	✓	✓		✓		✓	✓			✓	✓	✓				✓
May et al. (2002)															✓				
Brandt & Kasperkiewicz (2003)														✓					
Bamforth (2004)			✓	✓															
Gaal (2004)	✓	✓	✓	✓	✓				✓					✓					
REHABCON (2004)	✓	✓			✓		✓							✓					
Highways Agency (2006)		✓	✓		✓		✓		✓		✓		✓	✓	✓	✓			

In Table 5-1 a relationship between analysed publications and mechanisms (physical, chemical and biological) found is presented.

A complex solution can be found in (Branco & de Brito 2004). These researchers presented possible causes of defects of concrete bridges distinguishing them into the following groups:

- Design Errors;
- Construction Errors;
- Natural Accidental Factors;
- Man-Caused Accidental Actions;
- Environmental Actions;
- Natural Aggressive Factors;
- Man-Caused Aggressive Factors;
- Lack of Maintenance;
- Changes from Initially Planned Normal Use.

Each of these groups is divided by the particular defect causes. The proposed classification system presents impressive contribution in terms of defect causes. A great number of possible defect causes can be found there. However, some disadvantages of this system can be found as well. Several defect causes can be found in various groups of defect causes. For example wet / dry cycles can be found in the environmental actions as well as in the natural aggressive factors; biological action is attributed to the natural aggressive actions as well as the man-caused aggressive actions. Overload can be found in the man-caused accidental actions and also in the changes from initially planned normal use as an increase of the dead load due to repeated repaving. Also other examples may be found.

Though the cited references represent a significant advance toward the understanding of degradation mechanisms, a uniform solution covering all the processes is still missing.

5.2 General conception of classification

This chapter presents an approach of defining and classifying degradation processes occurring to railway reinforced concrete slab spans. The objective is to present the entire background of occurred defects as well as creating the basis for the unification of bridge condition assessment. Each degradation mechanisms will be briefly explained. A relationship between the degradation mechanisms and defects will be presented as well (Table 5-7).

In this study, taking into account nature of the degradation processes, the following groups of degradation mechanisms are distinguished:

- Chemical mechanisms – causing degradation of bridge structures as a result of chemical and biological reactions;
- Physical mechanisms – diminishing condition of bridge structures by influence of physical phenomena;
- Biological mechanisms – causing degradation of bridge structures as a result of biological reactions.

The proposed classification of basic degradation mechanisms identified in considered RC railway bridge spans is presented in Fig. 5-1.

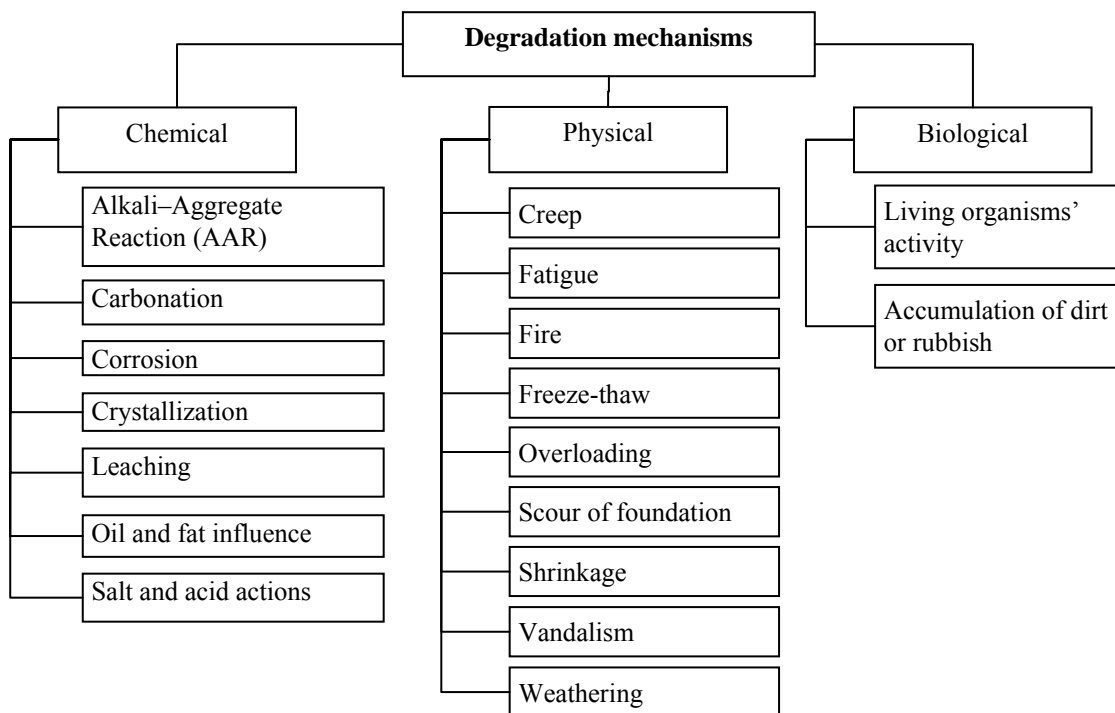


Fig. 5-1 Degradation mechanisms of RC railway bridges

5.3 Chemical degradation mechanisms

5.3.1 Alkali-Aggregate Reaction (AAR)

Alkali-Aggregate Reaction (AAR) is widely understood degradation mechanisms caused by presence of aggregates and alkali, which leads to an expansive reaction and deterioration of the concrete (Bijen 1989, Fagerlund 1997, Gaal 2004, REHABCON 2004). The AAR is believed to take three following forms: alkali-silica, alkali-silicate and alkali-carbonate. From among these reactions alkali-silica is the most common, and arises from a reaction between the silica of certain aggregates and the alkaline pore fluid arising from high alkali cements

(Highways Agency 2006). The product of the reaction (i.e. alkali-silica gel) imbibes water, swells and exerts pressure causing cracking of the hardened concrete. Cracking is the main external evidence for defect to concrete due to this degradation mechanism. Surface cracks may be characterised by a star shaped pattern (depending on the reinforcement configuration), they often follow the 'Isle of Man' pattern. In unrestrained concrete, the cracks develop into a random distribution, often referred to as 'map' cracking, where a network of fine cracks is bounded by a few larger cracks (Department of Transport 1993, Concrete Society 2000, Highways Agency 2006). An example of an effect of the AAR degradation mechanism is presented in Fig. 5-2.



Fig. 5-2 Effects of alkali-aggregate reaction (photographed by Author)

The AAR cracking may be associated with yielding of the reinforcing steel and weakening of the concrete. According to the report of Highways Agency (2006) it should be noted that at 0.1% of alkali-silica expansion, compressive strength decreases by about 12%, loss of flexural strength can be found to be as much as 50% and the elastic modulus is reduced by approximately 20%. Significant loss of bond strength can also occur. The considered mechanism may occur if three following conditions all are met. Firstly the concrete alkalinity must be sufficiently high. Secondly a critical amount of reactive silica must be present in the aggregate. It combines with the alkali when there is a sufficiently high concentration of hydroxyl ions in the pore solution. The last condition refers to the moisture of concrete. The gel may form in relatively dry conditions but to cause defect to the concrete there must be a sufficient supply of moisture available. Limiting the supply of water makes this process slower. Absence of any of these factors prevents damage from occurring (Department of Transport 1993, Concrete Society 2000).

5.3.2 Carbonation

Carbonation is a chemical process resulting in a reduction in the alkalinity of concrete. Carbon dioxide from the atmosphere combines with moisture in the concrete and subsequently forms carbonic acid which reacts with the calcium hydroxide in the pore water forming carbonates. Calcium carbonate is deposited in the pores of the concrete at the depth at which carbonation is occurring (Hobbs 1998, Lambert & Macdonald 1998, Concrete Society 2000, Bamforth 2004, Highways Agency 2006). The described reaction lowers the pH factor of concrete to about 9 (a pH of 8 means that the region is completely carbonated), causing loss of passivation of reinforcement, and corrosion of steel becomes possible.



Fig. 5-3 Effects of carbonation of concrete (Stańczyk 2000)

In the presence of moisture and oxygen carbonation may lead to corrosion-induced cracks parallel to reinforcement, followed by spalling, because the corrosion products form up to 2 to 4 times the volume of steel before it oxidized (Concrete Society 2000, Bamforth 2004, Highways Agency 2006). An example of carbonation effects is presented in Fig. 5-3. Another example of the effect of carbonation is presented in Fig. 5-4. A section photograph of a concrete core showing deep "V"-shaped carbonation front along a vertical crack can be seen. This section was treated with a phenolphthalein alcoholic solution which turns the non-carbonated concrete pink and the carbonation portion into light brown.

The reaction of carbon dioxide and calcium hydroxide is influenced by moisture content. This process is inhibited if concrete is very dry. Also fully saturated concrete stops this process because the moisture presents a barrier to the penetration of carbon dioxide. The most favourable condition for the carbonation reaction is when there is sufficient moisture, but not enough to act as a barrier, i.e. when the RH is between 50 and 70% (Concrete Society 2000, Bamforth 2004). The factors which increase the ability of concrete to carbonate are: lower

content of CaO, higher diffusion constant of CO₂, higher w/c value, cracks, lower strength of concrete, presence of mineral additives and also the lack of curing of concrete in moist environment (Bijen 1989, Fagerlund 1997, Gaal 2004, Ściślewski 1999, PN-86/B-01802).

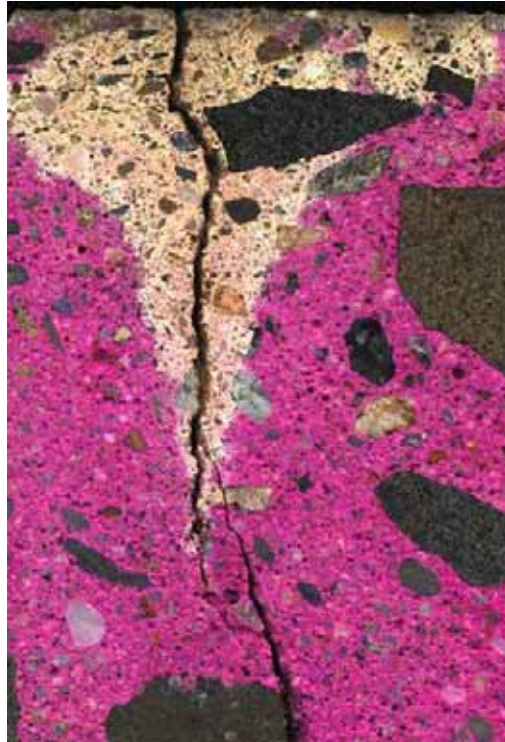


Fig. 5-4 Example the carbonated concrete highlighted by the bright coloration of calcium carbonate in a petrographic microscope, the picture downloaded from www.cmc-concrete.com/carbonation.htm

According to the report of Highways Agency (2006) carbonation-induced reinforcement corrosion is more common with reduced cover and/or poor quality concrete, and affects stirrups before main reinforcement. Despite several disadvantages carbonation is not generally harmful to the concrete itself. It may be beneficial, for example by increasing resistance to sulfate attack or by reducing permeability (Bamforth 2004). Another result of carbonation mechanism is localized hardening of concrete (British Standard 1986, Appraisal of existing structures 1996) indirectly resulting in the increasing the concrete strength (Ryall 2001).

5.3.3 Corrosion

Corrosion – the oxidation of steel initiated by the loosing of rebars passivation at the high electrolytic conductivity of concrete and the permanent supply of oxygen from outside. The factors increasing activity of this mechanism are: carbonation of concrete, chlorides and cracks (Fagerlund 1997, Ściślewski 1999, Gaal 2004, REHABCON 2004). Cracks parallel to the reinforcement, delamination and spalling of concrete or at least rusty weeping, are the main symptoms of corrosion in an advanced stage.



Fig. 5-5 Effects of corrosion at advanced stage with spalling of concrete (photographed by Author)

An example of the effect of corrosion is presented in Fig. 5-5. The nature of defect as a function of the bar size, spacing and cover was presented in the report of the Concrete Society (2000), see Table 5-2.

Table 5-2 Form of defect related to cover and bar diameter (Concrete Society 2000)

Cover / bar diameter	Likely type of damage on a flat surface
1	Cracks and possible local spalling
2	Larger cracks and risk of delamination
3	Delamination

Corroding reinforcement increases its volume, causing increased stress within the concrete. Various types of discontinuity occur. Widely spaced rebars situated close to the concrete surface tend to provoke cracks parallel to them.

If the reinforcement is located more deeply and close together, delamination (discontinuity parallel to the concrete face at the level of the steel) will be the most likely form of defect. Delamination primarily exerts an influence on bond strength. In the case of the compression zone, it may affect the compressive strength as well (Highways Agency 2006). Inadequate cover is invariably associated with areas of high corrosion risk due to both carbonation and chloride ingress. A cover survey would rapidly identify likely problem areas and permit preventative measures to be taken (Lambert & Macdonald 1998).

Reinforcement corrosion may be caused mainly by carbonation of concrete and chloride ingress and though the final result will be the same, significant differences in terms of the corrosion development can be observed. Carbonation-induced corrosion differs from corrosion resulting from chloride ions concentration. The first case is known as a degradation mechanism causing defects of relatively large extent. Corrosion caused by chloride ingress presents others symptoms. This mechanism occurs as at localized points commonly known as

pitting corrosion, resulting in failure of a bar situated close to sections in good condition. Chloride induced corrosion is also more likely to occur without external visual evidence, and in extreme cases can corrode deeply embedded bars with limited oxygen supply (Highways Agency 2006). Another difference between these two types of corrosion, described in the report of Concrete Society (2000), is the propagation period understood as the time between corrosion initiation and defect occurring. Though carbonation occurs in moderate environment (60-70% of humidity), even in these conditions the corrosion rate will be slow in relation to the structure life whereas, the propagation of chlorides relative to structure life is short

With regard to the condition appraisal of RC structures, with respect to the influence of reinforcement corrosion, two forms of crack should be taken into consideration; those present before the onset of corrosion which might assist the corrosion processes (for example cracks caused by Alkali-Aggregate Reactions or overloading), and those produced as a direct consequence of reinforcement corrosion (expansive corrosion products leading to cracking and spalling). More details can be found in the publication of Lambert & Macdonald (1998).

5.3.4 Crystallisation

This mechanism is caused by the reaction of aggressive substances from the surrounding environment with the concrete components resulting in the creation of salts in concrete pores. Salts crystallise enlarging their volume, this leads to the increase of tensile stresses, resulting in cracks of concrete and strength reduction. In the advanced stage loss of concrete may appear as well. The partial humidity of concrete and the possibility of the temporary steaming of water increase the activity of this mechanism (Ściślewski 1999).

5.3.5 Leaching

Leaching – degradation mechanisms caused by soft water, especially clear, distilled and also by the mountain streams and precipitations. This mechanisms is related to the dissolving and leaching of the concrete compounds (i.e. lime compounds) leading to the formation of calcium carbonate or calcium sulphate on the surface of the concrete known as efflorescence.

Two forms of leaching effects occur: lime bloom and lime weeping. The first form appears as white patches or an over-all lightening of the concrete surface (see Fig. 5-6) which is usually a cosmetic problem (Concrete Society 2000). Lime weeping is an effect of the precipitated degradation mechanism caused by the evaporating or leaking water mainly at discontinuities.



Fig. 5-6 Example of leaching effects – lime bloom (photographed by Author)

In case of serious water leakage stalactites (built up of white deposits on the concrete surface) may appear (Concrete Society 2000, Highways Agency 2006), see an example in Fig. 5-7.



Fig. 5-7 Example of leaching effects – lime weeping (photographed by Author)

The effects of leaching may be considered as indicators of severe problems, such as the likelihood of corrosion if the defects extend to reinforcement. When corrosion reaches reinforcement the white deposits may also be stained brown by corrosion products (Concrete Society 2000, Highways Agency 2006). The dissolving and leaching of the concrete compounds result in concrete strength reduction. Factors which increase activity of this mechanism are: cracks, higher value of w/c index, higher content of $\text{Ca}(\text{OH})_2$ and higher concrete permeability (PN-80/B-01800, PN-86/B-01802, Fagerlund 1997, Ścisławski 1999).

5.3.6 Oil and fat influence

Oil and fat influence – reaction of oils and/or fats with the calcium hydroxide. During this reaction a calcium soap is created as a greasy substance without bonding features. Apart from its influence on the bridge aesthetics this mechanism causes a strength reduction in the concrete (Ściślewski 1999).

5.3.7 Salt and acid actions

This degradation mechanism covers chemical reactions mainly of compounds of chlorine, sulphur, nitrogen and magnesium with structural material. The most common groups of these mechanisms are as follows.

Acid reactions This mechanism is usually caused by the reaction of concrete components with the aggressive acid environment at the external layer of concrete. Acids generally attack the surface of concrete by dissolving the matrix leading to surface disintegration. Acids may become more concentrated due to evaporation, leading to an increased rate of attack. This reaction may be caused by presence of carbon dioxide, sulphates, ammonium or magnesium and also strong mineral acids such as sulphuric, hydrochloric, nitric even diluted. The factors which increase activity of this mechanism are: hydrated cement and bad maintenance – organic materials can release sulphuric acid (Bijen 1989, Fagerlund 1997, Concrete Society 2000, Gaal 2004, REHABCON 2004, Ściślewski 1999, PN-80/B-01800, PN-86/B-01802).

Chloride penetration This degradation mechanism is defined as losing of the passivation of reinforcement caused by the presence of chloride ions which locally breaks the passive film. Chloride-free concrete effectively protects the reinforcement by means of a passive oxide film formed in the highly alkaline environment of cement paste where $\text{pH} > 13$. This film is being continuously corroded, but also continuously reinstated by the hydroxyl ions in the pore water (Bamforth 2004). The chloride ions (in sufficient quantities) which have reached the reinforcement may break down the protective film and (in the presence of moisture and oxygen) chloride-induced corrosion may be initiated causing defects such as discontinuities (parallel to reinforcement cracks) and material (reinforcement and concrete) losses (Hobbs 1998, Lambert & Macdonald 1998). Chlorides do not reduce the pH of concrete, but inhibit the mechanism by which the protective oxide layer is maintained (Concrete Society 2000).

Chlorides enter concrete during its mixing, diffusion and through capillary suction under wetting and drying conditions as well as through cracks (Lambert & Macdonald 1998, Hobbs 1998). The most favourable condition is dry concrete occasionally wetted (Concrete Society

2000). The factors increasing the activity of this mechanism are: high w/c, carbonization and moisture, low concentration of $\text{OH}^{(-)}$, mineral additives: silica dust, fly-ash, blast furnace slag, lower content of C_3A (Fagerlund 1997), the curing of concrete in moist environment even of small salt content, the salting on the construction surfaces subjected to the activity of the atmospheric factors (Fagerlund 1997, Ściślewski 1999, Gaal 2004).

Table 5-3 The risk of corrosion in relation to the level of chloride by binder weight (Bamforth 2004)

Chloride content (% weight of binder)	Risk of corrosion
< 0.4	Negligible
0.4 – 1.0	Possible
1.0 – 2.0	Probable
> 2.0	Certain

In order to assess whether the chlorides ingress may cause corrosion of reinforcement or not a threshold level of chloride ions, measured by binder weight, has been evolved. Reported values of this threshold level vary from 0.25% to 2.5% and the most common value of this threshold is 0.4%. In Table 5-3 a relationship between chloride content and corrosion risk is presented. More information on the chloride threshold level can be found in Bamforth (2004).

Sulphate reactions This mechanism is related to the reaction of concrete components with aggressive sulphate environment (i.e. water, especially seawater; decaying organic substance or industrial effluent). This reaction causes concrete surface disintegration such as cracks or losses of material permitting other contaminants to ingress. This mechanism can also be caused by aggregate that contains sulphates (Bijen 1989, Gaal 2004, Highways Agency 2006). Usually sulphate attack to concrete appears in two forms depending on the temperature, types and concentrations of sulphate and the concrete composition:

- Expansive formation of ettringite or gypsum causing cracks (up to 8 mm wide similar to AAR effects) and concrete losses (Concrete Society 2000, Highways Agency 2006);
- Thaumasite reducing the concrete to a pulpy mass which disintegrates, exposing the reinforcement to corrosion (Highways Agency 2006).

5.4 Physical mechanisms

5.4.1 Creep

This mechanism is defined as inelastic and only partly irreversible strains caused by long-time load (Mitzel et al. 1982). Generally creep may present detrimental consequences. Spans can deflect and reduce bridge headroom; columns can shorten, sometimes having a similar effect to settlement (Highways Agency 2006).



Fig. 5-8 Example of effect of creep (photograph courtesy of Zygmunt Kubiak, PKP)

With respect to the considered span structures (span lengths shorter than 20 m) creep causes insignificant deflections only, i.e. concrete elastic modulus reduction. An example of the span deformation presumably caused by creep (though it could also be related to badly performed formwork as well) is presented in Fig. 5-8.

5.4.2 Fatigue

Fatigue of material is the mechanism of sequential degradation characterized by the crack initiation and its increase to the critical size from which unstable escalation can take place. This mechanism causes material properties reduction. According to the fatigue tests described by Galloway et al. (1979) the residual flexural strength of five year old beams which had been subjected to 3.5×10^6 cycles of fatigue loading without failure, was about 6 % less than the mean strength of similar beams which had not been fatigue tested.

There are two main approaches of the fatigue behaviour analyses, i.e. bar axial tension test (favoured by the steel producers) and the testing of model reinforced concrete beams (preferred by the investigators with a civil engineering background). The results of the axially tested bars are affected by several factors such as bar diameter (fatigue strength decreases as bar size increases) while identical bars tested in RC elements appeared to display higher

fatigue strength. In case of the continuous reinforcement the cracks occur at the root of a transverse rib. The difference in results of these two approaches is related to nature of fatigue behaviour. The surface of rebars presents randomly distributed defects from which fatigue cracks can be initiated. In tests of RC elements such a defect will provide a crack initiation only if closely situated to the flexural crack in the concrete, where the rebar is subjected to the full stress. Unlike axial tests of rebars the entire length of the steel is fully stressed. For this reason the concrete elements appear to indicate higher fatigue strength. Also the relation between diameter of rebars and fatigue strength of axially loaded reinforcement can be explained. Rebars of bigger diameter are characterised by a bigger surface area for their unit length and the consequently greater probability of occurrence of a severe defect in a given length. Concerning the cranked lapped reinforcement these elements present much worse fatigue strength than the straight lapped which are close to that of the continuous reinforcement. In all cases of fatigue fracture of the mechanical splices, failure occurs in the vicinity of the coupler. The fatigue strength of reinforcement is reduced by the presence of welds, especially if carried out on site. In these locations concrete always cracks as a result of notch appearance. More information related to this paragraph can be found in Moss (1982) and Davies & Austen (1987). Another factor exerting an influence on the fatigue behaviour is the corrosion of reinforcement (Design Manual 1993). The experimental evidence from the tests performed on corroded bars indicates affected fatigue behaviour in comparison to the uncorroded bars.

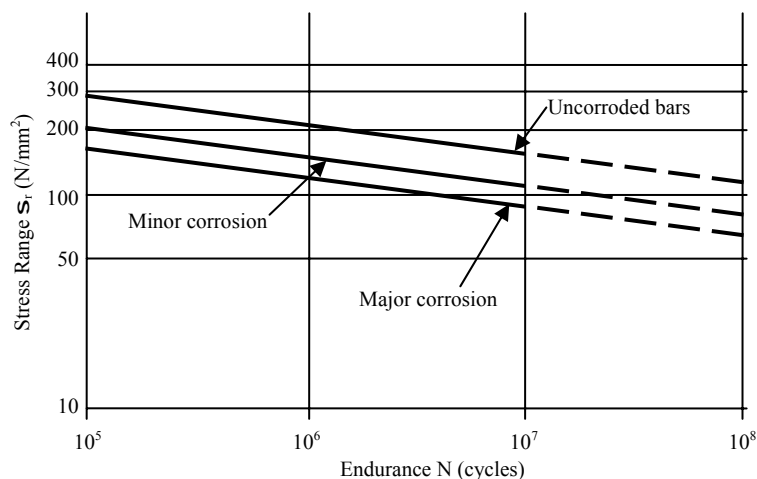


Fig. 5-9 Relationship between Stress Range and Endurance measured in number of cycles against condition of rebars related to their corrosion (Design Manual 1993)

According to this manual the fatigue behaviour can be significantly affected when reinforcement corrosion is characterized by the severe loss of steel. Usually it happens in case of the chloride-induced corrosion resulting in deep pits. Corrosion, as a result of carbonation

of the concrete, involves mainly superficially distributed loss of steel. In Fig. 5-9 the relationship between stress range and endurance of concrete element measured in number of cycles against the condition of rebars related to their corrosion is presented. The terms minor and major corrosion means the levels of intensity of reinforcement losses, i.e. minor corrosion – less than or equal to 25% of cross-section lost, major corrosion – more than 25%.

In this study the fatigue of material is considered as a reason of material parameters modification. The mentioned defects accompanying this phenomenon should be considered as indicators of a potential property modification of material.



Fig. 5-10 Example fatigue of material effects – cracks in concrete (photographed by Author)

An example of the fatigue effects, relating to the reinforcement and resulting in flexural cracks in the bottom surface of span, is presented in Fig. 5-10. The reduced strength of reinforcement causes an excessive effort of concrete.

5.4.3 Fire

This mechanism can be caused by rail or truck mounted tanker getting ignited accidentally in the vicinity of a bridge (Al-Serori et al. 1996, Mitzel et al. 1982). Fire may be initiated even during bridge construction in final stages. An example of fire damage occurred to a bridge over the American River in Sacramento (USA) is presented in Fig. 5-11. An Amtrak train went over the bridge about 15 minutes before the fire was reported. The crew of that train did not see any problems, which explains how fast this process is. All train traffic was immediately stopped. Almost one half of the bridge length was destroyed. Concrete which has been affected by fire and cooled to ambient temperature presents colour changes (Appraisal of existing structures 1996, Concrete Society 2000).



Fig. 5-11 Example of influence of high temperature mechanisms (fire of the Sacramento Bridge USA) – picture downloaded from http://www.uprr.com/newsinfo/2007/sacramento_bridge.shtml

Neville (1995) presented a relationship between colour changes in concrete subjected to fire against the temperature experienced, see Table 5-4. It may be used as a simple diagnostic method for concrete structures affected by a fire. Though concrete structures have high resistivity to elevated temperatures, prolonged fire conditions can cause serious defects such as: modification of physical features (reduction of strength and elastic modulus of concrete and reinforcing steel as well as loss of bond), discontinuities (cracks and delaminations) and loss of material (i.e. spalling of concrete) (Appraisal of existing structures 1996, Concrete Society 2000).

Table 5-4 Common colour changes in concrete subjected to fire according to Neville (1995)

Maximum temperature (°C)	Colour of concrete after cooling to ambient temperature
300-600	Pink
600-900	Grey
900-1200	Buff
Above 1200	Yellow

Discontinuities, i.e. cracks (visible or hidden) and delaminations, and losses of material (mainly spalling of concrete) are common external symptoms of distress caused by fire. This is induced in the concrete as it is being heated and the differential expansion of its successive layers occurs. Also, moisture in the concrete turns to super-heated steam causing internal pressure (Appraisal of existing structures 1996, Concrete Society 2000). Spalling of concrete takes place usually in the first 30 minutes after fire has occurred and continues to appear with disruptions removing layers of concrete of shallow depth (Appraisal of existing structures 1996). Cooling of concrete can be destructive for structure as well as its subjecting to fire. Sudden quenching, by spraying with water, may result in cracks and delaminations. Also

spalling of concrete is likely to occur (Appraisal of existing structures 1996, Concrete Society 2000). The loss of bond between concrete and steel is a consequence of delaminations and spalling of concrete. This defect depends mainly on the duration of fire action and the reinforcement type. A 30% loss of bond for the 100°C to 300°C range can be assumed, though this relationship is not well established yet (Appraisal of existing structures 1996, Highways Agency 2006).

Extremely high temperatures also exert an influence on material parameters, i.e. strength and modulus of elasticity (Appraisal of existing structures 1996, Perkins 1997). The reduction is approximately linear with temperature (Concrete Society 2000). The compressive strength of concrete can be reduced up to 15% in the temperature range between 100-300°C. Above 800°C it is unlikely to possess any viable structural strength. In Table 5-5 a relationship between temperatures reached and compressive strength reduction of concrete with corresponding damage factor according to (Appraisal of existing structures 1996) is presented.

Table 5-5 Residual strength of concrete after cooling and the corresponding fire-damage factor according to (Appraisal of existing structures 1996)

Temperature range (°C)	Resultant strength (%)	Damage factor
100-300	85	0.85
300-500	40	0.40
over 500	0	0.00

Fire can affect the strength of reinforcement as well. An increase in temperature is related to a reduction of elastic modulus as well. Above 100°C the steamed water is released from the concrete causing a reduction of 10% to 20% of this parameter. Further heating of the concrete causes development of elastic modulus reduction (Appraisal of existing structures 1996). Despite the described defects, reinforced concrete structures have a good fire resistance related to the low thermal diffusivity of concrete (about 1mm²/s). In the practice only the external (30-50mm) layer of concrete is likely to be subjected to high temperature (Appraisal of existing structures 1996).

5.4.4 Freeze-thaw

Freeze-thaw – This mechanism is caused by the expansion of pore water due to freezing. Factors increasing its effects can be listed as follows: a w/c ratio > 0.6; decreased air content; continuous storing of concrete in permanent contact with water without drying time; fine porous aggregate; alkalis content; mineral additives like cinder, fly-ash without aerating substances; cracks; structures sucking ground water; railway bridge troughs filled with mist

ballast (Fagerlund 1997, Brandt & Kasperkiewicz 2003, Gaal 2004, REHABCON 2004). Water occupying the capillary pores of cement paste and freezing at lower temperatures increases its volume and causes expansive forces (Concrete Society 2000). Increase of volume of water while turning to ice is about 8%. It means that concrete must be saturated in at least 90% of volume in order to cause the expansive pressure (Hobbs 1998).

Concrete which is permanently exposed to water or head water may be critically saturated. In case of cold concrete, its saturation is possible as well, if exposed to warm moist air. Also salt activity can result in critical saturation of concrete (Hobbs 1998). When the expansive pressure caused by freezing is greater than the local strength of concrete defects occur.



Fig. 5-12 Example of the result of freeze-thaw action (photograph courtesy of prof. Jan Bień, WUT)

If the pores are large, this mechanism does not influence freeze-thaw behaviour, because of the dominating presence of air (Concrete Society 2000). Freeze-thaw mechanism causes several defects. The most common are discontinuities and losses of material. An example of the freeze-thaw effects is presented in Fig. 5-12. The described expansive pressure results in cracking to the depth to which the freezing has penetrated (Hobbs 1998, Concrete Society 2000). The network of closely spaced cracks may appear even after the first winter of exposure (Highways Agency 2006). This mechanism can result in concrete surface scaling (Concrete Society 2000) also associated with the application of salts (Hobbs 1998). Spalling of concrete may be observed as well (Hobbs 1998). Freeze-thaw mechanism may result in pop-outs related to the susceptible coarse aggregate particles closely located to the concrete surface (Hobbs 1998, Concrete Society 2000). Repeated cycles of freezing and thawing have a cumulative effect and result in progressively deeper damage (Hobbs 1998, Concrete Society 2000).

5.4.5 Modification of foundation conditions

This mechanism is caused mainly by moving liquid (for instance a river or the soil mass) through the support zone and causing loss of support material as well as soil. Material from the bed of and banks of a channel is being removed by action of water or other liquid such as mud mass (May et al. 2002). Foundation displacements are the main effects of this mechanism. Scour of foundation causes changes in the global geometry of the structure (eg. Fig. 5-13). This phenomenon leads to the dangerous redistribution of internal forces and consequently stresses which may consequently exceed designed values of the load capacity, causing cracks, and potentially failure (Mitzel et al. 1982). Scour of foundation may also cause differential settlement leading to cracks and reinforcement yielding (Highways Agency 2006).

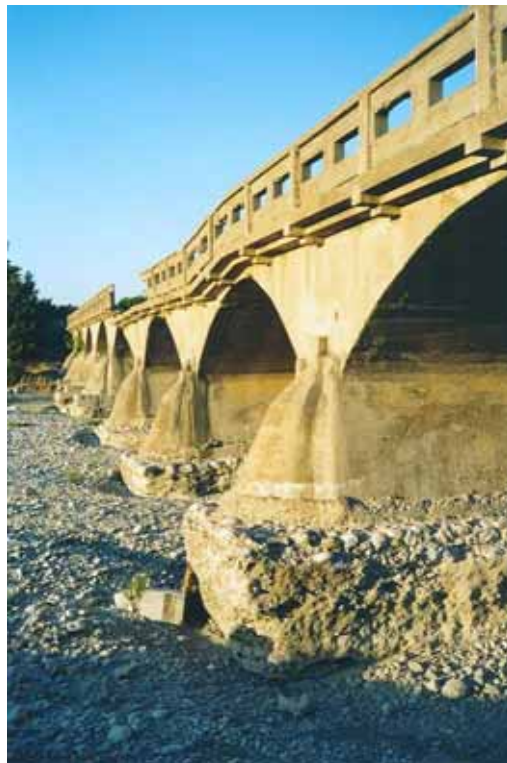


Fig. 5-13 Effects of scour of foundation (photograph courtesy of prof. Jan Bień, WUT)

In the Author's opinion defects related to global geometry modification of a structure should be considered not as defects but as failures requiring immediately a repair intervention.

5.4.6 Overloading

Overloading – exceeding the acceptable values of the load, is caused mainly by: changing of the load class; floods, earthquakes, explosions, collisions, war activities (especially the 2nd World War) or any other accidental loading. Usually, overloading results in the formation of cracks. Their pattern often allows the cause to be identified. Uniformly distributed cracks in

the middle of the slab soffit, orientated at right-angles to the span, are related to the excessive values of bending moment. Failure of the anchorage of reinforcement may lead to the formation of parallel cracks (Concrete Society 2000). Sometimes overloading leads to severe defects, Fig. 5-14 shows an example of failure of the support. Overloading caused by explosion may result in cracks and loss of material (Highways Agency 2006).



Fig. 5-14 Example of effects of overloading (photograph courtesy of Kazimierz Bieniek, WUT)

Another cause of this mechanism is earthquake, see an example Fig. 5-15. In such cases bridge structures must be immediately repaired or demolished and replaced. In extreme cases overloading may result in deformations or/and displacement.



Fig. 5-15 Example of effects of overloading caused by earthquake (photograph courtesy of prof. Jan Bień, WUT)

5.4.7 Shrinkage

Shrinkage is a mechanism caused by the internal constraint of element deformation by reinforcement resistance resulting in cracks of concrete (Fig. 5-14). It may also be caused by the external constraint of element movement by supports and can be caused by badly performed curing of concrete exposed to direct sunlight (Mitzel et al. 1982).



Fig. 5-16 Effects of shrinkage (photograph courtesy of prof. Jan Bień, WUT)

5.4.8 Vandalism

According to Cheetham (1994) vandalism may be defined as the wilful damage of property, often that owned by local or public authorities. It is an anonymous offence with a low rate of detection and conviction. It adversely affects the quality of life and the environment.



Fig. 5-17 Example of vandalism effects - graffiti (photographed by Author)

Though the analysed structure type is relatively resistant to the vandalism, its several forms may be considered, including: destroying balustrade, track elements and graffiti (Fig. 5-17). The last group is the most common. There is no easy solution to the problem of vandalism. It results from a complex network of interrelated factors: people, their attitudes and expectations, local social, political and economic conditions, and the nature of the physical environment (Cheetham 1994). Graffiti are defined as unwanted painting, writing, gouging or scratching on walls or other surface. They are most commonly found on publicly-owned property such as underpasses or bridges and on structures such as brick perimeter walls without apparent owners. The marking agents most commonly used for graffiti are paints, felt-tip markers, ball-

point pens and waxy substances. Other less common types of marking agent include pencil and chalk. Identification may be a problem, but discarded tins and pens may provide a clue (Wallace & Whitehead 1989). In general the graffiti is rather the cosmetic problem, but for some bridges their aesthetic attributes are crucial in terms of the local environment, especially when the bridge is situated over frequently used road or pedestrian passage.

5.4.9 Weathering

Weathering is a degradation mechanism related to the atmospheric conditions which have occurred during service life such as pollution, frost or sunlight exerting an influence on a structure. The main effect of weathering is various variations in visual appearance of the structure, for example dust from atmosphere may be deposited on the facade, flowing water or rainfall tends to cause significant differences in colours. Regular washing and painting the surface can reduce this effect. The dissolution of carbon dioxide in the atmosphere makes rainfall slightly acidic and tends to etch the concrete surface or at least cause its deterioration (Fig. 5-18). Until these substances have not concentrated, this degradation mechanism can be considered as a cosmetic problem only. More details can be found in Concrete Society (2000).



Fig. 5-18 Effects of weathering (photograph courtesy of prof. Jan Bień, WUT)

5.5 Biological degradation mechanisms

5.5.1 Accumulation of dirt or rubbish

Dirt and rubbish do not themselves attack concrete. Their presence is related rather to the aesthetics problems than to structure degradation. They play a role of the collector of aggressive substances or at least water. In this way they can be considered as reasons of other degradation mechanisms. Simple maintenance actions (cleaning) can reduce this problem.

5.5.2 Living organisms activity

Despite porosity of concrete its high alkalinity about pH 13 is not favourable for biological growth, but during bridge service life, as the concrete ages, the situation changes.



Fig. 5-19 Mosses on the concrete surface as an example of biological degradation mechanism effect
(photographed by Author)

Various atmospheric conditions such as carbonation of concrete or rainfall cause reduction of the alkalinity and concrete environment becomes better for biological growth. In the course of time various organisms can be found in concrete structure, i.e. algae, fungi and bacteria. Lichens and mosses appear as well (see an example in Fig. 5-19).



Fig. 5-20 Example of plants growing on concrete structure (photographed by Author)

Bacteria do not themselves attack concrete. They may play an active role in the conversion of essentially harmless substances into acids or other compounds causing degradation. Mixture of dirtiness (i.e. particles of grit, pollen, spores and toxic chemicals) and decaying remains of dead organisms provides conditions for more advanced biological growth. Organic growth

affects concrete durability as well. Trapping moisture in pores makes the concrete saturated even in relatively dry conditions. Some algae produce acids slowly dissolving the cement matrix of the concrete surface.

Roots of plants (Fig. 5-20) growing into cracks may cause bursting stresses resulting in increasing the size of cracks and spalling. More information can be found in the publication of Ściślewski (1999) and report of Concrete Society (2000).

5.6 Other methods of classification

In the previous section all the degradation mechanisms reported in the available literature which relate to RC structures have been distinguished into the chemical, physical and biological mechanisms. The presented mechanisms can be also classified by taking into account the duration of the degradation processes. The following groups can be distinguished:

- Incidental mechanisms – when the degradation process is very short (duration even below a second), e.g. overloading by collision or by earthquake;
- Short-time mechanisms – acting during hours or days, e.g. fire, scour of foundation occurred during flood;
- Long-time mechanisms – majority of chemical, physical and biological processes.

Fookers (1976) classified defects in terms of their typical time of appearance, see Table 5-6.

Table 5-6 Typical times of appearance of defects according to Fookes (1976)

Type of defect	Typical time of appearance
Plastic settlement cracks*	10 min. – 3 hours
Plastic shrinkage cracks*	30 min. – 6 hours
Construction defects*	On removal of formwork
Crazing	1 – 7 days, sometimes much later
Early thermal contraction cracks*	1 day – 2 or 3 weeks
Long-term drying shrinkage cracks	Several weeks or months
Chemical attack (incl. sulphates)	Few months up to several years depending on the materials
Freeze-thaw damage	After first severe winter
Damage due to structural loading	Probably several months, possibly much later
Damage due to temperature movements (seasonal)	Probably up to a year, but may be longer
Materials-related	Several years
Reinforcement corrosion	Several years, but may be sooner
Fire damage*	After severe fire

Note: *Once these have formed, they do not develop further

5.7 Effects of degradation mechanisms

Identified defects are usually caused by more than one degradation mechanism and correct understanding of the processes needs detailed analysis. Relationships between the degradation mechanisms and the basic types of defects are presented in Table 5-7.

Table 5-7 Degradation mechanisms and basic types of defects

Degradation mechanisms Defect types	Chemical						Physical							Biol.				
	AAR	Carbonation	Corrosion	Crystallization	Leaching	Oil and fat influence	Salt and acid actions	Creep	Fatigue	Fire	Freeze-thaw	Modific. of found. cond.	Overloading	Shrinkage	Vandalism	Weathering	Accum. of dirt or rubbish	Living organisms activity
Contaminations			✓		✓	✓				✓					✓	✓	✓	✓
Deformations								✓					✓					
Deterioration	✓	✓	✓	✓	✓	✓	✓	✓	✓	✓						✓		✓
Discontinuity	✓	✓	✓	✓			✓		✓	✓	✓	✓	✓	✓				✓
Displacements												✓	✓					
Loss of material		✓	✓	✓			✓			✓	✓		✓			✓		✓

The presented solutions in this section are similar to the methodology of the correlation matrices presented in Branco & de Brito (2004). These researchers presented a correlation matrix between defects and possible causes. In this matrix, in the intersection of each line (representing a defect) and each column (representing a possible cause), a coefficient representing the knowledge-based correlation degree between one and the other has been introduced. The criteria adopted for that coefficient are as follows:

- 0 – No correlation: no relation whatsoever (direct or indirect) between the defect and the cause;
- 1 – Low correlation: indirect cause of the defect, connected only with the early stages of the deterioration process; secondary cause of the deterioration process and not necessary for its development;
- 2 – high correlation: direct cause of the defect associated with the final stages of the deterioration process; one of the main causes of the deterioration process and essential to its development.

The correlation matrix is based on the defect classification presented by Branco & de Brito (2004) and discussed in Section 3.1. The presented disadvantages of this classification explain the Author's solutions applied.

In the solutions presented in Table 5-7 the Author has assumed the relationship between degradation mechanism and defect as uniform, i.e. the relationship exists or not. From the load capacity assessment point of view the diversity of relationship is not so important. Moreover this diversity should be based on a particular research which significantly goes beyond the area of this Thesis.

Chapter 6

Numerical modelling of slab spans with defects

6.1 Introduction

Modelling of bridge structures with defects requires the application of special techniques for representation of structure imperfections. Selection of the modelling technology should be determined by analysed structure type and by considered defects. In this study, as it has been presented in Chapter 2, entire attention is concentrated on the simply supported slab spans with a special focus on their defects. The modelling methodology of defects influencing the load capacity (see Table 3-6, page 42) of railway slab spans will be presented taking into account defects of concrete and reinforcement such as loss of material and material parameters modification, i.e. strength and elastic modulus. To describe the condition of a damaged construction the following three defect parameters, proposed by Bien (2002), are required:

- Defect intensity I_d ;
- Defect extent E_d ;
- Defect location L_d .

In this study, the Author will present his own proposal regarding the modelling of the defect intensity (i.e. loss of concrete, see Section 6.4.1), the defect extent (Section 6.5) and location (Section 6.6). All of these parameters allow for the precise description of a bridge structure

with defects and is the basis for further assessment of load capacity and bridge technical condition. The proposed solution of defect parameters makes this description uniform and collected information on defects can be stored in the data base and be used by other engineers working for the bridge infrastructure administration.

An approach for the definition of defect parameters can be found in the Network Rail (2004) handbook. Defects are described by means of two parameters; severity and extent. Their definitions are presented in Table 6-1 and Table 6-2 respectively. The main disadvantage of this methodology is lack of a uniform defect classification and imprecise definitions of the mentioned parameters. Concerning the defect classification this system loosely refers to the subjectively described defects. For example spalling is a kind of concrete loss. The presented system does not refer to the other forms of this defect for example honey-combing.

Table 6-1 Defect severity definition according to Network Rail (2004)

Severity	Definition
A	No visible defects
B	The most extensive from: <ul style="list-style-type: none"> • Surface damage/chips/scrapes/minor spalls • Indications of wetness/presence of water (define as percolation, run down etc excluding exposure to rainfall) • Staining (from aggregates, tying wire, nails or other minor metallic debris) • Cracking < 1mm wide without evidence of corrosion of reinforcement
C	The most extensive from: <ul style="list-style-type: none"> • Spalling (no exposed reinforcement) without evidence of corrosion of reinforcement • Cracking 1mm wide or greater without evidence of corrosion of reinforcement
D	The most extensive from: <ul style="list-style-type: none"> • Spalling (no exposed reinforcement) with evidence of corrosion of reinforcement (excludes staining from metallic debris). Includes delamination & drumminess • Cracking of any width (no exposed reinforcement) with evidence of corrosion of reinforcement (excludes staining from metallic debris)
E	Secondary reinforcement exposed
F	Primary reinforcement exposed
G	Structural damage to element. (Includes permanent distortion/displacement)

Regarding the parameter definitions the system provides their discrete gradations as a function of their occurrence. It can be clearly observed, especially in case of the defect extent. Defects of extent 11 and 50% are attributed to the same extent class “4”. On the other hand,

defects of extent 10 and 10.05 have to be described as damages of different extent level. Such illogical situations can be fixed by means of the continuous scale of defect parameters proposed in this Thesis.

Defect location has not been taken into account in this methodology. The load capacity is the main measure of bridge condition and in terms of its evaluation the defect location has a crucial meaning.

Table 6-2 Defect extent definition according to Network Rail (2004)

Extent	Definition	
	For all severities	For cracking of severity B, C & D
1	No visible defects	No visible defects
2	Localised defect due to local circumstances	Total length of all visible cracks of that severity regardless of orientation, as a % of the principal dimension of the element, < 20%
3	Defect occupies < 5% of surface of the element	ditto 20% up to 50%
4	Defect occupies 5 % up to 10% of the surface of the element	ditto > 50% up to 100%
5	Defect occupies > 10% and up to 50% of the surface of the element	ditto > 100% up to 200%
6	Defect occupies > 50% of the surface of the element	ditto > 200%

6.2 Geometry models

Models of geometry applied in the bridge engineering can be classified taking into account the following two parameters (Kmita et al. 1989):

- *Element dimension* used to create the bridge model:
 - one-dimensional e^1 ,
 - two-dimensional e^2 ,
 - three-dimensional e^3 ;
- *Space dimension*, in which the bridge model can be created:
 - one-dimensional s^1 ,
 - two-dimensional s^2 ,
 - three-dimensional s^3 .

Using the available parameter combinations, six basic geometry classes, presented in Table 6-3, can be created. For the particular classes an expression (e^n, s^m) , where e^n is understood as n -dimensional element and s^m is m -dimensional space, has been considered.

Table 6-3 Geometry models according to Kmita et al. (1989)

Space dimension \ Element dimension	s^1	s^2	s^3
e^1	e^1, s^1	e^1, s^2	e^1, s^3
e^2		e^2, s^2	e^2, s^3
e^3			e^3, s^3

The presented system allows precisely describing dimensions of element and its space as well. The space description has a special meaning regarding the structures composed of more than one part. Sometimes it is useful to use a simplified class description based on the element dimensions only, i.e. instead of (e^n, s^m) an expression (E^n) can be applied.

- E^1 class model for 1D elements (e^1, s^1) , (e^1, s^2) and (e^1, s^3) ;
- E^2 class model applicable in case of 2D elements (e^2, s^2) and (e^2, s^3) ;
- E^3 class model – 3D elements (e^3, s^3) .

6.3 Coordinates system

In order to describe defects as well as entire geometry, a uniform coordinate system is necessary. This system allows for unambiguous description of the considered structure geometry. The axis “ x ” is parallel to the longitudinal axis of the span, the axis “ y ” is parallel to width of the cross section and the axis “ z ” is perpendicular to the “ x - y ” plane.

However, the “ x, y, z ” system describes geometry in the global coordinates, in this study the Author has introduced a normalised coordinate system “ ξ, ψ, ζ ” based on the global coordinates but taking into account the span dimensions as well. Using this system the defect description presented and explained in the next sections will be clearer. In Fig. 6-1 the bridge structure against the global coordinates system is presented.

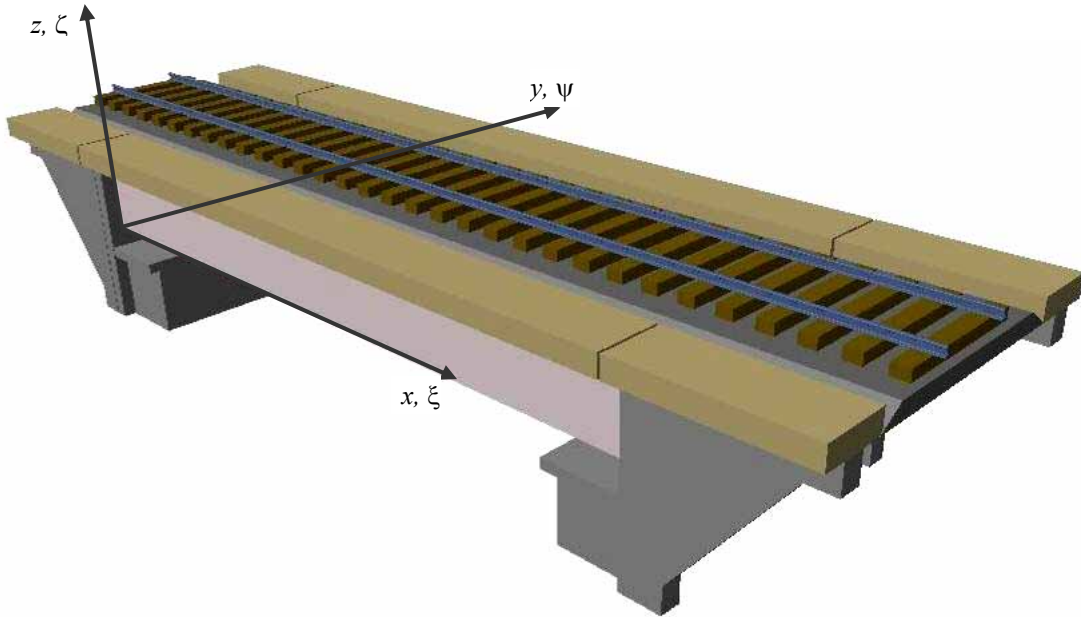


Fig. 6-1 The global coordinate system applied to geometry modelling (visualisation performed by means of DAGA program)

The relationship between the global and normalised systems is presented below:

$$\xi = x/L, \text{ where } L - \text{span length}, \quad (6-1)$$

$$\psi = y/B, \text{ where } B - \text{span width}, \quad (6-2)$$

$$\zeta = z/H, \text{ where } H - \text{span height}. \quad (6-3)$$

6.4 Defect intensity

This parameter can be defined by *defect intensity function* I_d related to the applied geometry model, i.e. E^1 , E^2 and E^3 , for each defect type separately. This function allows the representation of defect intensity distribution for the entire span. For defect types such as *loss of material* (concrete and reinforcement) the geometry models E^2 and E^3 , depending on applied structural model, can be introduced. The geometry model E^1 , where the vertical coordinate is eliminated, is not sufficient, because of importance of the analysed defect location along the vertical ζ axis. In this study, the Author has assumed constant distribution of material parameters along the cross section height (ζ axis) and the variable distribution along the span length (ξ axis) and width (ψ axis) depending on the considered model. Taking into account the assumptions the geometry models E^1 and E^2 can be applied.

6.4.1 Loss of concrete

From among various defect types influencing the load capacity, this defect is the most irregular in terms of its distribution of parameters. The proper modelling of concrete loss

requires its description along all of the coordinates. Only question is, if the coordinate ψ , parallel to the lateral axis of the span, should be included. For the simplified geometry, i.e. simply supported beam and its longer length, this coordinate may be omitted. The crucial meaning has the vertical axis ζ , which is considered during the strength evaluation. The analysis of efficiency of models with and without the ψ coordinate will be presented and discussed in Section 6.7 of this Chapter.

For constructions modelled using E^2 geometry model *defect intensity function* is expressed by the following formula:

$$I_d^{L,c}(\xi, \zeta) = \frac{\Delta w(\xi, \zeta)}{w(\xi, \zeta)}, \quad (6-4)$$

where:

$\Delta w(\xi, \zeta)$ – width reduction of the element at the point (ξ, ζ) measured along the “y” axis,

$w(\xi, \zeta)$ – designed element width at the point (ξ, ζ) measured along the “y” axis.

In the methodology proposed by Bień (2002) this defect is related to the element thickness (parallel to the vertical axis ζ). For concrete structures, modification of the thickness can be interpreted ambiguously in terms of the strength analysis. In Author’s opinion this defect should refer to the width and location of the damaged layer.

In case of the E^3 geometry model by the intensity function is presented below:

$$I_d^{L,c}(\xi, \psi, \zeta) = \begin{cases} 1 - \text{at the points, where loss of concrete occurred} \\ 0 - \text{at the other points of the structure} \end{cases}. \quad (6-5)$$

6.4.2 Loss of reinforcement

Loss of reinforcement modelled using E^2 geometry the *defect intensity function* can be evaluated by the following formula:

$$I_d^{L,s}(\xi, \zeta) = \frac{\Delta A_s(\xi, \zeta)}{A_s(\xi, \zeta)}, \quad (6-6)$$

where:

$\Delta A_s(\xi, \zeta)$ – reduction of the area of cross section of the reinforcement at the point (ξ, ζ) ,

$A_s(\xi, \zeta)$ – designed area of reinforcement at the point (ξ, ζ) .

In case of the E^3 model class the *defect intensity function* is expressed as follows:

$$I_d^{L,s}(\xi, \psi, \zeta) = \begin{cases} 1 - \text{at the points, where loss of reinforcement occurred} \\ 0 - \text{at the other points of the element} \end{cases} \quad (6-7)$$

6.4.3 Concrete Strength reduction

This defect has been distinguished into the compressive and tensile strength. Though the tensile strength has a secondary meaning, the Author has left the possibility of analysis for this material parameter as well. The defect intensity function for **compressive strength reduction in concrete**, modelled by means of E^1 , can be evaluated as follows:

$$I_d^{\sigma,c}(\xi) = \frac{\Delta\sigma_{c,c}(\xi)}{\sigma_{c,c}(\xi)}, \quad (6-8)$$

where:

$\Delta\sigma_{c,c}(\xi)$ – reduction of the compressive strength of concrete in cross section situated at the point (ξ) ;

$\sigma_{c,c}(\xi)$ – designed compressive strength of concrete at the point (ξ) .

In case of the E^2 geometry model the *defect intensity function* can be expressed by the following equation:

$$I_d^{\sigma,c}(\xi, \psi) = \frac{\Delta\sigma_{c,c}(\xi, \psi)}{\sigma_{c,c}(\xi, \psi)}, \quad (6-9)$$

where:

$\Delta\sigma_{c,c}(\xi, \psi)$ – reduction of the compressive strength of concrete in cross section situated at the point (ξ, ψ) ;

$\sigma_{c,c}(\xi, \psi)$ – designed compressive strength of concrete at the point (ξ, ψ) .

The defect intensity function for **tensile strength reduction in concrete**, modelled by means of E^1 geometry model can be expressed by the following equation:

$$I_d^{\sigma,t}(\xi) = \frac{\Delta\sigma_{t,c}(\xi)}{\sigma_{t,c}(\xi)}, \quad (6-10)$$

where:

$\Delta\sigma_{t,c}(\xi)$ – reduction of the tensile strength of concrete in cross section situated at the point (ξ) ,

$\sigma_{t,c}(\xi)$ – designed tensile strength of concrete at the point (ξ) .

In this case the defect intensity distribution along the span axis (ξ) has been considered.

For the E^2 geometry model the defect intensity function for this damage can be evaluated as follows:

$$I_d^{\sigma,c}(\xi, \psi) = \frac{\Delta\sigma_{t,c}(\xi, \psi)}{\sigma_{t,c}(\xi, \psi)}, \quad (6-11)$$

where:

$\Delta\sigma_{t,c}(\xi, \psi)$ – reduction of the tensile strength of concrete in cross section situated at the point (ξ, ψ);

$\sigma_{t,c}(\xi, \psi)$ – designed tensile strength of concrete at the point (ξ, ψ).

Concerning the E^2 geometry model these defect (the compressive as well as tensile strength in concrete) intensity distribution can be analysed considering the span length (ξ) and its width (ψ). The defect intensity distribution along the height of cross section (ζ) is considered as constant.

6.4.4 Elastic modulus reduction in concrete

Defect intensity function for the elastic modulus reduction in concrete modelled by the E^1 geometry model can be expressed as follows:

$$I_d^{E,c}(\xi) = \frac{\Delta E_c(\xi)}{E_c(\xi)}, \quad (6-12)$$

where:

$\Delta E_c(\xi)$ – reduction of the elastic modulus of concrete in cross section situated at the point (ξ),

$E_c(\xi)$ – designed elastic modulus of concrete at the point (ξ).

For the E^2 geometry model the following defect intensity function can be applied:

$$I_d^{E,c}(\xi, \psi) = \frac{\Delta E_c(\xi, \psi)}{E_c(\xi, \psi)}, \quad (6-13)$$

where:

$\Delta E_c(\xi, \psi)$ – reduction of the elastic modulus of concrete in cross section situated at the point (ξ, ψ),

$E_c(\xi, \psi)$ – designed elastic modulus of concrete at the point (ξ, ψ).

6.4.5 Strength reduction in reinforcement

For the E^1 geometry model the defect intensity function, regarding the strength reduction in reinforcement, can be expressed by the following equation:

$$I_d^{\sigma,s}(\xi) = \frac{\Delta\sigma_s(\xi)}{\sigma_s(\xi)}, \quad (6-14)$$

where:

$\Delta\sigma_s(\xi)$ – reduction of the strength of reinforcement in cross section situated at the point (ξ),

$\sigma_s(\xi)$ – designed compressive strength of reinforcement at the point (ξ).

This model includes the intensity distribution along the span axis (ξ) only. In order to include also the ψ axis the E^2 model is necessary.

The defect intensity function for E^2 geometry model is expressed by the following equation:

$$I_d^{\sigma,s}(\xi, \psi) = \frac{\Delta\sigma_s(\xi, \psi)}{\sigma_s(\xi, \psi)}, \quad (6-15)$$

where:

$\Delta\sigma_s(\xi, \psi)$ – reduction of the strength of reinforcement in cross section situated at the point (ξ, ψ),

$\sigma_s(\xi, \psi)$ – designed strength of reinforcement in cross section situated at the point (ξ, ψ).

6.4.6 Elastic modulus reduction in reinforcement

The defect intensity function for this defect type, using the E^1 geometry model, can be evaluated by the following equation:

$$I_d^{E,s}(\xi) = \frac{\Delta E_s(\xi)}{E_s(\xi)}, \quad (6-16)$$

where:

$\Delta E_s(\xi)$ – reduction of the elastic modulus of reinforcement in cross section situated at the point (ξ),

$E_s(\xi)$ – designed elastic modulus of reinforcement at the point (ξ).

Using this model the defect distribution along the span axis (ξ) only is considered.

In case of the E^2 geometry model the defect intensity function is expressed as follows:

$$I_d^{E,s}(\xi, \psi) = \frac{\Delta E_s(\xi, \psi)}{E_s(\xi, \psi)}, \quad (6-17)$$

where:

$\Delta E_s(\xi, \psi)$ – reduction of the elastic modulus of reinforcement in cross section situated at the point (ξ, ψ) ,

$E_s(\xi, \psi)$ – designed elastic modulus of reinforcement at the point (ξ, ψ) .

This model allows considering the defect intensity distribution also along the lateral direction ψ . Concerning the vertical direction ζ , this defect distribution is constant.

6.5 Defect extent

To express this parameter (E_d) the defect presence function e_d is introduced. This function is based on defect intensity function I_d described for particular defect types in Section 6.4 and can be expressed by the formulas listed below in regarding the geometry model class. For E^1 geometry model the occurrence function e_d is expressed by (6-18).

$$e_d(\xi) = \begin{cases} 1 & \text{for } I_d(\xi) \neq 0 \\ 0 & \text{for } I_d(\xi) = 0 \end{cases} \quad (6-18)$$

In case of E^2 geometry model class, this function can be described by (6-19).

$$e_d(\xi, \zeta) = \begin{cases} 1 & \text{for } I_d(\xi, \zeta) \neq 0 \\ 0 & \text{for } I_d(\xi, \zeta) = 0 \end{cases} \quad (6-19)$$

For E^3 geometry model the occurrence function e_d is expressed by (6-20).

$$e_d(\xi, \psi, \zeta) = \begin{cases} 1 & \text{for } I_d(\xi, \psi, \zeta) \neq 0 \\ 0 & \text{for } I_d(\xi, \psi, \zeta) = 0 \end{cases} \quad (6-20)$$

The defect extent parameter E_d proposed by Bień (2002) is expressed as it has been presented in the equations (6-18) to (6-20) above. The Author of this study has made the next step by integrating these expressions to create new forms of this parameter for various geometry models. This solution represents the defect extent much better, because it returns a number, i.e. percentage, related to the real defect extent. This parameter varies between 0.0 (defect has not appeared) and 1.0 (defect has occupied entire domain, i.e. space).

For geometry model E^1 the *defect extent function* has the following formula depending on applied geometry model class:

$$E_d = \int e_d(\xi) d\xi . \quad (6-21)$$

In case of geometry model E^2 the following formula has been introduced:

$$E_d = \iint e_d(\xi, \zeta) d\xi d\zeta . \quad (6-22)$$

Regarding geometry model E^3 the following formula has been introduced:

$$E_d = \iiint e_d(\xi, \psi, \zeta) d\xi d\psi d\zeta . \quad (6-23)$$

An example of *extent* parameter distribution (for geometry model E^1) is presented in Fig. 6-2.

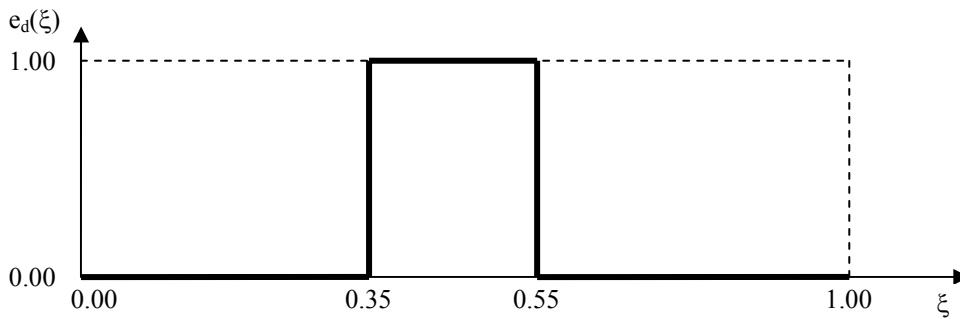


Fig. 6-2 Example of evaluation *defect extent* parameter for geometry model E^1

By this function defect extent parameter E_d can be evaluated in simple way like follows:

$$E_d = (0.55 - 0.35) \cdot 1.00 = 0.20 = 20\% . \quad (6-24)$$

For other geometry models evaluation of this parameter is analogical.

6.6 Defect location

According to the methodology presented by Bień (2002) the extent (E_d) and location (L_d) parameters are expressed by the same formulas, see the equations from (6-18) to (6-20). It is expected that these values represent different parameters. In order to attribute them a proper meaning another expressions have been proposed. The defect location L_d can be based on defect intensity function I_d (section 6.4) or by the defect occurrence function e_d (section 6.5). From the geometrical point of view the defect location L_d is expressed as a gravity centre point of the occurrence or intensity function graph. This parameter can be expressed for each of observed defects separately.

For geometry model E^1 the defect extent function has the following formula:

$$L_d = \left(\frac{\int \xi \cdot f_d(\xi) d\xi}{\int f_d(\xi) d\xi} \right). \quad (6-25)$$

In case of geometry model E^2 the following formula has been introduced:

$$L_d = \left(\frac{\iint \xi \cdot f_d(\xi, \zeta) d\xi d\zeta}{\iint f_d(\xi, \zeta) d\xi d\zeta}, \frac{\iint \zeta \cdot f_d(\xi, \zeta) d\xi d\zeta}{\iint f_d(\xi, \zeta) d\xi d\zeta} \right). \quad (6-26)$$

Regarding geometry model E^3 the following formula has been introduced:

$$L_d = \left(\frac{\iiint \xi \cdot f_d(\xi, \psi, \zeta) d\xi d\psi d\zeta}{\iiint f_d(\xi, \psi, \zeta) d\xi d\psi d\zeta}, \frac{\iiint \psi \cdot f_d(\xi, \psi, \zeta) d\xi d\psi d\zeta}{\iiint f_d(\xi, \psi, \zeta) d\xi d\psi d\zeta}, \dots, \frac{\iiint \zeta \cdot f_d(\xi, \psi, \zeta) d\xi d\psi d\zeta}{\iiint f_d(\xi, \psi, \zeta) d\xi d\psi d\zeta} \right). \quad (6-27)$$

In these expressions the function f_d can be the defect intensity function I_d or the defect occurrence function e_d . In case of the presented example in Fig. 6-2 location is equal to 0.45.

Another example presented in Fig. 6-3 illustrates in the better way these parameters. The maximum value of this function should be understood as defect intensity I_d , the area of this graph (A) can be interpreted as defect extent E_d and the center of gravity of this area (ξ_0) is the defect location L_d .

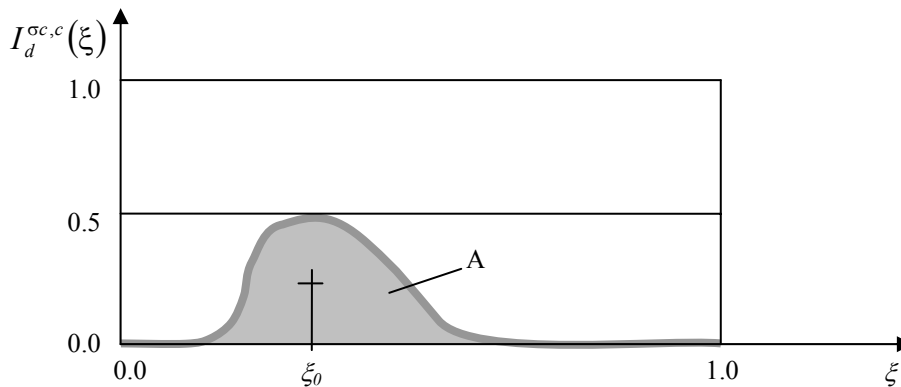


Fig. 6-3 Intensity distribution of concrete strength changes in bridge span modeled in E^1 geometry model class

6.7 Analysis of the simplified model efficiency

6.7.1 Introduction

As it has been presented in the section 2.2, the biggest population of railway bridge structures are spans situated along single tracks. For this reason a possibility of the structural model simplification by eliminating the lateral coordinate ψ (see Fig. 6-1) seems to be reasonable to discuss. The objective of this section is to present the range of application for the simplified model and to propose a methodology of railway RC slab span assessment, for which this simplification is unsuitable.

For longer spans (more than 15.0m of span length) this simplification could be justified, because the considered constructions works as beams and the internal force distribution along the mentioned lateral axis “y” is uniform. In case of shorter span lengths, especially when the ratio L/B (span length and span width respectively) is close to one, the situation is more complicated. The considered construction works as a slab and the internal force distribution along the “y” axis is not uniform.

Another problem is a defect occurrence which influences the element stiffness (for example loss of reinforcement or elastic modulus reduction in concrete) and causes the disturbance of internal forces distribution.

In the previous sections the modeling methodology, using E^1 , E^2 and E^3 geometry model classes, has been presented. The considered construction types (slab spans) are flat and coordinate ζ (parallel to the slab height) from the static point of view has a meaning in terms of the influence on the element stiffness only. The discussion presented in this section is related to the possibility of application of models created in a 1D space, i.e. (e^1, s^1) , against the models built in the 2D space, i.e. (e^1, s^2) , where the lateral coordinate “y” (see Fig. 6-1) is taken into account.

6.7.2 Geometry

To analyse the efficiency of (e^1, s^1) geometry model, several span cases (with various lengths) have been considered. In Fig. 6-4 a schematic bridge span geometry is presented. In order to perform required analyses the program SAP has been used. The RC slab has been substituted by a grillage composed of bar elements.

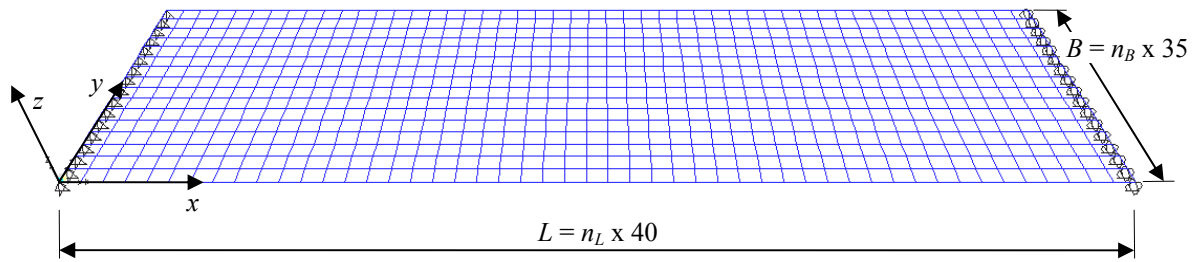


Fig. 6-4 Geometry of the considered bridge span model, where n_B – number of the longitudinal bar elements across the span length (constant value, $n_B=17$), n_L – number of the transversal bar elements along the span length (variable value); dimensions expressed in centimeters

The geometry parameters of applied grillage construction are presented in Table 6-4. By modifying the number of transverse elements it is possible to obtain various span lengths and in this way six various span have been analysed ($L = 19.6, 15.2, 10.0, 8.0, 6.0$ and 4.0 meters).

Table 6-4 Geometry parameters, dimensions expressed in centimeters

	Height	Width	Number of elements					
Longitudinal	90	40	17					
Transversal	90	35	49	38	25	20	15	10
			1960	1520	1000	800	600	400
			Span length					

6.7.3 Material

Concerning the material the following values of modulus of elasticity (for concrete and steel) has been considered:

- Elastic modulus of the concrete, $E_c = 24.0$ GPa;
- Elastic modulus of the steel, $E_s = 200.0$ GPa.

6.7.4 Loads

The intensities of applied loads (dead and moving) are related to the PN-85/S-10030.

Concerning the **dead load** each longitudinal element is subjected by the linear uniformly distributed load of 1.4 kN/m intensity. This load is an equivalent of the track elements (railway, ballast) and concrete sidewalks. Regarding the RC slab the volumetric weight 24.0 kN/m³ of concrete has been applied.

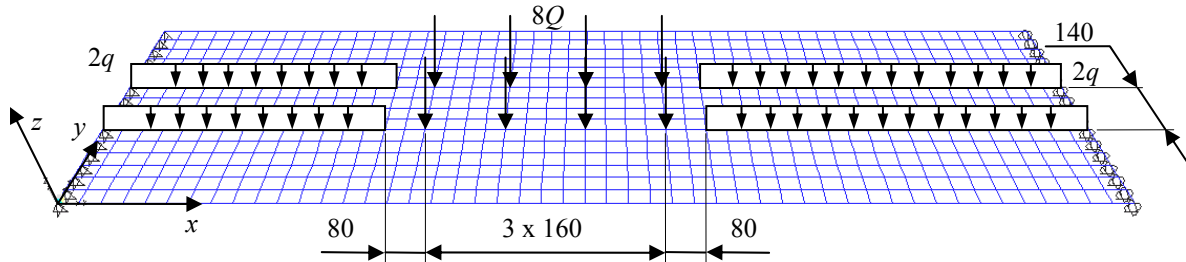


Fig. 6-5 Schema of the applied moving load according to the PN-85/S-10030, where q – intensity of the uniform load, Q – intensity of the concentrated load, dimensions expressed in centimeters

The **moving load** consists of the eight concentrated forces (four axles of the train) of 150 kN intensity and the uniformly distributed load of 48kN/m intensity. In Fig. 6-5 a schematic moving load causing the maximal bending moment in the middle of the span is presented.

All of these forces (moving load) have been transformed into the superficial uniformly distributed loads as a consequence of the significant thickness of bridge deck layers (i.e. rails, sleepers, ballast and slab). In Fig. 2-17 and Fig. 2-18 a distribution of the applied load, along the longitudinal and transversal direction respectively, is presented.

The combination of the applied loads is expressed by the formula (6-28) below:

$$M = \gamma_{g1} \cdot M_{g1} + \gamma_{g2} \cdot M_{g2} + \gamma_q \cdot M_q \quad (6-28)$$

where:

M – bending moment caused by the combination of all the loads,

M_{g1} – bending moment caused by the equivalent of the track elements (railway, ballast) and concrete sidewalks,

M_{g2} – bending moment caused by the weight of the concrete slab,

M_q – bending moment caused by the moving load,

$\gamma_{g1} = 1.5$ – load factor for non-constructural elements,

$\gamma_{g2} = 1.2$ – load factor for constructional elements,

$\gamma_{g2} = 1.5$ – load factor for moving load.

6.7.5 Analysis of structures without defects

The objective of this section is to establish a range of application for the simplified geometry model (e^1 , s^1). The analysis is composed of several bridge span cases distinguished by the span length L_t (4.0; 6.0; 8.0; 10.0; 15.2 and 19.6 meters) and slab depth H (0.3; 0.6 and 0.9 meters) – 18 cases. Each structure has been subjected to the same load combination presented in the section 6.7.4. This analysis, focused on the bending moment distribution of the

longitudinal elements, is concentrated on the cross section located in middle of the span (where $\xi = 0.5$). The ratio between the maximal (located in the middle of cross section, $\psi = 0.5$) and average bending moment (according to the value obtained by means of the (e^1, s^1) geometry model class) has been considered. The results of this analysis are presented in Fig. 6-6. The low value of this ratio means the uniform distribution of internal forces (in the considered cross section) and the possibility of application of the simplified geometry model.

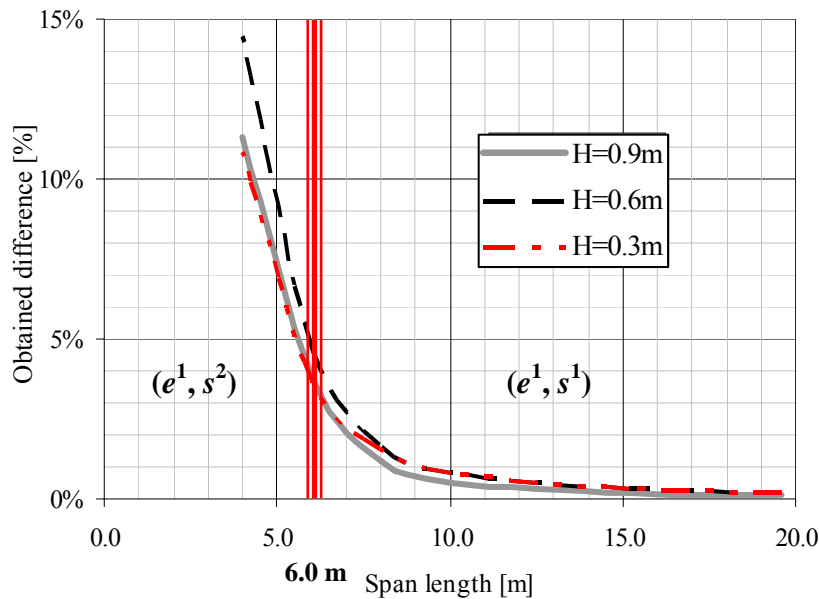


Fig. 6-6 The percentage difference between the maximal and average bending moment in cross section located in the middle of the span in the function of span length evaluated for various slab heights

In this study the Author considered the 5% of this ratio as a classifying criterion. For spans of at least 6.0 meters length the distribution of internal forces is almost uniform. For shorter bridges more advanced model (i.e. grillage or slab) is required. As it has been mentioned before, the analysis was performed for various slab depth. This factor influences the results, but its coexistence with variable distribution of moving load through the cross section layers makes this relationship more uniform.

The presented results allow applying the simplified geometry model for undamaged slab spans of length at least 6.0m. The proposed model can be also used for damaged structures with uniformly distributed defects along the considered cross section. Possibilities of defect distribution disturbance will be analysed in the next section.

6.7.6 Analysis of structures with defects

The possibility of application of (e^1, s^1) model class gives engineer a very fast (and easy to check as well) tool for load capacity assessment of not damaged railway slab spans. As it has been presented in the previous section the undamaged bridge spans, but non shorter than 6.0

meters, can be assessed by means of the (e^1, s^1) class model. For shorter structures more sophisticated model (at least (e^1, s^2)) is required. If along the analysed cross section the defect intensity is constant, then model class (e^1, s^1) can be applied as well. The situation becomes more complicated, when construction is with defects influencing its rigidity and the defect intensity is not constant. The redistribution of internal forces makes the considered model complicated and much more difficult to assess. The aim of this section is to distinguish a group of damaged spans (longer than 6 meters) for which the (e^1, s^1) class model can be applied. Several parametric analyses of the load capacity evaluation have been performed. In the Table 6-5 the considered parameters of the performed analyses are presented. The slab height and material parameters are set in order to obtain the maximal effort of cross section in the middle of the span.

Table 6-5 Material and geometry parameters applied in the analysis

L_t [m]	H [mm]	R_c [Mpa]	R_s [Mpa]	ρ [%]
6.0	400	40	180	0.980
8.0	500	40	200	1.079
10.0	500	50	300	1.143
15.2	700	50	450	1.011
19.6	800	50	500	1.333

The reinforcement ratio is approximately equal to 1.0% in order to assure the proper cooperation between concrete and steel.

The most common and severe defect which causes the stiffness modification is loss of reinforcement. Loss of concrete occurs mainly in the tensile zone. The compressive part of cross section is usually covered by track components and for this reason influence of this defect has been omitted and only reinforcement losses have been taken into consideration. Concerning the defect intensity, several levels (5%, 10%, 15% and 20%) were analysed. The defect extent of 0.24 of asymmetrical location (see Fig. 6-7) has been applied.

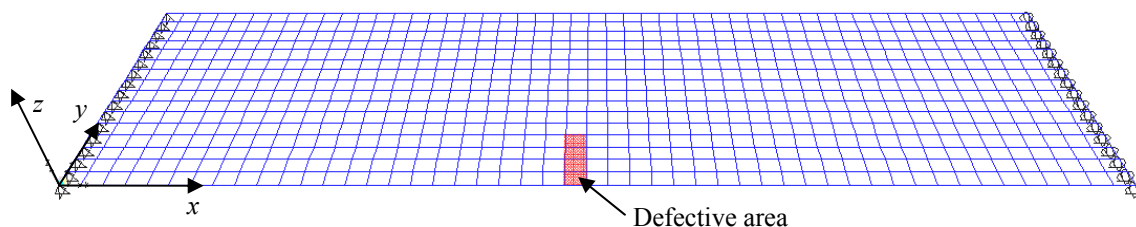


Fig. 6-7 Defect scenario

For each bridge case (each span length and each defect intensity) the load capacity is being evaluated as the load class coefficient α (factor for the moving load class) according to the PN-85/S-10030. It means that, the objective is to find (by an iteration process) the maximal

value of the α coefficient, for which the maximal acceptable effort of the construction is reached. In the next step the obtained values of the α coefficient are being compared with bridge span cases damaged by the same defect but with constant intensity along the considered cross section.

An example of the load capacity analysis for the considered cross section is presented in Fig. 6-8. Both graphs present the same defect (in terms of its intensity against the analysed cross section) occurred in the middle of the 6.0 meters span. Fig. 6-8 Fig. 6-9

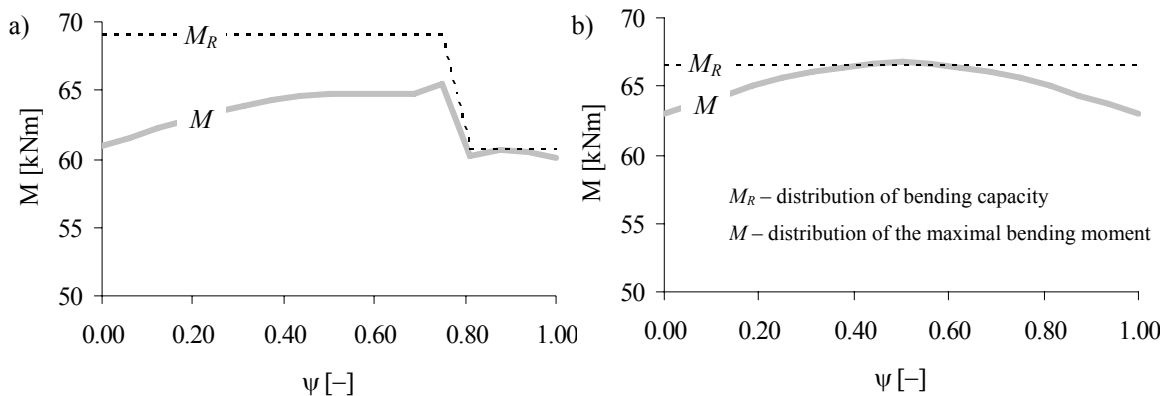


Fig. 6-8 Comparison of different defect modeling ways for the span of 6.0m length and reinforcement loss of 15% intensity; a) concentrated and asymmetrically located defect; b) uniformly distributed defect; obtained difference: 7.5%

The graph on the left (Fig. 6-8a) presents the concentrated reinforcement loss of 15% intensity. This defect causes a local reduction of the bending capacity M_R and lower contribution in the internal forces transmission M . It can be observed, that the load capacity in this section is reached ($M = M_R$). The graph on the right (Fig. 6-8b) can be understood as an alternative assessment way. In Fig. 6-8a loss of reinforcement is substituted by a uniformly distributed defect. The bending capacity M_R has been reduced along the entire cross section. This operation generates some difference regarding the previous solution. In this figure the load capacity has been reached as well, but the α coefficient is 7.5% higher than in Fig. 6-8a. The presented percentage difference can be considered as a measure of efficiency of proposed class model (e^1, s^1). If this difference is equal or less than 5%, then considered case can be understood as applicable for analysis by means of the simplified (e^1, s^1) geometry model. Otherwise this model (e^1, s^1) cannot be applied.

Another analysis example is presented in Fig. 6-9. In this case the span length is equal to 15.2m and the structure is damaged by loss of reinforcement of 20% intensity. On the left (Fig. 6-9a) this defect is applied asymmetrically and the bending capacity is reached. Like in the previous example this defect causes a local reduction of the bending capacity M_R and lower

contribution in the internal forces M transmission of the cross section. In order to reach the load capacity M_R for the damaged structure presented in Fig. 6-9, the moving load should be increased 15% (α coefficient), which also eliminates this situation. The presented examples in Fig. 6-8 and Fig. 6-9 do not allow applying the (e^1, s^1) geometry model class, but there is a group of span structures, for which this simplified model can be used. Entire results of the comparison analysis are presented in Fig. 6-10 to Fig. 6-12.

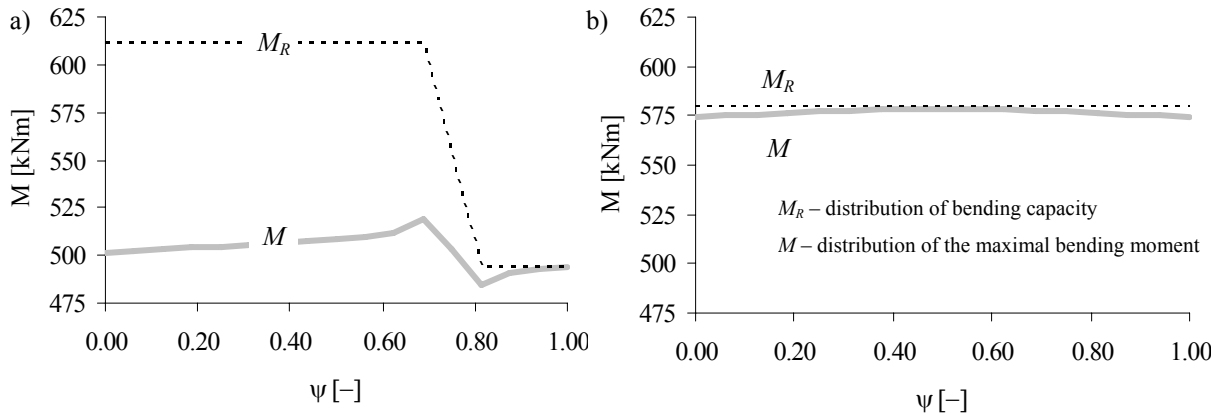


Fig. 6-9 Comparison of different defect modeling ways for the span of 15.2m length and reinforcement loss of 20% intensity; a) concentrated and asymmetrically located defect; b) uniformly distributed defect; obtained difference: 15%

In Fig. 6-10 efficiency of the (e^1, s^1) geometry model class as the percentage difference of a coefficient α for moving load for various span lengths in the function of the defect intensity is presented.

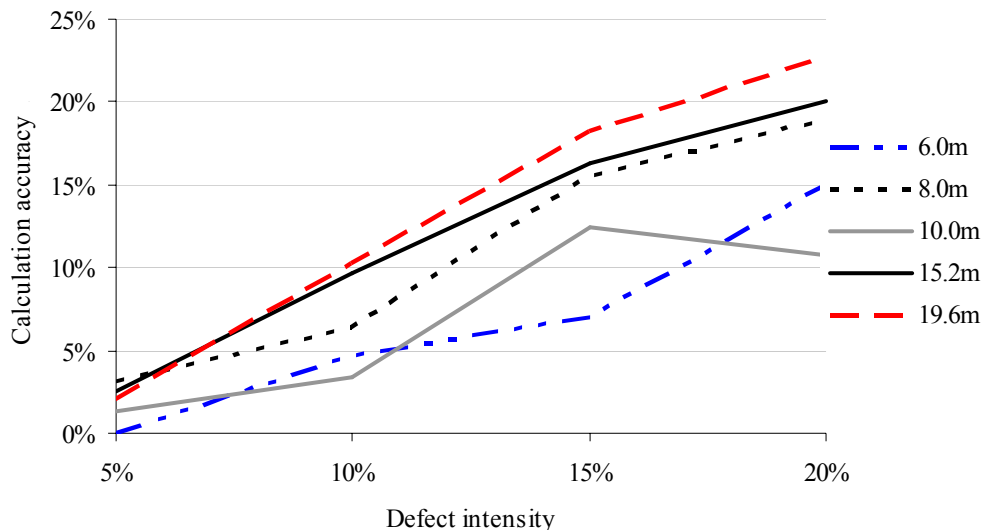


Fig. 6-10 Percentage difference of the maximal acceptable load class level (load capacity of span) in function of considered defect intensity (loss of reinforcement) evaluated by means of the (e^1, s^1) and (e^1, s^2) geometry models

The best results are obtained for the spans of 6.0 and 8.0 meters and defect intensity no higher than 10%. In case of longer spans (10.0, 15.2, and 19.6 meters) the defect intensity of 7-8%

seems to be the maximal acceptable level in terms of possibility of application. The analogical results are presented in Fig. 6-11, but instead of the α coefficient the summation of bending moment along the analysed cross section has been taken into consideration. The difference between both defect scenarios is smaller. Despite some occurred disturbance of presented relationships (especially for the span of 10.0m length and 15% of defect intensity) the tendency is that for longer spans the structure is more sensitive for model simplifications.

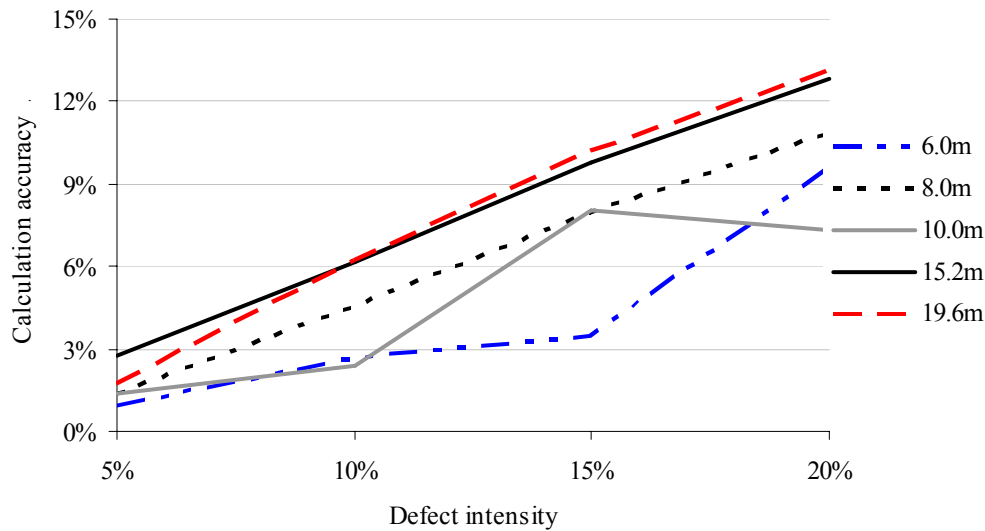


Fig. 6-11 Percentage difference of the sum of bending moment values of considered cross section (in the middle of the span) according to the maximal load class in function of considered defect intensity (loss of reinforcement) evaluated by means of the (e^1, s^1) and (e^1, s^2) geometry models

The next two figures present also the obtained results but for various defect intensities and in the function of span length. Fig. 6-12 is related to the percentage difference of the α coefficient.

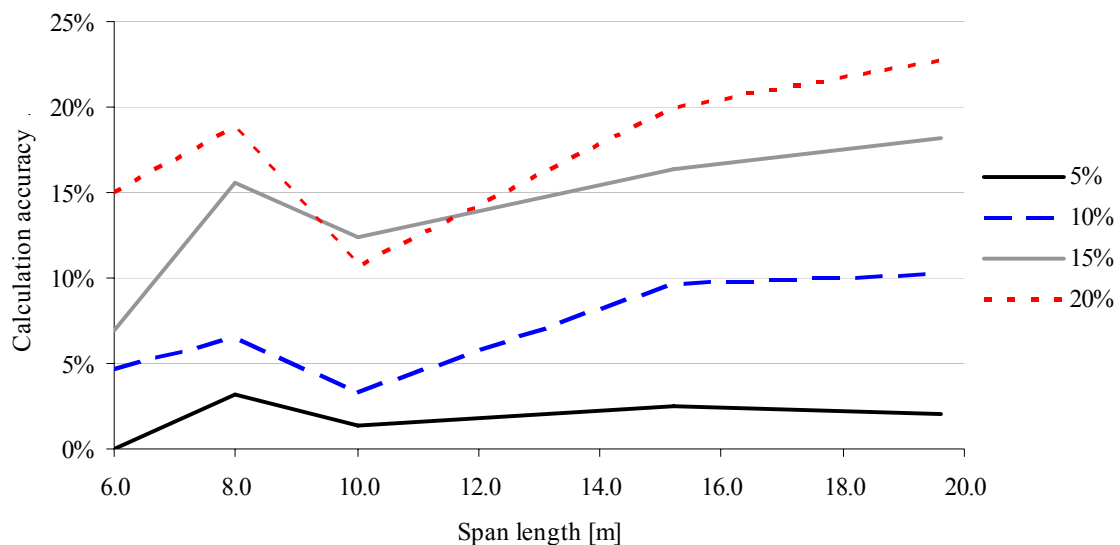


Fig. 6-12 Percentage difference of the maximal acceptable load class level (load capacity of span) in function of span length (loss of reinforcement) evaluated by means of the (e^1, s^1) and (e^1, s^2) geometry models

In case of Fig. 6-13, the percentage difference of sum of the bending moment in the analysed cross section has been considered.

Longer spans are more sensitive for the model simplification in terms of the load capacity assessment. All of these figures present this tendency.

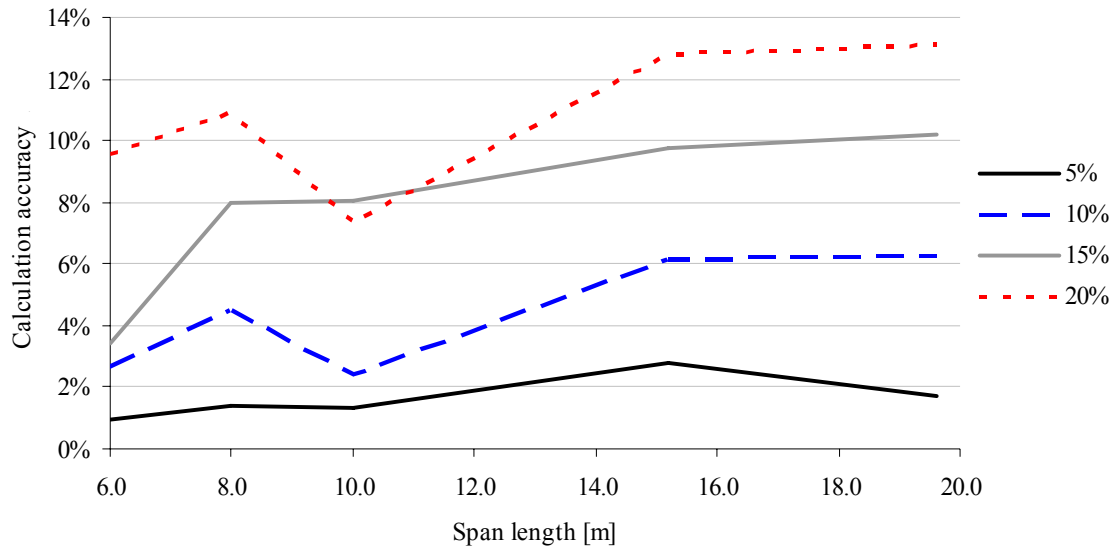


Fig. 6-13 Percentage difference of the sum of bending moment values of considered cross section (in the middle of the span) according to the maximal load class in function of span length (loss of reinforcement) evaluated by means of the (e^1, s^1) and (e^1, s^2) geometry models

The analysed defect intensities should be treated as disturbances of their distribution along the considered cross section. For example the possibility of application of an asymmetrically applied defect of 10% intensity means also the possibility for a damage of 20% intensity against the 10% intensity along the rest of cross section.

Chapter 7

Analysis of damaged structures by means of DAGA program

7.1 Introduction

During bridge service life degradation mechanisms take place causing various defects. Some of them significantly influence the bridge load capacity, which is usually the main measure of the bridge condition. Repair or strengthening of damaged constructions, evaluation of acceptable class of live load and analysis of bridge replacement conditions are the most common problems to solve for the railway infrastructure administration. Time we live is an intensive development of computer technology, data processing, testing method and advanced assessment. The objective is to combine them into the one powerful methodology.

7.1.1 Computer devices

The newest advances in the computer technology allows bridge inspector reducing the number of mistakes related to the human errors made on field inspection while updating the traditional paper-based information collected in reports, sketches, photographs, manuals etc. By means of the computer technology all of information and data collected on the field inspection can be immediately stored and integrated with data basis of bridge management systems. Inspector can also have access to the previous inspection reports and update them if necessary. The recent hardware development (supporting the bridge defects evaluation

especially identified on the field inspections) like mobile and wearable computer devices are briefly presented in this section. From among various technologies the following positions are briefly mentioned here: pen-based tablet computers, wearable computers, personal digital assistants (PDA), computer sketching, handwriting recognition, speech recognition and also photogrammetry.

Operation of the **pen-based tablet computers** requires from the user (bridge inspector) both hand. Its display allows, for example, handwriting and using the tablet computer digital pen to "gesture", e.g., scratching out digital ink on the display with a digital pen to erase the digital ink. An example of the pen-based computer is presented in Fig. 7-1.



Fig. 7-1 Example of pen-based computer provided by Lenovo Group of the IBM Personal Computing Division

If the field condition does not allow inspector using his both hands the **wearable computers** are the suitable solution. This kind of device can be attached directly to the body of the user (see an example in Fig. 7-2). Computers used on site can also be connected by means of the wireless communications with remote server.



Fig. 7-2 Example of wearable computer provided by the Simple Abilities company

In terms of data acquisition the exchange between bridge engineer and his office makes the assessment process much more effective.

7.1.2 Technologies

The data collection process may also be supported by computer sketching, write recognition as well as photogrammetry.

Though the presence of computer in bridge engineering is irreplaceable, sometime simple sketching allows engineer to express his thoughts and support his process of thinking. The **computer sketching** allows enriching existing bridge digital graphic documentation like drawings or pictures by marking symbols, lines, circles etc. Currently it is possible to convert hand-made drawing into the CAD formatted files providing also some animations (Alvarado & Davis 2001).

The **handwriting recognition** is an intelligent feature allowing the inspector writing text using electronic stylus on the electronic pad like traditionally they used to do with paper. The system automatically recognizes the writings and converts into the digital data. In case of low text accuracy a dialog box appears in order to be verified and corrected. This technology allows also entering samples of handwriting or particular letters that are difficult to recognize so it is possible to train the handwriting engine to more accurately recognize writing style. More information on this handwriting recognition can be found in the bulletin of Microsoft (Wacom 2006).

Another intelligent feature available for bridge inspectors is the **speech recognition**. This technology is essentially useful in task that requires both hand of inspector. Profits and disadvantages of this technology are presented and discussed by Neti et al. (2000). Before its operation for voice recognition training is required. In this way the measurements obtained by inspectors can be enriched by the spoken comments to be converted to the digital data and stored within bridge database. However, this system is not recommended to be applied in noisy environment.

Photogrammetry, another powerful technology, is defined as the “science of measurement from photographs” (Appraisal of existing structures 1996). The advantages of the technique are the documentary value of the photographs and the relative speed and simplicity of the measurements. Basing on the report presented by Jáuregui et al. (2006) the following aspects of photogrammetry can be underlined. The accuracy of this technique meets that of traditional hand measurements. It is possible to obtain measurements between two points, a point and a line, a point and a surface, etc. This technology allows for interaction between visual inspections, documentation study and information updating. Accuracies to within 1 to 2 mm can be obtained (Appraisal of existing structures 1996).

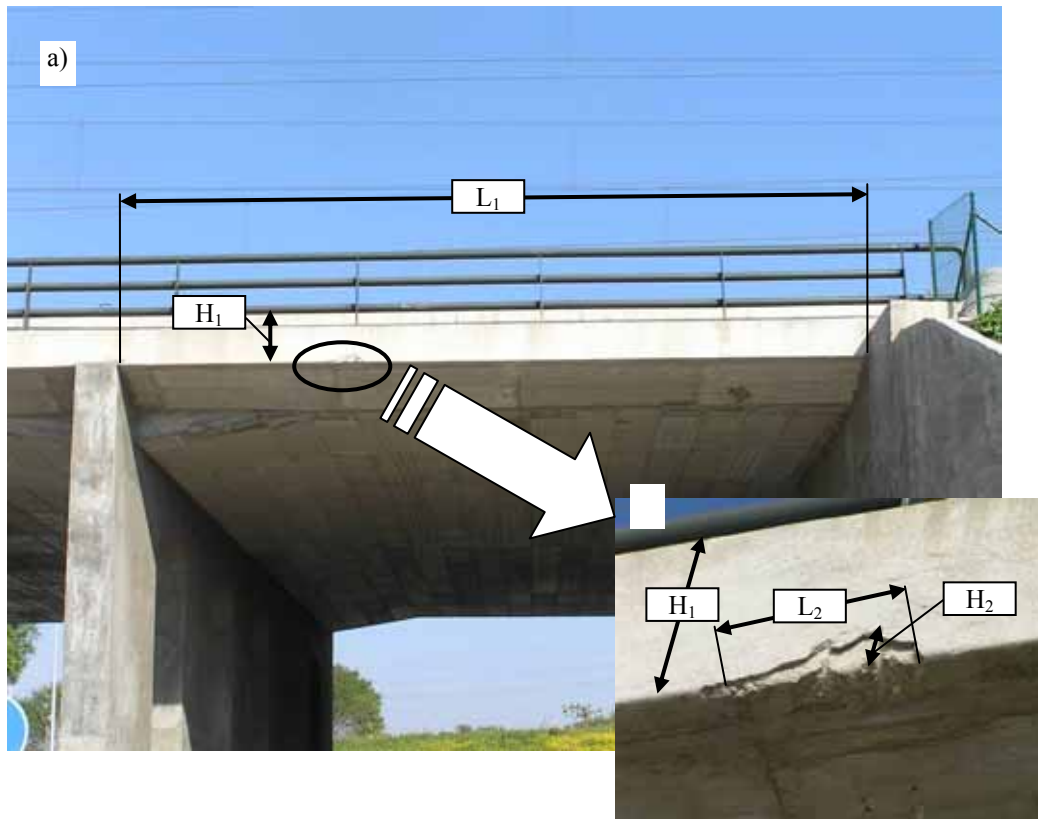


Fig. 7-3 Example of application of photogrammetry (photographed by the Author)




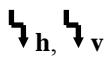








This technique can find a very practical application during visual inspection. In Fig. 7-3 an example of railway RC bridge with loss of concrete is presented. By means of photogrammetry it is possible to measure the Extent of defect occurred. In terms of real geometry no dimension needs to be measured. Only relationship between particular distances should be established. In this figure, by simple measurements made in the digital data a relationship between L_1 and L_2 as well as H_1 and H_2 allows the Extent of this defect to be measured.

7.1.3 Graphic tools for assessment of defects

Occurred defects influence the current load capacity and the further service conditions in the future. In this section the most common computer-aided tools supporting the current load capacity assessment or at least the visual inspections are presented.

One of the simplest ways is the application of the conventional marks system for defects proposed by Kushtch (1996). This system includes marks for basic defects of RC bridge constructions. In the Table 7-1 the conventional marks for RC span structure are presented. The conventional marks are drawn on diagrams of bridge elements.

Table 7-1 Conventional marks for concrete bridge defects proposed by Kushtch

Defect	Conventional Marks
Baring of working reinforcement	
Shearing of concrete	
Stalactite of concrete surface	
Crack (horizontal, vertical)	
Water flows on concrete surface	
Baring of web reinforcement	
Filtration of water	
Spalling of concrete	
Deadening of rainwater pipe	
Rainwater pipe is not long enough	
Deviation of construction surface from shuttering dimensions	
Destruction of butts of diagram beams	

The system called Inspection On Hand (IOH) developed by Trilon (1999) is a tool designed to collect and manage information extracted from field inspections. This tool is compatible with Pontis Bridge Management System (BMS). IOH allows inspectors to create complete or update inspection reports using the handheld computer with a stylus interacting with an intuitive graphic user interface. This system allows for application of handwriting recognition and sophisticated connectivity with conventional computers.

Another solution can be found in the work of Bień (2002). The computer program called SEZAM allows creating bridge models composed of non-dimensional (e^0) and one-dimensional (e^1) elements in 2D (s^2) or 3D (s^3) space. Experience of this researcher confirms the high efficiency and the practical serviceability of the presented tool. In particular cases more sophisticated evidential bridge models composed of two-dimensional (e^2) or even three-dimensional (e^3) elements is necessary. This solution has been applied in RUBIKON computer system for supporting of the long-term monitoring of bridge condition. The computer programs SEZAM as well as RUBIKON allow graphically modelling of defects by means of the built-in 2D graphic editor.

A scanning measurement system combining NDT methods (impulse radar, ultrasonic-echo and impact-echo) for 2D concrete surfaces has been developed by Stoppel & Niederleithinger (2004). The modular system is adapted and tested with the special demands on railway concrete box girder bridges. The system allows the locating of reinforcement and tendon

ducts as well as the detection of compaction faults, injection faults and honeycombing with a high accuracy in positioning and reproducibility in a yet unknown speed. The system delivers online measurement data for all three measurement methods related to one coordinate system with an accuracy of 1 mm. The main advantage of the system is a possibility of determining the position and orientation of e.g. tendon ducts or reinforcement when no plans are available or accuracy is doubtful.

The potential mapping proposed by Jensen et al. (2006) allows evaluating the extent and rate of corrosion. This technology helps the engineer to get a good overview of corrosion and deterioration of concrete structures.

The pattern recognition method for crack classification presented by Mikumo et al. (2006) allows extracting the crack pattern parameters from digital images of slab surfaces and classifying them in order to obtain defect level.

The multi-mapping procedure presented by Wawrusiewicz (2006) couples various maps of particular RC surfaces incorporating corrosive state of reinforcement, concrete strength, the range of carbonation, the thickness of concrete cover, the contents of chlorides, the permeability of concrete cover etc. The overlapping of these maps will enable to specify the areas requiring special diagnostic control, or estimation of complex hazards of structure durability.

ScanPrint, provided by Advitam, is a set of software, database and graphic tools managing all information relating to structures, inspection, maintenance and diagnosis within a one combined tool. This system can support bridge inspectors in terms of drawings, data transmission, reporting etc. By means of the pen-based computers the bridge inspector can introduce to data base results of inspection. This system is equipped with features allowing providing photographic documentation with defects exposed and digitally processed.

7.1.4 Defect analysis

These solutions represent large effort in terms of current bridge condition appraisal, but they do not offer suitable support for defect modelling in terms of the load capacity assessment. A connection between the graphic modelling of damaged RC structures and static-strength analysis engine is still required. The main problem of existing RC bridges is corrosion of the reinforcement. In available literature there are many publications on this phenomenon (Bertagnoli et al. 2006, Capozucca 1995, Dekoster et al. 2003, Fang 2006, Fang et al. 2006, Hover 1996, Kato et al. 2006, Legat et al. 2004, Oh & Kim 2004, Rodriguez et al. 1997,

Sanchez & Venturini 2007, Shayanfar et al. 2006, Teughels et al. 2002); their reasons (Capozucca 1995, Dekoster et al. 2003); its modelling (Capozucca 1995, Oh & Kim 2004, Sanchez & Venturini 2007) and the occurred repercussions like steel-concrete debonding mechanism (Bertagnoli et al. 2006, Capozucca 1995, Fang 2006, Fang et al. 2006, Hover 1996, Shayanfar et al. 2006); load capacity (Capozucca 1995, Enochsson et al. 2006, Hover 1996, Kato et al. 2006, Oh & Kim 2004, Plos et al. 2006, Rodriguez et al. 1997, Shirakura et al. 2004, Yun et al. 2006); ductility (Capozucca 1995, Hover 1996, Kato et al. 2006) and strength of material (Bertagnoli et al. 2006, Bakhshi et al. 2006, Capozucca 1995, Dekoster et al. 2003, Plos et al. 2006, Sanchez & Venturini 2007, Shayanfar et al. 2006).

Basically two forms of corrosion occur: uniform – primarily caused by carbonation and localised – caused by the chlorides. In case of the uniform corrosion authors of the studies (Capozucca 1995, Dekoster et al. 2003, Fang et al. 2006, Kato et al. 2006, Val et al. 1995) suggest consideration the influence of the concrete-steel bond loss on the load capacity reduction. Their opinion has been proved by series of laboratory tests. On the other hand the localized corrosion leads to substantial local reductions in the bar cross-section. According to Bertagnoli et al. (2006) and Rodriguez et al. (1997) load capacity of RC elements can be evaluated by concrete compressive strength reduction (due to longitudinal cracks and spalling) and by reinforcement loss.

To evaluate the load capacity of RC elements with corroded bars only losses of material (concrete and steel) and material parameter modifications will be considered and for the steel-concrete debonding mechanism a simplified solution will be proposed.

7.2 Architecture of the DAGA program

To deal with these problems the Author has developed his own computer program called Damage Assessment Graphic Analyser (DAGA). Proposed solution enables fast and effective computer-aided analysis of damaged RC slab spans of railway bridges. The program supports the evaluation of the most frequent defects, which exert an influence on the load capacity of the span. These defect types are listed below:

- loss of concrete;
- loss of reinforcement;
- modification of strength (concrete and steel).

The aim of this program is to create a three-dimensional (3D) model of railway slab span also with defects and evaluate its load capacity. The analysis can be performed for any location,

intensity and extent of any combination of the listed defects. All information about the analysed structure are stored in a special data base of DAGA and can be used for more sophisticated analysis, e.g. by means of the finite element method (FEM). The detailed description of this program can be found in the Appendix B (DAGA – User’s Manual).

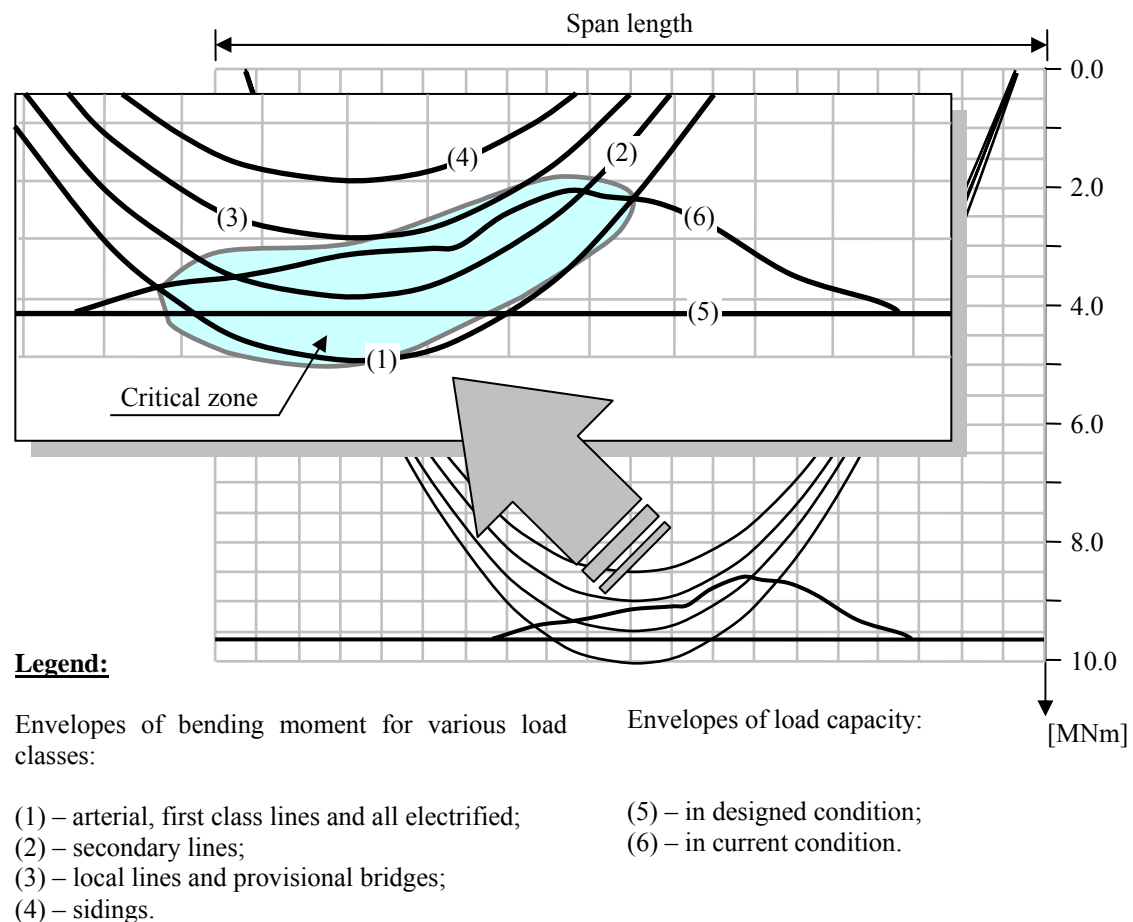


Fig. 7-4 Example result of the static-strength analysis performed by means of DAGA program

The output of this program is the graphs of the load capacity against envelopes of bending moment (see an example in Fig. 7-4). The results consists of the envelopes of bending moment (1), (2), (3) and (4) caused by various load classes and envelopes of the load capacity for the designed (5) and current (with defects) condition (6). The “critical zone” (where the value of the maximal bending moment exceeds the load capacity of the cross section) is also exposed. Obtained results can give the basis to the repair actions introduction or the moving load class reduction if the budget of railway administration is not sufficient.

Operation with this program consists of the following three steps presented in Fig. 7-5: modelling, analysis and results. The **modelling** is destined to deliver all required information on geometry, defects, material and loads by means of graphic editor to the system. Introduced information about 3D discrete model of span is saved in the data base and processed by means of SQL computer language.

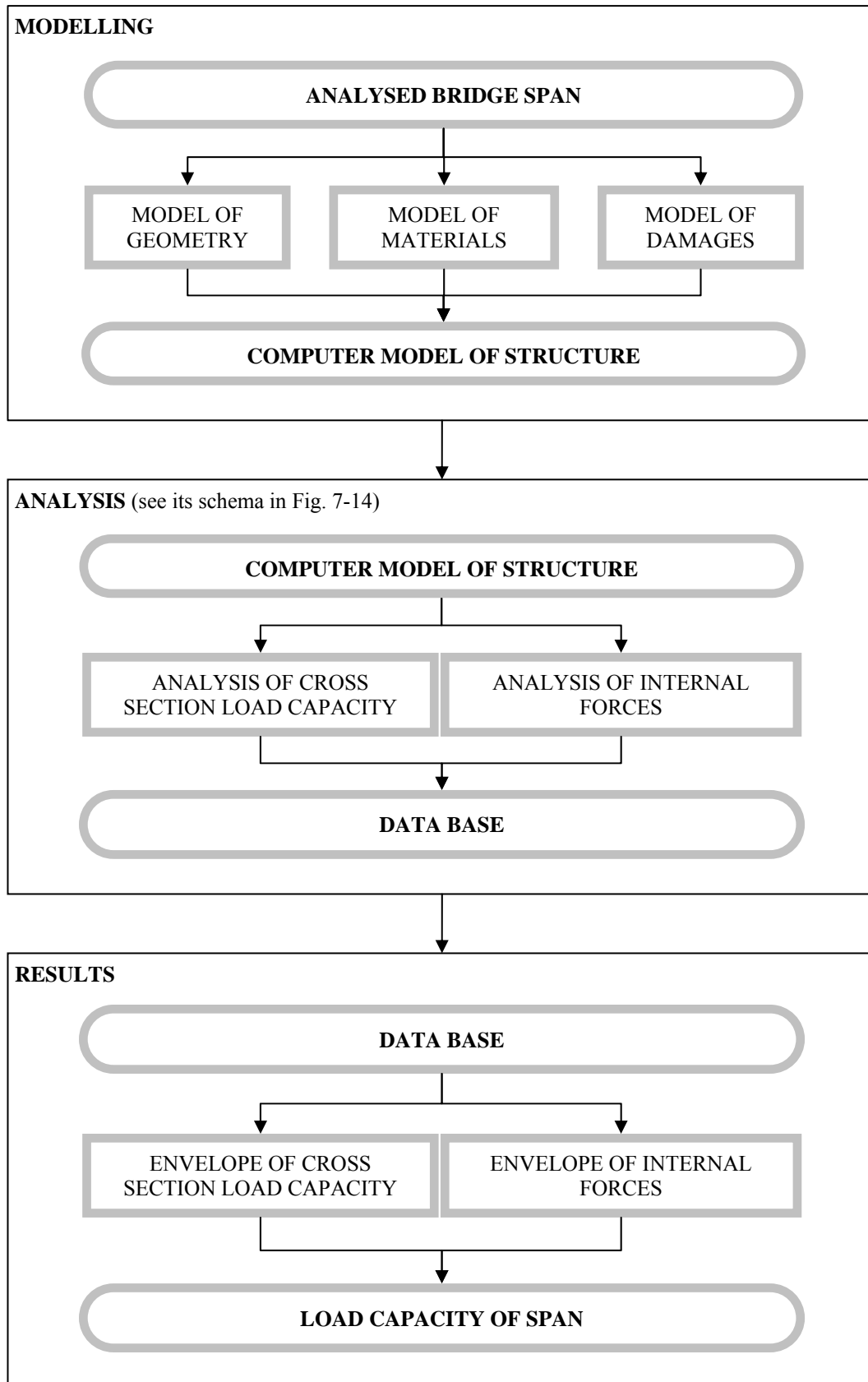


Fig. 7-5 Functional scheme of DAGA program

The model structure, created in 3D space, allows processing all this information. The **analysis** processes the data introduced before, the user selects the calculation code and DAGA performs the static-strength analysis. The **results** are the final step of procedures as graphs for

example envelopes of bending moment and load capacity and also defect intensity distributions. In order to present the possibility of application of the DAGA program a simulation of damaged railway RC slab span will be performed and discussed. In the next sections an example will be presented to show the whole assessment procedure.

7.3 Geometry

To analyse load capacity of the considered bridge structure its geometry must be provided to the system. Basically they are: length of the span, dimensions of the cross-section and some parameters of track components. To illustrate the possibilities of DAGA an example the analysis of railway RC bridge is presented in this chapter. The analysed structure of span length 16.0 meters has the bearings situated in distance of 0.5 meters from the ends of superstructure. It means that the theoretical span length L_t is equal to 15.0 meters. The dimensions of the cross-section of the considered span are presented in Fig. 7-6 below.

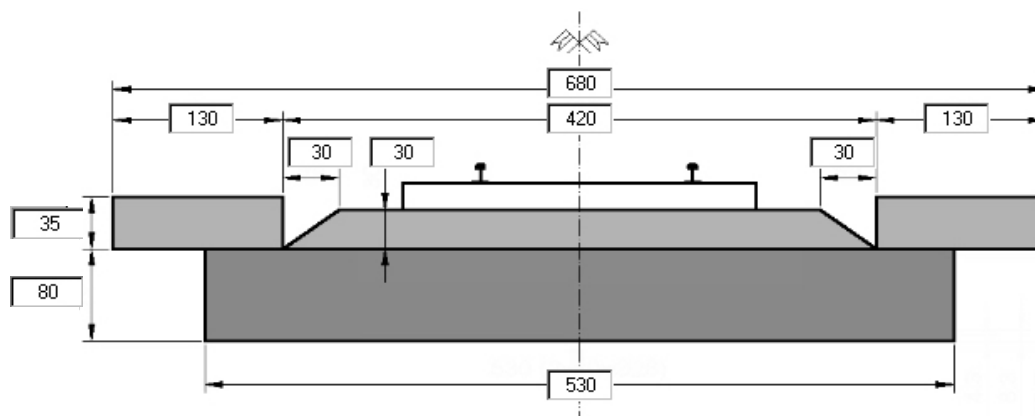


Fig. 7-6 Cross section of the analysed structure (dimensions expressed by centimetres)

The considered bridge structure (also with defects) is presented as 3D object. All information (dimensions, co-ordinates of points, defect parameters, etc.) is stored in the data base. This feature allows introducing a more sophisticated way of static and strength (i.e. Finite Element Method).

Regarding the methodology presented and discussed in Chapter 6 the load capacity assessment analysis is performed by means of the mixed model of geometry. Table 7-2 presents model classes applied in the analysis. The static analysis is performed using (e^1 , s^3) model (simply supported beam). In the case of the strength analysis the geometry model depends on the particular defect type.

Basically load capacity assessment requires the location of the damaged cross-section to be provided. The relationship between the maximal bending moment and the particular capacity of cross-section determine whether the maximal effort of cross-section is exceeded or not. To

analyse the construction in terms of the bending moment distribution the basic geometry class (e^1, s^3) is sufficient.

Regarding the material properties its uniform distribution along the particular cross-section has been assumed (basing on consultations with bridge engineers and inspectors). The assumed uniform distribution of the material properties results in applying the basic geometry class (e^1, s^3) as well.

Table 7-2 Geometry models applied in the static-strength analysis

Defect	Strength analysis	Static analysis
Loss of concrete	(e^2, s^3)	(e^1, s^3)
Loss of reinforcement		
Modification of concrete strength	(e^1, s^3)	
Modification of reinforcement strength		

Losses of material require a more precise modeling of defects, their location against the cross-section height must be provided. These features can be represented by (e^2, s^3) model class.

7.4 Loads

7.4.1 Dead load

The loads of bridge structures consist of dead and moving loads. The cross section geometry determines the intensity of dead load. In Table 7-3 intensities of dead load of the analysed railway bridge is presented.

Table 7-3 Dead load defining (in accordance to PN-85/S-10030)

Load item	Geometry of cross section of load items [cm]	Volumetric weight [kN/m ³]	Linear weight [kN/m]	Load factors	Dead load [kN/m]	
					Items	Total
railway track	-	-	1.2+1.6	1.5	4.2	193.7
ballast	0.5·(420+360)·30	20.0	23.4	1.5	35.1	
two sidewalks	2·(35·130)	24.0	21.8	1.5	32.3	
concrete slab	80·530	24.0	101.8	1.2	122.1	

7.4.2 Moving load

The moving load with the Dynamic Amplification Factor (*DAF*) has been defined in accordance to the PN-85/S-10030. The formulas of *DAF* and values of standard moving load

intensities are presented in Appendix B, section B.5. The DAF value for the considered example, evaluated according to formula (B-1), is presented below:

$$DAF = 1.212.$$

This program allows applying other DAF values, i.e. evaluated from the field tests.

7.5 Material parameters

The strength analysis requires the material parameters to be provided to the system. The following features have been introduced (according to PN-91/S-10042) as typical for the existing railway reinforced concrete bridge structures:

- strength of the bottom reinforcement: $R_{s,b} = 280 \text{ MPa};$
- strength of the top reinforcement: $R_{s,t} = 280 \text{ MPa};$
- compressive strength of the concrete: $R_c = 40 \text{ MPa};$
- elastic modulus of the reinforcement: $E_s = 200 \text{ GPa};$
- elastic modulus of the concrete: $E_c = 41.4 \text{ GPa}.$

7.6 Reinforcement

The analysed bridge structure is characterised by reinforcement of approximately 1% ratio as for a typical concrete structure.

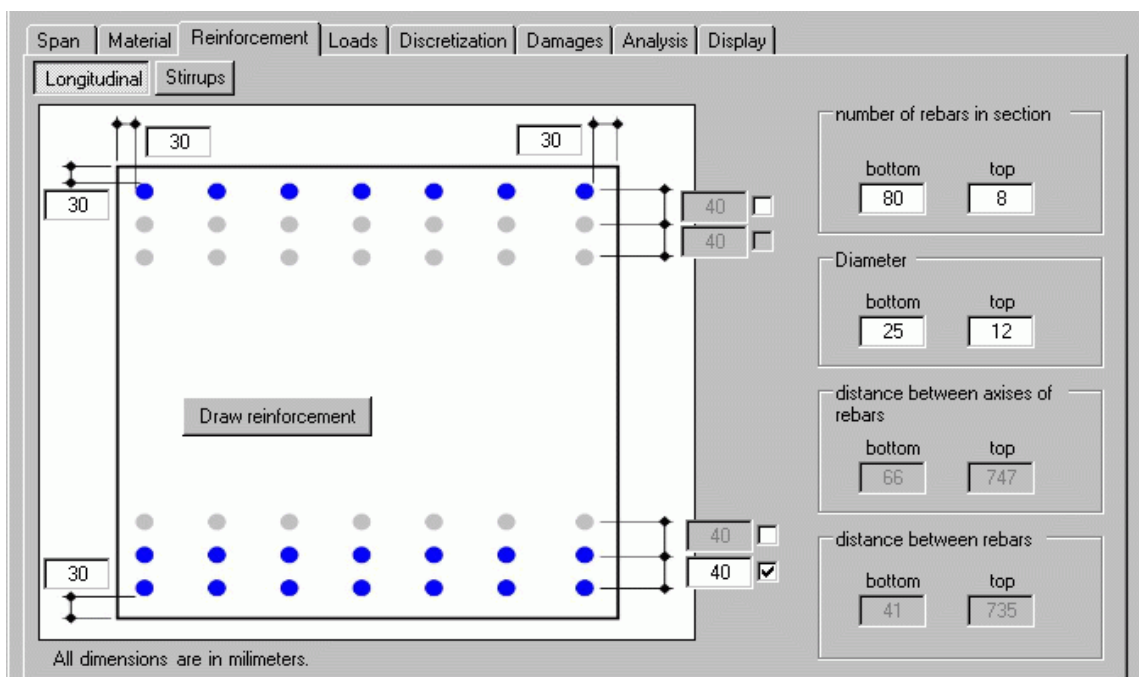


Fig. 7-7 Defining procedure for the longitudinal reinforcement

The geometry of the reinforcement is presented in Fig. 7-7. The bottom part of rebars is composed of two layers ($80\phi 25$) and the top part – single layer ($8\phi 12$).

7.7 Defects

During service life of the considered railway bridge structure the following defect types have occurred:

- Losses of the bottom reinforcement;
- Reduction of the compressive strength of the concrete;
- Reduction of the strength of the bottom reinforcement.

The DAGA program allows modelling defects and performing their visualisation.

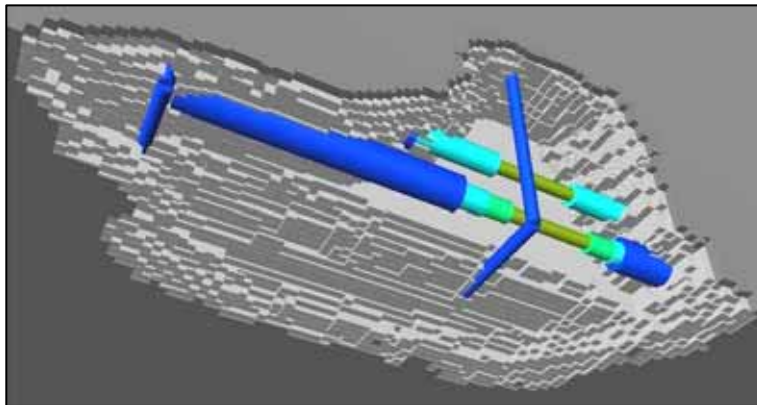
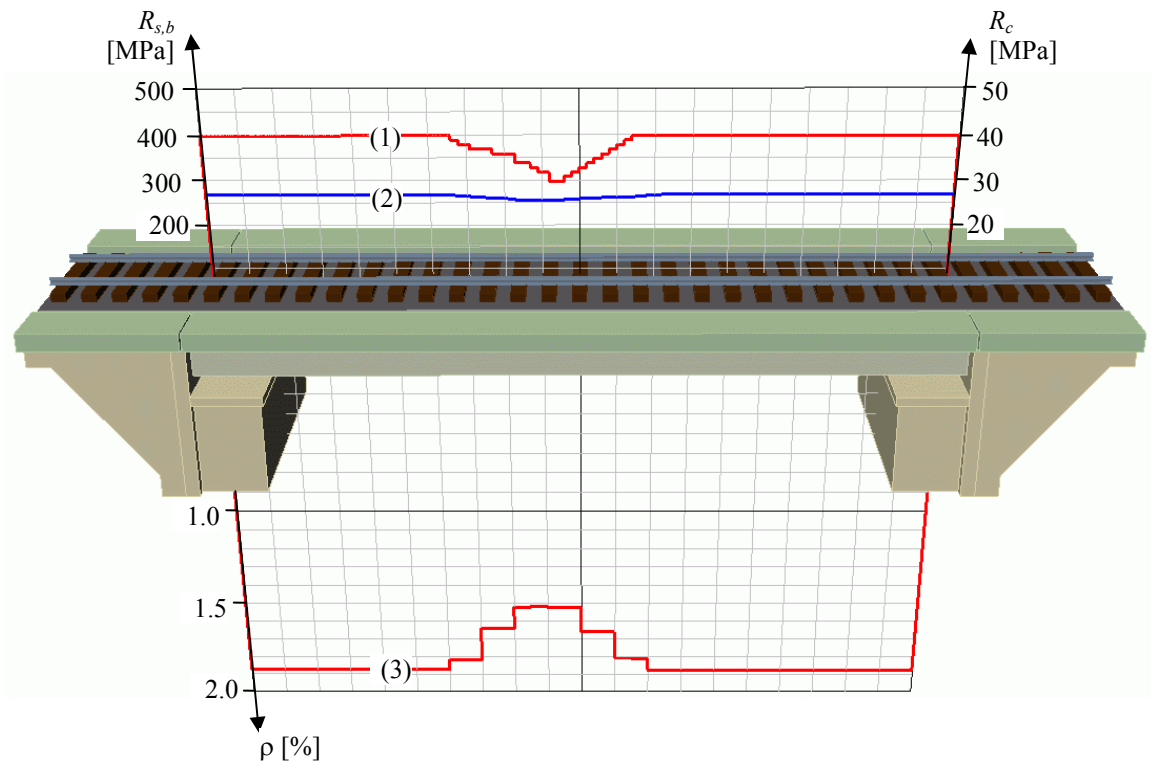


Fig. 7-8 Model of the combination of defects (loss of concrete and loss of reinforcement) visualised by means of DAGA program

In Fig. 7-8 an example of defect combination (losses of reinforcement and concrete) is presented. Applied discretisation methodology (described in the section B.6 of Appendix B) allows modelling every defect parameters. The colour of rebars as well as the diameter variation corresponds to the current condition of the concrete element. This kind of defect visualisation allows for better understanding of occurred phenomena. The presented defects influence the load capacity of the structure.

In Fig. 7-9 the distribution of occurred defects is presented. In case of the loss of steel, the distribution of the reinforcement ratio ρ has been exposed and varies between 1.87% (designed condition) and 1.52 (current condition in the worst defect case). The compressive strength of concrete σ_c varies between 40 MPa (designed condition) and 30 MPa (current condition). The maximum value of the strength of reinforcement σ_s is equal to 270 MPa (designed condition) and in the worst case this parameter is equal to 256 MPa (current condition).



Legend:

- (1) – Compressive strength of the concrete R_c [MPa] (the left axis);
- (2) – Strength of the steel in the bottom part of the reinforcement $R_{s,b}$ [MPa] (the right axis);
- (3) – Reinforcement ratio ρ [%].

Fig. 7-9 Distribution of defects occurred

Regarding the losses of reinforcement the procedure of the effective steel area evaluation procedure is required. The following procedure presented in Design Manual (1993) may be applied. From available bridge documentation the specified nominal diameter may be considered for evaluation of the nominal area. Usually the documentation of bridge is not complete or even does not exist. In these cases a measurement at the undamaged and damaged sections of the bar is required. Two measurements of the bar diameter at 90° to each other should be taken at an uncorroded section. The nominal area should then be based on the average of the measurements. Measurements of the actual cross-sectional area should be taken at the position of worst bar condition. The method of measurement depends on the loss shape.

For the corrosion case presented in Fig. 7-10a the cross sectional area of the corroded bar can be evaluated by the formula (7-29):

$$A_{corr} = \pi \frac{x \cdot y}{4}, \tag{7-29}$$

where:

x, y – widths of the rebar measured at 90° to each other, where either x or y records the minimum width.

Fig. 7-10a and b present deeply pitted reinforcement losses. From the measurement of their depth and width the loss of cross-sectional area can be determined. The last example (Fig. 7-10c) illustrates an irregular boundary of damage which is not covered by the previous examples. Since measurements are difficult in this case an approximation may be made in evaluating the loss of cross-sectional area.

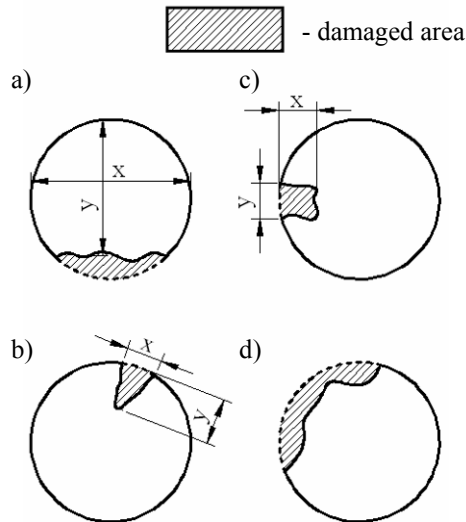


Fig. 7-10 Measurements to determine cross sectional area of a corroded bar (Design Manual 1993)

Another solution regarding evaluation of the residual area of corroded has been proposed by Horrigmoe (2004). This researcher distinguishes reinforcement losses caused by uniformly distributed corrosion as well as pitting (Fig. 7-11).

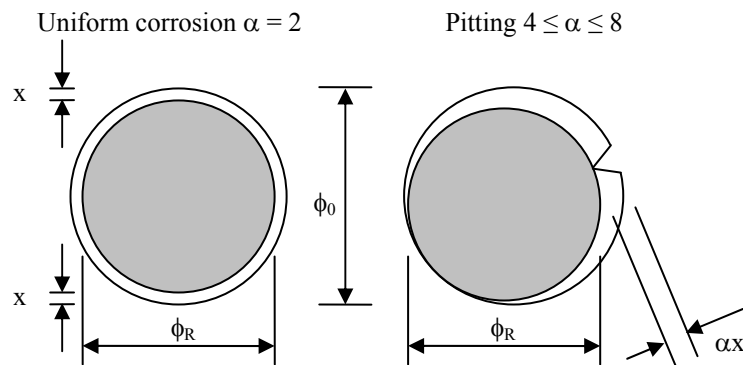


Fig. 7-11 Residual steel bar cross section proposed by Horrigmoe (2004)

The residual bar diameter ϕ_R can be estimated from the nominal bar diameter ϕ_0 (7-30):

$$\phi_R = \phi_0 - \alpha \cdot x, \quad (7-30)$$

where:

ϕ_R – residual bar diameter;

ϕ_0 – nominal bar diameter;

α – coefficient depending on the type of attack.

In case of localized pitting attack, the reduced cross sectional area is highly irregular and the net loss of area may be significantly greater than for uniform corrosion. The presented solution by Horrigmoe (2004) seems to be reasonable approach, which allows assuming the reduced cross-section as circular against Design Manual (1993).

7.8 Procedure of load capacity assessment

7.8.1 Limit states

According to the safety standards (Euro Code 2, PN-91/S-10042) each structure must meet the safety requirements defined by the ultimate limit states (ULS) and serviceability limit states (SLS). The ULS concern the danger potential associated with collapse of the structure or other forms of structural failure. The ULS can be distinguished as for: bending and longitudinal force, shear; torsion; punching; structural deformation. The SLS correspond to a structural state beyond which the specified service requirements are no longer met, i.e. limit states of cracking; limit states of deformation; limit states of displacement and finally corrosion risk. Regarding the ULS for considered slab span constructions the Author considered only bending as a dominant influence on load capacity assessment. The longitudinal force is related to the prestressed structures. Shear force in the slab structures is of little importance because of the cross section geometry. An influence of torsion and punching at considered moving load (centrically situated) type can be also omitted. In case of SLS the limit states of cracking can be considered at the design of bridge. During service life the cracking influences mainly on the bridge durability increasing the corrosion process. In some cases cracks can be interpreted as compressive reduction of concrete. This parameter has been considered. Deformations of slab spans can be considered as a theoretical case only, because of its large flexural stiffness. The corrosion risk is related to the bridge durability. Concerning all these reasons the SLS has been excluded from consideration in this study.

7.8.2 Analysis

The assessment of the load capacity of damaged spans consists of two steps:

1. Load capacity evaluation of each cross section for the design and current bridge condition and then plotting graphs of envelopes of bending moment for various load classes and envelopes of the load capacity;
2. Comparison the load capacity of damaged spans with the maximum value of bending moments; Selection of the load class ensuring that for the whole span the bending moment does not exceed the cross section load capacity.

Evaluation of damaged spans requires a uniform symbols (Fig. 7-12). Every cross section has identification $i = 1, 2, \dots, n$ and each layer of cross section is represented by $j = 1, 2, \dots, m$.

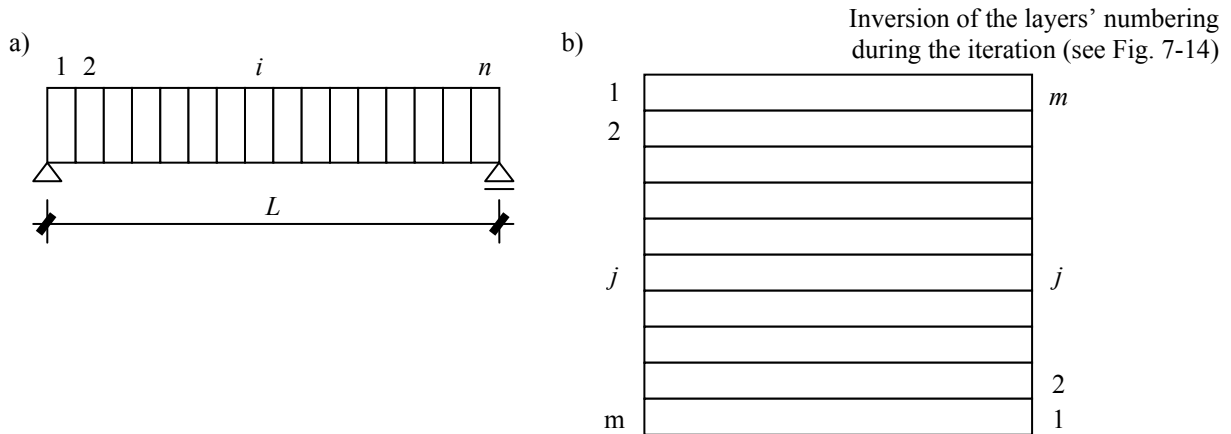


Fig. 7-12 Symbols used in load capacity assessment: a) considered span; b) analysed cross section

The following symbols allow describing strains, stresses, and internal forces:

F_{ij}^c - force in concrete at layer “j” of cross section “i”;

F_{ij}^s - force in reinforcement at layer “j” of cross section “i”;

ε_{ij} - strain at layer “j” of cross section “i”;

σ_{ji}^c - stress in concrete at layer “j” of cross section “i”;

σ_{ji}^s - stress in reinforcement at layer “j” of cross section “i”.

The index “max” means the maximal acceptable value of strain/stress according to the code. The load capacity algorithm (see Fig. 7-14) is an iteration process based on the incremental strain modification.

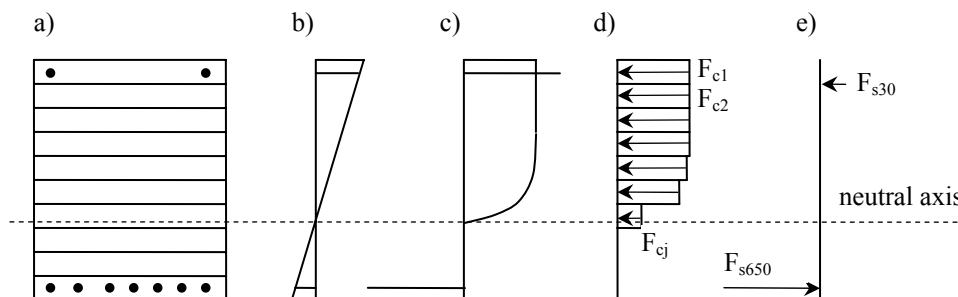


Fig. 7-13 Distribution of internal forces: a) division of the cross section into horizontal layers and location of reinforcement; b) strain distribution; c) stress distribution; d) distribution of internal forces in concrete (F_{bi}) for each layer of the cross section, e) distribution of internal forces in steel (F_{si}) for each reinforcement layer

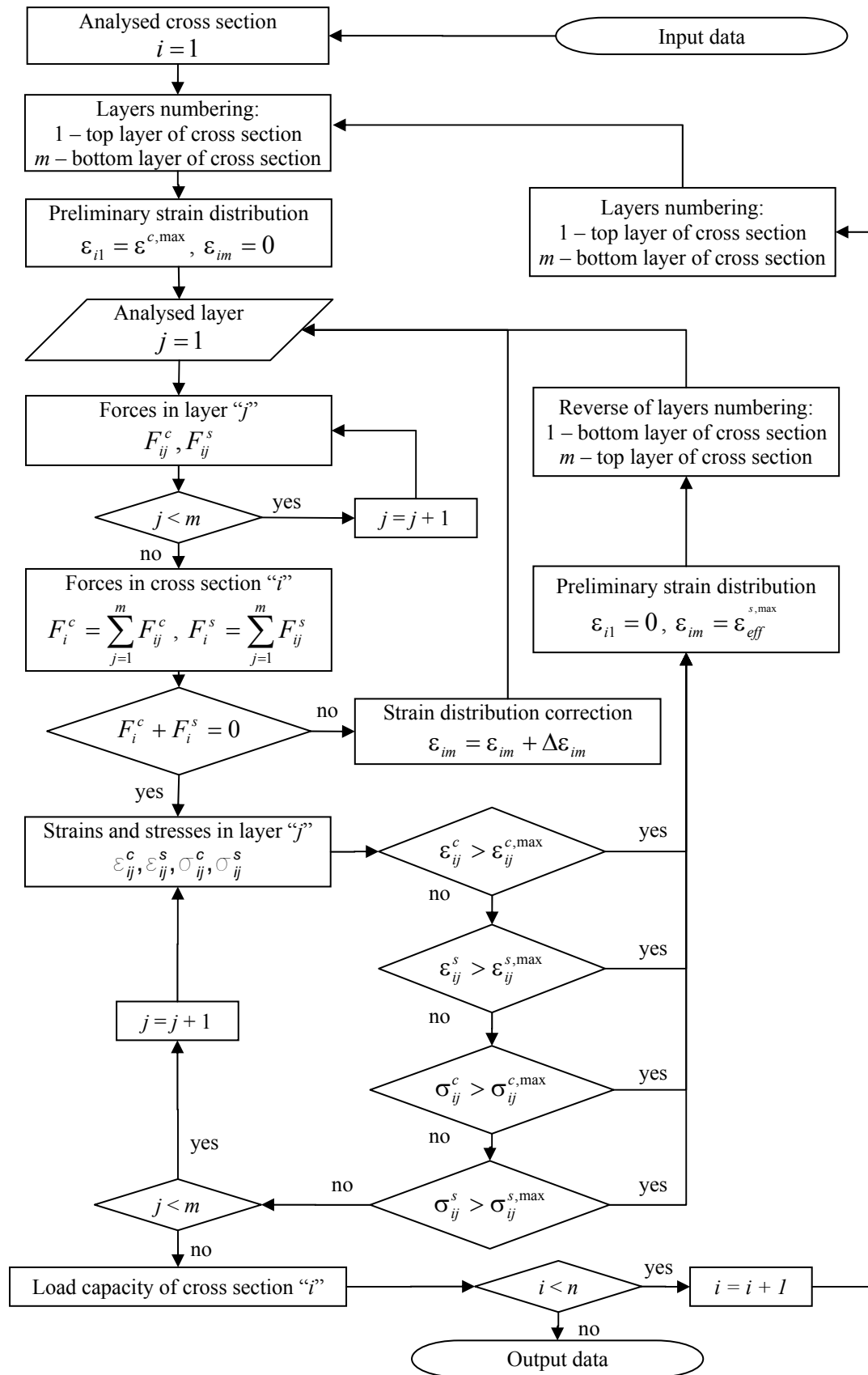


Fig. 7-14 Flowchart describing strength calculation in DAGA program

The $\Delta \varepsilon_{im}$ controls the program flow. The $\varepsilon_{eff}^{s,max}$ (introduced in preliminary strain distribution) is a strain in the bottom concrete layer, while the bottom layer of reinforcement has the

maximal acceptable strain. The cover of reinforcement is subjected to the higher strain and for this reason this parameter is enriched by the “*eff*” (effective) index. Schema of cross section discretisation and internal forces distribution is presented in Fig. 7-13.

At the beginning of the analysis the top layer of cross section is subjected to strain causing maximum effort of concrete $\varepsilon_{i1} = \varepsilon^{c,max}$. The strain in the bottom layer of cross section ε_{im} is equal to zero. At this moment the cross section is not at equilibrium of forces. In order to find this equilibrium, the iteration loop is started. The stress at the bottom layer is increased. From strain distribution it is possible to pass to the stress distribution (using the relations $\sigma = f(\varepsilon)$) and then to the internal forces distribution. The equilibrium of forces is checked. Increasing of strain is performed until the sum of forces is equal to zero. While the equilibrium of forces is reached, the location of neutral axis can be found. The next step is a verification of strains or stresses, whether in the particular layers the maximal values are not exceeded. If strains or stresses exceed the limits, then initial conditions have to be inverted, it means the bottom layer of cross section is subjected to strain $\varepsilon_{eff}^{s,max}$ causing maximum effort of bottom reinforcement and strain at the top layer is equal to zero. The next steps are similar.

When the equilibrium of forces is reached, then the load capacity of cross section can be evaluated according to the following formula (7-31):

$$M_R = \sum_{i=1}^{ns} (F_{si} \cdot r_{si}) + \sum_{i=1}^{nc} (F_{ci} \cdot r_{ci}), \quad (7-31)$$

where:

M_R – load capacity of analysed cross section;

F_{si} – value of the force in the current layer of the reinforcement;

r_{si} – location of current rebar layer against the neutral axis of the cross section;

n_s – total number of reinforcement layers;

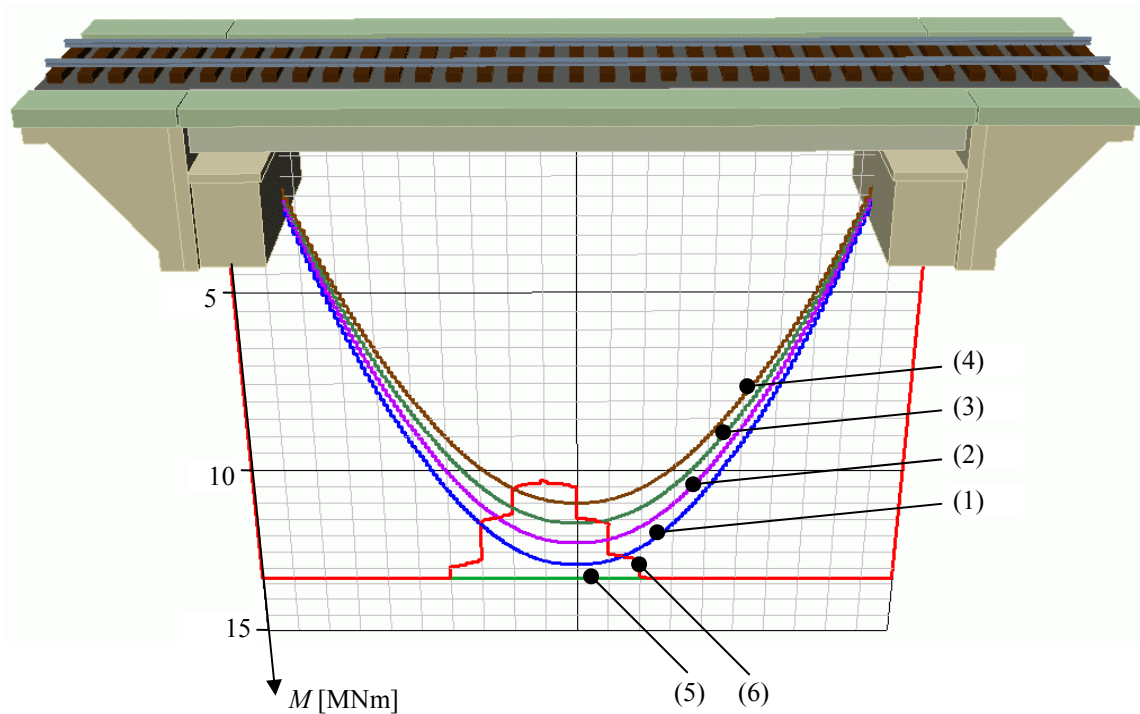
F_{ci} – value of the force in the current layer of the concrete;

r_{ci} – location of current concrete layer against the neutral axis of cross section;

n_c – total number of concrete layers.

7.9 Results of the analysis

The mentioned defects cause reduction of the load capacity of the analysed span. In Fig. 7-15 the results of the performed static and strength analyses have been presented.

**Legend:**

Envelopes of the bending moment:

- (1) – arterial, first-class line and all electrified lines;
- (2) – secondary lines;
- (3) – local lines and provisional bridges;
- (4) – sidings.

Envelopes of the load capacity:

- (5) – the designed condition;
- (6) – the current (with damages) condition.

Fig. 7-15 Results of the static-strength analysis

7.10 Defect modelling based on photos

The modelling of damaged bridge structures in terms of defect parameters (i.e. intensity, extent and location) requires an input data engine of high precision. Usually defects are characterized by irregular forms making this process very difficult. Non-adequate defect representation in the model may cause severe consequences regarding load capacity assessment. The simplest way is to describe the defect geometry (dimensions, depth of concrete loss etc.) based on direct measurements performed by inspectors, but this way would be very laborious and time consuming. Besides, the accuracy of this operation probably would leave a lot to be desired.

In order to simplify this problem an additional tool has been introduced to the DAGA software. Instead of the direct measurement a collected photographic documentation from visual inspections can be applied. This procedure is especially useful when the access to the bridge is limited (for example high riverside). Presented technology is related to the photogrammetry. During visits on-site inspector takes picture of the surface of damaged part

of the bridge. The collected documentation should be carefully described. The pictures are located in the folders sorted by inspection dates.

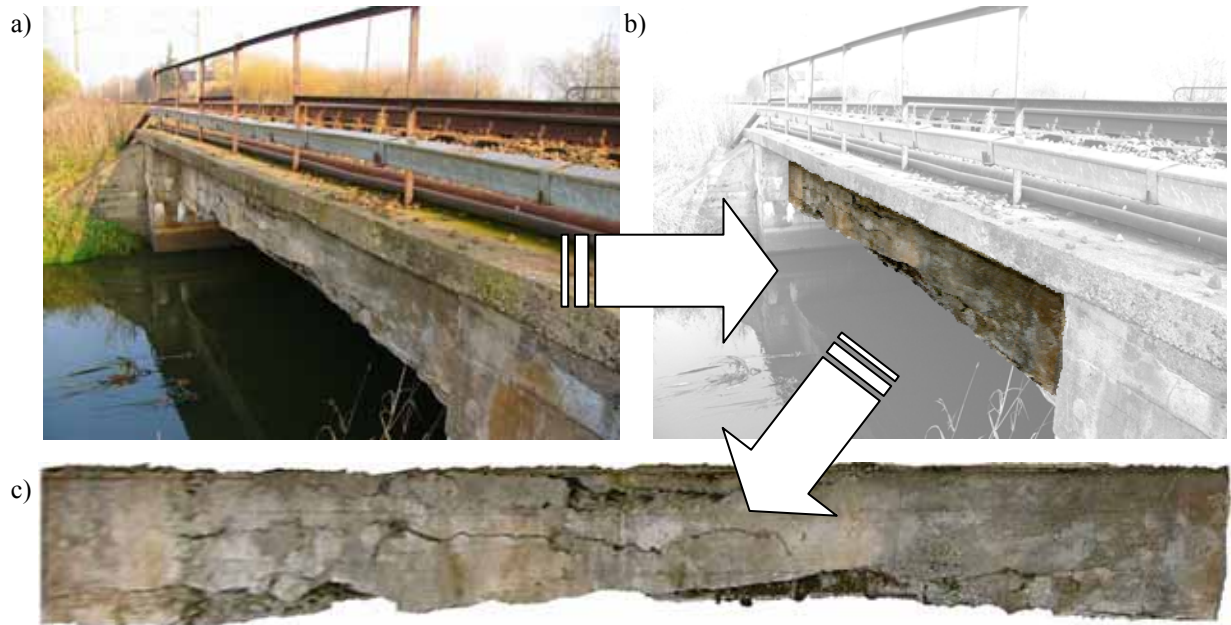


Fig. 7-16 Acquisition of the slab surface image procedure, the analysed bridge construction (a - *photograph courtesy of Jerzy Czastkiewicz, PKP*), the extracted surface image (b), the geometrically transformed image applicable in the DAGA system

Then the picture is geometrically transformed to be applied in DAGA program. In order to geometrically transform the picture the common programs for image editing (i.e. ACD FotoCanvas, Corel, Photoshop etc.) can be applied. In Fig. 7-16 the procedure of slab surface image acquisition and transformation is presented. After the picture of the considered bridge span (Fig. 7-16a) is taken, the area of the considered span surface (Fig. 7-16b) has to be extracted. The final result (Fig. 7-16c) can be applied in the analysis.

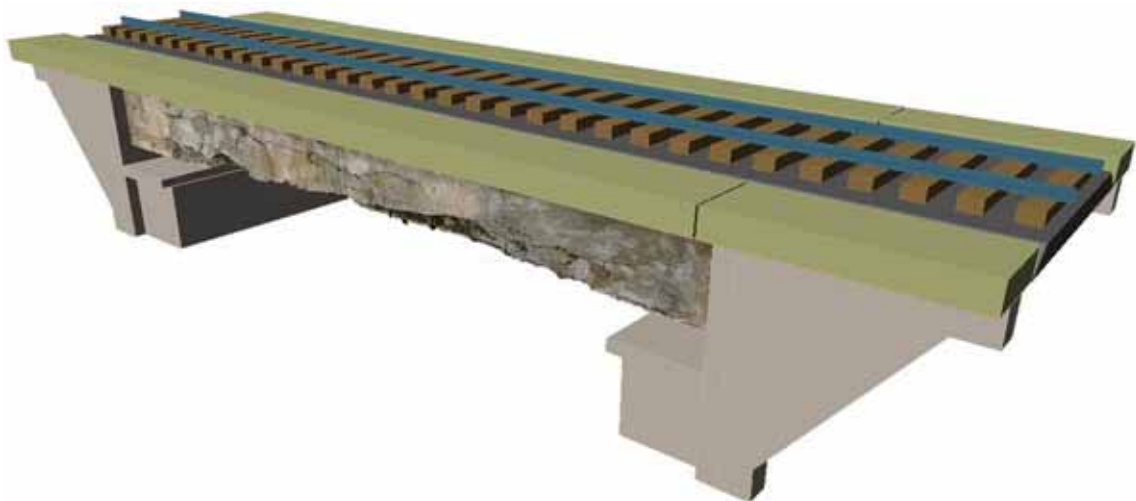


Fig. 7-17 Application of the 3D photo documentation from visual inspections

The particular pictures are automatically attributed to the surfaces of the bridge span model and ready to be displayed. The user selects the date of the visual inspection and in this moment inserted pictures allow for the proper defect representation and load capacity assessment. An example of application of this facility has been presented in Fig. 7-17. Severe losses of material are visible and easy to represent in the model.

Another advantage of this solution is a possibility of the monitoring of the bridge degradation progress based on visual inspections every reasonable period of time (for instance every two years). The superposition of collected results allows for reconstruction of degradation progress during bridge operation and prediction its future condition. Though DAGA system is designed to deal with the current load capacity only, in the future this program can be extended into the tool supporting also remaining life time evaluation as well as degradation mechanisms modelling.

Chapter 8

Neural network technology for the load capacity assessment

8.1 Introduction

8.1.1 General motivations

A question “Why is it worth to know Neural Network Technology (NNT)?“ should be asked before an analysis by means of this technique has started. Last time NNT is widely investigated and successfully applied in various domain of human life. This fact manifests itself in a huge number scientific publications and innumerable conferences on NNT. Basically NNT represents a possibility of knowledge processing in terms of its acquisition, storing, modifying and applying. This technique reflects simplified actions of human brain as a system (i.e. artificial neural network) able to change its structure basing on information flowing through the network. Data modelling and decision making are the main advantage of the NNT application. The utility of artificial neural network lies in fact that they can be applied to infer a function from observation. This is especially useful when an unknown function of more than 3-4 variables needs to be modelled. NNT can be used to model complex relationships between inputs and outputs or to find patterns in data. Introducing values of an unknown function with corresponding variables the artificial neural network is able to perform an approximation of this function and regression analysis, including time series prediction and modelling. It can be done by a training of the network.

The application area of NNT is wide and diverse. This technology was applied for system identification and control (vehicle control, process control), game-playing and decision making (backgammon, chess, racing), pattern recognition (radar systems, face identification, object recognition, etc.), sequence recognition (gesture, speech, handwritten text recognition), medical diagnosis, financial applications, data mining (or knowledge discovery in databases, "KDD"), visualisation and e-mail spam filtering. Also civil engineering was partly supported by application of NNT as an alternative procedure to analytic analyses.

8.1.2 Basic principles on Neural Network Technology

From the biological point of view, nerve cell, called also neuron, constitutes a basic element of the nerve system. Each neuron is composed of cell body (i.e. soma), dendrites (inputs) and axon (output). By means of axon the neuron is able to send a signal to another nerve cell. A single neuron receives signals from a large group (up to one thousand) of neurons. The human brain consists of about 10^{11} neurons interacting together by means of about 10^{15} connections. The neuron transfers a signal to the others by means of nerve joints, called synapses. A signal transmission is based on the complex electrochemical processes. Synapses play a role of information transmitters causing increasing or reduction of the signal.

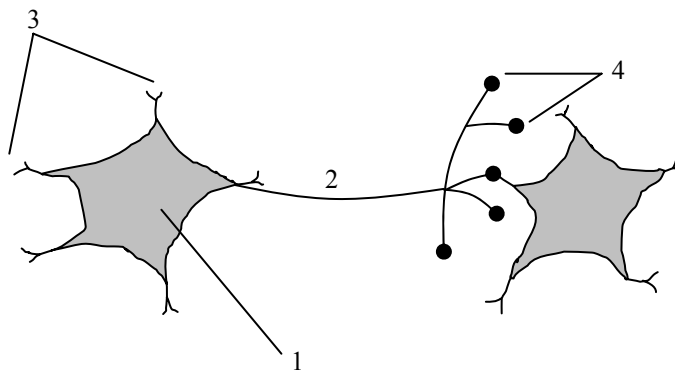


Fig. 8-1 Simplified scheme of a neuron and its connections with another nerve cell: neuron body (1), axon (2), dendrites (3), synapses (4)

By means of synapses, the neuron receives various signals. Some of them may be stimulating and others can be restraining. The neuron adds all of these signals and if their algebraic sum exceeds some threshold value then output signal is transferred, by axon, to another neuron. A simplified scheme of neuron is presented in Fig. 8-1.

An artificial neural network is a computing method loosely modelled on cortical structures of the brain. The network is composed of interconnected elements called neurons that work together to produce an output signal. As a result, it has the unique property of being able to perform its overall function even if some neurons are not functioning. This means that it can

tolerate error or failure. Operation mode of particular neurons is defined by *activation function* f_a , also called *transfer function*. This function determines the relationship between input and output signals of the neuron. Weights are attributed to all connections; their values are specified in the training process. Concerning their architecture it is possible to distinguish neural network types regarding:

- *direction of signal flow*:
 - unidirectional signal flow;
 - bidirectional signal flow;
- *number of neuron layers*:
 - networks without hidden layers;
 - networks with hidden layers;
- *type of neural activation function*:
 - linear;
 - non-linear.

Activation function f_a of neuron describes relationship between the output signal u_i and the input signals x_j as well as weights w_{ij} attributed to the particular inputs. The general formulation of neuron output has been presented below (8-1):

$$u_i = f_a(e_i) = f_a\left(\sum_{j=1}^n (w_{ij}x_j + w_{i0})\right), \quad (8-1)$$

where:

e_i – net input of neuron i ,

w_{i0} – weight of the special input x_0 (bias) which signal is always equal to one.

Concerning the learning strategy neural networks can be distinguished as follows:

- supervised, which involves a mechanism of providing the network with the desired output signals,
- unsupervised, where the network has to make sense of the inputs without outside help.

In supervised learning, the learner is given a set of instances of the form $\langle \vec{x}, y \rangle$, where y represents the variable that we want the system to predict, and \vec{x} is a vector of values that represent features thought to be relevant to determining y . The goal in supervised learning is

to induce a general mapping from \vec{x} vectors to y values. That is, the learner must build a model, $\hat{y} = f(\vec{x})$, of the unknown function f , that allows it to predict y values for previously unseen examples. In unsupervised learning, the learner is also given a set of training examples but each instance consists only of the \vec{x} part; it does not include the y value. The goal in unsupervised learning is to build a model that accounts for regularities in the training set (Craven & Shavlik 1998).

When a neural network has a specified structure for some application, training process can be started. To start this process the weights of connections are defined randomly. In this work the supervised mechanism of neural network training has been applied.

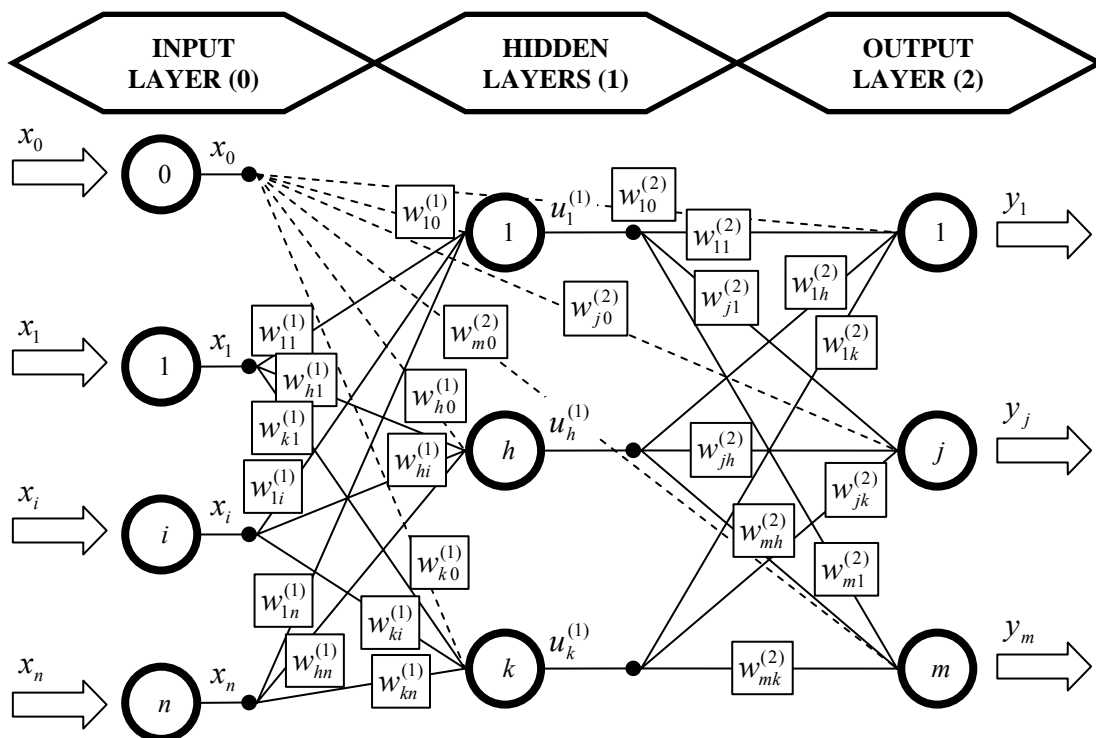


Fig. 8-2 Example of multi-layer neural network

In Fig. 8-2 an example of the multi-layer unidirectional neural network is presented. This kind of component has been applied in this study for knowledge representation. The most important advantages are:

- solving problems concerning symbolical description of knowledge,
- theoretical as well as empirical data can be used in training process,
- easy modification of stored knowledge by its updating,
- speed and reliability in its operation.

The basic properties of the multi layer neural network are:

- network is composed of at least three layers: input, hidden (any number) and output;
- each layer should consist of at least one neuron;
- network is composed of layers with regular connections; the input of each neuron of particular layer is connected to the outputs of all the neurons of the previous layer;
- only neurons of neighbouring layers are connected;
- neurons of input layer transmit the signal to interior of the network only;
- output signals are generated by the neurons of output layer;
- multi-layer networks with multiple nodes are capable of memorizing data.

The weights of connections have random values at the beginning of the training process. While processing the inputs and comparing resulting outputs against the desired outputs an error occurs. In order to adjust the weights which control the system, errors are propagated back. The procedure of weight adjustment of the neural network is called Back-Propagation (BP) algorithm. The set of data which enables the training is called the training set or the pattern. This process is run until the differences between expected and real output values are below the required error margin. Training and testing processes occur simultaneously. A number of training set elements is reserved for testing.

Sometimes a network cannot solve the problem. In this case the knowledge engineer has to review entire training set and network architecture. These modifications determine entire process called the “art of neural network creating, training and testing”.

Kröse & van der Smagt (1996) noted that there are some aspects which make the algorithm not guaranteed to be universally useful. Most troublesome is the long training process. Outright training failures generally arise from two sources: network paralysis and local minima. Concerning the network paralysis, as the network trains, the weights can be adjusted to very large values. The total input of hidden or output units can therefore reach very high values, and because of the sigmoid activation function, the unit will have an activation very close to zero or very close to one. For the weight adjustments close to zero the training process can come to a virtual standstill. With regard to the local minima, the error surface of a complex network is full of hills and valleys. Because of the gradient descent, the network can get trapped in a local minimum when there is a much deeper minimum nearby. Probabilistic methods can help to avoid this trap, but they tend to be slow. Another suggested possibility is

to increase the number of hidden units. Although this will work because of the higher dimensionality of the error space, and the chance to get trapped is smaller, it appears that there is some upper limit of the number of hidden units which, when exceeded, again results in the system being trapped in local minima.

Though NNT works fast and effectively, its lack of a transparent procedure of working constitutes a “black box”. This fact requires its user to trust that network works correctly. It is especially important when NNT is applied as a big component representing an incomprehensible model. Craven & Shavlik (1998) presented algorithms to extract symbolic rules from trained neural networks in terms of the data mining. These algorithms promote comprehensibility by translating the functions represented by trained neural networks into languages that are easier to understand. A broad range of rule-extraction methods has been developed. The primary dimensions along which these methods vary are their (i) representation languages, (ii) strategies for mapping networks into the representation language, and (iii) the range of networks to which they are applicable.

8.1.3 Historical outline

The Neural Network Technology appeared at the moment of publication of McCulloch & Pitts (1943), where a mathematical formula of the nerve cell had been presented first time. This description was also connected with data processing problem. Ability for data processing in the parallel way was identified as the most valuable property of Neural Network.

Perceptron is the first, widely known example of well constructed and working neural network Rosenblatt (1968). The system was created as partly electromechanical and partly electronic. Its changeable synaptic weights were constructed using potentiometers controlled by electric motors. The ability to operate after destroying some its elements was the main advantage of Perceptron. Moreover it was the first, really working, imitation of the nerve network.

In 1960 Bernard Widrow from University of Stanford constructed a network composed of electrochemical learning elements called Adaline (Adaptive Linear Element). This network, called Madaline (Many Adalines), was composed of maximally 8 neurons with 128 connections. Madaline was capable to work at the speed of 10^4 activations per second. It was the first neurocomputer offered commercially. This type of network is used in radars, sonar and telephonic lines.

The development of the Neural Network Technology was stopped after 1970 due to the book (Mins69). This publication discouraged many researchers, because it proved that the area of application of single-layer neural networks was very limited. Only few scientific centres with researchers such as Gossberg, Widrow, von der Malsburg, Amari, Fukishima or Kohonen continued further investigations on NNT. This impasse (lasting about 15 years) was broken only after a series of publications had appeared, proving that multi-layered non-linear neural network did not have limitations mentioned before. Also methodologies of training of multi-layered networks were introduced. In those times the following devices were constructed. In 1970 Stephen Grossberg (University of Boston) built a network called Avalanche to speech recognition and to control movements of arm of a robot. In 1978 K. Fukishimo constructed a network Neocognitron to recognition of hand-written signs (also Chinese). This system was able to read any signs and also was insensitive to their deformations, sizes, displacements, etc., but required a huge number of elements and connections.

In the eighties, regarding to a technology of producing of nerve cells as integrated circuits, solutions of big sizes and computational powers appeared. Usually, those devices were capable to use only some fragment of properties of nerve networks, such as especially adaptivity of parameters of neuron.

In those times first approaches related to recurrent neural networks appeared. That type of network was destined to look for the state of equilibrium during a long dynamic iteration process. As an example, systems developed in 1982 by J. Hopfield from AT&T Bell Labs for reconstruction of images from their fragments can be mentioned. This kind of network can also be applied in optimization tasks.

Since the middle of the eighties a real race (between laboratories and companies producing electronic components) can be observed. Number of elements in a network, number of connections and also speed of these devices are significant achievements in this race.

NNT has been applied in various domains of human life such as speech recognition, medicine, meteorology, marketing, computer science etc.

Tebelskis (1995) presented an advantage of NNT for purposes of the speech recognition.

Hansen B. (1997) summarized a state of the art on NNT application in meteorology such as minimum temperature forecasting, lightning prediction, hurricane tracking, cloud recognition and classification and many others.

Yao et al. (1999) presented an application of NNT for purposes of stock index forecasting basing on the data from Kuala Lumpur Stock Exchange. They captured the relationship between the technical indicators and the levels of the index in the market under study over time. They proved that useful predictions can be made without the use of extensive market data or knowledge.

8.1.4 Application of Neural Network Technology in civil engineering

The NNT has also been successfully applied in civil engineering. In this section a brief description of NNT application in civil engineering is presented.

Brancaleoni et al. (1993) presented experiences in application of neural networks for detecting defects of civil engineering structures. Learning strategies, network organisation-topology, error and convergence characteristics, normalisation procedures have been discussed. The dynamic response of structures, comprising artificial signals from numerical models, experimental signals from laboratory tests and some examples on full scale structures, was adopted as network input. The cracking and the presence of nonviscous dissipation were examined in that research.

Hsu & Yeh (1993) presented an idea of using neural network technology to detect structural deterioration. They presented a case study to inspect loss of stiffness and locate damage in a multistory building composed of shearwalls. The net they described was trained to achieve the machine learning purpose. The net was then used to deduce stiffness degradation in each story. This was done by inputting the measured eigenvalues of the damaged building.

Logar & Turk (1995) proposed an approach of constitutive modelling of non-linear material such as soil by means of NNT. A neural network used in predicting the oedometer loading curve was trained by 40 oedometer curves obtained from tests made on marshland soil. The neural network was tested on 6 oedometer curves which were not included in the learning process. The oedometer curves and the clay parameter were evaluated. Good agreement between measured and predicted values was obtained, which implies that the neural networks can serve as an effective constitutive model as well as predicting sample behaviour.

Satorre (1995) developed a system to automatically detect changes in parameters among several measures taken at different times. The system is proposed to check the evolution of the surfaces by using a video-camera. A neural network learns a sequence of events and marks a representative set of changing parameters (i.e. pixels of images obtained by means of a video-camera). The network recognises whether the new set of parameters falls in the

admissible range or if these values are not suitable. In order to demonstrate the effectiveness of the system, a simulation of the movement of a joint in a railway was considered.

Flood et al. (2001) presented a solution of NNT application to model the performance of externally reinforced beams. This research was based on laboratory observations of actual beam behaviour. The presented solution is particularly useful, because the numeric tools used to analyze such beams are computationally expensive making them slow to arrive at an answer, especially when dealing with complicated three-dimensional composite forms.

Tarighat (2004) presented an application of NNT in purposes of concrete durability analysis. In this study a neural network model has been developed from the experimental data to predict the concrete carbonation coefficient of Fick's second law in diffusion theory. The proportion of water to binders, condensed silica fume to binders ratio and relative humidity percentage were considered as input parameters for that analysis. The advantage of that approach was that predicted values were based on derived patterns from real tests instead of a given mathematical function.

Kwak et al. (2006) performed a tensile test with self-manufactured hybrid Fibre Reinforced Polymer (FRP) rod. The results acquired (mainly strains and deflections) have been used for purposes of the neural network training. Comparison of the obtained results with analytically performed analyses confirmed the suitability of NNT in this field.

Madan (2006) presented an approach for unsupervised training of neural networks in active control of earthquake-induced vibrations in building structures. The proposed methodology obviates the need for developing a mathematical model of structural dynamics or training a separate neural network to emulate the structural response for implementation in practice.

Pu & Mesbahi (2006) proposed NNT to be applied to predict the ultimate strength of unstiffened plates under uni-axial compression. The obtained network models were trained and cross-validated using the existing experimental data. It was found that those models can produce a more accurate prediction of the ultimate strength of panels than the existing empirical formulae.

Inel (2007) presented the possibility of the potential use of NNT in deformation estimates of RC columns dominated by flexural failure. Experimental data of 237 rectangular columns from an existing database were used to develop a neural network model. The input parameters were selected based on past studies such as aspect ratio, longitudinal reinforcement ratio, yield strength of longitudinal reinforcement, concrete strength, yield strength of transverse reinforcement, transverse steel spacing, ratio of transverse steel parallel to the direction of

loading and axial load ratio. Ultimate displacement estimates of RC columns by the model were compared to the existing semi-empirical and empirical models. The ANN model was found to perform well.

Pendharkar et al. (2007) developed a methodology of using NNT for the continuous composite beams to predict the inelastic moments (considering instantaneous cracking and rheology of concrete) from the elastic moments (neglecting instantaneous cracking and time effects) using eight input parameters. These models were validated for four example beams and the errors were shown to be small.

Hozjan et al. (2007) presented an alternative approach to the modelling of the mechanical behaviour of steel frame material when exposed to the high temperatures expected in fires. Based on a series of stress–strain curves obtained experimentally for various temperature levels, an artificial neural network was employed in the material modelling of steel. A non-linear analysis of plane frame structures subjected to fire was performed by Finite Elements Method. The numerical results were compared with the measurements, and shown a good agreement.

8.1.5 Application of Neural Network Technology in bridge engineering

NNT can be used as a major instrument in assessing the condition of RC bridges. The methodology presented here has wide application in designing of Expert Tools for load capacity evaluation of damaged structures. This section presents a brief review of the application of this technique in bridge engineering.

Miyamoto et al. (1995) developed a concrete bridge rating expert system with machine learning. The aim of this was to evaluate structural serviceability of bridges on the basis of the specifications of target bridges, environmental conditions, traffic volume and results of visual inspection.

Nagaraja & Melhem (1995) developed a rebar corrosion expert system using machine learning programs. The objective was to provide a tool for assessing the extent of corrosion in a structure and predicting its service life. The system is composed of two modules. The first module determines the degree of corrosion and type of remedial action. The second module predicts the serviceability life of the structure. The system is developed and implemented with numeric and symbolic data and considers material, structural and environmental factors.

Waszczyszyn (1995) presents applications of neural network technology in bridge engineering. In traditional bridge engineering, the Winkler tables created for extreme values

of bending moments (in the middle of the span and at the supports) evaluation for continuous beams are used. Other neural network applications include:

- Design of rectangular cross section of the RC beam with single reinforcement layer;
- Approximating discrete results extracted from tests performed on concrete specimens to obtain a uniform relationship between concrete strains and stresses.

Žnidarič & Peruš (2000) developed an application to bridge condition assessment, based on visual inspection and basic test results. Defects are evaluated taking into account:

- Their types and effect on the safety and/or durability of analysed structural member;
- The impact of the affected structural part on the safety and durability of the structure;
- The defect parameters (intensity and extent) and expected propagation.

These parameters are stored as numbers to be processed by analytical function. The objective of this is to obtain the deterioration factor, attributed description of the condition, and determine what intervention is needed. However, they found no connection between applied factors and results of static-strength analysis.

Brandt & Kasperkiewicz (2003) presented another application of neural network, to evaluating freeze resistance. As a result of test results on concrete freeze resistance, a database of 183 records was created. Test results such as concrete density, air content, specific surface of pores, pore spacing factor, compressive strength at 28 days, were input attributes. Resistance of concrete to freezing was its output.

Bień & Rawa (2004) presented the application of neural network technology in the bridge management system. The developed system, called Neuritis, is based on the multilevel hybrid network technology based on neural, fuzzy and functional components. These researchers enabled representation of information in the form of an advanced knowledge base. All the information coded in the form of data is stored and processed in the computer system. It is then interpreted in a specific context to make it ready for use in decision processes.

Amen et al. (2006) described a system based on the neural network technology for prediction of the final shrinkage at dry condition with low relative humidity of ambient air. This system can predict shrinkage based on parameters such as ratio of moisture loss, volume of paste and concrete compressive strength.

Vianna et al. (2006) applied NNT to evaluate the strength of shear connectors “Perfobond” in composite concrete slab / steel girder constructions. This took account of material and geometry parameters. Acquired knowledge was represented by neural networks.

8.2 General functional scheme of ANACONDA program

This chapter presents the Author’s own conception of load capacity assessment of defective railway RC slab spans. This is done by means of neural networks involved within the expert tools, based on the hybrid network technology. The knowledge acquired from the parametric analyses performed by DAGA program is used for neural network training as well as the expert tool architecture adjusting.

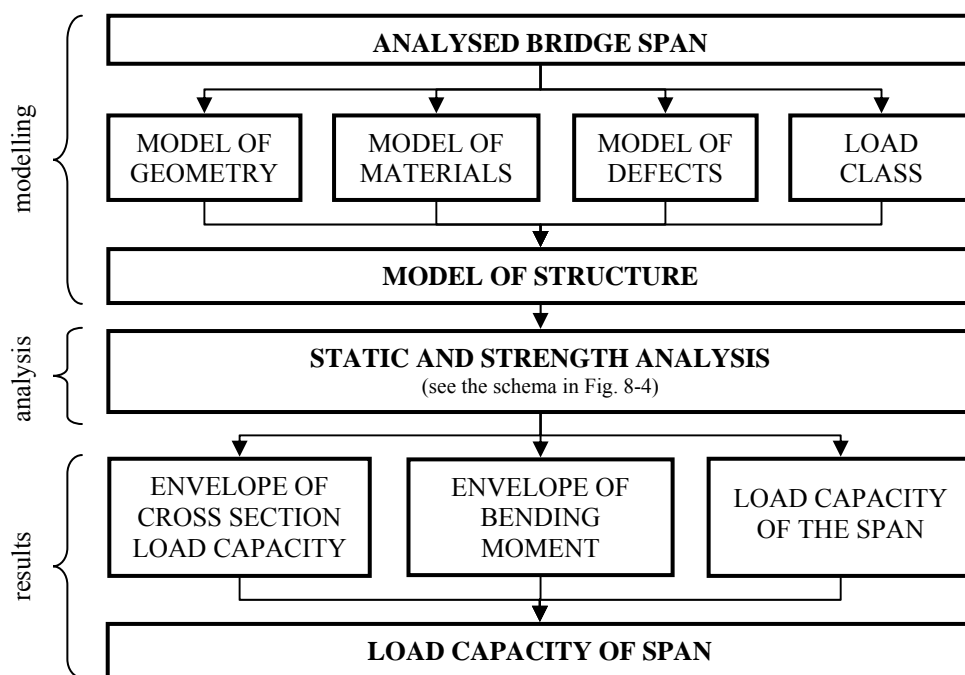


Fig. 8-3 Functional scheme of ANACONDA program

To present the possibilities of analysis of load capacity of damaged spans by the neural network technology, the Author will present an expert tool “ANACONDA” (ANALYSIS of CONcrete spans with DAMages). User’s Manual with an example of the analysis performed by means of this tool can be found in Appendix C. The general functional scheme of this tool is presented in Fig. 8-3.

This system consists of three modules: modelling, analysis and results. The **modelling** module creates the model of analysed bridge span structure. The geometry, materials, defect parameter and load class are input to the structural model.

The structural model is input to the **analysis** module. In this central module the static-strength analysis takes place, on each virtually created cross-section. The system evaluates the

maximal bending moment for specified load class and compares it with the load capacity. This module is composed of several components - neural and functional.

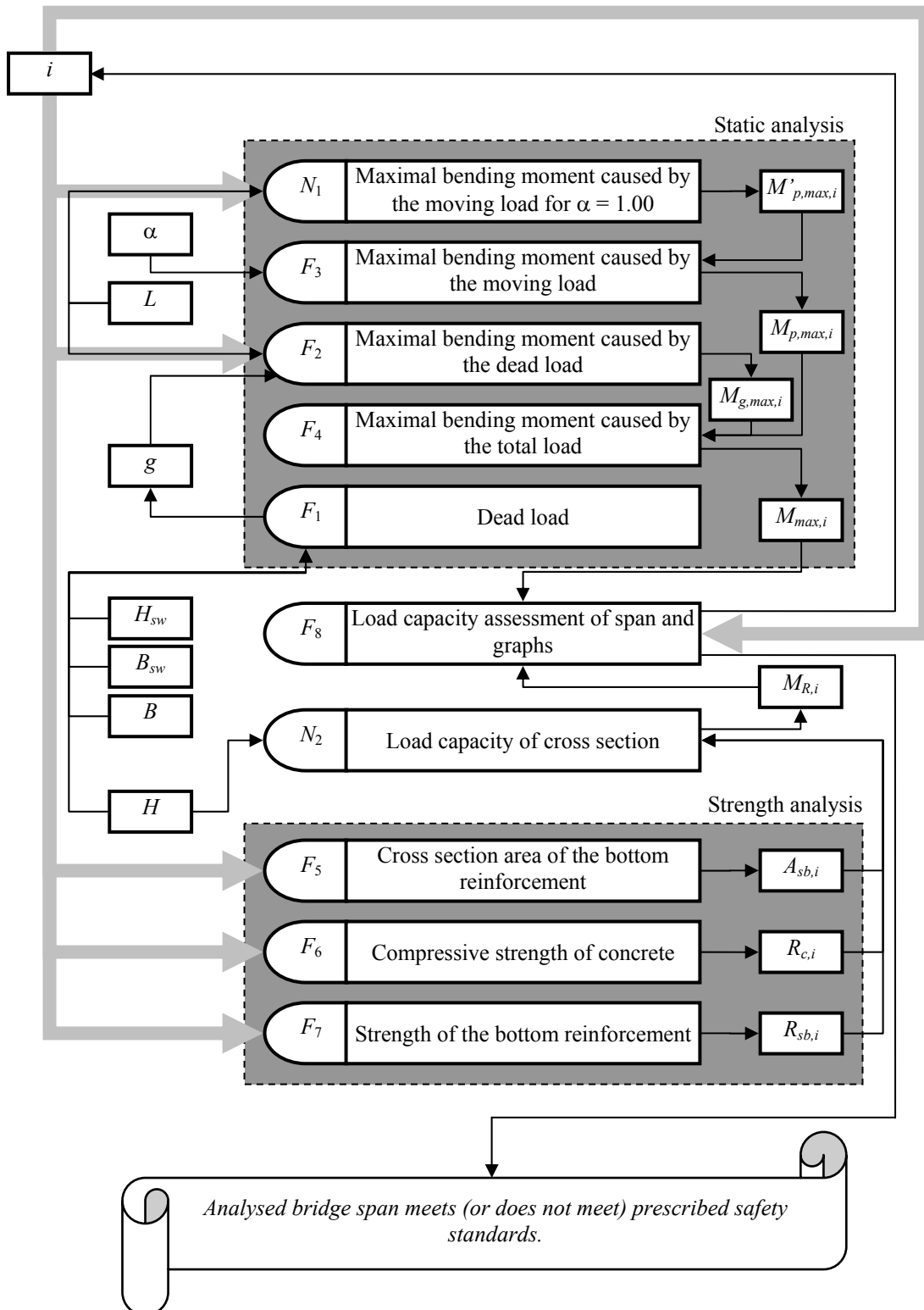


Fig. 8-4 Data flow system in Analysis module of ANACONDA program

The architecture of the analysis module is presented in Fig. 8-4. The **results** are the third module of the ANACONDA program, in the form of graphs (envelopes of bending moment

and load capacity) to determine whether the span meets the prescribed safety standards. Sections below present the neural and functional components.

8.3 Neural components (composition, training and testing)

The aim of this section is to obtain a uniform description of the relationships based on the discrete results of performed parametric analyses performed by DAGA program. The results of these analyses will be used as a knowledge base for expert tool based on the neural network technology. While analysing an influence of more than 3 parameters, the expected problems related to the description of these relationships (for example a mathematical formula) occur. In this situation an analytical description is usually very difficult and for some of them the neural network technology seems to be the most profitable. This technology allows performing the global approximation of the problem for any number of input parameters.

In the expert tool presented in Fig. 8-4 two neural components are used. The first element N_1 has been created for approximation of bending moment values caused by the moving load (trains). The component N_2 is destined for approximating the cross section load capacity. To create neural networks for resolving particular problems several network architectures have been compared in order to find the most suitable solution. By comparison of their sufficiency the best results have been typed for application in the ANACONDA. For both components the multi-layer unidirectional neural network technology with the back propagation training algorithm has been applied. To create all the networks as well as perform their training and testing a program BrainMaker (Lawrence & Fredrickson 1993) has been used.

8.3.1 Neural component N_1

To create this component the parametric analysis has to be performed. The set of discrete results should be stored in a knowledge-base. In this case the analysis has been performed in accordance to the Polish Code for the bridge loads (PN-85/S-10030) for the single load class (local lines and provisional bridges, where load class coefficient $\alpha = 1.0$). In this analysis span length L_t and cross section location ξ are the parameters taken into the consideration and the maximal bending moment $M'_{p,max}$ caused by the mentioned load is the single result. The results of these simulations have been presented in Fig. 8-5. Theoretical span length L_t and location of cross section ξ are its inputs. The maximal bending moment $M'_{p,max}$ is the output of this component.

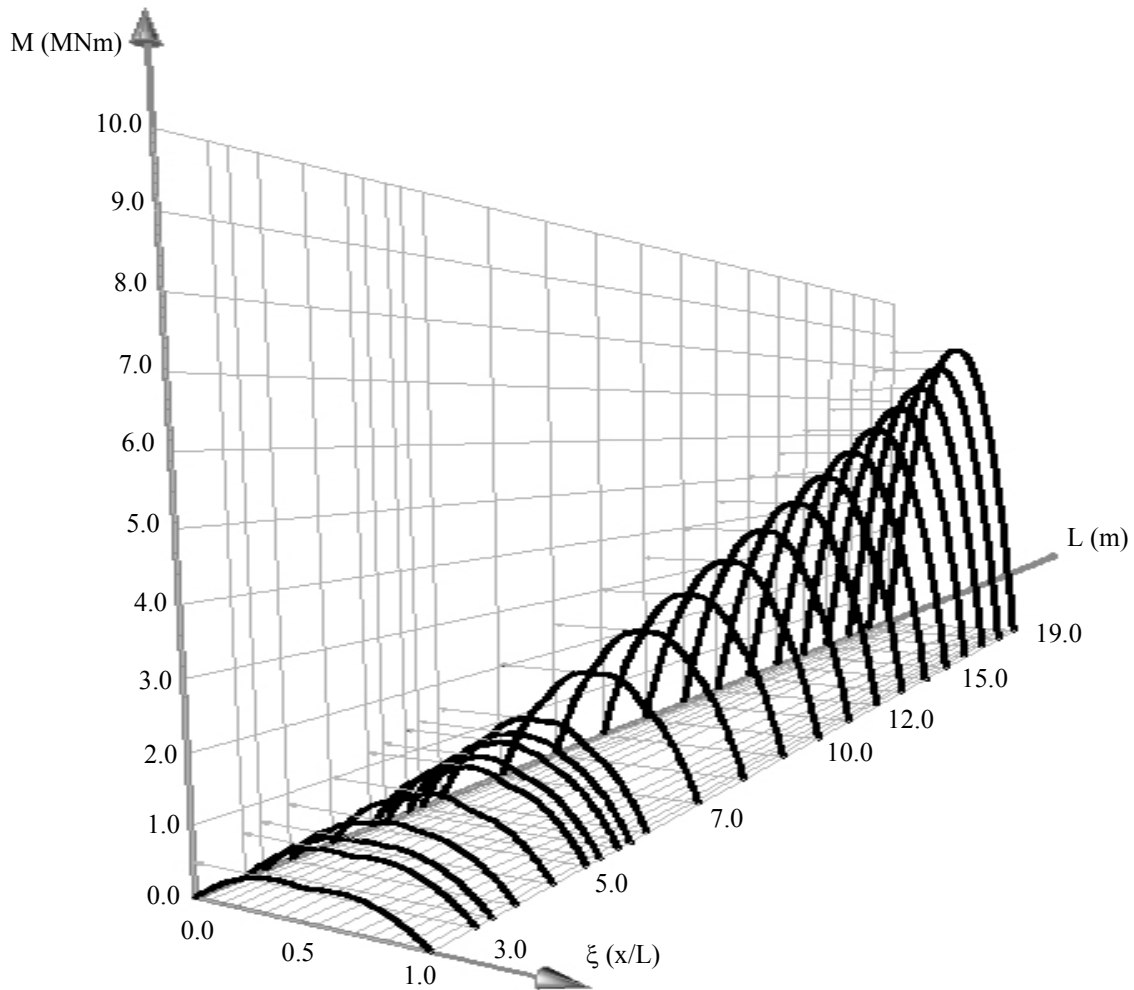


Fig. 8-5 Results of the static analysis: envelopes of bending moment caused by moving load (for local lines and provisional bridges, $\alpha = 1.00$) for various length of spans

The following neural network architecture has been proposed:

- input layer related to the parameters of analysis with the following input parameters: theoretical span length L_t and cross section location ξ ,
- hidden layer(s),
- output layer with one output signal of the network $M'_{p,max}$.

Before training and testing processes each envelope of bending moments (Fig. 8-6, line 2) needs to be transformed because of the problems with approximation of boundary conditions. The symmetrical form of the envelopes allows for analysing of their halves only (Fig. 8-6, line 1). The mentioned graphs have been extended by their mirror reflection on the left (Fig. 8-6, line 3) and by horizontal line on the right (Fig. 8-6, line 4). The mentioned problems moved to the new boundaries but fortunately outside of the analysed domain.

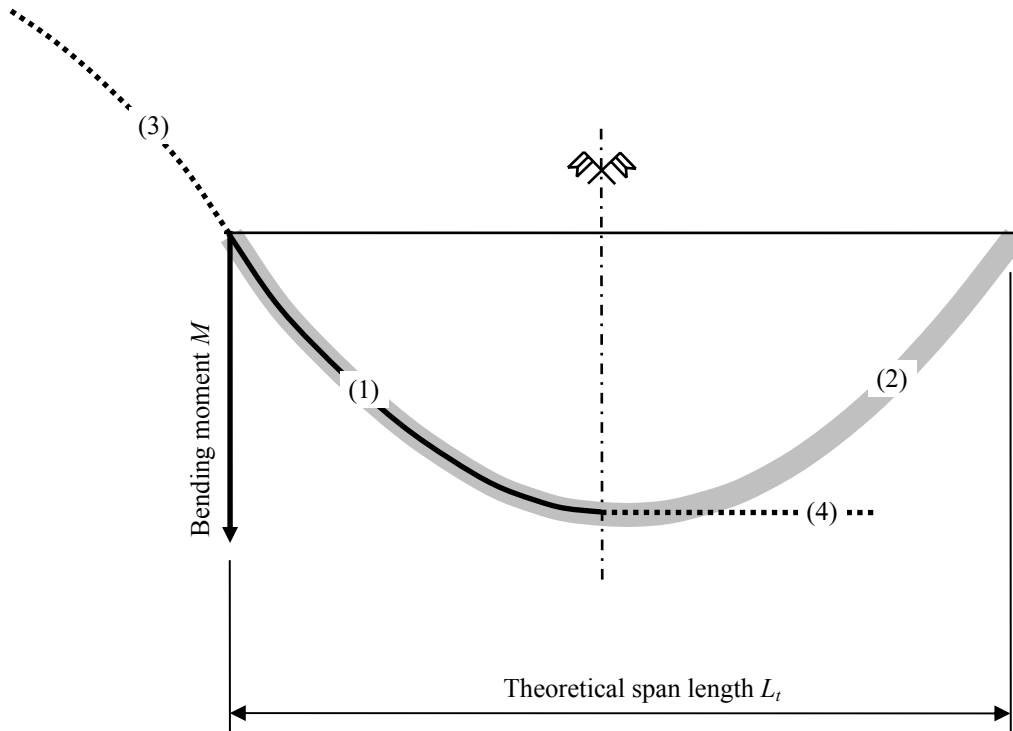


Fig. 8-6 Example of bending moment envelope and its transformation for application in NNT

Three neural networks of various architectures (Fig. 8-7, Fig. 8-8 and Fig. 8-9) have been analysed and compared during creation of N_1 component.

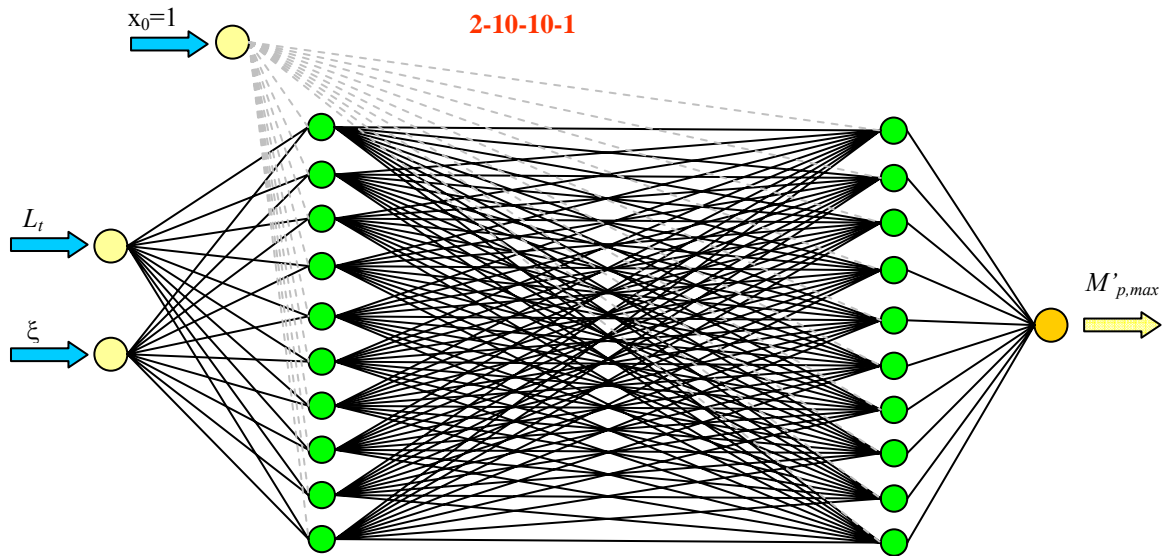


Fig. 8-7 Component N_1 : network architecture “2-10-10-1”

The first network (Fig. 8-7) consists of four layers (input, two hidden and output layer). The input layer corresponds to the parameters of the analysis and consists of two neurons (L_t and ξ). Each of the hidden layers consists of the ten neurons. The output layer is composed of the single neuron ($M'_{p,max}$). Architecture of the network determines its name: “2-10-10-1”.

The next neural network example (see Fig. 8-8) consists of three layers (input, one hidden and output layer). The input layer consists of two neurons (L_t and ξ). The hidden layer is

composed of 20 neurons. The output layer is composed of the single neuron ($M'_{p,max}$). Architecture of the network determines the network name: “2-20-1”.

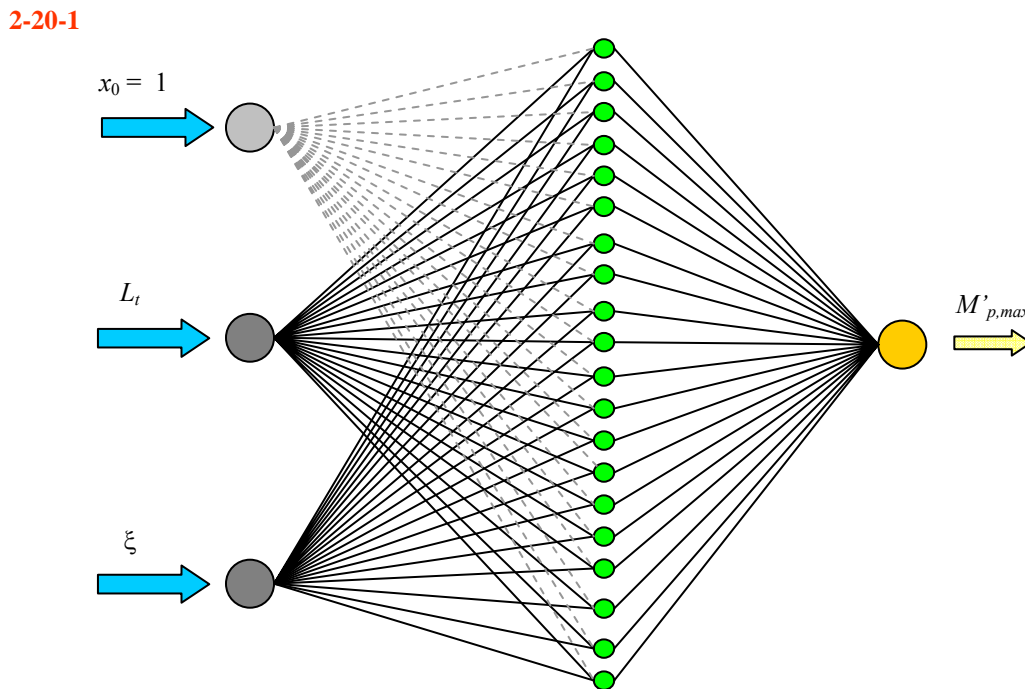


Fig. 8-8 Component N_1 : network architecture “2-20-1”

The third neural network example has been presented in Fig. 8-9. The network is composed of four layers (input, two hidden and output layer). The input layer consists of two neurons (L_t and ξ). Each of the hidden layers consists of ten neurons.

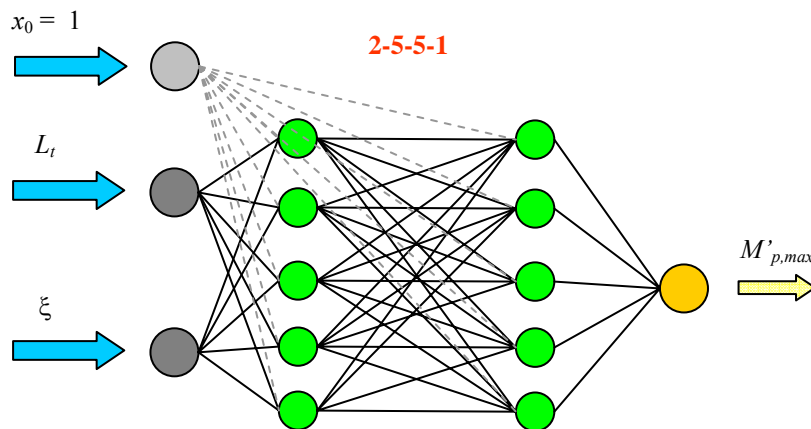


Fig. 8-9 Component N_1 : network architecture “2-5-5-1”

The output layer is composed of the single neuron ($M'_{p,max}$). Architecture of the network determines the network name: “2-5-5-1”.

To analyse efficiency of created neural networks a comparison of accuracy achieved by three various architectures of designed neural networks have been presented in Table 8-1.

Table 8-1 Component N_1 : training and testing errors of various network architectures

Network architecture	Training error		Testing error	
	Avg	RMS	Avg	RMS
2-5-5-1	0.0075	0.0091	0.0104	0.0117
2-10-10-1	0.0061	0.0057	0.0095	0.0092
2-20-1	0.0057	0.0054	0.0067	0.0064

This table presents two error groups (training and testing). The efficiency of the trained neural networks is presented also graphically, i.e. response of these networks against expected and analytically obtained values of envelopes of bending moments for various span lengths (Fig. 8-10 to Fig. 8-15). In this way the response of the neural networks can be easily compared and discussed in order to select the best architecture for further application in the expert tool.

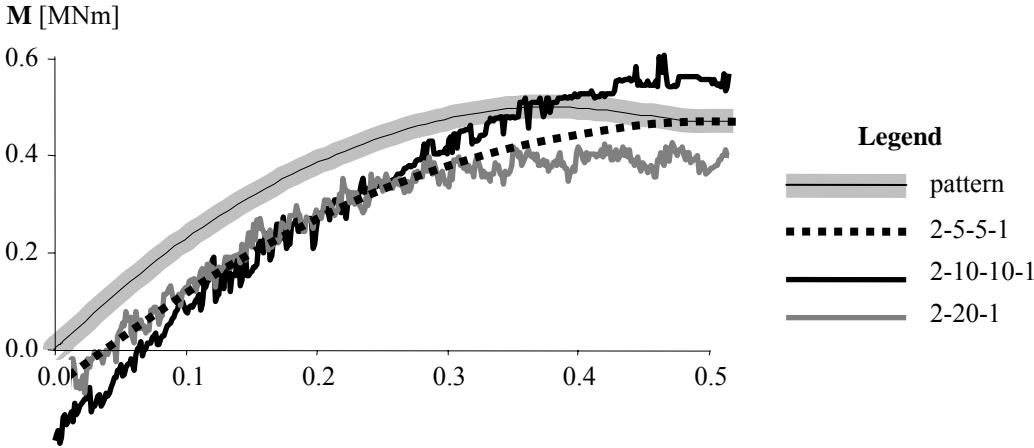


Fig. 8-10 Component N_1 : the network answers and expected values for $L_t = 3.0$ m

The presented results cover span lengths between 3.0 and 19.0 m and the worst behaviour of all networks can be observed for the shortest span length, $L_t = 3.0$ m (Fig. 8-10).

During the creation and training of neural networks some problems with the approximation of boundary conditions occurred. To solve this problem the analysed set of data has been extended by points related to the shorter spans ($L_t = 3.0$ m) and though the range of application of this methodology starts from 6.0 m, for the training purpose these spans have been considered. For the spans of length $L_t = 3.7$ m (Fig. 8-11) the accuracy of this analysis leaves a lot to be desired, but for longer spans the results are much better (Fig. 8-12).

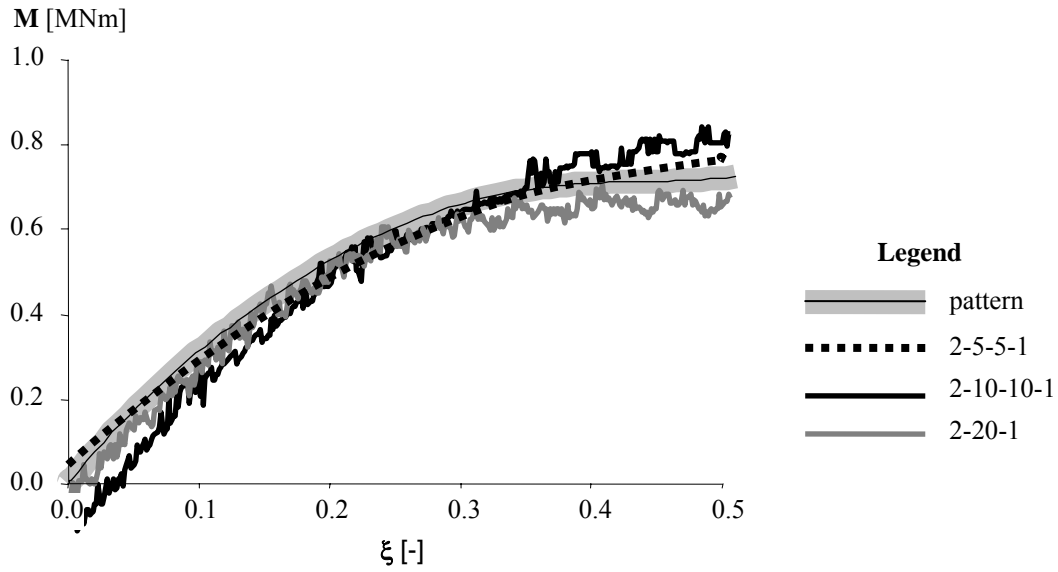


Fig. 8-11 Component N_1 : network answers and expected values for $L_t = 3.7$ m

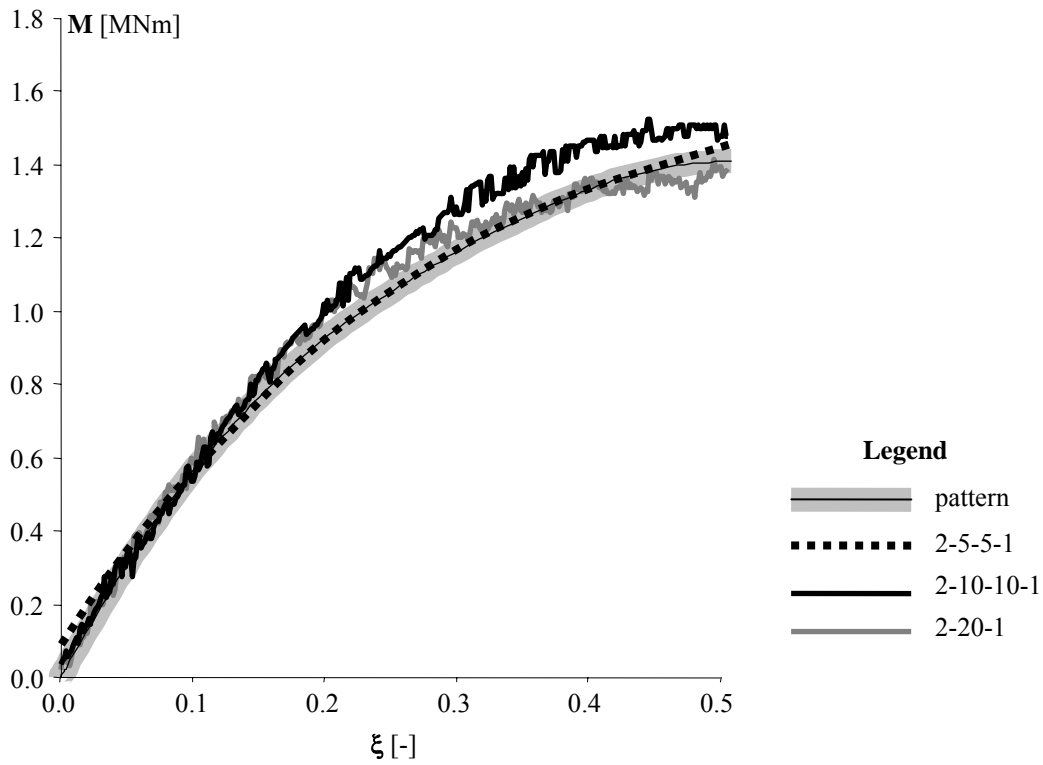


Fig. 8-12 Component N_1 : network answers and expected values for $L_t = 5.5$ m

In the presented figures various behaviours of the created networks can be observed. The network of the architecture “2-5-5-1” represents the best performance.

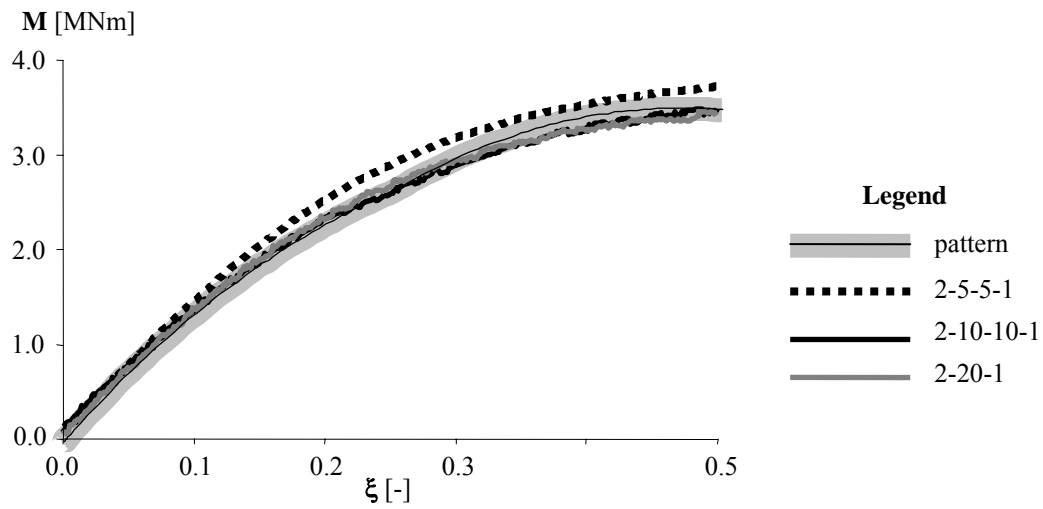


Fig. 8-13 Component N_1 : network answers and expected values for $L_t = 10.0$ m

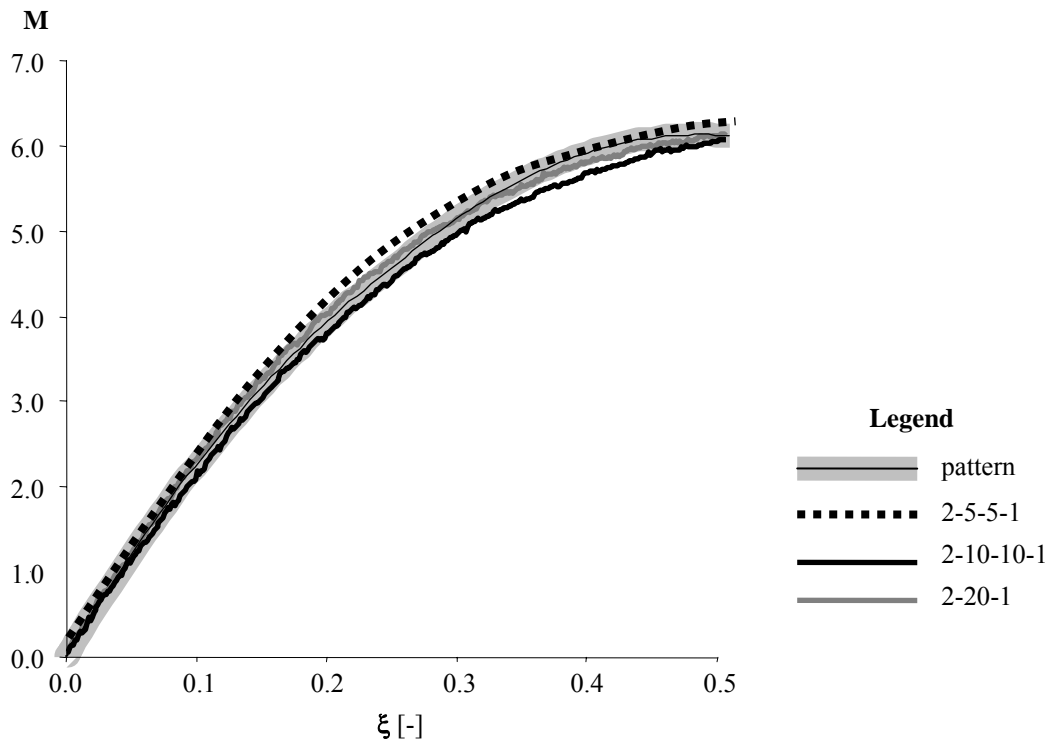


Fig. 8-14 Component N_1 : network answers and expected values for $L_t = 15.0$ m

The simulations for 10.0, 15.0 and 19.0 meters (Fig. 8-13 to Fig. 8-15) represent the highest accuracy of obtained results. The best accuracy has been achieved for the architecture called “2-5-5-1” and this composition has been typed for component N_1 of the expert tool.

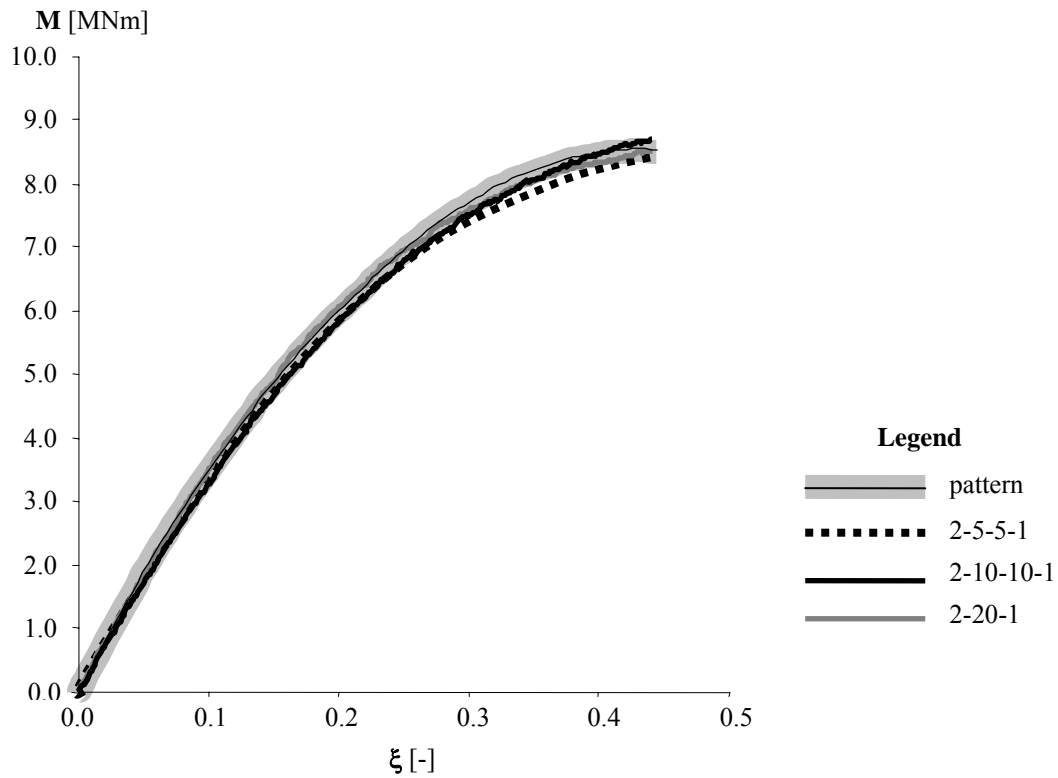


Fig. 8-15 Component N_1 : network answers and expected values for $L_t = 19.0$ m

8.3.2 Neural component N_2

This component has been created and applied for the load capacity assessment of the particular cross section of the analysed span. There are many parameters (related to the geometry as well as material parameters) influencing this value. Some of them are presented in Fig. 8-16.

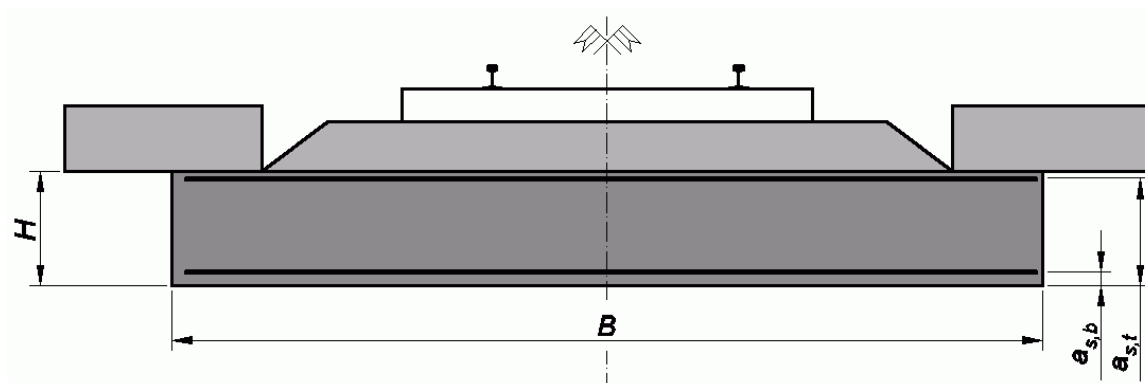


Fig. 8-16 Cross section of the considered RC span to be assessed by means of ANACONDA

To analyse the load capacity of cross section the following parameters should be considered:

- Slab width B ;
- Slab height H ;
- Cross section area of the bottom layer of reinforcement $A_{s,b}$;
- Cross section area of the top layer of reinforcement $A_{s,t}$;
- Location in cross section of the bottom layer of reinforcement $a_{s,b}$;
- Location in cross section of the top layer of reinforcement $a_{s,t}$;
- Compressive strength of concrete R_c ;
- Strength of the top layer of reinforcement $R_{s,t}$;
- Strength of the bottom layer of reinforcement $R_{s,b}$;
- Elastic modulus of the concrete E_c ;
- Elastic modulus of the bottom layer of reinforcement $E_{s,b}$;
- Elastic modulus of the top layer of reinforcement $E_{s,t}$.

The number of parameters and their variability may cause technical problems with presenting of the analysis results. It seems to be clearer, if some of them are considered as variable and the rest – as constant values. The following parameters are considered as constant:

- Slab width, $B = 530$ cm;
- Cross section area of the top layer of reinforcement, $A_{s,t} = 2.26$ cm²;
- Location in cross section of the bottom layer of reinforcement, $a_{s,b} = 8.0$ cm;
- Location in cross section of the top layer of reinforcement, $a_{s,t} = H - (3.6)$ cm;
- Strength of the top layer of reinforcement $R_{s,t}$ has been considered as equal to the strength of the bottom layer of reinforcement $R_{s,t} = R_{s,b}$;
- Elastic modulus of concrete E_c – empirical equation (8-2) based on the strength of reinforcement R_c :

$$E_c = -0.0175(R_c)^2 + 1.3992(R_c) + 13.406; \quad (8-2)$$

- Elastic modulus of the bottom layer of reinforcement, $E_{s,b} = 200$ GPa;
- Elastic modulus of the top layer of reinforcement, $E_{s,t} = 200$ GPa.

Parameters considered as variable in this analysis are listed as follows:

- Cross section height, H ;
- Cross section area of the bottom layer of reinforcement $A_{s,b}$;
- Compressive strength of the concrete R_c ;
- Strength of the bottom layer of reinforcement $R_{s,b}$;

The variable parameters (H , $A_{s,b}$, $R_{s,b}$, and R_c) have the following ranges of variation:

- H – varies between 60 and 105 cm;
- $A_{s,b}$ – varies between 77.0 and 770.0 cm²;
- R_c – varies between 10.0 and 60.0 MPa;
- $R_{s,b}$ – varies between 150.0 and 400.0 MPa.

Each neural network needs to be trained. For this reason a knowledge base containing the relationships between the input parameters (H , $A_{s,b}$, R_c , $R_{s,b}$) and the network's output (load capacity of cross section) is necessary. This base has been created using results of the parametric analysis performed by the DAGA program. In Appendix A the results of this analysis, in the form of 3D graphs, are presented (Fig. 10-2 to Fig. 10-25). All these graphs present the load capacity distribution in function of the cross section area of the bottom part of reinforcement $A_{s,b}$ and various compressive strengths of concrete R_c . Each graph is related to the various slab height H and to the type of steel distinguished by its strength $R_{s,b}$. This analysis allows training and testing of the component N_2 . For the required neural component the following three network architecture have been assumed and compared in order to select the best network:

- “4-9-9-9-9-1”;
- “4-15-15-15-1”;
- “4-19-12-10-22-1”.

Each of these networks consists of:

- input layer related to the parameters of analysis (H , $A_{s,b}$, $R_{s,b}$ and R_c),
- hidden layers,
- output neuron representing the load capacity of cross-section M_R .

In Fig. 8-17 the architecture of the neural network called “4-9-9-9-9-1” is presented.

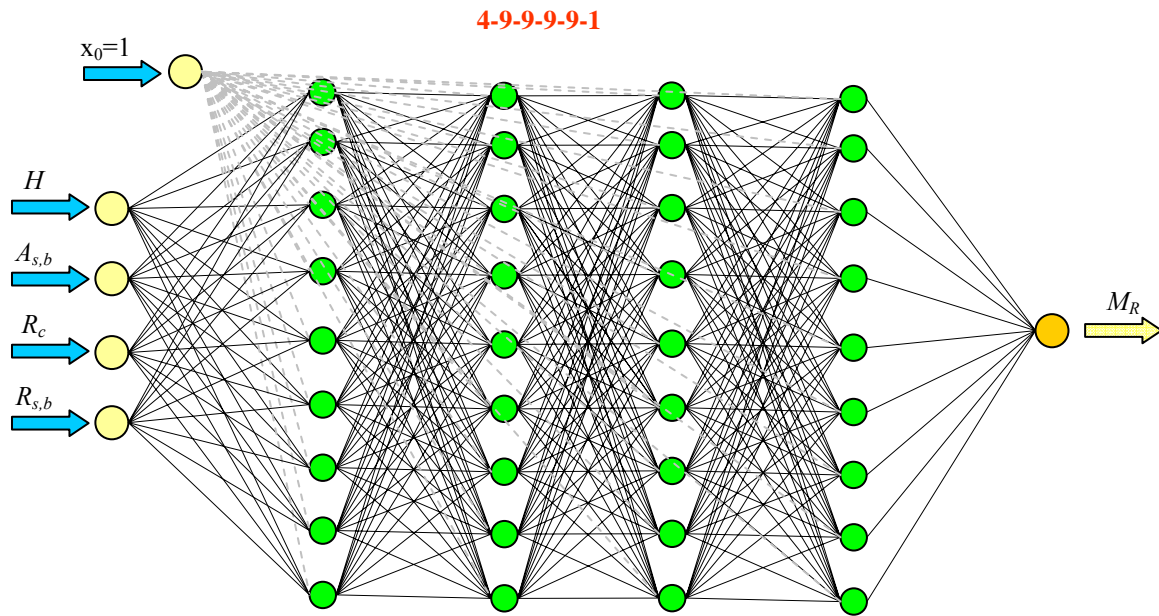


Fig. 8-17 Component N_2 : network architecture “4-9-9-9-9-1”

Modifications of the $A_{s,b}$, $R_{s,b}$, and R_c can be interpreted as defects (loss of reinforcement, compressive strength reduction in concrete and strength reduction of reinforcement).

In the next part of this section efficiency of the created networks will be analysed in order to select the best architecture for the N_2 component. The comparison of these networks will be based on the analyses of the training and testing error (Table 8-2). Moreover the graphic representation of the pattern and the answer of the various networks types, in the function of the single parameter, will be plotted (Fig. 8-18 to Fig. 8-23).

Table 8-2 Component N_2 : training and testing errors of various network architectures

Network architecture	Training error		Testing error	
	Avg	RMS	Avg	RMS
4-9-9-9-9-1	0.0099	0.0117	0.0158	0.0171
4-15-15-15-1	0.0081	0.0073	0.0146	0.0138
4-19-12-10-22-1	0.0076	0.0069	0.0109	0.0102

The main problem with approximation of the analytically performed results occurs when there is a sharp alteration of the angle of the line (see Fig. 8-18, Fig. 8-21, Fig. 8-22 and Fig. 8-23). This problem can be solved by increasing number of the points in the critical zone. Another solution can be dividing the neural network’s domain in the critical point. In the particular case of $H = 60$ cm, $R_c = 10$ MPa, $R_{s,b} = 150$ MPa (Fig. 8-18) this point could be situated for $A_{s,b} = 300$ cm².

For the purpose of this Thesis the accuracy of this analysis is sufficient and the objective of this research is to distinguish the best architecture of the neural network to be applied in the expert tool.

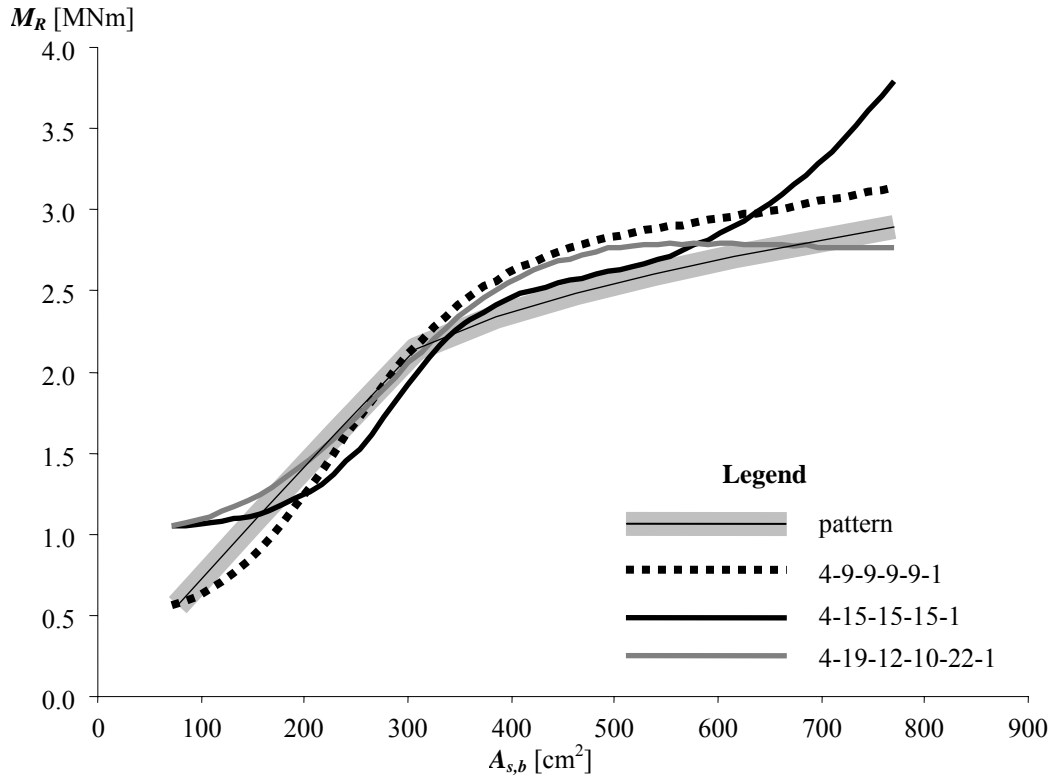


Fig. 8-18 Component N_2 : network answers and expected values for $H = 60$ cm, $R_c = 10$ MPa and $R_{s,b} = 150$ MPa

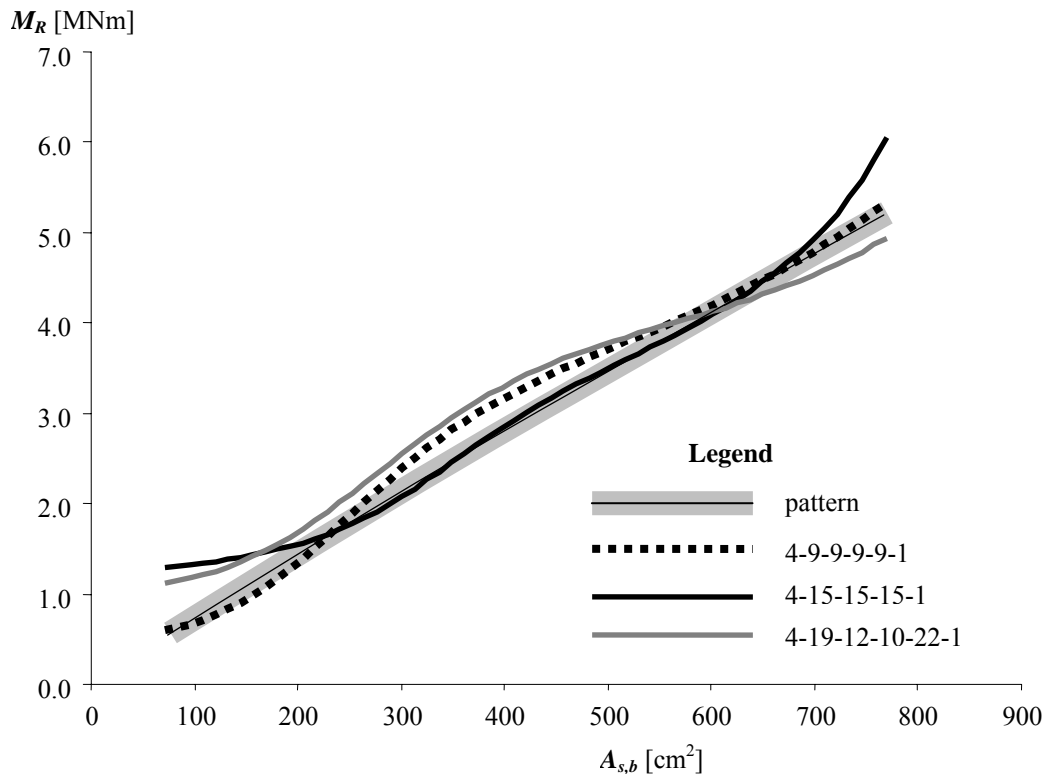


Fig. 8-19 Component N_2 : network answers and expected values for $H = 60$ cm, $R_c = 40$ MPa and $R_{s,b} = 150$ MPa

The results presented in Fig. 8-19 and Fig. 8-20 present much better quality. This is caused by the simpler form of the graph.

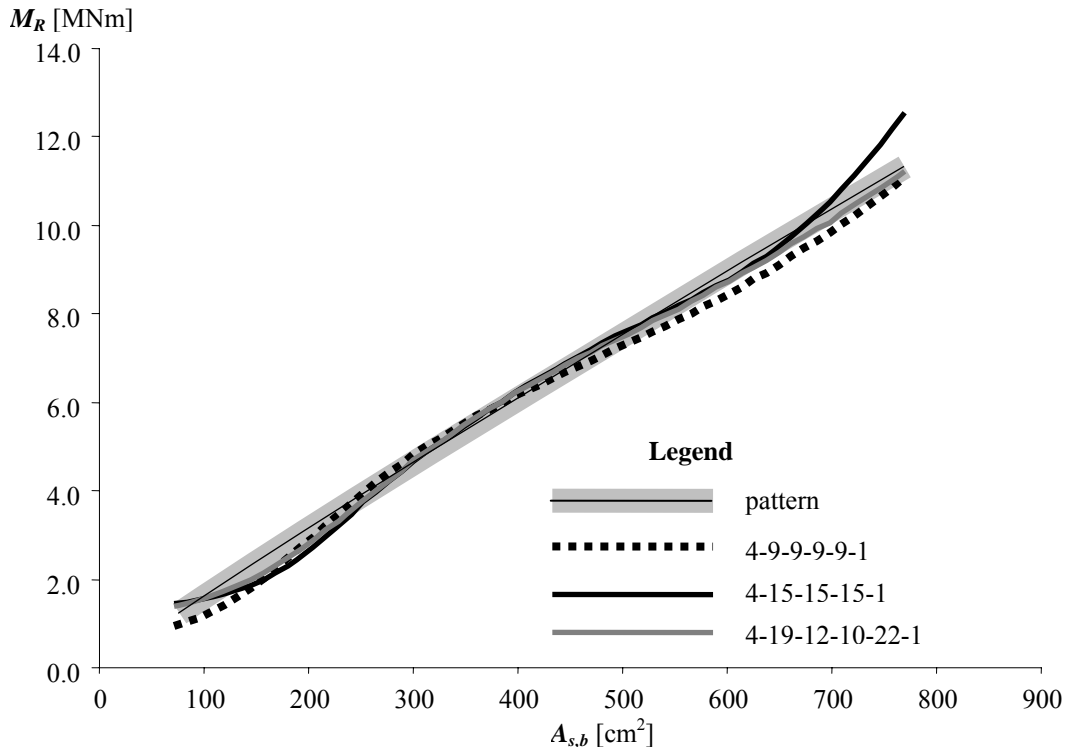


Fig. 8-20 Component N_2 : network answers and expected values for $H = 75$ cm, $R_c = 30$ MPa and $R_{s,b} = 250$ MPa

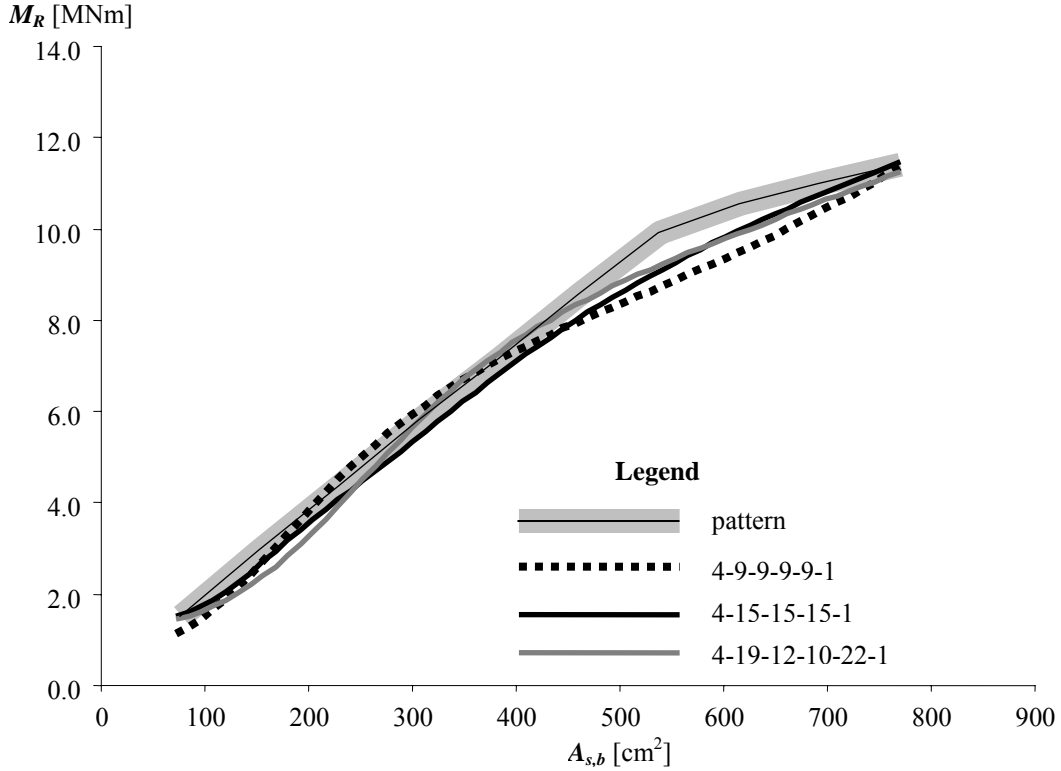


Fig. 8-21 Component N_2 : network answers and expected values for $H = 90$ cm, $R_c = 20$ MPa and $R_{s,b} = 250$ MPa

In these graphs (Fig. 8-21 and Fig. 8-22) the conformity is still relatively high. The best performance can be observed in the network called “4-9-9-9-9-1”.

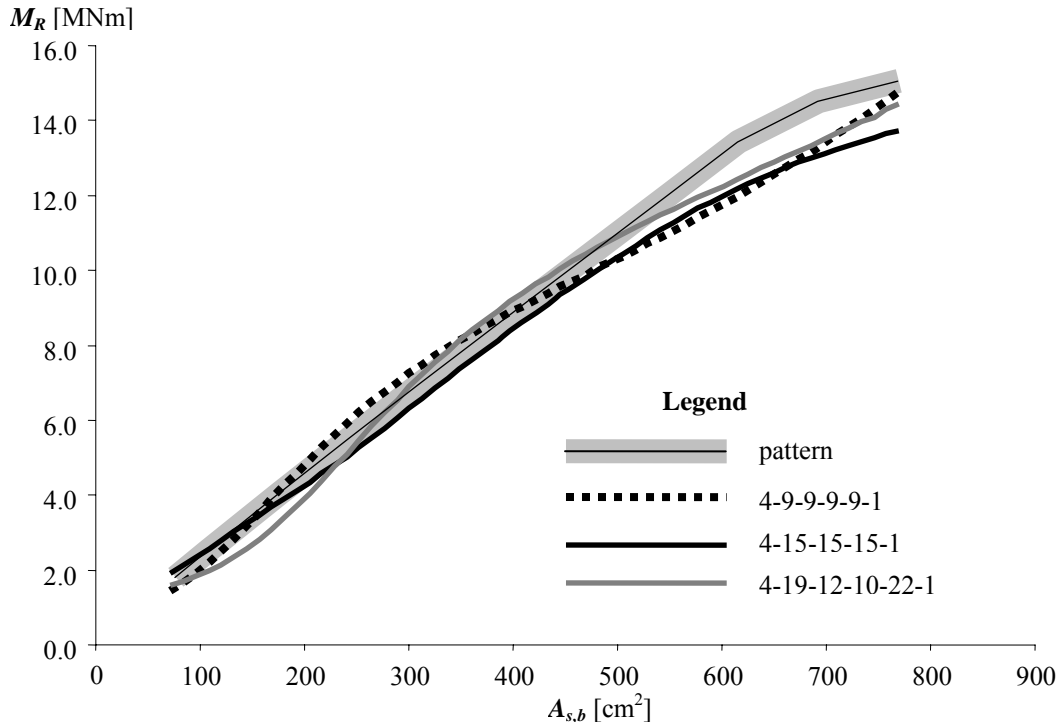


Fig. 8-22 Component N_2 : network answers and expect. values for $H = 105$ cm, $R_c = 20$ MPa and $R_{s,b} = 250$ MPa

The last graph presents worse quality of the analysis than before. It is caused by the form of the line. The network “4-9-9-9-9-1” presents the best accuracy.

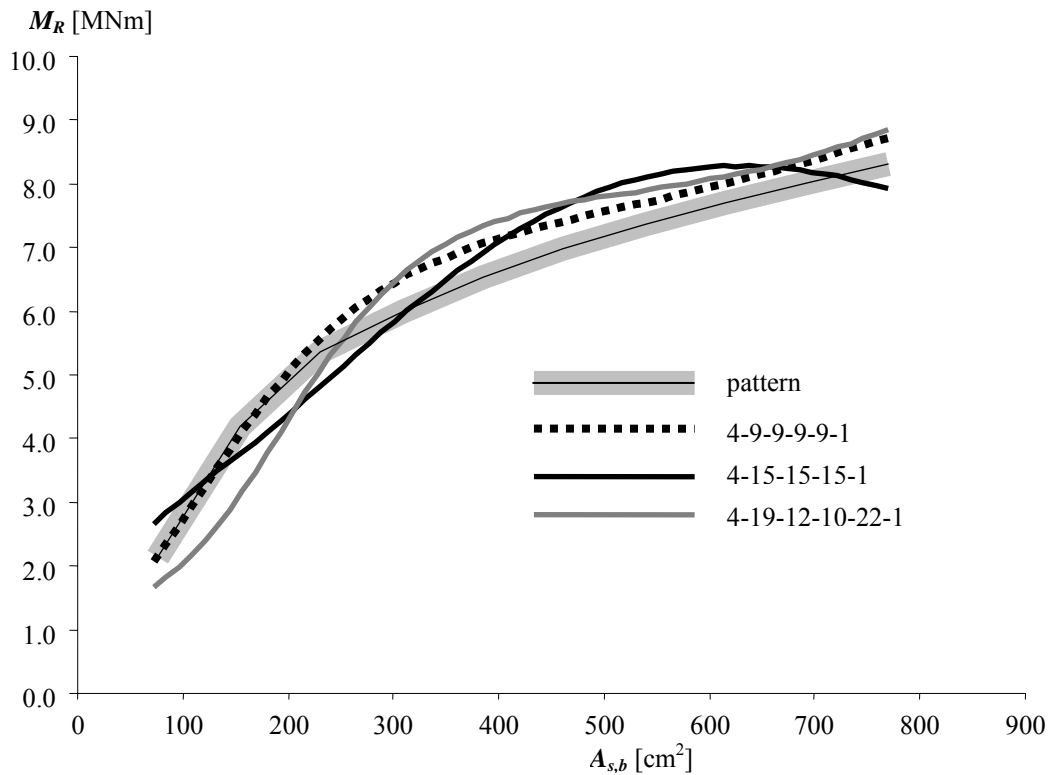


Fig. 8-23 Component N_2 : network answers and expect. values for $H = 105$ cm, $R_c = 10$ MPa and $R_{s,b} = 300$ MPa

For the further application in the expert tool the network 4-9-9-9-9-1 has been typed.

8.4 Functional components

Functional components are destined for the symbolical knowledge representation by means of mathematical functions describing the relationships between their input and output signal. ANACONDA contains of the eight functional components (see Fig. 8-3). They evaluate outputs to be used as the input parameters by other components of the network. These outputs can be listed as follows: intensity of the dead load (F_1); maximal bending moment caused by dead load (F_2); maximal bending moment caused by the moving load taking into account load class factor (F_3); total maximal bending moment in section (F_4); cross section parameters (F_5 , F_6 and F_7) and finally load capacity of the span by comparison the maximal bending moment and the load capacity in the single cross section (F_8).

8.4.1 Functional component F_1

This component, presented in Fig. 8-24, has been created for evaluating intensity of the dead load g . The output value is evaluated by the formula (8-3).

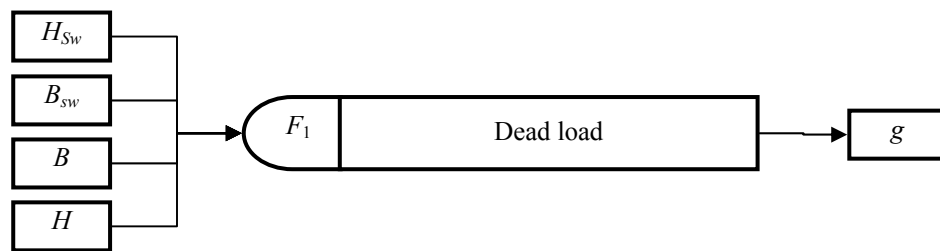


Fig. 8-24 Component F_1 : functional schema

$$g = \gamma_2 \cdot 2(H_{sw} \cdot B_{sw} \cdot \gamma_c) + \gamma_1 \cdot H \cdot B \cdot \gamma_c + \gamma_2 \cdot A_b \cdot \gamma_b + \gamma_2 \cdot g_t, \quad (8-3)$$

where:

H_{sw}, B_{sw} – Side walk height and width;

H, B – Slab height and width;

A_b – Cross section area of the ballast;

g_t – Linear weight of rail track;

γ_1, γ_2 – Load safety coefficient for constructional and non-constructional parts;

γ_b, γ_c – Weight by volume of the ballast and concrete.

In the presented version of ANACONDA only slab height H , ballast thickness H_b and dimensions of the side walks B_{sw} and H_{sw} are the inputs accessible for the user. The rest of the parameters are considered as the constant values as follows: $A_b = 12\,000\text{ cm}^2$ (for ballast thickness $H_b = 30\text{ cm}$); $g_t = 2.8\text{ kN/m}$; $\gamma_1 = 1.2$; $\gamma_2 = 1.5$; $\gamma_b = 20.0\text{ kN/m}^3$; $\gamma_c = 24.0\text{ kN/m}^3$.

8.4.2 Functional component F_2

This component is created for evaluating of the maximal bending moment caused by dead load (Fig. 8-25). The dead load intensity g (evaluated by the functional component F_2), theoretical span length L_t and cross section number i are its three inputs. The mentioned maximal bending moment in section i caused by dead load $M_{g,max,i}$ is its output.

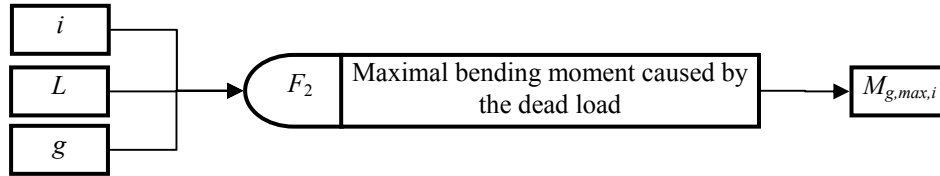


Fig. 8-25 Component F_2 : functional schema

The mathematical formula (8-4) of this component is presented below:

$$M_{\max,g}(g, L_t, \xi) = \frac{1}{2} \cdot g \cdot L_t^2 \cdot \xi \cdot (1 - \xi). \quad (8-4)$$

where:

$M_{g,max}$ – The maximal bending moment caused by the dead load;

L_t – Theoretical span length;

ξ – Cross-section location.

8.4.3 Functional component F_3

This component is created for evaluating of the maximal bending moment $M_{p,max,i}$ caused by the moving load for each load class in section i . In Fig. 8-26 the schema of this element is presented. The maximal bending moment in section i caused by moving load for load class $\alpha = 1.0$ $M'_{p,max,i}$ and load class coefficient α are its two inputs.

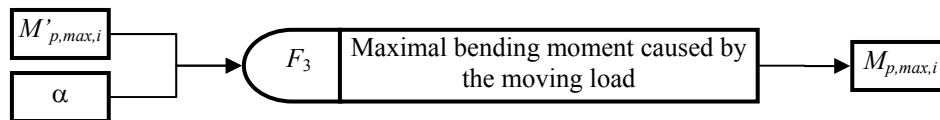


Fig. 8-26 Component F_3 : functional schema

The output of this component is evaluated by (8-5).

$$M_{p,max,i} = \alpha \cdot M'_{p,max,i}, \quad (8-5)$$

where:

$M'_{p,max,i}$ – The maximal bending moment in section i caused by moving load for load class $\alpha = 1.0$ evaluated by the neural component N_1 ;

α – Load class coefficient.

8.4.4 Functional component F_4

This component is created for evaluating value of the total maximal bending moment in section i (Fig. 8-27). The maximal bending moment in section i caused by moving load $M_{p,max,i}$ and the maximal bending moment in section i caused by dead load $M_{g,max,i}$ are its two inputs. The total maximal bending $M_{max,i}$ is its output.

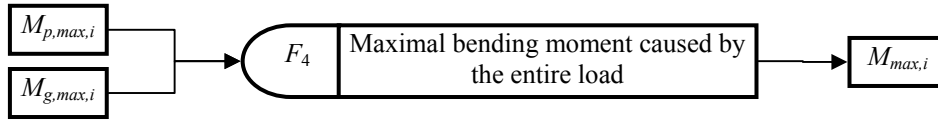


Fig. 8-27 Component F_4 : functional schema

The mathematical formula of this component is presented below (8-6).

$$M_{max,i} = M_{p,max,i} + M_{g,max,i}, \quad (8-6)$$

where:

$M_{p,max,i}$ – The maximal bending moment in section i caused by moving load evaluated by the functional component F_3 ;

$M_{g,max,i}$ – The maximal bending moment in section i caused by dead load evaluated by the functional component F_2 .

8.4.5 Functional components F_5 , F_6 and F_7

These components work in the same way (Fig. 8-28 to Fig. 8-30). The cross section number i are their single inputs. For the section i these components (F_5 , F_6 and F_7) evaluate the cross section area of the bottom reinforcement $A_{sb,i}$, the strength of the bottom reinforcement $R_{sb,i}$ and the compressive strength of the concrete $R_{c,i}$. All these parameters are saved in the vector form defined previously by user (see Fig. 10-46 in Appendix C), where the section number i is related to the element of this vector.

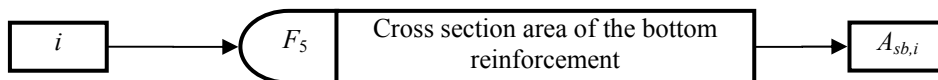


Fig. 8-28 Component F_5 : functional schema



Fig. 8-29 Component F_6 : functional schema

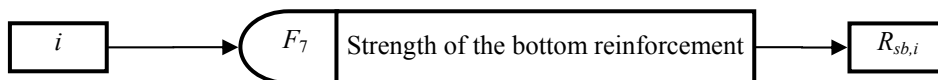


Fig. 8-30 Component F_7 : functional schema

8.4.6 Functional component F_8

This component (Fig. 8-31) is created for evaluating the load capacity of the span by comparison the maximal bending moment in the cross section i ($M_{max,i}$) with load capacity of cross section in the section i ($M_{R,i}$). Also the graphic part as envelopes of the bending moment and distribution of the load capacity of cross sections are being performed here.

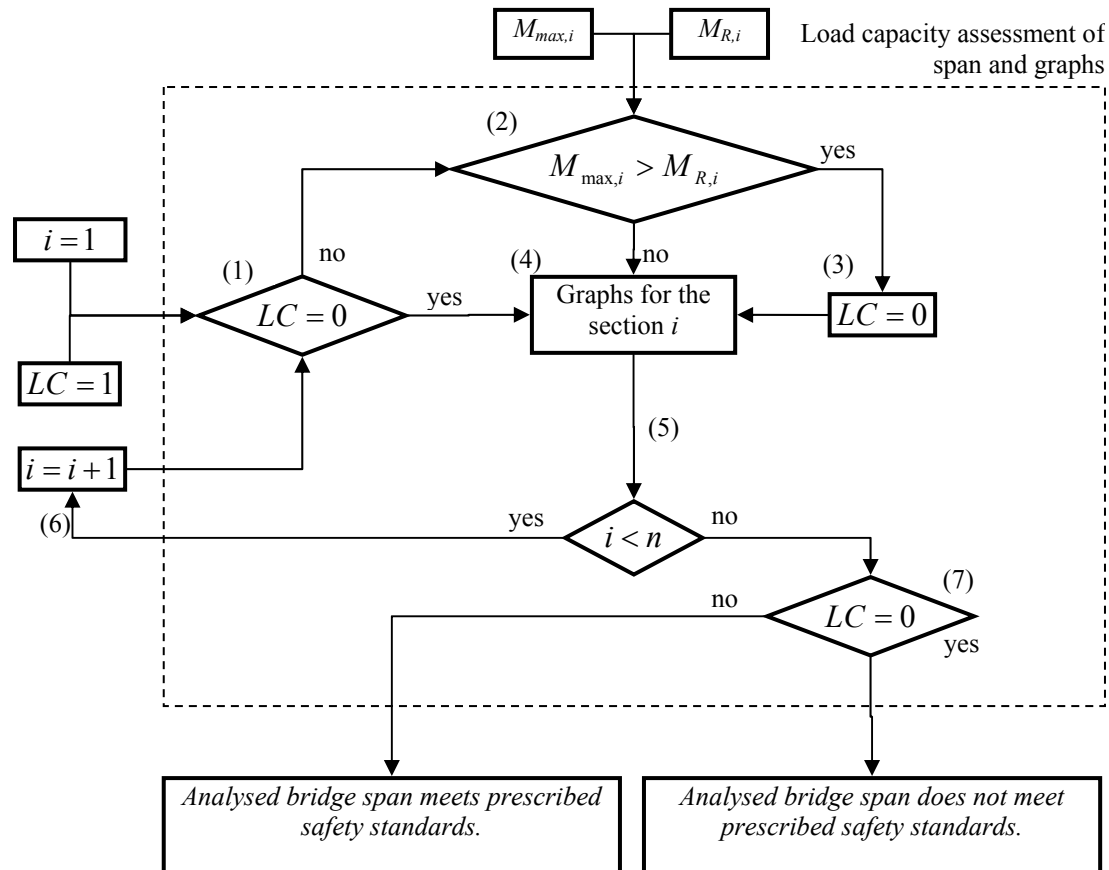


Fig. 8-31 Component F_8 : functional schema

The span is divided into n virtual cross sections. This component works as a loop through all cross sections from $i=1$ to n . Firstly the load capacity parameter is assumed as $LC=1$, which means that the load capacity of the considered span is not exceeded. The program checks whether the load capacity parameter is equal to zero (1). The first step of this loop is to check that the assumed load capacity is not exceeded. Then program compares the bending moment with the load capacity for the analysed cross section (2). If the load capacity is exceeded then the load capacity parameter is set to $LC=0$ (3). In terms of this parameter the loop is finished, but the program continues in order to plot (4) the relationship between the maximal bending moment and the load capacity for each cross section. At the end of the particular step of this loop the program checks whether the current cross section is the last (5). If the number of current cross section is less than n , then program goes to the next cross section (6) and the

loop processes again. The last operation of this component is to check the load capacity parameter when the loop has reached the last cross section (7). Basing on this parameter the final answer of this component can be returned.

Chapter 9

Conclusions

9.1 General conclusions

The objective of this Thesis was to propose a complete methodology of the load capacity evaluation of railway RC slab spans with defects. In the next sections conclusions related to the particular elements of Thesis will be presented.

9.2 Bridge survey

The presented statistical information on the existing railway bridge infrastructure shows that RC structures are one of the most common construction types. According to bridge span profile, spans of length between 4 and 20 meters constitutes the biggest group of the railway bridge population with domination of structures situated along single tracks. Moreover, in case of multi-track lines the span construction is longitudinally divided and each line is carried by a separated structure.

For these reasons the analysis of efficiency of the simplified geometry model has been considered. Concerning the age of bridges, constructions of 20-100 years old form the biggest group, which explains a need of analysis of deteriorated structures.

9.3 Taxonomy of defects

In this study the Author presented a uniform classification of defects occurring to the considered structures. A special attention has been paid for defect reasons (i.e. degradation mechanisms) as well as testing method for their identification. Moreover relationships between degradation mechanisms, defects and testing methods have been presented.

9.3.1 Classification of defects

Concerning modelling of deteriorated structures unambiguous definition of defects is required. The solutions described in the literature are characterised by the lack of uniform criteria at the level of the creation of the defect classification. In this study a uniform classification of defects based on the “cause” criterion has been presented. This solution allows creating numerical models of defects to be applied for the load capacity evaluation of the considered structure types. Defect identification can be strongly supported by means of the richly illustrated catalogue of railway defects (Bień et al. 2007b). Identified defects by bridge inspectors and described according to the presented system can be unambiguously interpreted during a further analysis of considered structure (Maksymowicz et al. 2006a, Maksymowicz et al. 2006b). Proposed classification of defects can be applied for all types of structural (i.e. concrete, masonry and steel) and non-structural bridge parts. This methodology has been already presented and discussed in the international forum of discussion (Bień et al. 2004a, Maksymowicz et al. 2006c) and also accepted and applied in the framework of the European research project “Sustainable Bridges” (Bień et al. 2004b, Bień et al. 2007a, Sustainable Bridges 2007).

9.3.2 Testing methods

Each defect and geometry parameter (i.e. length of span, reinforcement location etc.) to be considered in the load capacity evaluation needs to be measured. Basing on the available solutions, described in the literature, the Author presented various testing methods for RC slab span assessment. The relationship presented between defect types with respect to the load capacity assessment and available testing methods enables selection of methods of condition appraisal of RC railway bridges.

9.3.3 Mechanisms of degradation

Presented classification of degradation mechanisms of RC slab spans together with defects and testing methods creates a basis for a consistent identification and description of the railway bridge defects as well as for comparable assessment of their load capacity

(Maksymowicz et al. 2006a, Maksymowicz et al. 2006b). Defined relationships between degradation mechanisms and defects should help in optimisation of the maintenance strategies and in reliable foresight of the bridge infrastructure lifetime. This research has been applied in the framework of the European scientific project “Sustainable Bridges” (Bień et al. 2004b, Bień et al. 2007a, Sustainable Bridges 2007) as well as discussed in the international forum of discussion of IABMAS conference (Maksymowicz et al. 2006c).

9.4 Defect modelling

In Chapter 6 a complete methodology for damaged railway RC slab spans modeling has been presented. The solutions cover the defect types which cause load capacity reduction, i.e. losses of material (concrete and reinforcement) and material parameters modifications (strength, elastic modulus). This methodology is presented against the (e^1, s^1) and (e^1, s^2) geometry model classes.

According to the statistical information presented in Chapter 2, the analysis of the possibility of geometry model simplification, i.e. simply supported beam, has been presented and discussed. The analysis has been divided into the analysis of undamaged and damaged slab spans.

Concerning the undamaged spans, the analysis results showed that the simply supported beam can be applied for span of length at least 6.0 meters, practically independently on the slab height. In order to assess shorter slab spans a more advanced model (for example grillage) is necessary. This conclusion is applicable also for damaged spans of constant defect intensity along the considered cross section.

Regarding damaged constructions, another set of analyses has been performed. The aim of this study was to analyse the influence of asymmetrically applied defect (against the uniformly distributed) along the cross section on the load capacity assessment. The obtained results have been presented in a function of span length and have lead to the conclusion that longer spans are more sensitive in terms of model simplification.

9.5 Load capacity assessment

Two approaches of the load capacity assessment have been proposed. The first is related to the analytically performed analysis; the second approach has been carried out by means of the expert tool based on the hybrid network technology with neural and analytical components incorporated. Both solutions have been applied by two computer programs developed by the

Author, i.e. DAGA (“Damage Assessment Graphic Analyser”) and ANACONDA (“ANALYSIS of CONcrete spans with DAmages”).

9.5.1 Program DAGA

The presented program DAGA enables fast and precise analysis of load capacity of railway RC slab spans taking into account common defects, i.e. losses of material and material property modifications. Due to its user-friendly interface and simple graphic editor this program can be used on intuitive way. The example of analysis illustrates all of these features. The system does not require user training in modelling, analysis and strength evaluation of damaged RC constructions. DAGA can be used on every level of infrastructure bridge management. Only standard computer environment is required. The programme makes possible the quick processing of data and immediate results delivering. The description of this program as a use’s manual can be found in Appendix B.

The presented solutions have been already presented in the international forum of discussion (Maksymowicz et al. 2006a) and also in the national conference in Poland (Maksymowicz et al. 2006b).

9.5.2 Program ANACONDA

In Chapter 8 a conception of the load capacity assessment of damaged railway RC slab spans has been presented. The Author proposed his own expert tool (ANACONDA) based on the hybrid network technology. The engine of this program is composed of the neural and functional components. The knowledge stored in the neural components has been acquired from the results of parametric analyses performed by means of the DAGA program. Systematic analysis for all important parameters influencing load capacity enabled creation of the knowledge base built on the results of large numbers of the calculations (see Appendix A). The parametric strength analysis can be extended for the other parameters in order to obtain full view of relationship between the load capacity of cross section and various factors. Concerning the neural networks their several architectures have been provided and the efficiency analyses have been performed. The best networks were implemented into the system. The system can be used for analysis of the individual structures as well as for parametric analysis of the structure sensitivity to each factor. The proposed tool, despite simplified description of the damaged span, guarantees high precision of the load capacity evaluation (by simple interface – see the User’s Manual in Appendix C) because of high quality knowledge involved. In this appendix the parametric analysis of the load capacity of

cross section has been presented. The results with input parameters can be saved in the knowledge base for the purposes of neural network training and testing. The possibilities of the practical application of this analysis can be found in Appendix C.

9.6 Further developments

Though in this study a complete methodology of load capacity assessment of railway RC slab spans with defects has been proposed, its several elements can be extended and a further research will be fruitful.

Concerning testing method a non-destructive technique for the reinforcement strength assessment is still missing, but the market is under a continuous development process offering newer and newer solutions and hopefully some technique will appear. Otherwise a sample extraction will be only solution.

Regarding to the load capacity evaluation by DAGA program there are potential gaps to be filled in the future. Though this program is destined to the effective graphical modelling of defects and the static-strength analysis the considered geometry model makes this analysis limited. In Chapter 6 the range of application of the simplified model applied in the analysis has been presented and discussed. The consideration of other geometry models applied in structure analysis, e.g. (e^2, s^3) and (e^3, s^3) would extend the range of DAGA's application for other structure types, e.g. hyper-static constructions, multi-track bridges and so on. Also other load models and strength analysis procedure would be applied.

ANACONDA program offers very fast analysis of damaged slab spans, but also in this case its range of application can be extended. Analysis engine provided into this system is based on the limited input parameters such as compressive strength of concrete, strength of the bottom layer of reinforcement with cross-sectional area and also slab depth. These parameters can vary within the specified ranges which can be extended, but also other parameters can be provided in order to expand the possibilities of ANACONDA system. For example the location of reinforcement and other types of cross section would be considered as the first step. Like in case of DAGA program this software is based on the simplified geometry model. By providing to the geometry at least the lateral dimension of the span with all consequences for the analysis, the range of application would increase significantly. Unfortunately such expansion is related to the large increase of size of the knowledge base which would make a knowledge acquisition work consuming.

The load capacity assessment is a practical measure of bridge condition. Time goes by and the load capacity changes. Taking the time into account, i.e. modelling of the degradation mechanisms, a possibility of expansion of this methodology appears.

References

- Al-Serori M.Sh., Jávor T. & Nad L. (1996), Influence of Temperature on the Degradation of the Concrete Quality, Proceedings of the 2nd RILEM International Conference, Štrbské pleso, Slovakia, October 7-11, pp. 506-509;
- Alvarado C. & Davis R. (2001), Resolving Ambiguities to Create a Natural Computer-Based Sketching Environment, Proceedings of IJCAI'01 Workshop on Ontologies and Information Sharing, Seattle, WA, USA;
- Amen D.K.H., Al-Lashi, R.S. & Al-Rawi R.S. (2006), Prediction Model for the Final Shrinkage of Concrete Using Artificial Neural Network, Proceedings of the 2nd FIB Congress, Naples, Italy;
- Appraisal of existing structures (1996), The Institution of Structural Engineers, Second edition, London;
- Bakhshi M., Mahoutian M. & Shekarchi M. (2006), The Gas Permeability of Concrete and Its Relationship with Strength, Proceedings of the 2nd FIB Congress, Naples, Italy;
- Bamforth P.B. (2004), Concrete Society, Technical Report No. 61, Enhancing reinforced concrete durability, Guidance on selecting measures for minimising the risk of corrosion of reinforcement in concrete;
- Bertagnoli G., Mancini G. & Tondolo F. (2006), Bond Deterioration Due to Corrosion and Actual Bearing Capacity, Proceedings of the 2nd FIB Congress, Naples, Italy;
- Bień J. (2002), Modelling of Bridge Structures during their operation (in Polish), Publishing House of the Wroclaw University of Technology;
- Bień J. & Rawa P. (2004), Hybrid Knowledge Representation in BMS, Archives of Civil and Mechanical Engineering 4(1): 41-55;

- Bień J., Król D., Rawa P. & Rewiński S. (1997), Komputerowa ewidencja obiektów inżynierskich, Seria wydawnicza: System Zarządzania Mostami Kolejowymi SMOK, Dyrekcja Generalna PKP, Warszawa (in Polish);
- Bień J., Cruz P.J.S. & Maksymowicz M. (2004a), Unified classification of damages of railway concrete bridges, V-th Scientific-Technical Conference – Design, construction and maintenance problems of short and medium span bridges, Wrocław, Poland, pp. 31-40 (in Polish);
- Bień J., Rawa P., Jakubowski K., Kamiński T. & Maksymowicz M. (2004b), Deliverable D3.3 - Possibilities of unification of bridge condition evaluation, Sustainable Bridges – Assessment for Future Traffic Demands and Longer Lives;
- Bień J., Jakubowski K., Kamiński T., Kmita J., Rawa P., Cruz P.J.S. & Maksymowicz M. (2007a), Railway bridge defects and degradation mechanisms, “Sustainable Bridges – Assessment for Future Traffic Demands and Longer Lives”, Dolnośląskie Wydawnictwo Edukacyjne, Wrocław 2007;
- Bień J., Jakubowski K., Kamiński T., Rabięga J., Rawa P., Zwolski J., Cruz P.J.S. & Maksymowicz M. (2007b), Sustainable Bridges, D3.15 Guideline for inspection and condition assessment of railway bridges, Annex 2: Defect catalogue;
- Bijen J.M.J.M. (1989), Maintenance and repair of concrete structures, HERON, Netherlands school for advanced studies in construction 34(2);
- Brancaleoni F., Spina D. & Valente C. (1993), Structural Damage State Assessment via Neural Networks, Colloquium of the International Association for Bridge and Structural Engineering „Knowledge Support Systems in Civil Engineering”, Beijing, China, IABSE, Zurich, Switzerland, 1993, Vol. 68, pp. 341–350;
- Branco F.A. & de Brito J. (2004), Handbook of concrete bridge management, American Society of Civil Engineers ASCE;
- Brandt A.M. & Kasperkiewicz J. (2003), Diagnosis of Concrete and High Performance Concrete by Structural Analysis, Institute of Fundamental Technological Research at Polish Academy of Science, North Atlantic Treaty Organization, Scientific Affairs Division, Warsaw, Poland: Argraf (in Polish);
- Bridge Inspection Manual (1996), Swedish National Road Administration, Publication 1996:036(E);
- British Standard (1986), Testing concrete – Part 201: Guide to the use of non-destructive methods of test for hardened concrete;
- Capozucca R. (1995), Damage to reinforced concrete due to reinforcement corrosion, Construction and Building Materials, Vol. 9, No. 5, pp. 295-303;
- Cheetham D.W. (1994), Dealing with vandalism – a guide to the control of vandalism, CIRIA Special publication 91;
- Concrete Society (2000), Technical Report No. 54, Diagnosis of deterioration in concrete structures, Identification of defects, evaluation and development of remedial action;
- Craven M.W. & Shavlik J.W. (1998), Using Neural Networks for Data Mining, Future Generation Computer Systems issue on Data Mining;

- Currie R.J. & Robery P.C. (1994), Repair and maintenance of reinforced concrete, Building Research Establishment Report;
- Davies C.M. & Austen I.M. (1987), The fatigue performance of reinforced concrete beams, Contractor Report 53, Transport and Road Research Laboratory, Department of Transport;
- Dekoster M., Buyle-Bodin F., Maurel O. & Delmas Y. (2003), Modelling of the flexural behaviour of RC beams subjected to localised and uniform corrosion, *Engineering Structures* 25, pp. 1333–1341;
- Department of Transport (1993), Highways, Safety and Traffic, Inspection and repair of concrete highway structures, Departmental advice note BA 35/90;
- Design Manual for Roads and Bridges (1993), Volume 3, Section 4, BA 38/93 Assessment of the fatigue life of corroded or damaged reinforcing bars;
- Diggest (2000), Corrosion of steel in concrete, Investigation and assessment, Part 2;
- Domsa J. (1996), Some aspects concerning the defects of concrete structures and their remedy, Proceedings of the 2nd RILEM International Conference, Štrbské Pleso, Slovakia, pp. 435-438;
- Enochsson O., Elfgrén L., Olofsson T., Täljsten B., Töyrä B., Kronborg A. & Paulsson B. (2006), Assessment and condition monitoring of a concrete railway bridge in Kiruna, Sweden, Proceedings of the 3rd International Conference on Bridge Maintenance, Safety and Management, IABMAS, Porto, Portugal;
- Fagerlund G. (1997), Durability of concrete constructions, Warsaw: Arkady (in Polish);
- Fang C. (2006), Bond-slip behaviour of corroded reinforcing steel in concrete bridges, Proceedings of the 3rd International Conference on Bridge Maintenance, Safety and Management, IABMAS, Porto, Portugal;
- Fang C., Lundgren K., Plos M. & Gylltoft K. (2004), The effect of corrosion on concrete bridges, Proceedings of the 2nd International Conference on Bridge Maintenance, Safety and Management, IABMAS, Kyoto, Japan;
- FIB (2003), Monitoring and safety evaluation of existing concrete structures, FIB Bulletin 22;
- Flood I., Muszynski L. & Nandy S. (2001), Rapid analysis of externally reinforced concrete beams using neural networks, *Computers & Structures*, Vol. 79, Issue 17, July 2001, pp. 1553-1559;
- Folic R.J. & Ivanov D. (1996), Damage classification of concrete structures, Proceedings of the 2nd RILEM International Conference, Štrbské pleso, Slovakia, pp. 403-412;
- Fookes P. (1976), A plain man's guide to cracking in the Middle East, *Concrete*, Vol. 10, No. 9, pp. 20-22;
- Gaal G.C.M. (2004), Prediction and deterioration of concrete bridges (PhD Thesis), Corrosion of reinforcement due to chloride ingress and Carbonization, Delft: DUP Science;
- Galloway J. W., Harding H.M. & Raithby K.D. (1979), Effects of age on flexural, fatigue and compressive strength of concrete, Transport and Road Research Laboratory, department of the Environment, Department of Transport, TRRL Laboratory Report 865;

German Instruments (2003), NDT systems for Durability of New Structures, Service Life Estimation, Fact Construction, Structural Integrity, Repair Quality, Monitoring, Catalog NDT, Copenhagen, Denmark;

Grimes T.C., Gauntt F.M. & Davidson J.S. (2001), Local Roads Bridge Replacement Prioritization Database (BRPD) Program, University Transportation Center for Alabama, UTCA Report Number 00219;

Hansen B. (1997), State of the Art of Neural Networks in Meteorology, Midterm Paper for course in Neural Networks, Technical University of Nova Scotia;

Helmerich R. & Niederleithinger E. (2005), Deliverable D3.16 - Guideline for Condition Assessment and Inspection, Subdeliverable D3.16-1: NDT-toolbox for the Inspection of Railway Bridges (draft version), Sustainable Bridges – Assessment for Future Traffic Demands and Longer Lives;

Highways Agency (2006), Design manual for roads and bridges, Vol. 3 Highway structures – Inspection and maintenance, Section 1 Inspection, Part 7 Advice notes on the non-destructive testing of highway structures;

Hobbs D.W. (1998), Minimum requirements for durable concrete, Carbonation- and chloride-induced corrosion, freeze-thaw attack and chemical attack, British Cement Association, Berks, Great Britain;

Horváth B. & Popa I. (1996), Diagnosis of reinforced concrete structures, Proceedings of the 2nd RILEM International Conference, Štrbské pleso, Slovakia, October 7-11, pp. 423-428;

Horrigmoe G. (2004), D3.11: Specifications for Finite Element Modelling of Reinforced Concrete Structures Attacked by Corrosion, Sustainable Bridges – Assessment for Future Traffic Demands and Longer Lives;

Hover K.C. (1996), Special problems in evaluating the safety of concrete bridges and concrete bridge components, Construction and Building Materials, Vol. 10, No. 1, p. 3943;

Hozjan T., Turk G. & Srpčič S. (2007), Fire analysis of steel frames with the use of artificial neural networks, Journal of Constructional Steel Research, Volume 63, Issue 10, October 2007, pp. 1396-1403.

Hsu D.S. & Yeh I.C. (1993), Damage detection using artificial neural system, Colloquium of the International Association for Bridge and Structural Engineering „Knowledge Support Systems in Civil Engineering”, Beijing, China, IABSE, Zurich, Switzerland, 1993, Vol. 68, pp. 263–272;

Inel M. (2007), Modelling ultimate deformation capacity of RC columns using artificial neural networks, Engineering Structures, Volume 29, Issue 3, March 2007, pp. 329-335;

Jensen B.B., Frølund T. & Pedersen T. (2006), Current use of NDT in bridge condition assessments Proceedings of the 3rd International Conference on Bridge Maintenance, Safety and Management, IABMAS, Porto, Portugal;

Jáuregui D.V., Tian Y. & Jiang R. (2006), Photogrammetry Applications in Routine Bridge Inspection and Historic Bridge Documentation, Report NM04STR-01, New Mexico Department of Transportation Research Bureau 7500B Pan American Freeway NE Albuquerque, NM 87109;

- Kato E., Iwanami M. & Yokota H. (2006), Deterioration in Ductility of RC Beams with Corroded Reinforcement, Proceedings of the 2nd FIB Congress, Naples, Italy;
- King E.S. & Dakin J.M. (2001), Specifying, detailing and achieving cover to reinforcement, Construction Industry Research and Information Association CIRIA, London;
- Kmita J., Bień J. & Machelski C. (1989), Computer-Aided Bridge Design, WKŁ, Warszawa (in Polish);
- Kröse B. & van der Smagt P. (1996), An introduction to Neural Networks, The University of Amsterdam, Eight edition, November 1996;
- Kushtch N.N. (1996), Conventional Marks for Defects of Ferroconcrete Bridges, Proceedings of the 2nd RILEM International Conference, Štrbské pleso, Slovakia, pp. 590-593;
- Kwak, K.H., Jang, H.S., Yang, D.O. (2006), Prediction of Deflection of Hybrid FRP Rod Using Neural Networks, Proceedings of the 2nd FIB Congress, Naples, Italy;
- Lambert P. & Macdonald M. (1998), Reinforced Concrete – History, Properties and Durability, Monograph No. 1, Corrosion Prevention Association;
- Lauer K.R. (1991), Classification of Concrete Damage Caused by Chemical Attack, International Conference „Diagnosis of Concrete Structures”, Bratislava, pp. 473–479;
- Lawrence J. & Fredrickson J. (1993), BrainMaker Professional, User’s Guide and Reference Manual, California Scientific Software;
- Legat A., Leban M. & Bajt Ž. (2004), Corrosion processes of steel in concrete characterized by means of electrochemical noise, *Electrochimica Acta* 49, pp. 2741–2751;
- Logar J. & Turk G. (1995), Modelling of the Oedometer Test by Neural Networks Colloquium of the International Association for Bridge and Structural Engineering (IABSE) „Knowledge Support Systems in Civil Engineering”, Bergamo, Italy, 1995, Vol. 72, pp. 273–281;
- Łakomy T. (2004), Practical experiences with applying merged method of potential and resistance mapping to estimate the corrosion risk in RC structures, *Badania materiałów budowlanych i konstrukcji inżynierskich*, Dolnośląskie Wydawnictwo Edukacyjne, Wrocław;
- Madan, A. (2006), Active Control of Building Structures Using Featuresensitive Neural Networks, Proceedings of the 2nd FIB Congress, Naples, Italy;
- Maeck J., Feltrin G. & De Roeck G. (2002), Vibration Based Damage Identification on a Concrete Highway Bridge, Proceedings of the 1st European Workshop on Structural Health Monitoring (SHM2002);
- Madaj A. & Wołowicki W. (1997), “Concrete bridges – design and construction”, Wydawnictwa Komunikacji i Łączności, Warszawa (in Polish);
- Maksymowicz M., Bień J. & Cruz P.J.S. (2006a), “Assessment of load capacity of railway RC slab spans with reinforcement losses”, Proceedings of the 2nd FIB Congress, Naples, Italy;
- Maksymowicz M., Bień J. & Cruz P.J.S. (2006b), “Evaluation of load capacity of railway slab spans with damages”, Proceedings of the conference “Technological topics at design and construction of concrete bridges”, Wrocław, Poland, pp. 199-208 (in Polish);

- Maksymowicz M., Cruz P.J.S., Bień J. & Helmerich R. (2006c), Concrete railway bridges – Taxonomy of degradation mechanisms and damages identified by NDT methods, Proceedings of the 3rd International Conference on Bridge Maintenance, Safety and Management, IABMAS, Porto, Portugal;
- Mathews S.L. (1998), Application of subsurface radar as an investigative technique, Construction Research Communications, Building Research Establishment Ltd, London;
- May R.W.P., Ackers J.C. & Kirby A.M. (2002), Manual on scour at bridges and other hydraulic structures, Construction Industry Research and Information Association CIRIA, London;
- McCulloch W.S., Pitts W. (1943), A logical calculus of the ideas immanent in nervous activity, Bulletin of Mathematical Biophysics, No. 5, 1943, pp. 115-133;
- Mikumo Y., Hirokane M., Furuta H., Kusunose Y. & Yasuda K. (2004), A Study of Crack Classification in Concrete Slabs by Using Pattern Recognition Methods, Proceedings of the 2nd International Conference on Bridge Maintenance, Safety and Management, IABMAS, Kyoto, Japan;
- Mitzel A., Stachurski W. & Suwalski J. (1982), Failures of concrete and masonry constructions, Warszawa, Poland, Arkady (in Polish);
- Miyamoto A., Kushida M. & Kinoshita K. (1995), Concrete Bridge Rating Expert System with Machine Learning, Colloquium of the International Association for Bridge and Structural Engineering „Knowledge Support Systems in Civil Engineering”, Bergamo, Italy, IABSE, Zurich, Switzerland, 1995, Vol. 72, pp. 301–306;
- Moczko A. (2004), Modern testing methods for „In-situ” non-destructive examination of concrete structures, Badania materiałów budowlanych i konstrukcji inżynierskich, Praca zbiorowa, Dolnośląskie Wydawnictwo Edukacyjne, Wrocław, p. 65 (in Polish);
- Monks W. (1981), The control of blemishes in concrete, Cement and Concrete Association, Slough, United Kingdom;
- Moss D.S. (1982), Bending fatigue of high-yield reinforcing bars in concrete, TRRL Supplementary Report 748, Transport and Road Research Laboratory, Department of the Environment, Department of Transport;
- Nagaraja S. & Melhem H.G. (1995), A Rebar Corrosion Decision System Using Machine Learning, Colloquium of the International Association for Bridge and Structural Engineering „Knowledge Support Systems in Civil Engineering”, Bergamo, Italy, IABSE, Zurich, Switzerland, 1995, Vol. 72, pp. 293–296;
- Neti C., Potamianos G., Luetttin. J, Matthews L., Glotin H., Vergyri D., Sison J., Mashari A. & Zhou J. (2000), Audio-visual speech recognition, Workshop 2000 Final Report;
- Network Rail (2004), Structures Condition Marking Index Handbook for Bridges, London, United Kingdom;
- Neville A.M. (1995), Properties of concrete, Harlow, Longman Scientific and Technical, fourth edition;
- Nowak A.S. (1990), Bridge Evaluation Repair and Rehabilitation, NATO ASI Series, Series E: Applied Sciences – Vol. 187;

- Oh B.H. & Kim D.W. (2004), Development of Evaluation System for Load Capacity of Concrete Bridges Incorporating Load and Environmental Factors, Proceedings of the 2nd International Conference on Bridge Maintenance, Safety and Management, IABMAS, Kyoto, Japan;
- Pendharkar U., Chaudhary S. & Nagpal A.K. (2007), Neural network for bending moment in continuous composite beams considering cracking and time effects in concrete, Engineering Structures, Volume 29, Issue 9, September 2007, pp. 2069-2079;
- Perkins P.H. (1997), Repair, Protection and Waterproofing of Concrete Structures, Third Edition, E&FN SPON;
- Plos M., Gylltoft K., Lundgren K., Elfgrén L., Cervenka J., Brühwiler E., Thelandersson S. & Rosell E. (2006), Structural assessment of concrete railway bridges: Non-linear analysis and remaining fatigue life, Proceedings of the 3rd International Conference on Bridge Maintenance, Safety and Management, IABMAS, Porto, Portugal;
- Pu Y. & Mesbahi E. (2006), Application of artificial neural networks to evaluation of ultimate strength of steel panels, Engineering Structures, Volume 28, Issue 8, July 2006, pp. 1190-1196;
- REFER EP. (2005), Direcção de Estruturas Especiais, Departamento de Pontes, Cadastro de pontes, Alvenaria, betão armado / P.E. e metálico, Lisboa;
- REHABCON (2004), Strategy for maintenance and rehabilitation in concrete structures, EC DG ENTR-C-2, Innovation and SME Programme, IPS-2000-0063;
- Rodriguez J., Ortega L.M. & Casal J. (1997), Load carrying capacity of concrete structures with corroded reinforcement, Construction and Building Materials, Vol. II, No. 4, pp. 239-248;
- Rosenblatt F. (1968), The Perceptron, A theory of statistical separability in cognitive system, Cornell Aeronautical Lab. Inc. Rep. No. VG-1196-G-1, 1968;
- Ryall M.J. (2001), Bridge Management, Betterworth – Heinemann, First published;
- Satorre R. (1995), Image-Based Analysis of Evolution by Using Neural Network, Colloquium of the International Association for Bridge and Structural Engineering (IABSE) „Knowledge Support Systems in Civil Engineering”, Bergamo, Italy, 1995, Vol. 72, pp. 307–310;
- Shayanfar M.A., Safiey A. & Ghalehnovi M. (2006), “Investigation of Corrosion Effects on Bond-slip and Tensile Strength of Reinforced Concrete Members”, Proceedings of the 2nd FIB Congress, Naples, Italy;
- Shirakura A., Kawashima Y., Yonezawa Y. & Morikawa H. (2004), Condition rating method for performance evaluation of existing RC bridges, Proceedings of the 2nd International Conference on Bridge Maintenance, Safety and Management, IABMAS, Kyoto, Japan;
- Stańczyk S. (2000), Slab spans of railway bridges made of reinforced concrete – methods of technical condition evaluation and rehabilitation, Master Thesis, Wrocław University of Technology (in Polish);
- Stoppel M. & Niederleithinger E. (2004), D3.6 Prototype of 2D-scanning system for automated measurements on concrete surfaces with impulse radar, ultrasonic echo and impact-echo, Sustainable Bridges – Assessment for Future Traffic Demands and Longer Lives;

Structural Assessment, Monitoring and Control SAMCO (2003), Work Package 9: Practical bridge management, Task 9.1 Bridge end-user needs, D.9.1.1 End-user practical bridge management requirements <http://www.samco.org>;

Sustainable Bridges (2005), WP1-02-T-2004-04-14-D-Summary of questionnaire answers, Sustainable Bridges European Project, Work Package 1;

Sustainable Bridges (2007), Deliverable D3.15, "Guideline for Inspection and Condition assessment of railway bridges", Sustainable Bridges European Project, Work Package 3, www.sustainablebridges.net;

Ściślewski Z. (1999), Preservation of reinforcement concrete constructions, Warsaw, Arkady (in Polish);

Tadeusiewicz R. (1998), "Elementary introduction to the neural network technology with examples of programs", Akademska Oficyna Wydawnicza PLJ, Warszawa 1998 (in Polish);

Tarighat A. (2004), Application of neural network and Monte Carlo Method for concrete durability analysis, Proceedings of the 2nd International Conference on Bridge Maintenance, Safety and Management, IABMAS, Kyoto, Japan;

Tebelskis J. (1995), Speech Recognition using Neural Networks, PhD Thesis, School of Computer Science Carnegie Mellon University, Pittsburgh, Pennsylvania, USA;

Teughels A., Maeck J. & Roeck G.D. (2002), Damage assessment by FE model updating using damage functions, Computers and Structures 80, pp. 1869–1879;

Trilon (1999), Inspection On Hand (IOH), User's Manual, Version 3.4, Trilon, Inc., 1999;

Val D.V., Stewart M.G. & Melchers R.E. (1995), Effect of reinforcement corrosion on reliability of highway bridges, Engineering Structures, Vol. 20, No. 11, pp. 1010-1019;

Vianna J.C., Andrade S.A.L., Vellasco P.C.G. & Vellasco M.M.B.R. (2006), Neural network modelling of perfobond shear connector resistance, Proceedings of the 3rd International Conference on Bridge Maintenance, Safety and Management, IABMAS, Porto, Portugal;

Wacom (2006), Windows Vista Pen Experience , Product Marketing Bulletin, Vol. 1106-02;

Wallace J. & Whitehead C. (1989), Graffiti removal and control, Design Note 48, Department of Education and Science Architects & Building Group, Construction Industry Research and Information Association CIRIA, London, Great Britain;

Waszczyszyn Z. (1995), Application of artificial neural networks in civil engineering, XLI Konferencja Naukowa Komitetu Inżynierii Lądowej i Wodnej PAN i Komitetu Nauki PZITB "Problemy naukowo-badawcze budownictwa", Kraków-Krynica, Politechnika Krakowska, Kraków, T. 9, pp. 251-288 (in Polish);

Wawrusiewicz, A. (2006), Evaluation of the State of Concrete Structures by Multi Mapping, Proceedings of the 2nd FIB Congress, Naples, Italy;

Wibrerg U. (1995), Checking Concrete by Quantitative Ultrasonics, Extending the Lifespan of Structures, IABSE Symposium, San Francisco, USA, pp. 189-194;

Woodward R.J., Cullington D.W., Daly A.F., Vassie P.R., Haardt P., Kashner R., Astudillo A., Velando C., Godart B., Cremona C., Mahut B., Raharinaivo A., Lau M.Y., Markey I., Bevc L. & Peruš I. (2001), Bridge Management in Europe – Final Report. BRIME PL97-2220.

Wójtowicz M. (2004), Badania w laboratoriach akredytowanych dla potrzeb rzeczoznawstwa budowlanego, VIII Konferencja Naukowo-Techniczna, Problemy Rzeczoznawstwa Budowlanego, Cedzyna 21-23 kwietnia 2004 (in Polish);

Yao J, Tan C. L., & Poh H.-P. (1999), Neural networks for technical analysis: A study on KLCI, International Journal of Theoretical and Applied Finance, Vol. 2, No. 2 (1999), 221-241;

Yun C.B., Cho S., Yi J.H., Lee C.G. & Lee W.T. (2006), Evaluation of load carrying capacity of bridge based on ambient acceleration measurements, Proceedings of the 3rd International Conference on Bridge Maintenance, Safety and Management, IABMAS, Porto, Portugal;

Žnidarič J. & Peruš I. (2000), Condition Rating Method for concrete structures, 16th Congress of the International Association for Bridge and Structural Engineering “Structural Engineering for Meeting Urban Transportation Challenges”, Lucerne, Switzerland, pp. 270-277;

PN-80/B-01800, Protection against corrosion in building, Concrete and reinforced concrete structures, Classification and determination of environment (in Polish);

PN-85/S-10030, Bridges, Loads (in Polish);

PN-86/B-01802, Protection against corrosion in building, Concrete and reinforced concrete structures, Nomenclature definitions (in Polish);

PN-91/S-10042, Bridges, Concrete, reinforced concrete and prestressed concrete structures, Design (in Polish).

Appendix A

Parametric analysis of load capacity of cross-section for RC slab spans with defects

A.1. Introduction

This appendix is related to the methodology of load capacity assessment by means of the expert tool technology described and discussed in Chapter 8. The proposed ANACONDA program (see its User's Manual in Appendix C) is based on the hybrid network technology and contains of the functional and neural components. Its functional scheme is presented and explained in Section 8.2 (Fig. 8-3). The engine of this tool is situated in the Analysis module responsible for the static-strength analysis. The functional scheme of this module is presented in Fig. 8-4 where the network composed of the neural and functional components can be seen. All of these components are presented and explained in 8.3 (the neural components) and 8.4 (the functional components). Despite some limitations of the functional components the relationship between input data and its output is described by mathematical formulas modeling these relationships. Concerning the neural components the knowledge acquisition, network training and testing are definitely required. The knowledge acquisition is based on the parametric analysis performed in this case by means of the DAGA program (see its description in Chapter 7 and the User's Manual of this program in Appendix B). The presented ANACONDA system contains two neural components: N_1 (8.3.2) and N_2 (8.3.2). The first (N_1) contains the knowledge related to the static analysis presented in Fig. 8-5. The

knowledge contained in the component N_2 is related to the strength analysis. Number of the parameters makes its results huge and difficult to present for further analysis. The objective of this appendix is to present the results of this analysis against its parameters to be used in the neural network component (N_2) creating, training and testing.

A.2. Analysis

The aim of this analysis is to present the relationship between the cross section parameters (considered as geometry and material properties) and the load capacity M_R . Each result of this analysis will be saved with the input parameters as a single record in the knowledge base to be used for neural network training and testing. Basically the load capacity of cross section depends on various parameters (see Fig. 10-1).

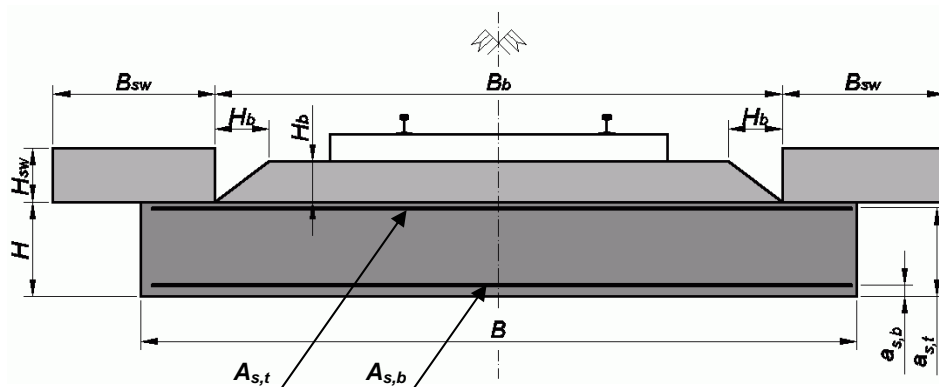


Fig. 10-1 Cross section of the considered span with geometry parameters

The load capacity of cross section is a function of its width (B) and height (H), reinforcement cross sectional area ($A_{s,b}$, $A_{s,t}$ for bottom and top layer respectively) and location ($a_{s,b}$, $a_{s,t}$ for bottom and top layer respectively) and also material parameters such as concrete and reinforcement strength (R_c , $R_{s,b}$, $R_{s,t}$ – concrete and two reinforcement layers). The situation is even more complicated when the analysed cross section is formed as other shape than rectangular. In this situation the number of parameters influencing the load capacity increases. This study is based on the rectangular form of cross section and other forms can be considered as outlook of this research only.

For the purposes of this research the number of parameters exerting the influence on load capacity of cross section has been reduced: cross section height (H), area of the bottom layer of reinforcement ($A_{s,b}$), strength of concrete (R_c) and strength of reinforcement (R_s). The rest of parameters have been considered as constant values, but in the future they can be considered as variables as well.

The results of this analysis are graphically presented in this appendix (Fig. 10-2 to Fig. 10-25). Each graph presents the load capacity of cross-section (according to PN-91/S-10042) in the

function of the bottom reinforcement area and the compressive strength of concrete. These graphs are distinguished by the strength of reinforcement and cross-section height. Modifications of these parameters can be interpreted as defects occurred such as losses of reinforcement and material parameter modifications. Each point of these graphs is to be taken as input value for the neural network training and testing.

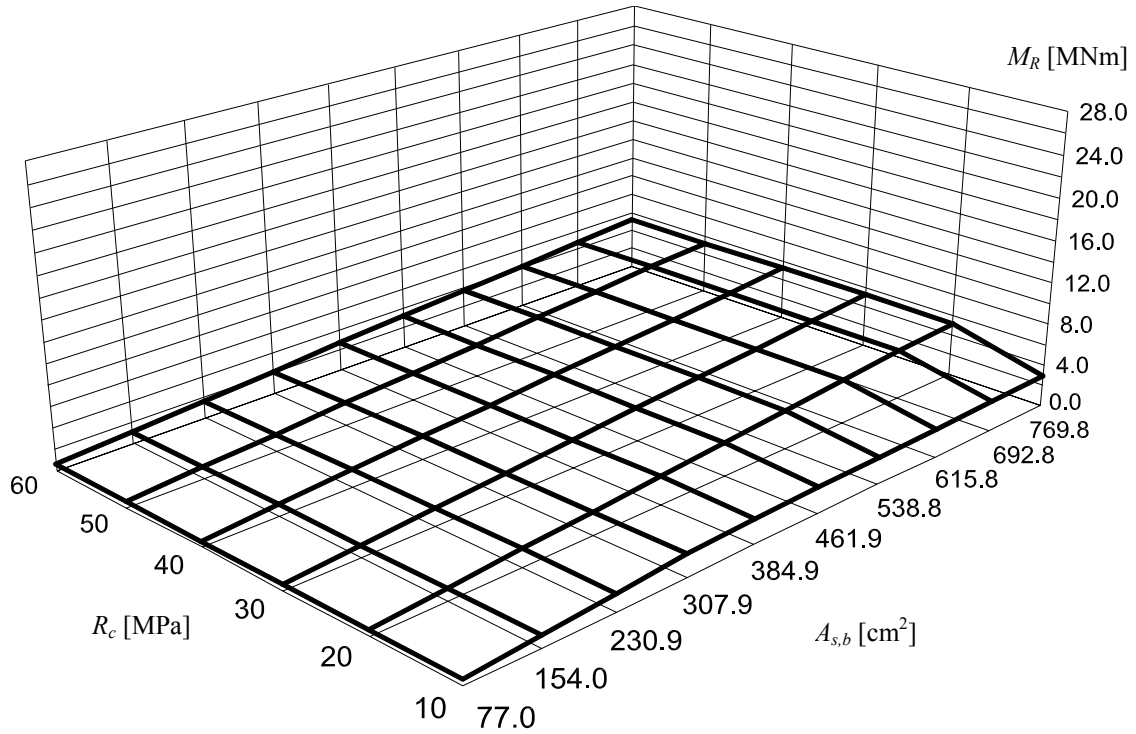


Fig. 10-2 Load capacity of cross section for $H = 60$ cm and $R_s = 150$ MPa

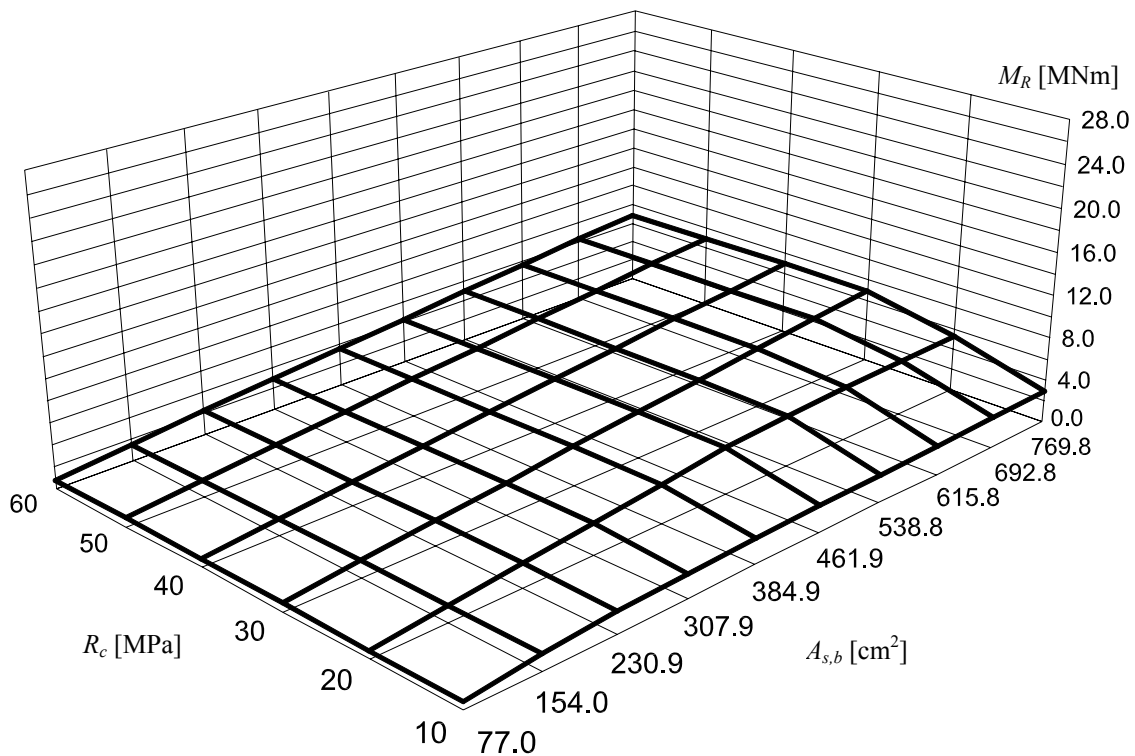


Fig. 10-3 Load capacity of cross section for $H = 60$ cm and $R_s = 200$ MPa

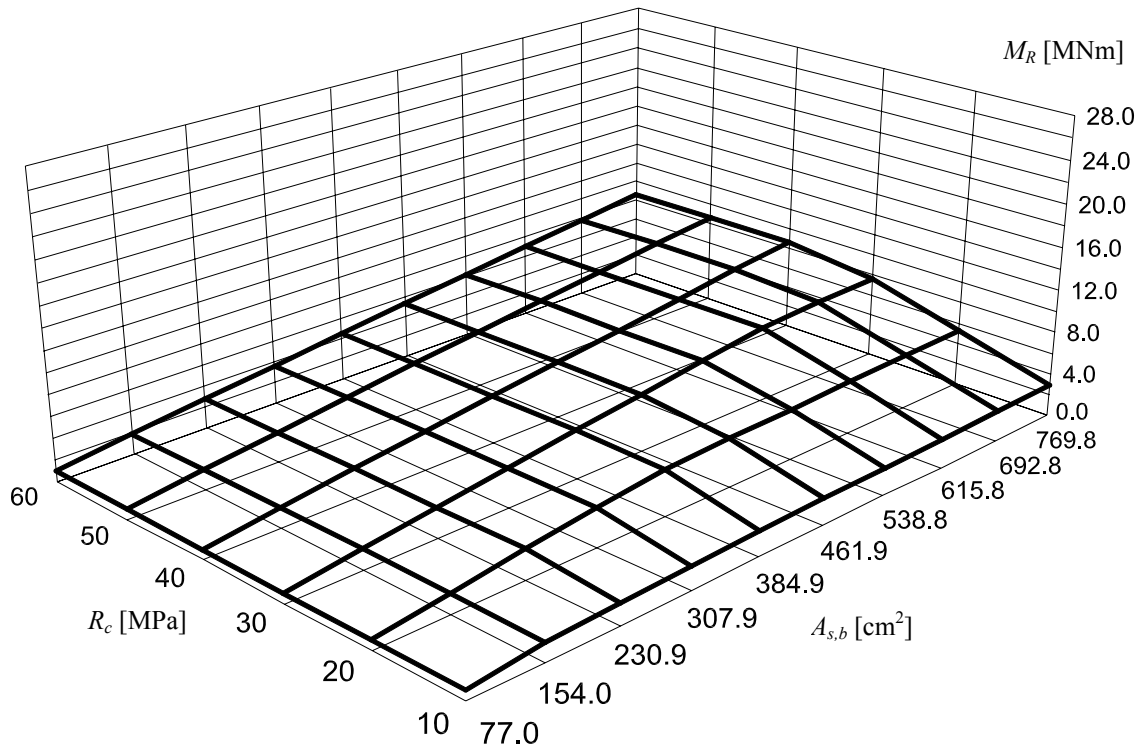


Fig. 10-4 Load capacity of cross section for $H = 60$ cm and $R_s = 250$ MPa

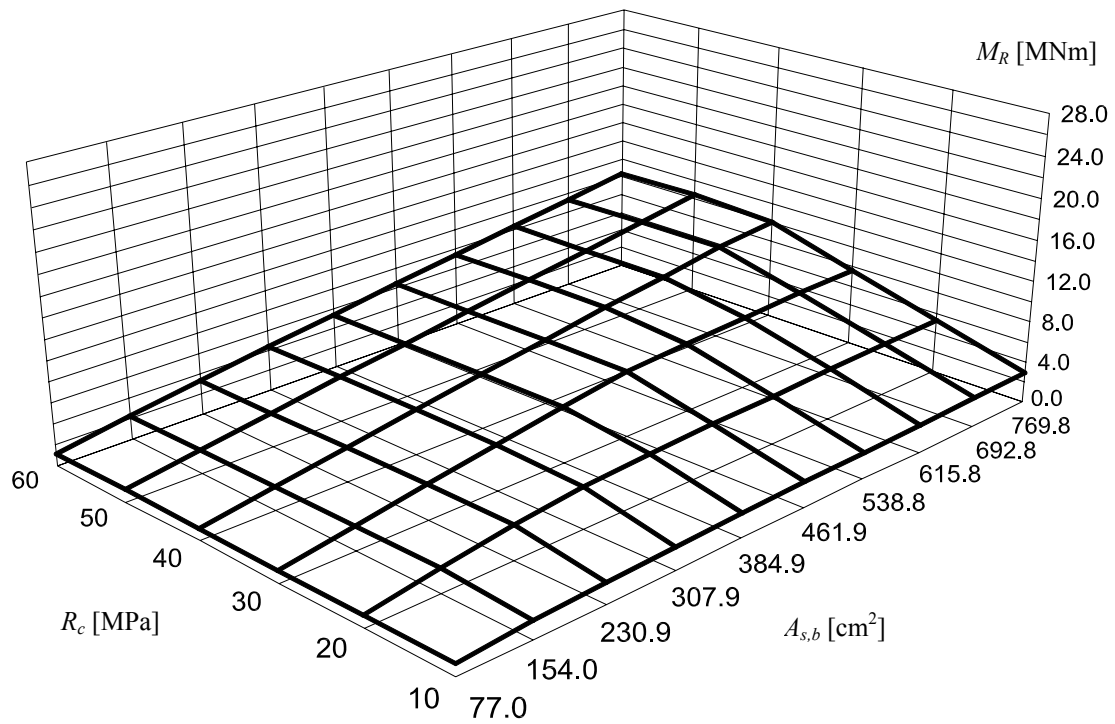


Fig. 10-5 Load capacity of cross section for $H = 60$ cm and $R_s = 300$ MPa

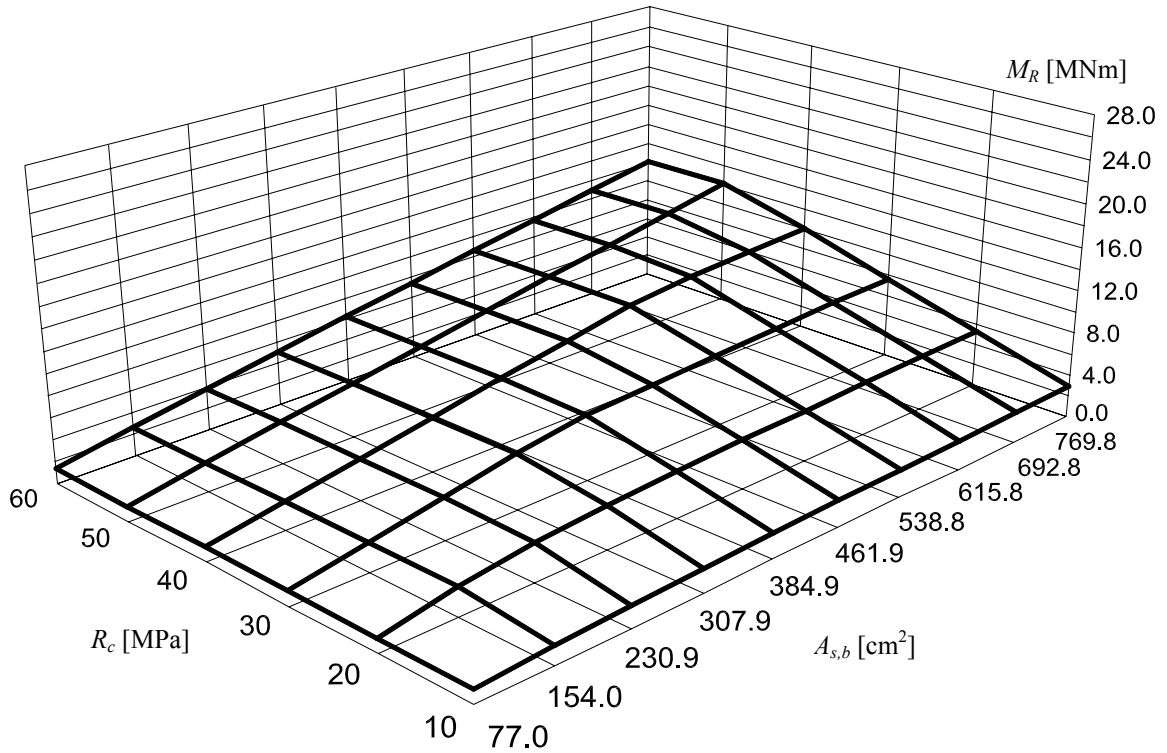


Fig. 10-6 Load capacity of cross section for $H = 60$ cm and $R_s = 350$ MPa

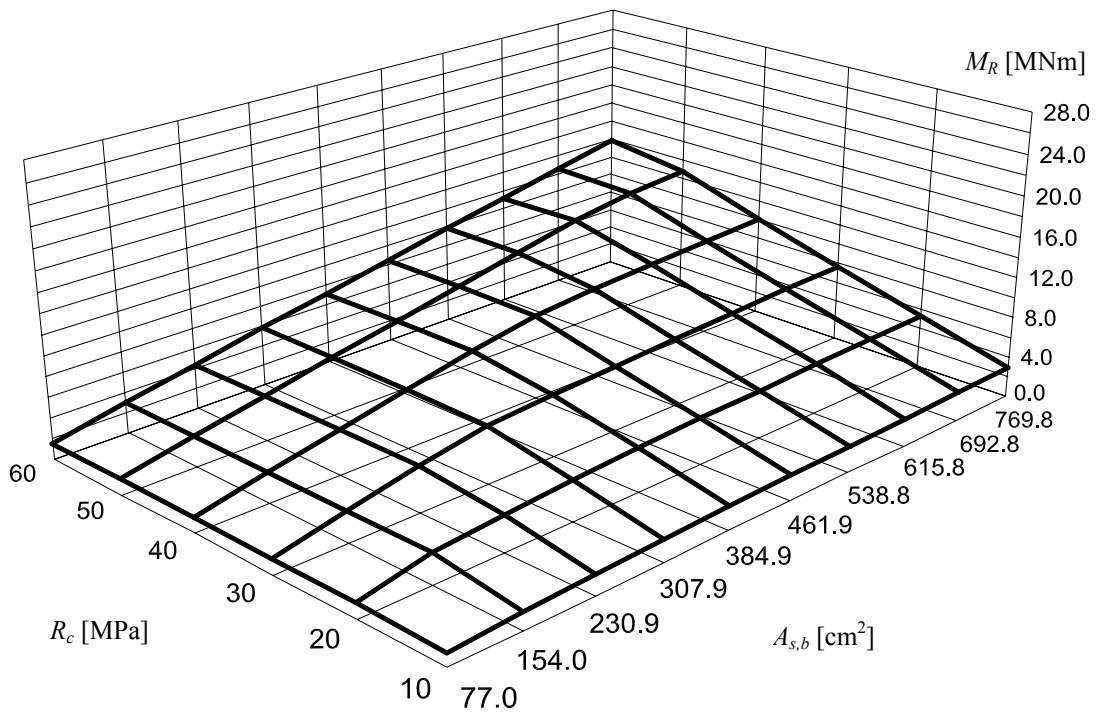


Fig. 10-7 Load capacity of cross section for $H = 60$ cm and $R_s = 400$ MPa

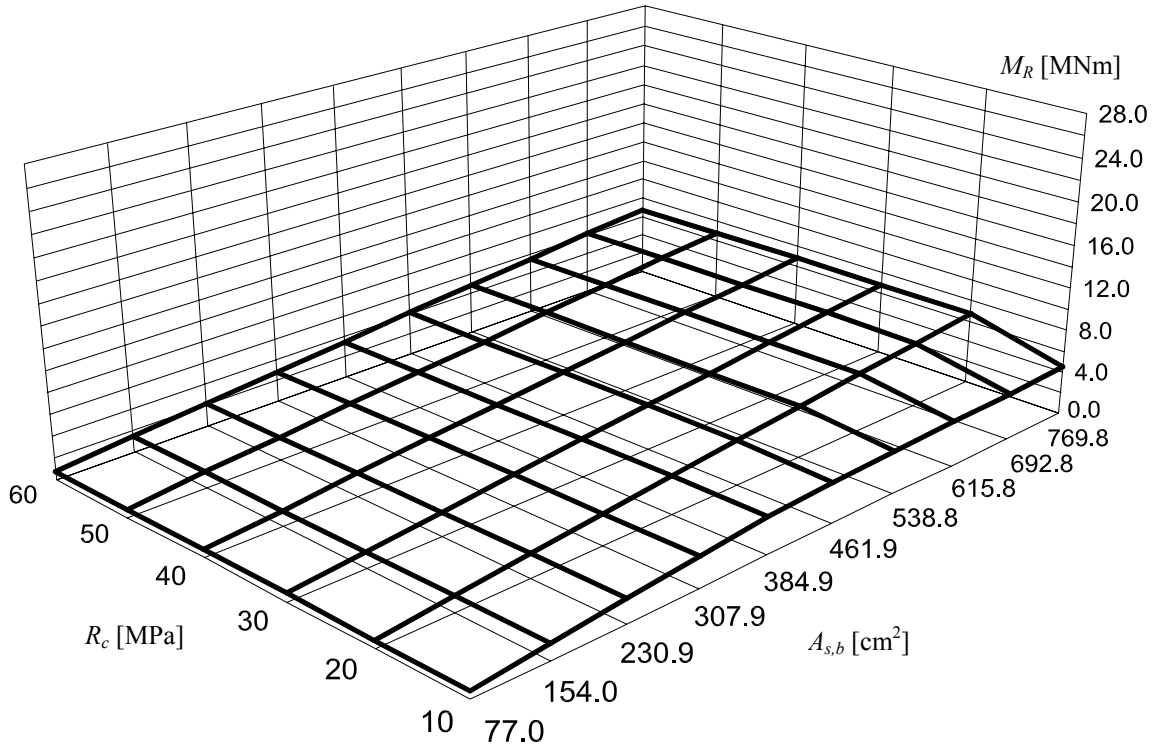


Fig. 10-8 Load capacity of cross section for $H = 75$ cm and $R_s = 150$ MPa

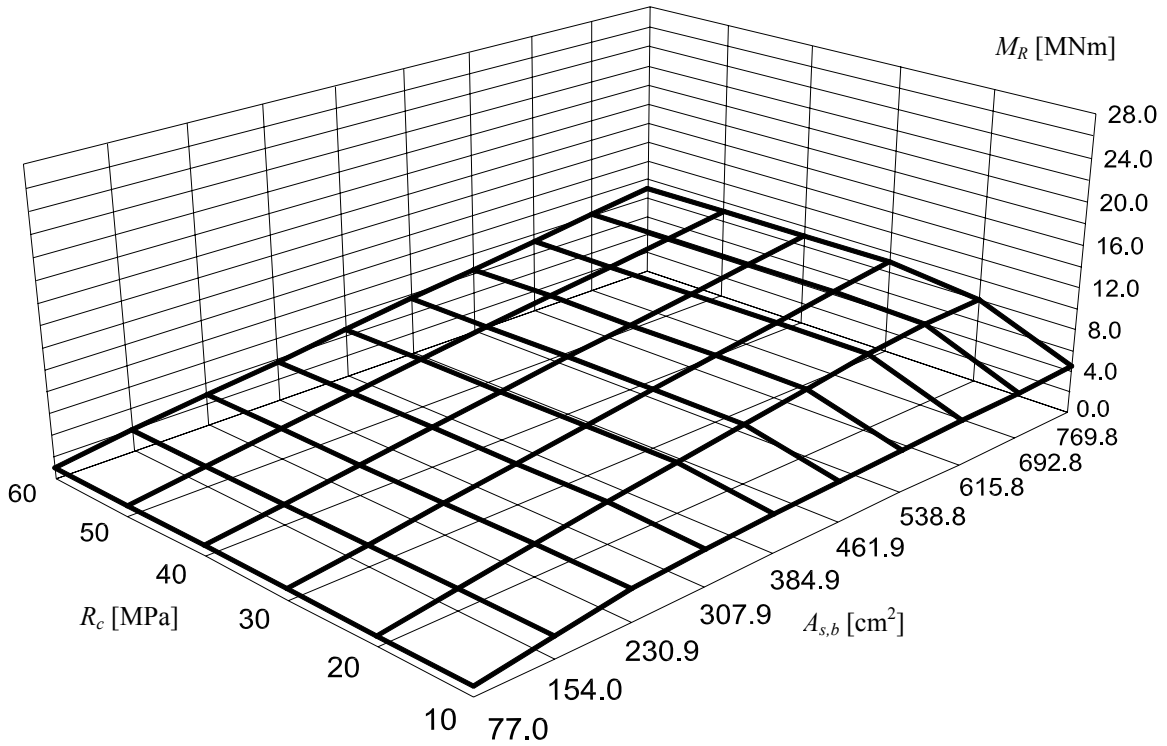


Fig. 10-9 Load capacity of cross section for $H = 75$ cm and $R_s = 200$ MPa

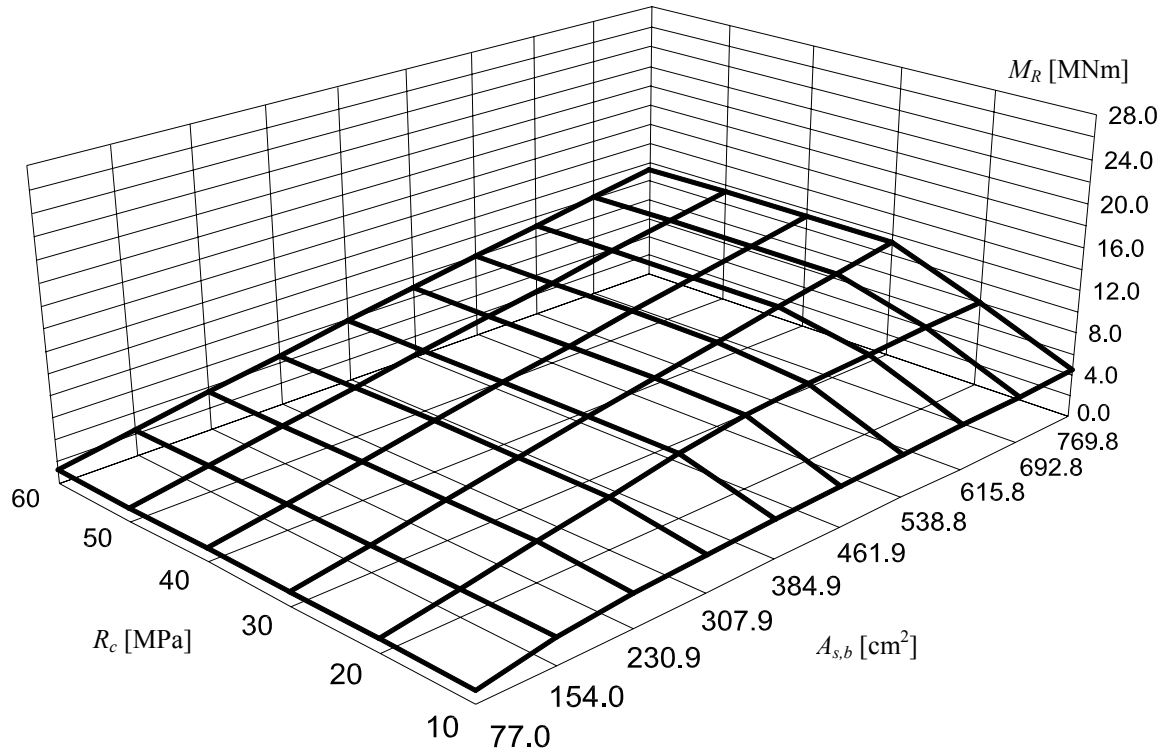


Fig. 10-10 Load capacity of cross section for $H = 75$ cm and $R_s = 250$ MPa

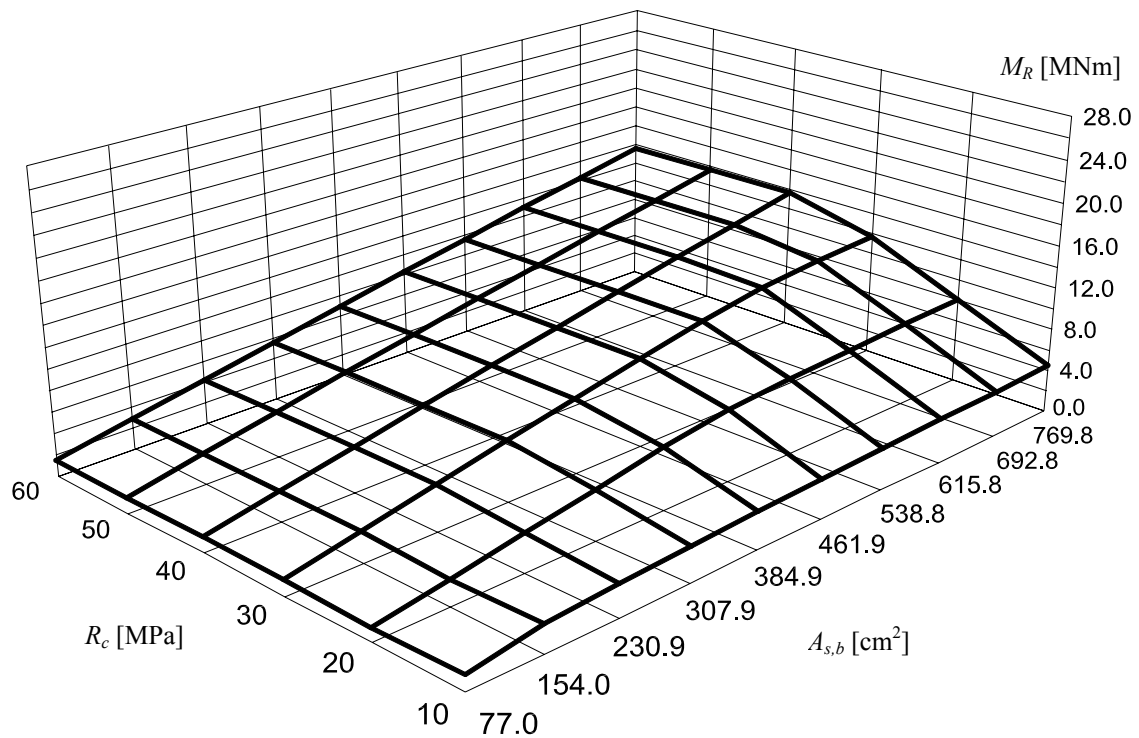


Fig. 10-11 Load capacity of cross section for $H = 75$ cm and $R_s = 300$ MPa

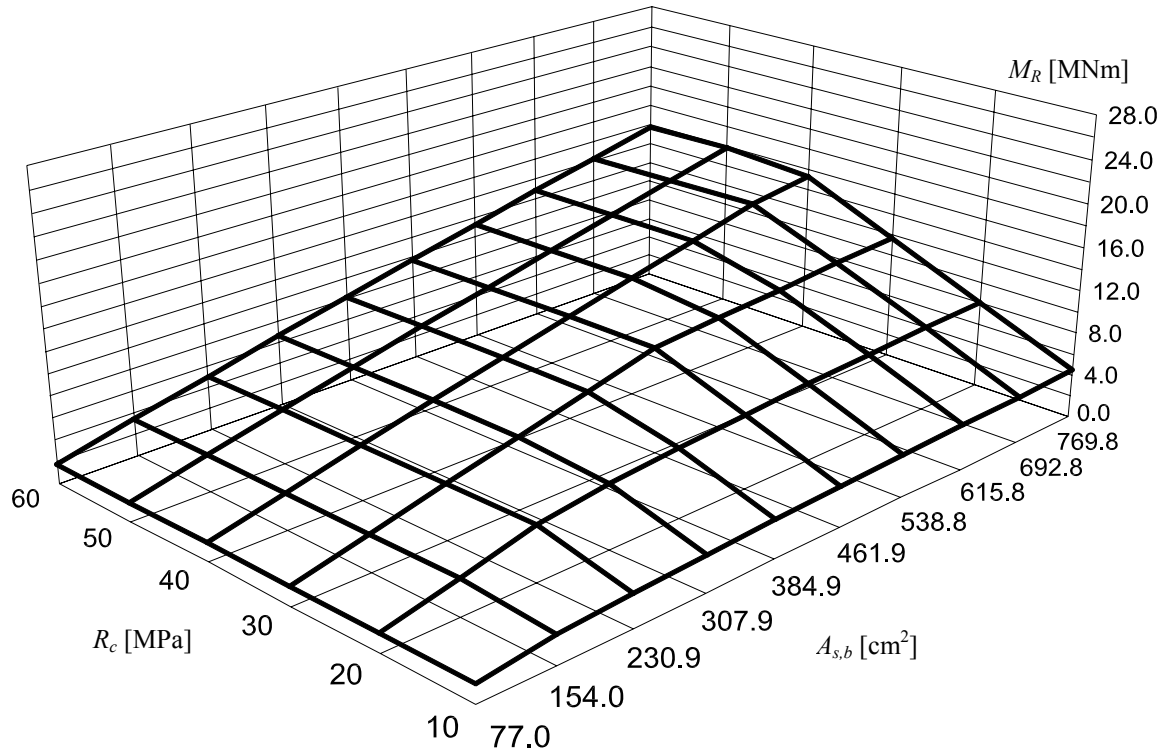


Fig. 10-12 Load capacity of cross section for $H = 75$ cm and $R_s = 350$ MPa

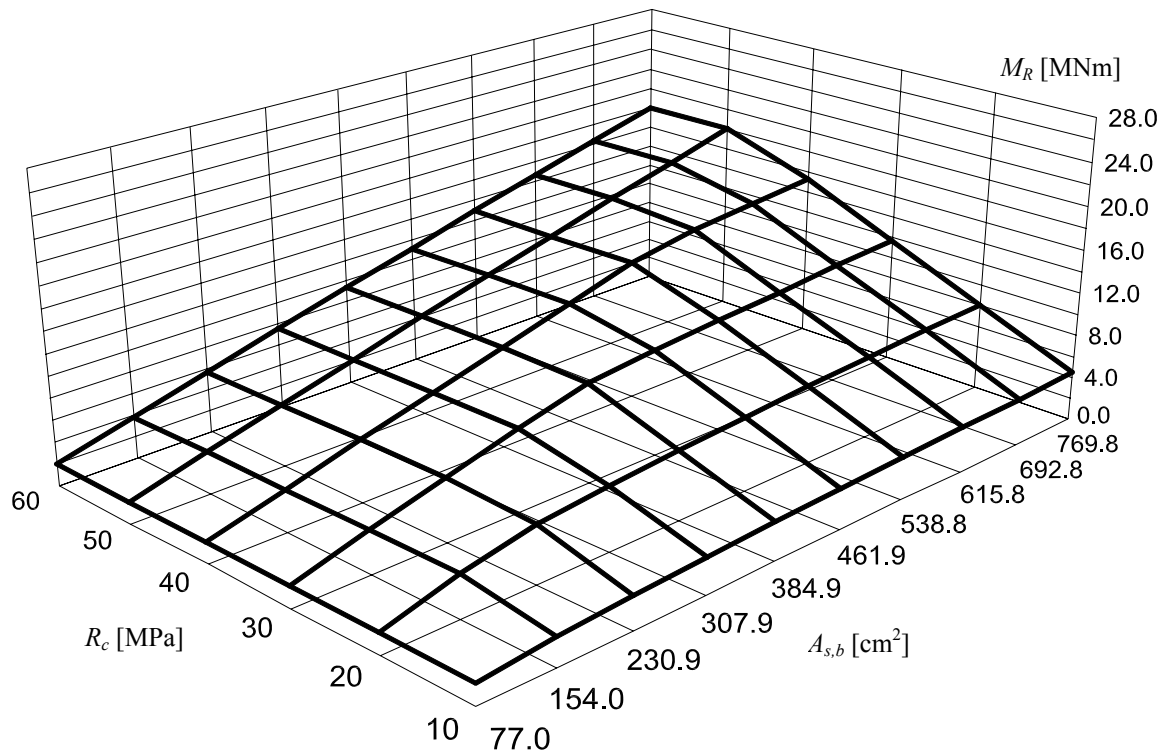


Fig. 10-13 Load capacity of cross section for $H = 75$ cm and $R_s = 400$ MPa

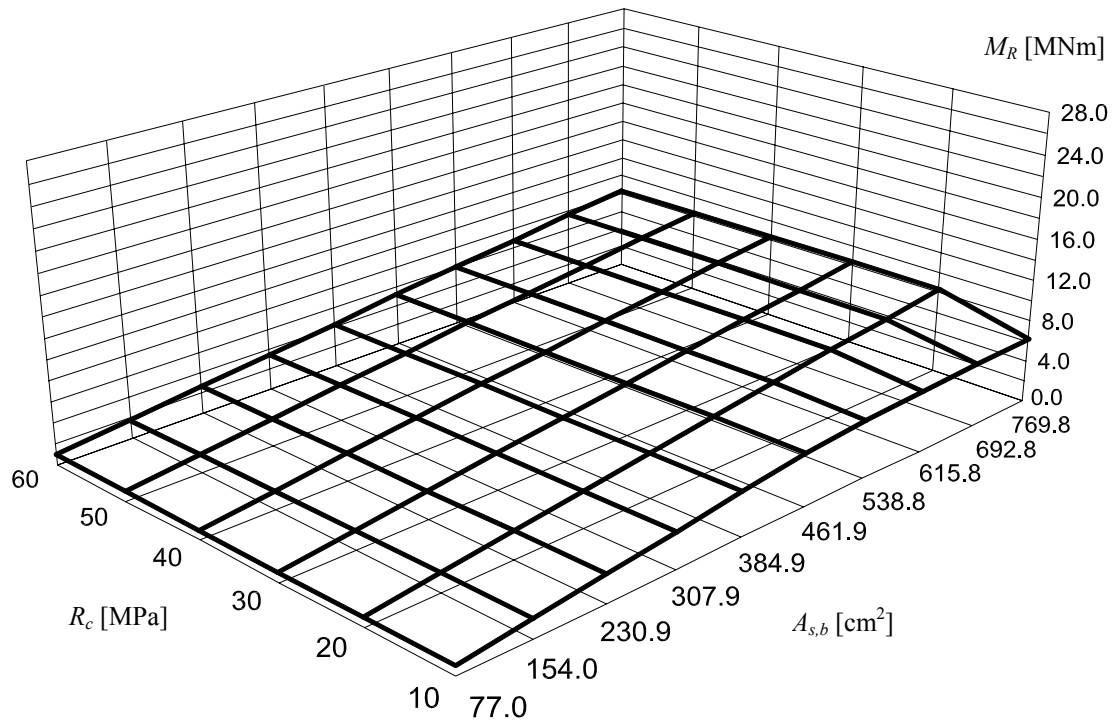


Fig. 10-14 Load capacity of cross section for $H = 90$ cm and $R_s = 150$ MPa

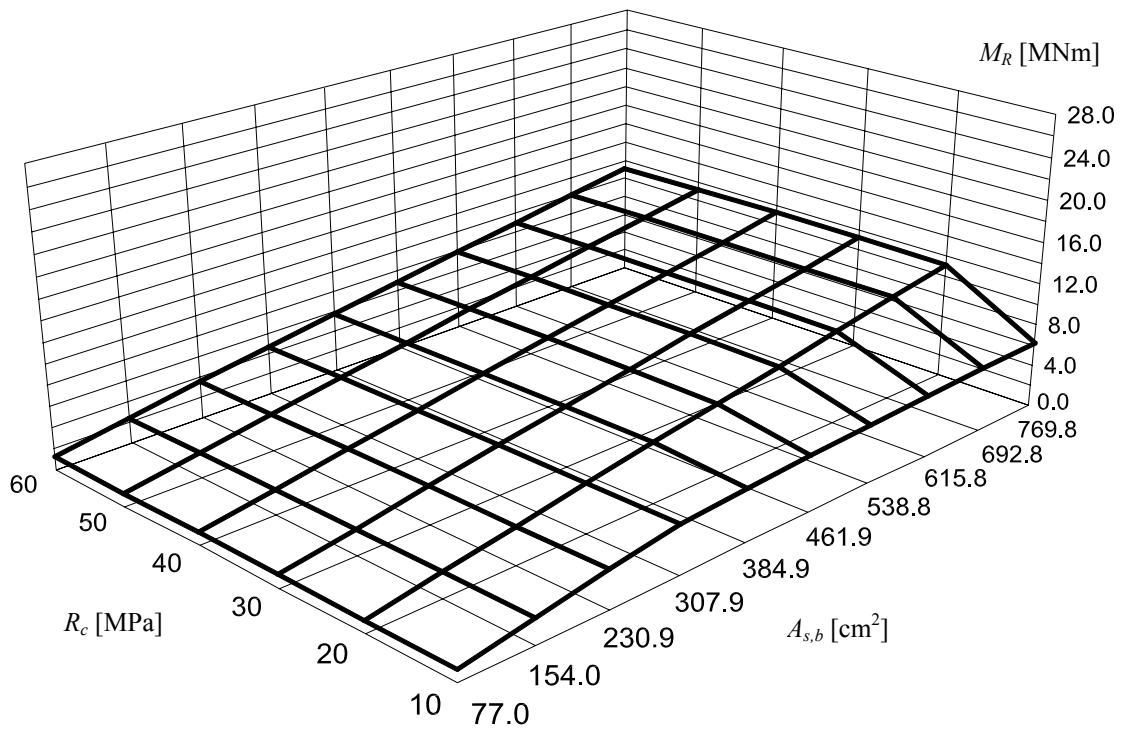


Fig. 10-15 Load capacity of cross section for $H = 90$ cm and $R_s = 200$ MPa

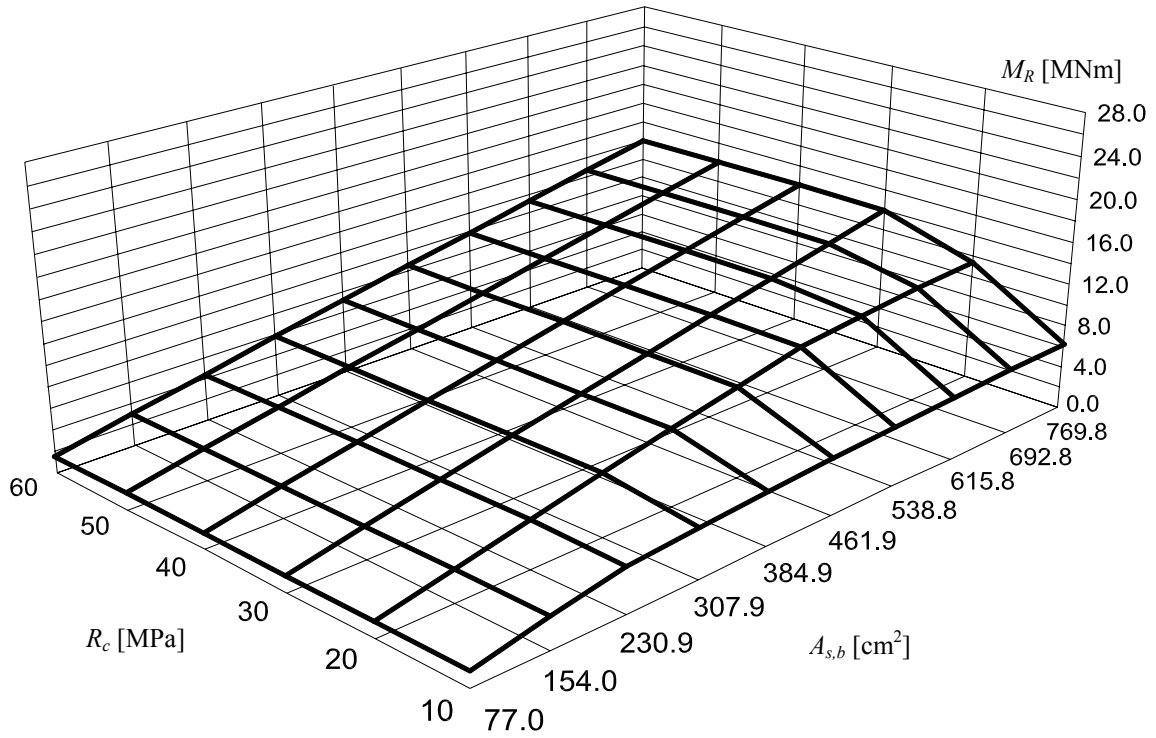


Fig. 10-16 Load capacity of cross section for $H = 90$ cm and $R_s = 250$ MPa

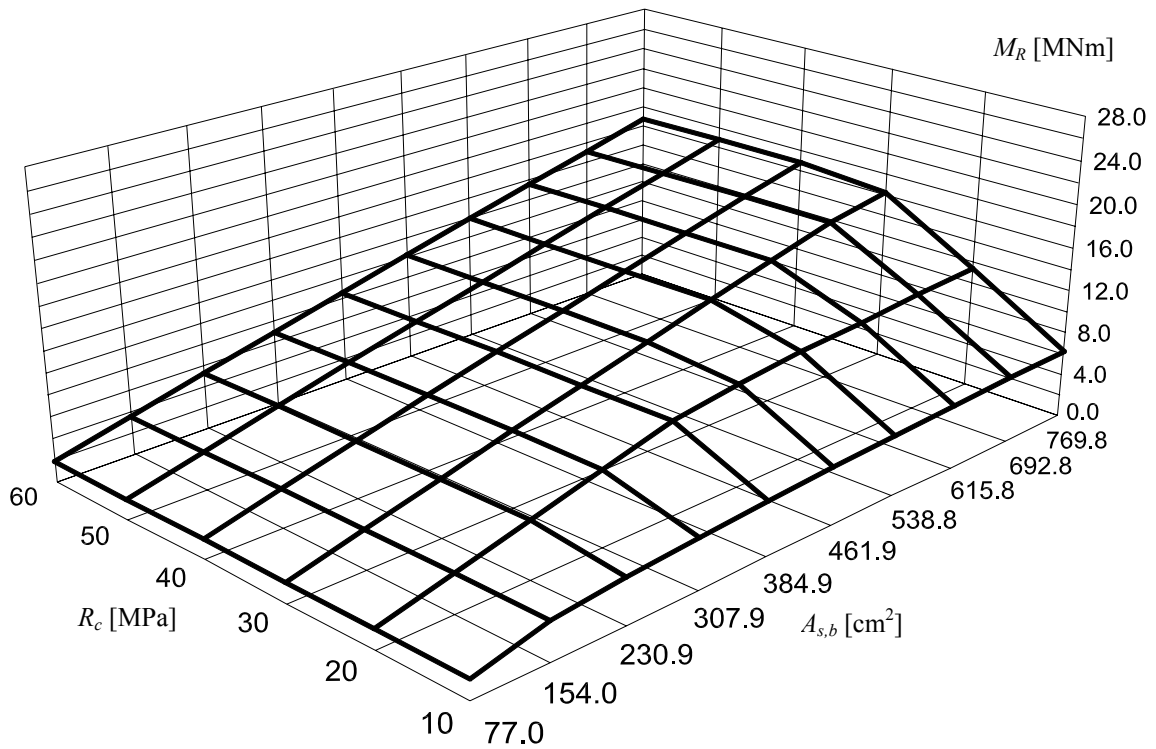


Fig. 10-17 Load capacity of cross section for $H = 90$ cm and $R_s = 300$ MPa

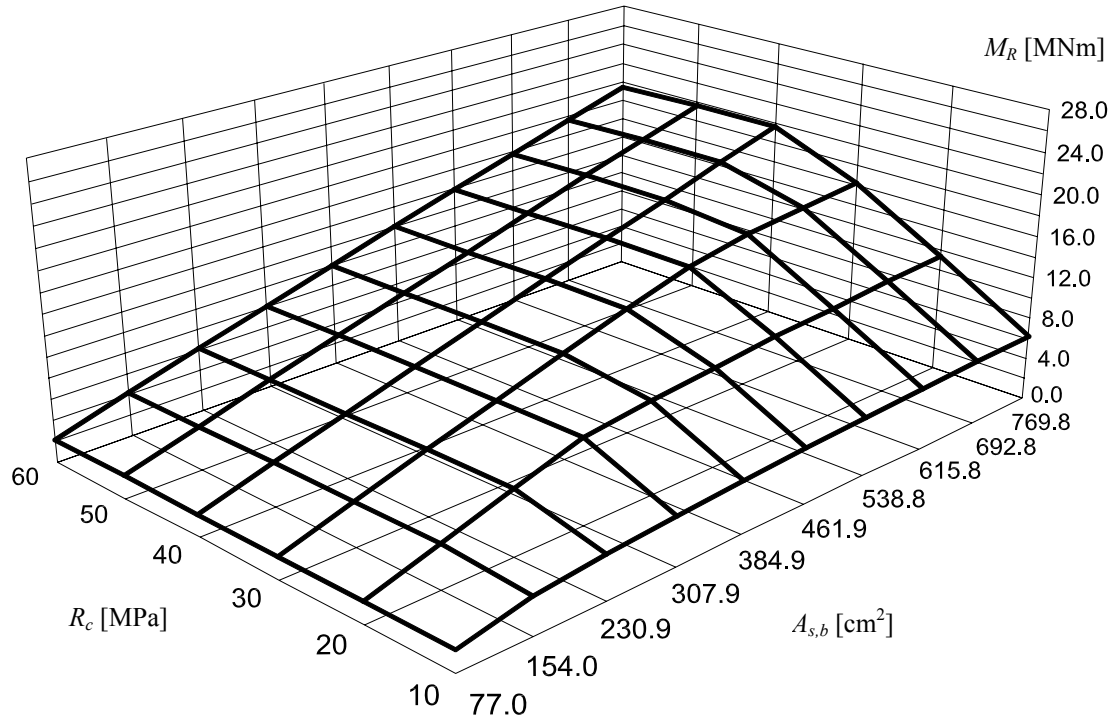


Fig. 10-18 Load capacity of cross section for $H = 90$ cm and $R_s = 350$ MPa

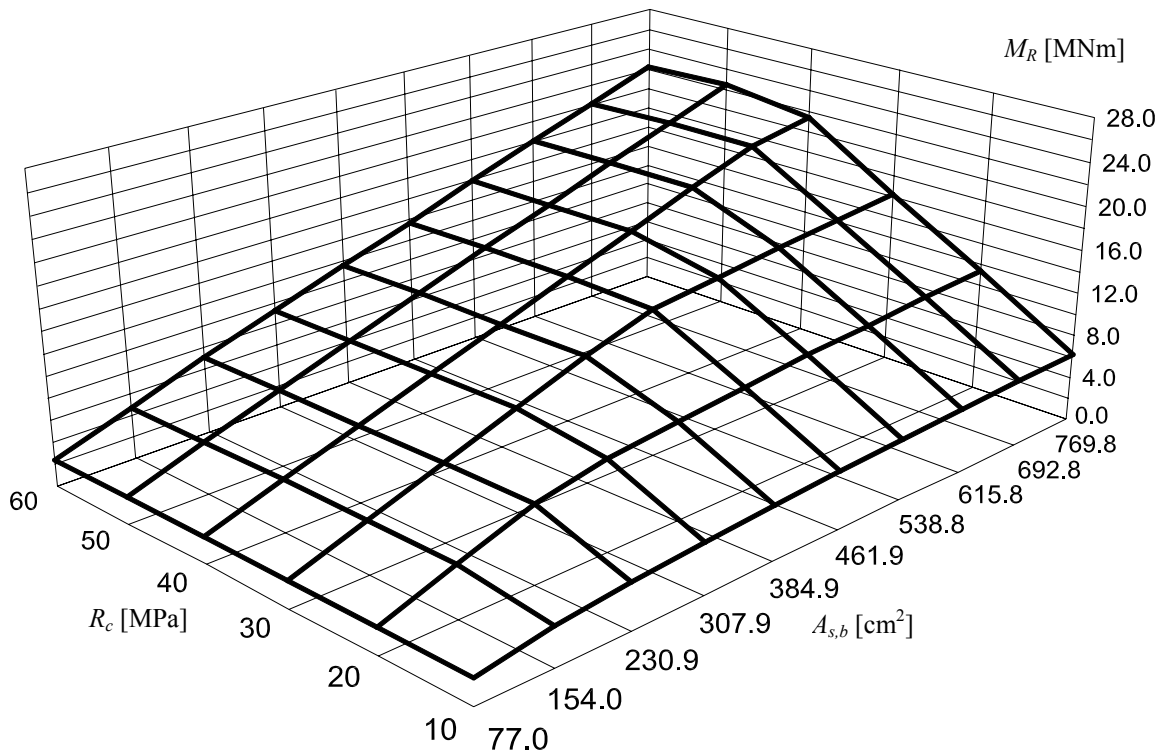


Fig. 10-19 Load capacity of cross section for $H = 90$ cm and $R_s = 400$ MPa

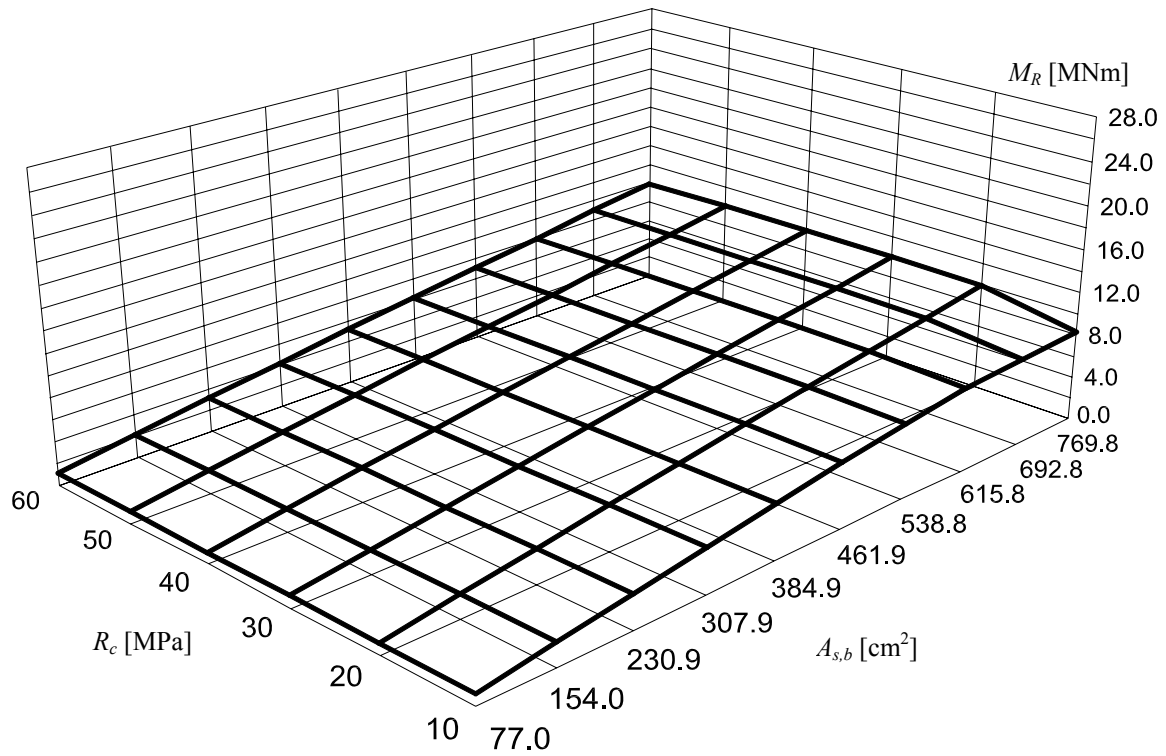


Fig. 10-20 Load capacity of cross section for $H = 105$ cm and $R_s = 150$ MPa

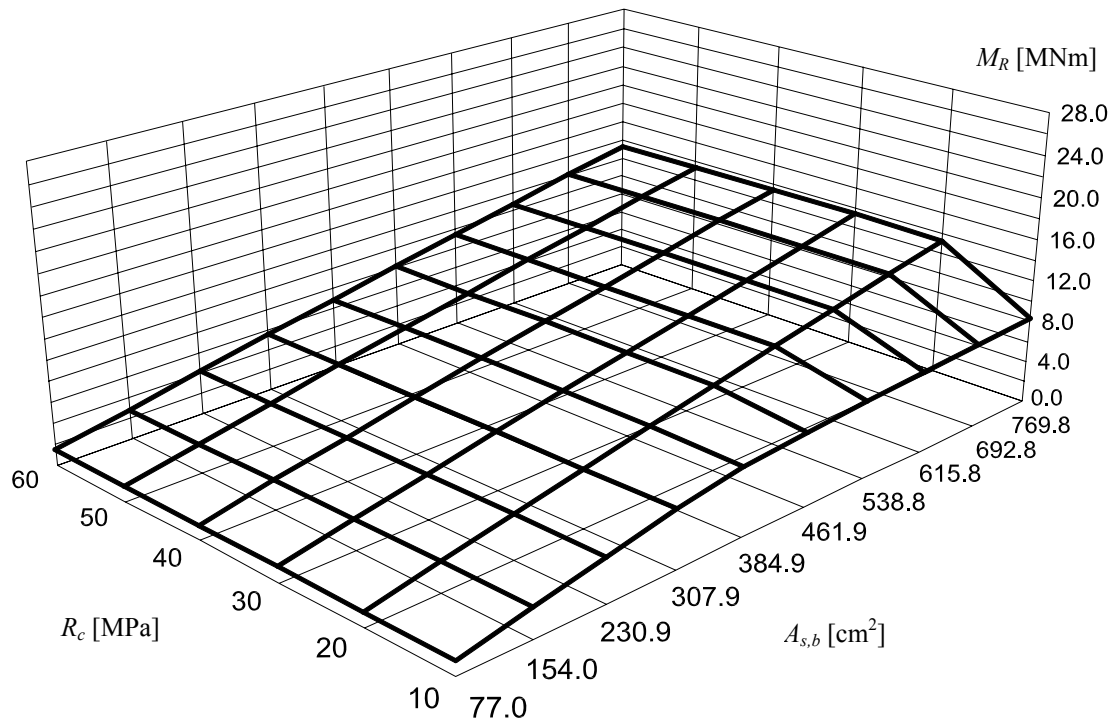


Fig. 10-21 Load capacity of cross section for $H = 105$ cm and $R_s = 200$ MPa

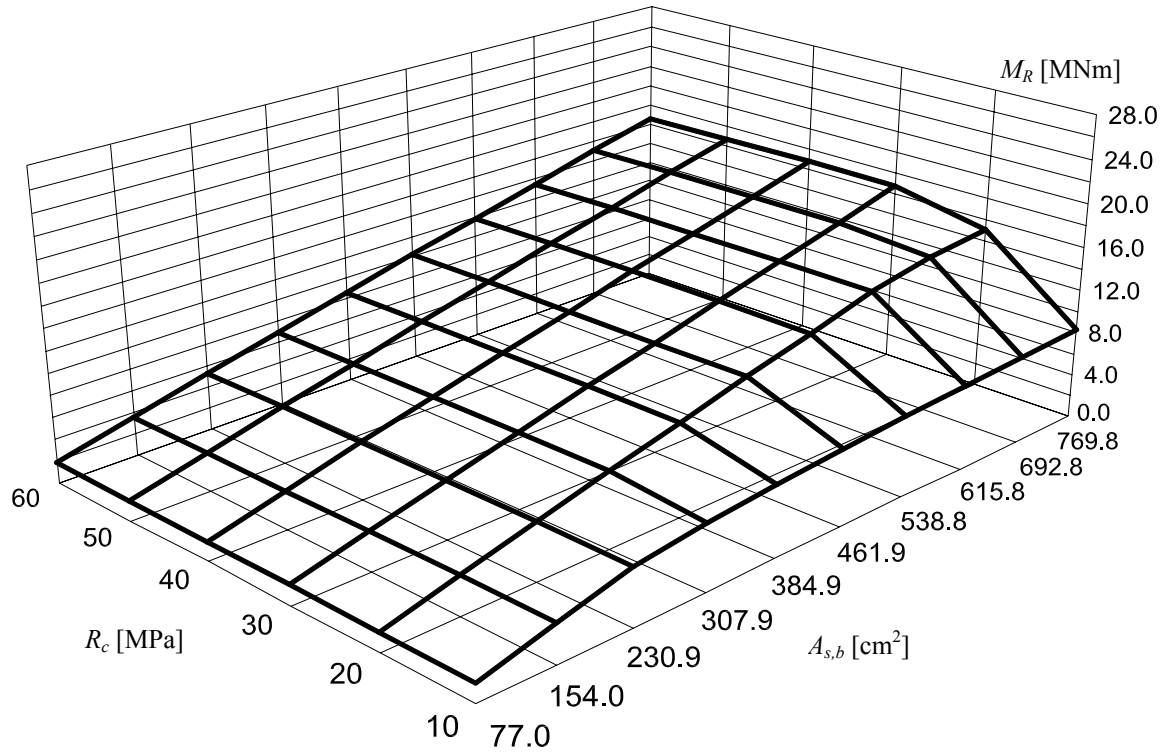


Fig. 10-22 Load capacity of cross section for $H = 105$ cm and $R_s = 250$ MPa

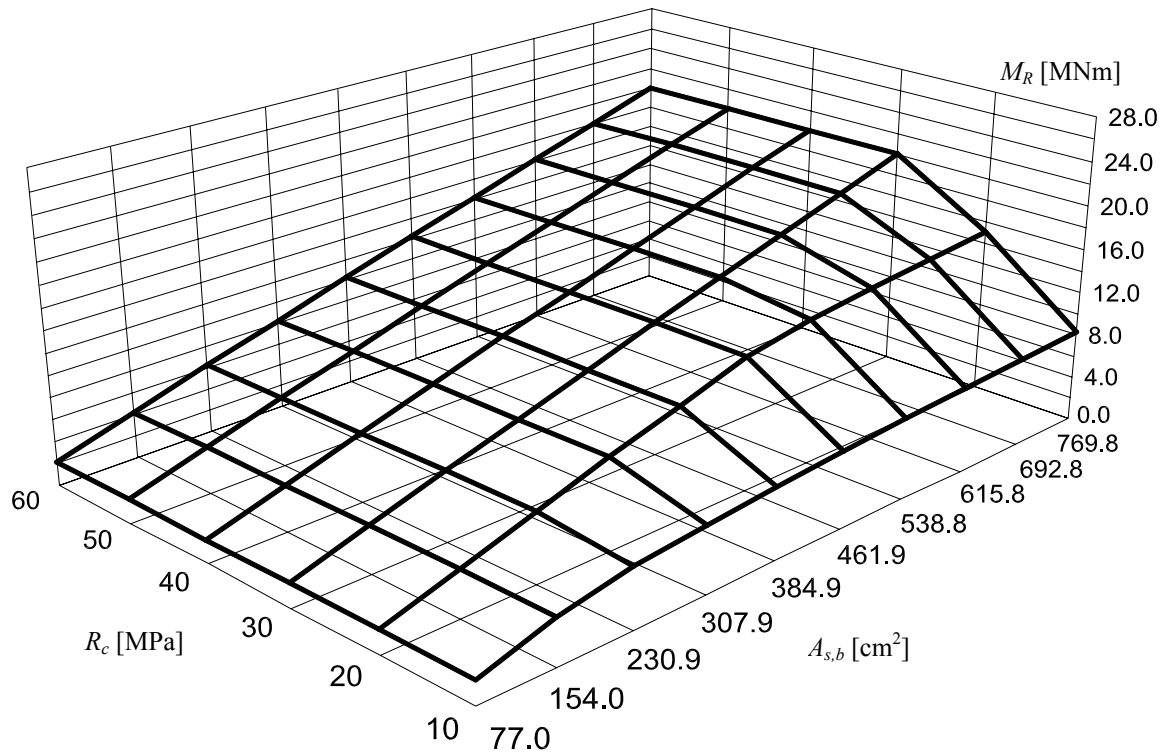


Fig. 10-23 Load capacity of cross section for $H = 105$ cm and $R_s = 300$ MPa

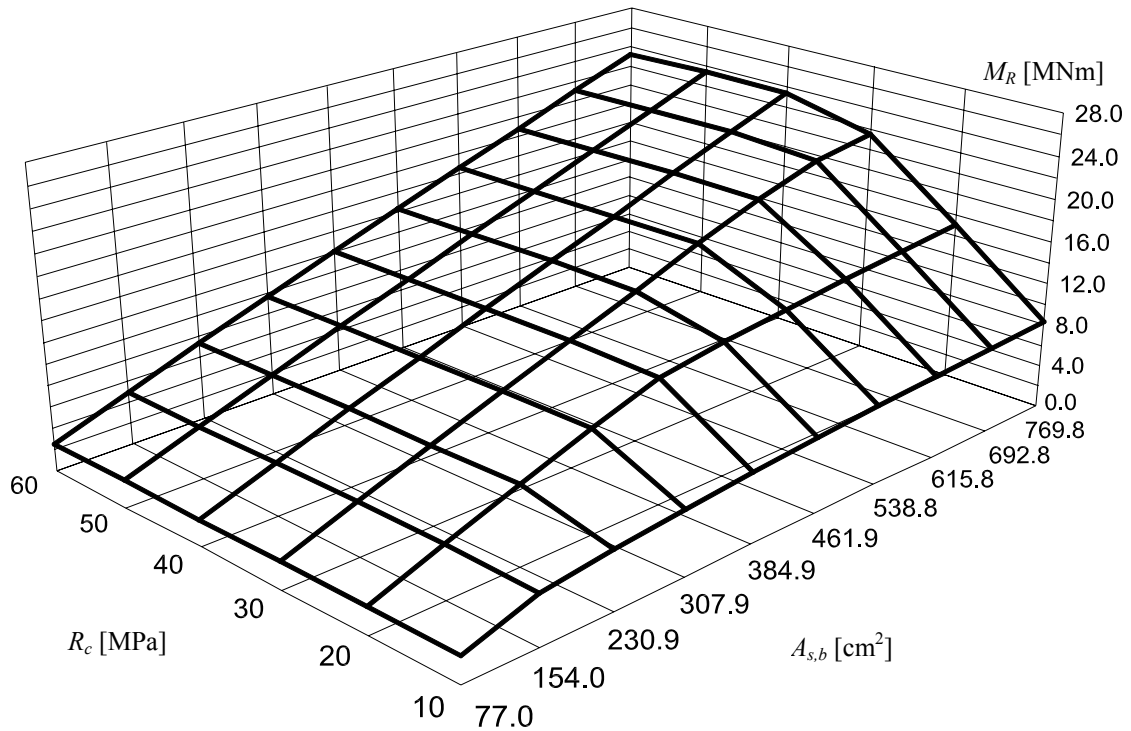


Fig. 10-24 Load capacity of cross section for $H = 105$ cm and $R_s = 350$ MPa

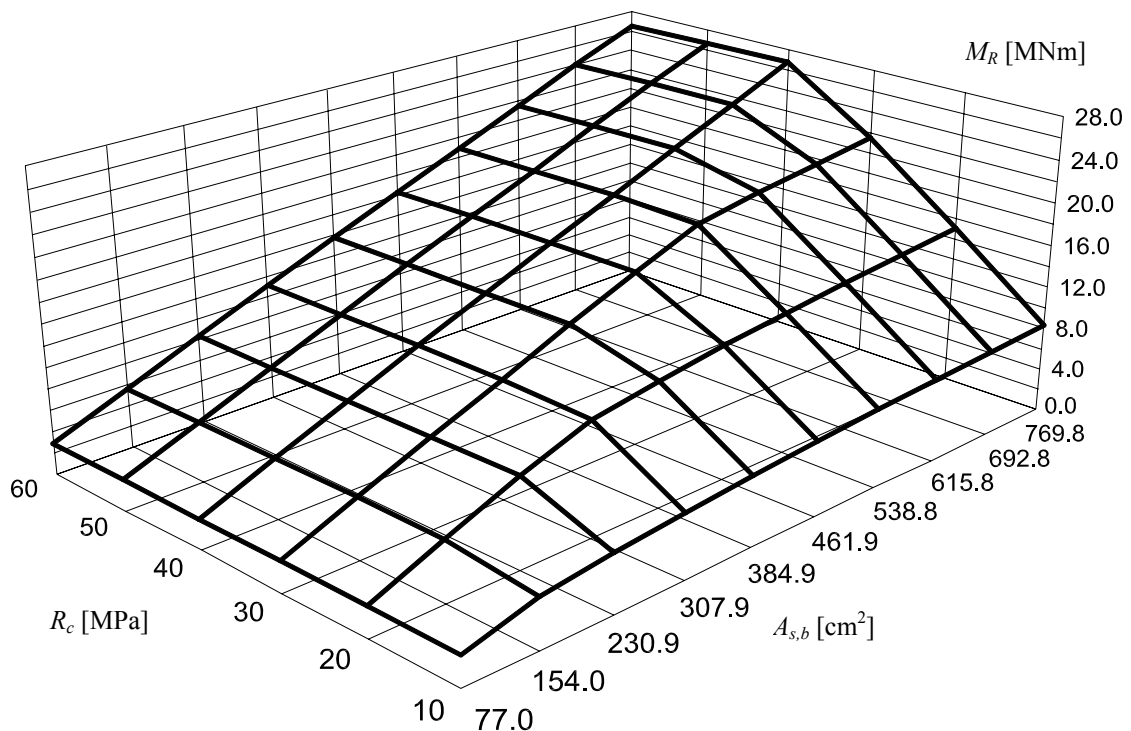


Fig. 10-25 Load capacity of cross section for $H = 105$ cm and $R_s = 400$ MPa

A.3. Conclusions

In this appendix the parametric analysis of the load capacity of cross section has been presented. The results with input parameters can be saved in the knowledge base for the purposes of neural network training and testing. The possibilities of the practical application of this analysis can be found in Appendix C.

Appendix B

User's Manual of DAGA program

In Chapter 7 the possibilities of load capacity assessment of railway *RC* slab spans with defects by means of DAGA (Damage Assessment Graphic Analyser) program has been presented. The objective of this appendix is to present these procedures in terms of the User's Manual of DAGA. Actually this program is in the process of design and testing. DAGA has been developed by means of the Visual Basic Net (VB.NET) programming language with some elements of the Structured Query Language (SQL) DAGA. Moreover DAGA uses the object model of some external applications like AutoCAD and MS Word.

DAGA creates the bridge record where all information (i.e. geometry, material and available codes) to be used during further analysis is saved in the data base. Also additional information related to the defects provided are saved and used in the analysis. This program processes information saved in the data base and using the object model of the AutoCAD application it performs 3D visualisation of entire bridge construction and presents results as graphs.

DAGA program allows modelling *RC* railway slab spans with defects. The user provides to the system basic geometry information with reinforcement parameters. This information enriched by the material parameters allows DAGA to draw entire bridge in 3D space.

The next step is defects modelling. DAGA provides a graphic tool for modelling defects influencing the load capacity, i.e. losses of material (concrete and reinforcement) and material parameters modifications (strength and modulus of elasticity of concrete and reinforcement).

As a consequence of irregular forms of defects a tool for discretisation of span elements has been implemented too. The final step of the DAGA operation is evaluation of the load capacity of analysed bridge span. This program calculates all necessary loading and performs the static-strength analysis. In the presented version of the DAGA program several codes (load and design) have been implemented.

B.1. Interface

This program consists of the following modules (Fig. 10-26):

- Span (creating in 3D space entire bridge construction), see B.2;
- Reinforcement (defining entire network of reinforcement), see B.3;
- Material (description of material properties of concrete and reinforcement), see B.4;
- Loads (load class definition), see B.5;
- Discretization (defining model accuracy), see B.6;
- Defects (specifying defect types and their parameters), see B.7;
- Analysis (load capacity of each cross section as well as for entire span), see Chapter 7;
- Display (control panel for drawing components displaying), see B.8.

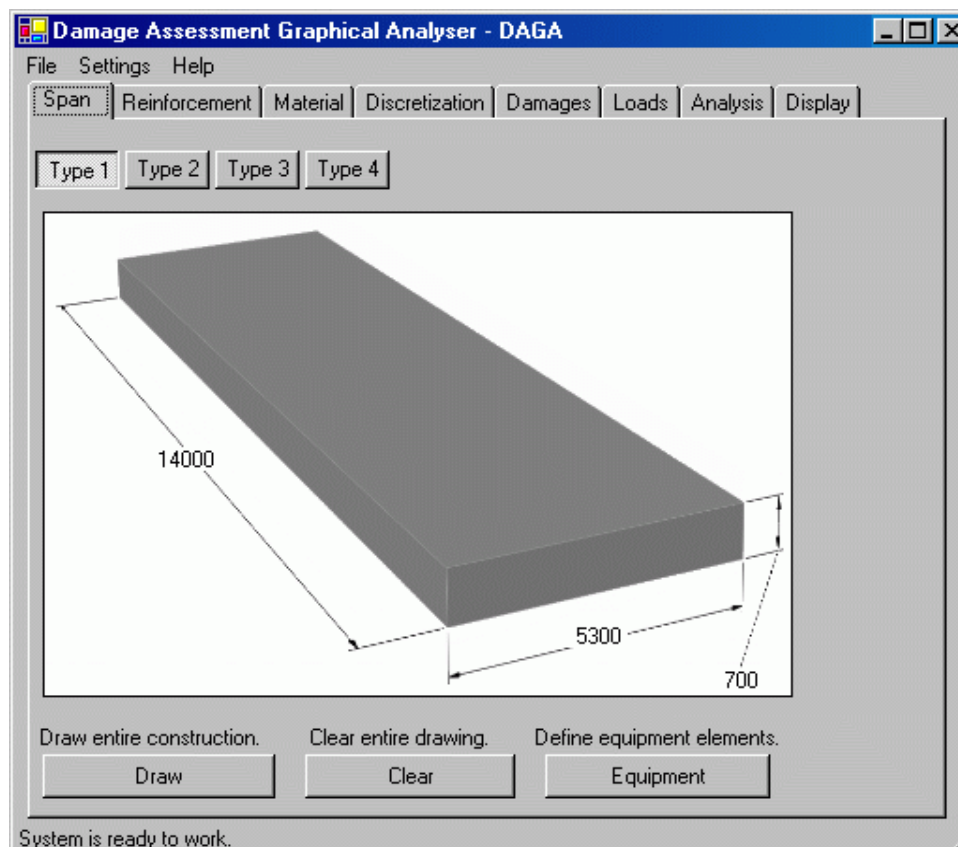


Fig. 10-26 The main interface of DAGA program

B.2. Geometry of the span

Creation of the 3D model of the bridge span is the first step in operation of DAGA system. In the presented version of this system only the rectangular cross section type (Fig. 10-27) is considered, but in the future version of DAGA software also other types of RC slab span will be available. Dimensions of the span are editable and should be defined by the user.

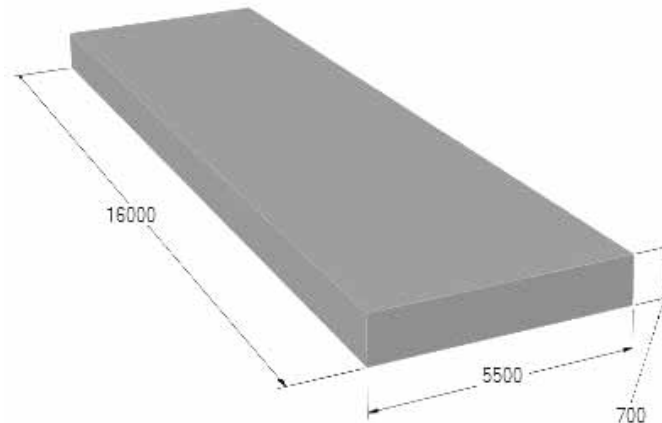


Fig. 10-27 Considered type of span

Additionally by means of the button “equipment” (presented in Fig. 10-26) another procedure for equipment elements defining can be run, see Fig. 10-28. Dimensions here are also editable and should be specified by the user. The specified cross section type as well as track components determine exactly the dead load used in load defining (see B.5). Weights are defined according to PN-85/S-10030 and presented in Table B-1.

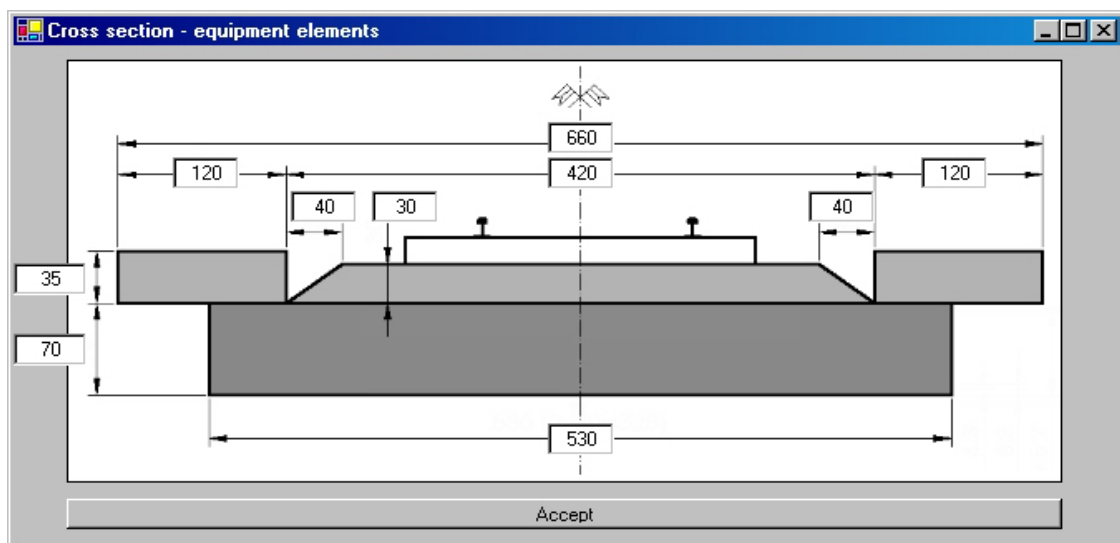


Fig. 10-28 Defining of cross section geometry of span

Analysed bridge span can be modelled together with abutments and track components. An example of axonometric view of the span model is presented in Fig. 10-29.

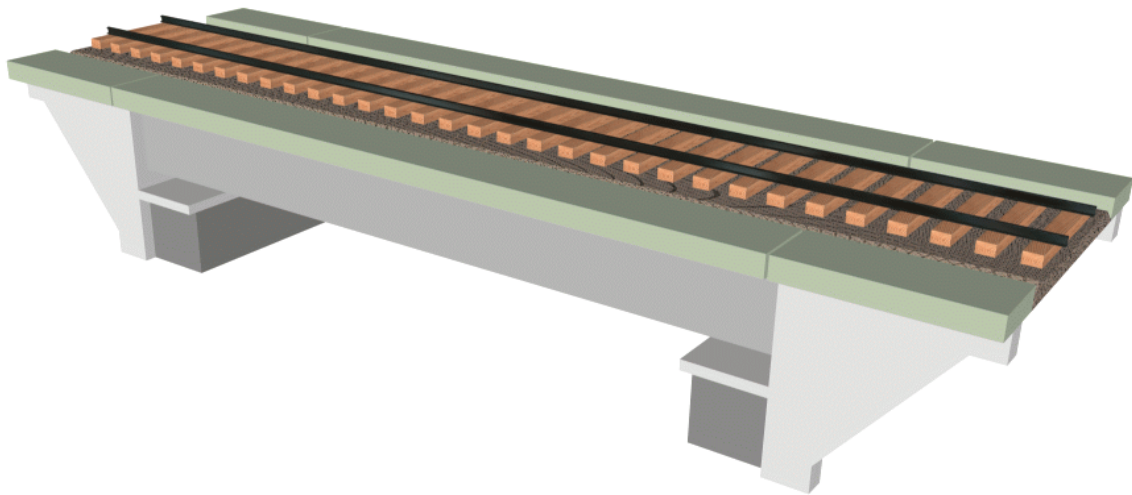


Fig. 10-29 Model of bridge span generated by means of DAGA

B.3. Reinforcement

The rebar network in *RC* structures consists of the longitudinal bars and stirrups. For this reason in DAGA program each type of these components is defined separately.

B.3.1. Longitudinal reinforcement

In Fig. 10-30 an interface for longitudinal reinforcement modelling is presented. Required dimensions (thickness of cover from top, bottom, left and right side), number of rebars and their can be defined. By means of checkboxes the user can add each reinforcement layer at the top as well as at the bottom.

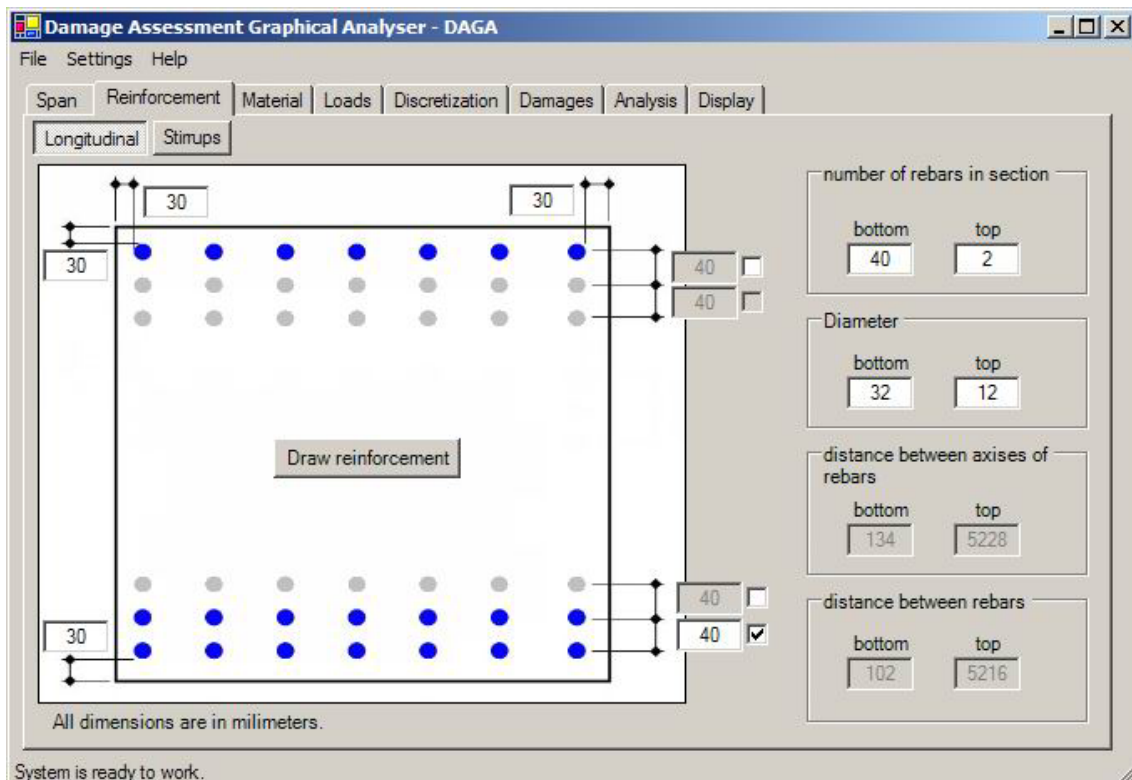


Fig. 10-30 Defining procedure of longitudinal reinforcement

The maximum number of these layers at the top as well as at the bottom of cross section is 3. In the example (see Fig. 10-32) a single top layer and double bottom layer of reinforcement have been defined. All dimensions are expressed in millimetres.

B.3.2. Stirrups

Regarding the considered structure type only bending moments play the main role in the load capacity assessment. Stirrups are related to the shear force transmission and they are considered as a graphic supplement of the main reinforcement. The next versions of DAGA will be extended for other structure types where shear forces play at least the same role like bending moment in considered structure type.

This part of the reinforcement can be specified by zones along the span axis. All parameters (distances from the first and the last stirrup to the front and back face of the slab respectively, number of the stirrups zones, number of rebars and their diameter at each zone) have to be specified by user (Fig. 10-31).

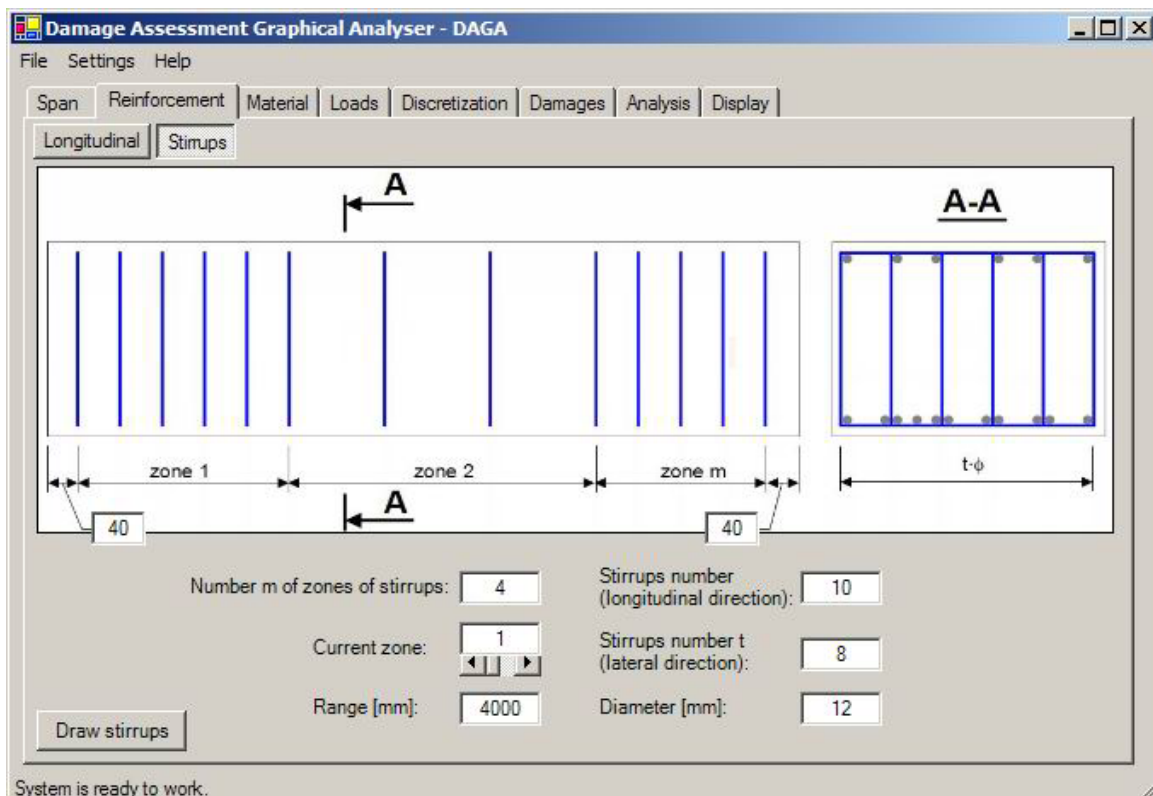


Fig. 10-31 Defining procedure of stirrups

An example of the 3D model of bridge slab reinforcement with enlarged detailed view is presented in Fig. 10-32. Various diameters of rebars can be observed. It helps to distinguish all reinforcement components. The graphic presentation of reinforcement network allows applying defects identified in existing concrete railway structures while inspecting.

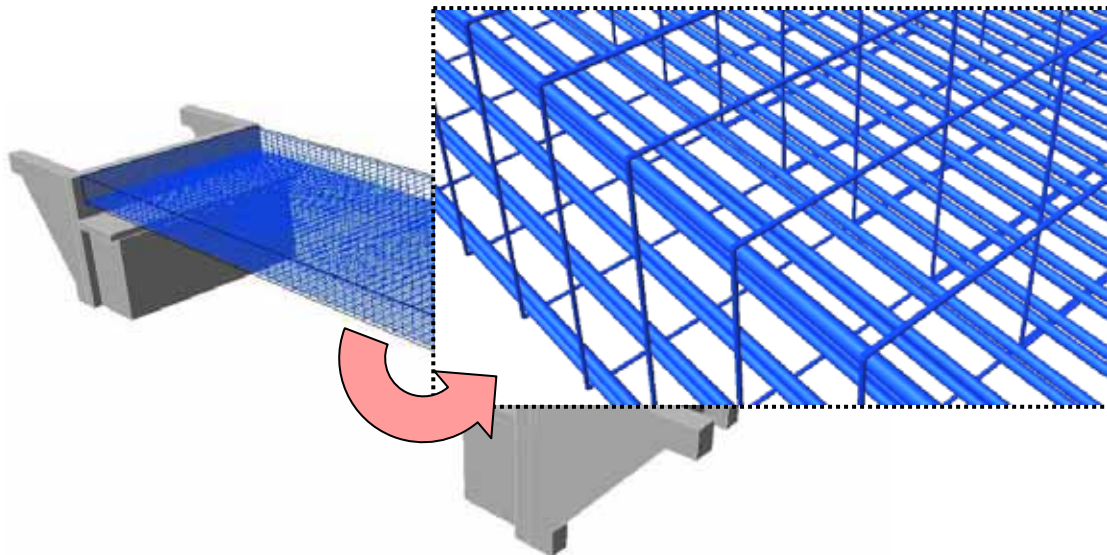


Fig. 10-32 Example reinforcement generated by means of DAGA program

B.4. Material properties

After the dimensions of span have been defined the material parameters of the slab can be set (Fig. 10-33). The user can define compressive and tensile strengths of concrete, strength of reinforcement and elastic modulus of concrete and reinforcement. The values introduced to DAGA are saved in the data base to be processed during further static-strength analysis in accordance to the selected code (see 7.8). Modifications of these parameters in terms of defects are possible and they are available in “Damages” module of DAGA.

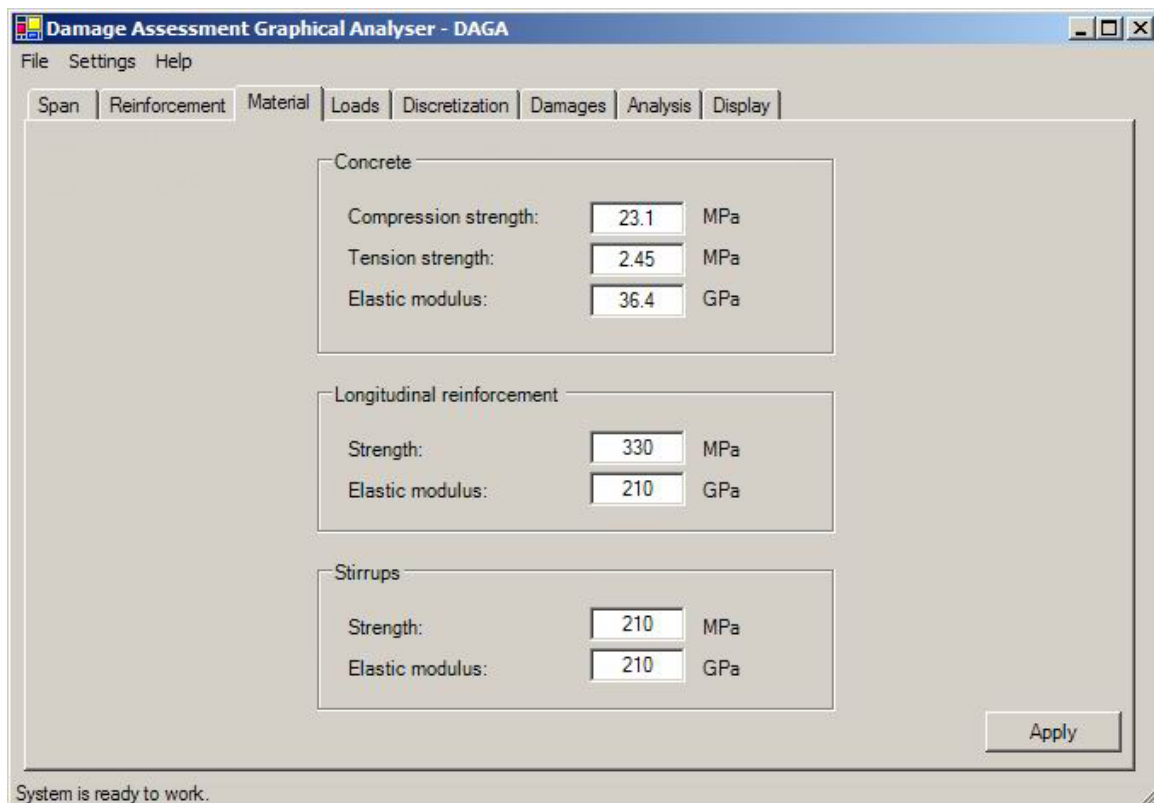


Fig. 10-33 Defining procedure of material parameters

B.5. Loads

The considered load consists of two parts: the dead and live load. In the presented version of DAGA both of them have been implemented in accordance to the PN-85/S-10030. In the next version of DAGA other load models will be available.

B.5.1. Dead load

Values of the dead load intensity (volumetric weights) are determined by the cross section dimensions and by the track construction (see B.2). In Table B-1 values of the dead load items applied in the DAGA are presented.

Table B-1 Values of the dead load items according to PN-85/S-10030

Load item	Volumetric weight [kN/m ³]	Linear weight [kN/m]	Load factors
track	-	1.2+1.6	1.5
ballast	20.0	-	1.5
sidewalk	24.0	-	1.5
slab	24.0	-	1.2

B.5.2. Live load

The moving load consists of four concentrated forces and two uniform loads. The user can select one or more load classes to be considered in the analysis (Fig. 10-34).

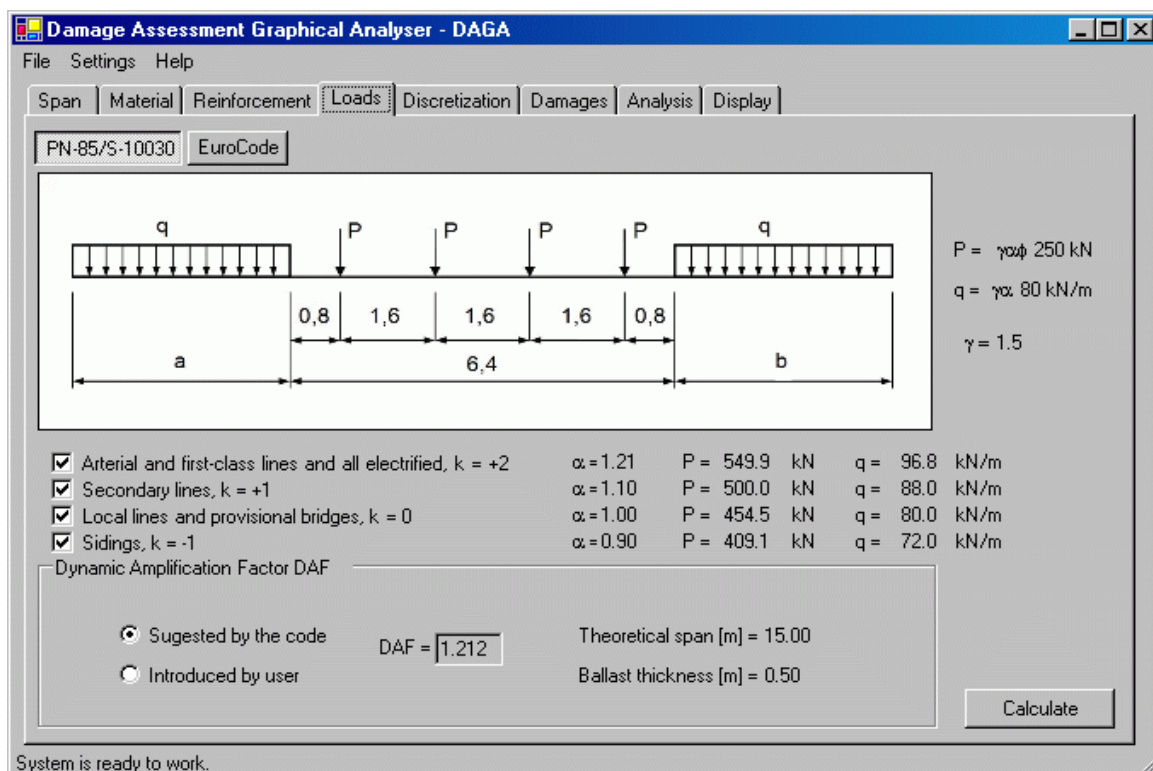


Fig. 10-34 Defining procedure of loads, distances a and b are variable and depend on span length.

Values of load components have to be multiplied by the safety coefficient $\gamma = 1.5$ and the load class factor $\alpha = 1.21$ (arterial, first-class line and all electrified lines), 1.10 (secondary lines), 1.00 (local lines and provisional bridges) or 0.90 (sidings) respectively to the load class.

Moreover the concentrated forces should be multiplied by the *Dynamic Amplification Factor (DAF)*. DAGA program allows the user introducing the default *DAF* value related to the considered code, expressed by the general formula (B-1), formula taking the ballast thickness H_b into account (B-2) or another formula (B-3) modified by an influence of non-standard train traffic velocity v . The user can also introduce other value (e.g. obtained from field tests) if necessary.

$$1.00 \leq DAF = \frac{1.44}{\sqrt{L_t} - 0.2} + 0.82 \leq 1.67, \quad (\text{B-1})$$

where:

L_t – theoretical span length, expressed by meters.

For tracks situated on the ballast the *DAF* has to be expressed by the following formula (B-2):

$$DAF_b = \begin{cases} DAF & \text{for } H_b \leq 0.5m \\ 1.0 + \frac{(1.0 - H_b)(DAF - 1.0)}{0.5} & \text{for } 0.5m \leq H_b \leq 1.0m, \\ 1.0 & \text{for } H_b \geq 1.0m \end{cases}, \quad (\text{B-2})$$

where:

H_b – ballast thickness, expressed by meters

DAF – value evaluated by formula (B-1).

In case of reduced velocity of trains ($v < 80$ km per hour) the dynamic influence has to be expressed by the following formula (B-3):

$$DAF_v = \begin{cases} 1.0 & \text{for } v \leq 10km/h \\ 1.0 + \frac{DAF - 1.0}{80} \cdot v & \text{for } v > 10km/h \end{cases}, \quad (\text{B-3})$$

where:

v – predicted velocity of trains;

DAF – value evaluated by (B-1) or taking into account ballast thickness.

The required *DAF* value is being calculated automatically and its value is displayed on the screen (Fig. 10-34).

B.6. Discretisation

Irregular forms of defects make their modelling much more difficult. To represent defect parameters with required accuracy, the bridge model discretisation is necessary. In Fig. 10-35 a procedure of model discretisation is presented. For concrete as well as for reinforcement various procedures (explained in the next sections) are provided. An example of defect visualisation has already been presented in Fig. 7-8 (page 131).

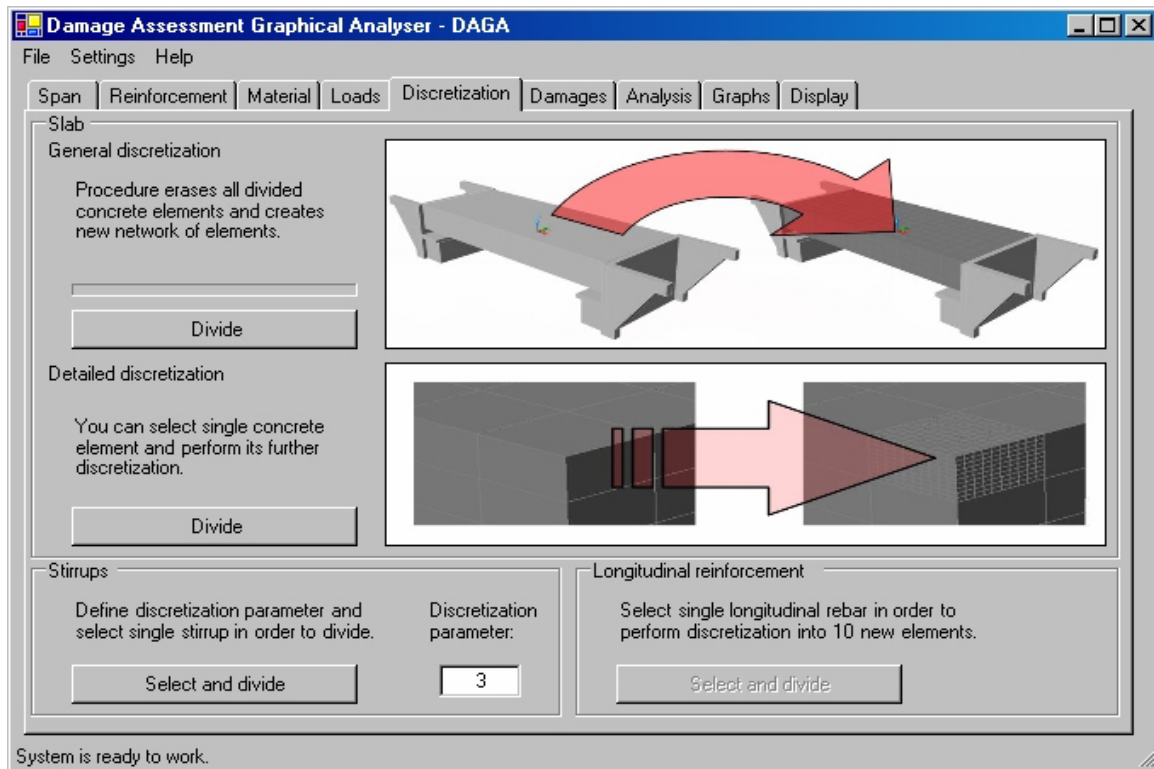


Fig. 10-35 Discretization procedure

B.6.1. Longitudinal reinforcement

Discretization of the longitudinal reinforcement is carried out at the moment of its modelling and causes creation of 20 elements along their axes. Each of them can be divided once again into the 10 new smaller elements. Moreover, to increase the accuracy, each of them can be divided in this way once again.

B.6.2. Stirrups

Though in this version of the DAGA shear forces are not considered, discretisation of the stirrups is possible to make the defect modelling available as well. At this moment this feature can be used only for defect visualisation. Division of the stirrups can be performed with the density defined by the user.

B.6.3. Concrete

The slab is firstly divided into 640 elements (20 in longitudinal direction, 8 in lateral and 4 in vertical). Moreover each of them can be divided into the 1000 (10x10x10) elements. To increase the accuracy each of them new element can be divided once again into the 1000 (10x10x10) elements. In case of common bridge construction of 14.0 meters span presented program allows modelling loss of concrete exact to 5-7 millimetres. An example of defect visualisation with the discretisation methodology applied is presented in Fig. 7-8 (page 131).

B.7. Modelling of defects

So far DAGA allows implementing defects related to concrete and reinforcement such as losses of material and material parameter modifications. Usually defects of RC slabs are complex and coexist with others. For example corroded rebars can be also exposed (loss of reinforcement and concrete). Strength reduction of reinforcement as a consequence of fatigue degradation process occurs also with cracks causing the reinforcement corrosion (strength reduction + loss of reinforcement). DAGA makes defect combinations modelling available. An example of such a “multi-defect” visualisation has been presented in Fig. 7-8 (page 131).

B.7.1. Loss of reinforcement

For the defect modelling a graphic editor presented in Fig. 10-36 can be used.

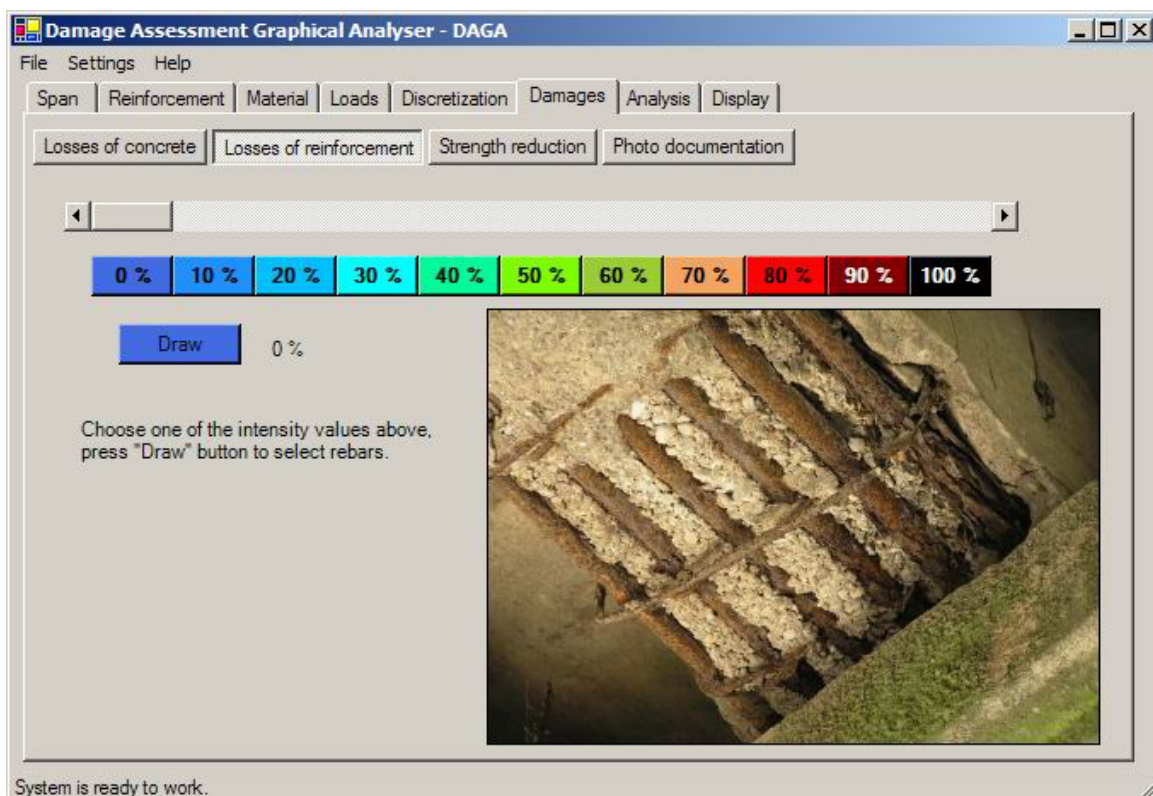


Fig. 10-36 Defining procedure of reinforcement losses

User specifies the intensity of the reinforcement loss and selects rebars to apply the defect. Intensity corresponds to the various colours of rebar as a current corrosion indicator. Defect intensity of 100% means a fracture of considered rebar and causes a visual elimination of this element from the drawing space. Moreover loss of steel is presented in graphic model of the structure as changes of rebars diameter. An example this defect is presented in Fig. 10-37.

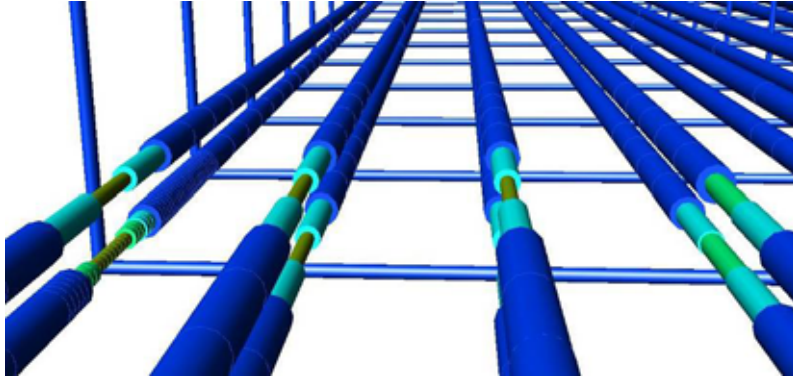


Fig. 10-37 Three-dimensional visualisation of the reinforcement losses

B.7.2. Loss of concrete

The concrete loss modelling is based on the discretisation methodology presented in B.6. By means of the graphic editor (see Fig. 10-38) the user selects elements missing in the real structure and removes them from the drawing space. In Fig. 7-8 an example of the visualisation of RC slab with a combination of concrete and reinforcement losses is presented.

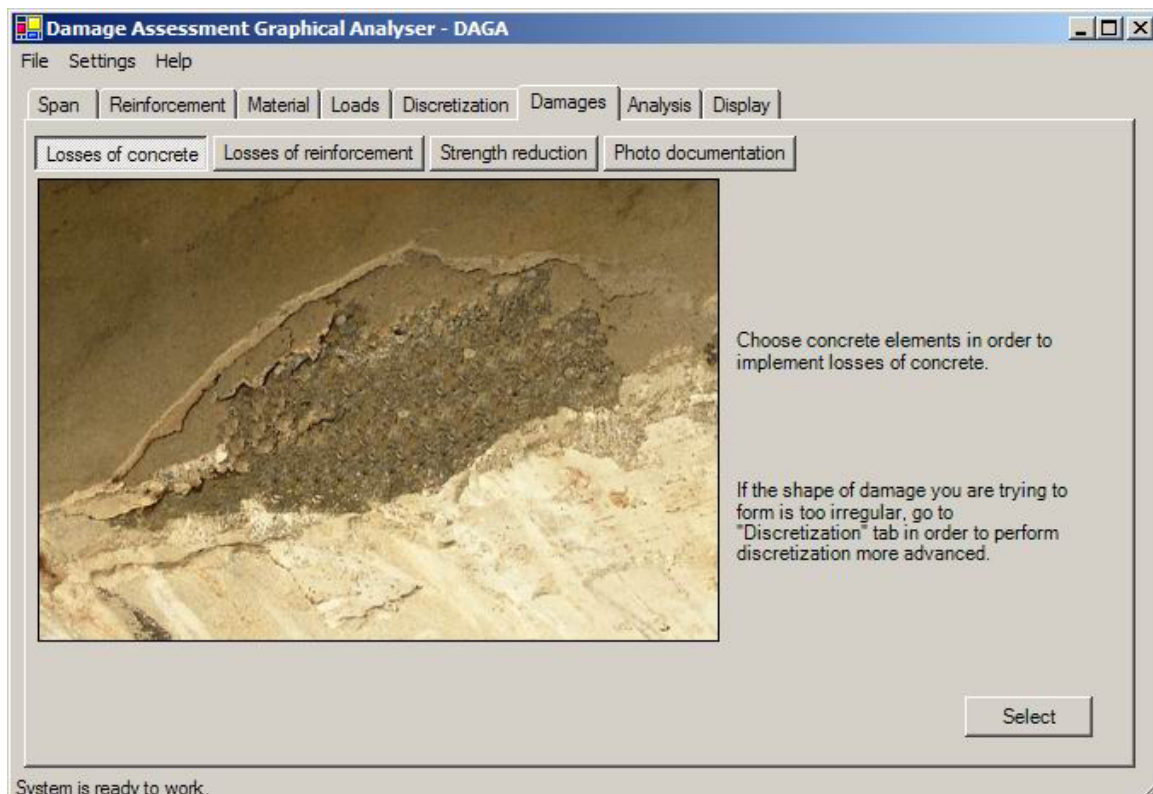


Fig. 10-38 Defining procedure of loss of concrete

B.7.3. Loss of bond concrete-reinforcement

Loss of bond between concrete and reinforcing steel is one of the factors decreasing the load capacity. Though in this study the conservative way of load capacity assessment has been taken into consideration (loss of reinforcement, loss of concrete and material parameters modification), the implementation of the loss of concrete-steel bond is also available.

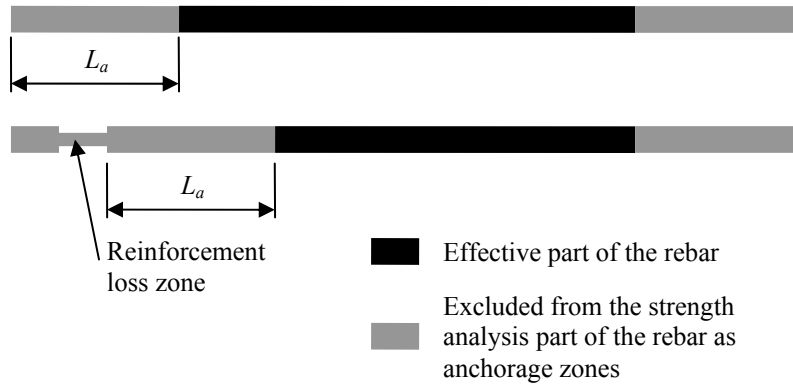


Fig. 10-39 Modification of rebar anchorage zone as a consequence of the corrosion effect – reinforcement loss

In case of non-corroded rebars applying the reinforcement losses along their anchorage lengths L_a will sufficiently represent this defect. In case of corrosion occurred in the rebar anchorage zone its effective length should be reduced (Fig. 10-39).

B.7.4. Strength modification

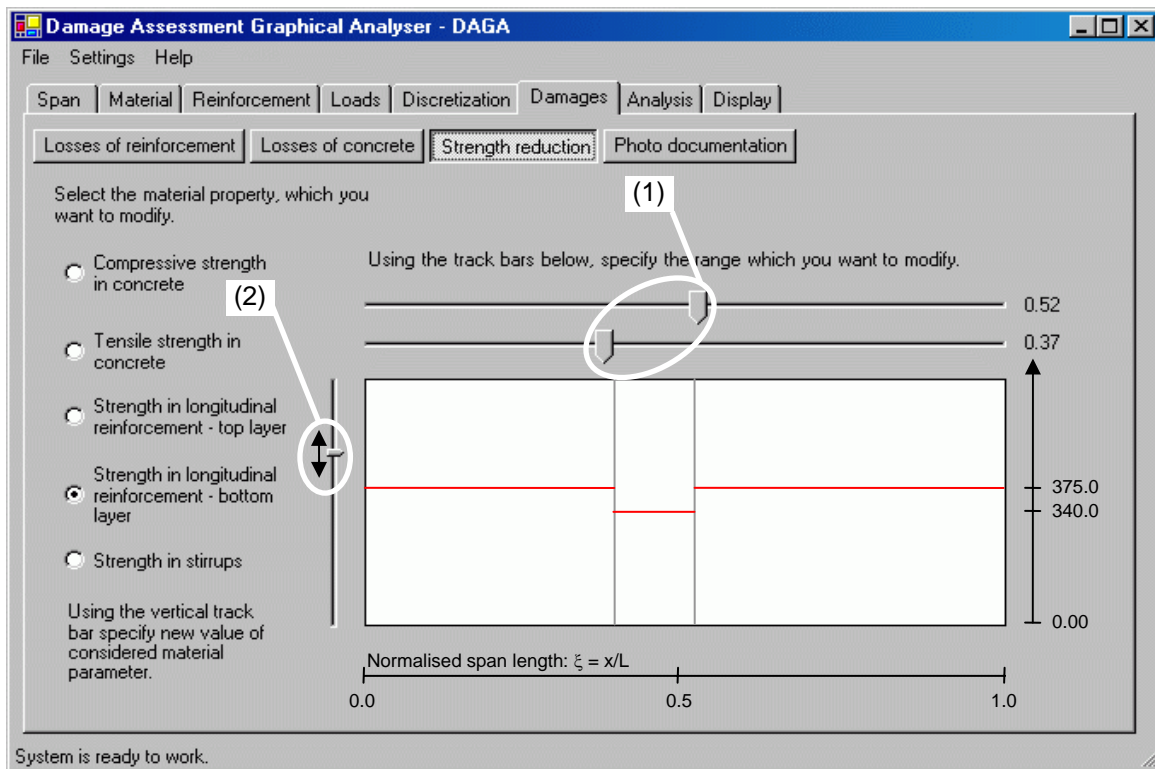


Fig. 10-40 Defining procedure of strength reduction of reinforcement

Defect combinations can be enriched by material parameters modification. Usually this defect occurs without visual symptoms. This program allows modifying the following parameters:

- Concrete strength (compressive and tensile) strength;
- Strength of reinforcement (in both layers) and stirrups.

By means of the graphic editor the selected material strength parameter can be modified. In Fig. 10-40 an example of strength modification for the bottom layer of longitudinal reinforcement is presented. In the central part of this dialog box the distribution of the selected parameter along the length of the span is shown. Above this graph there are two track bars to specify the modification zone (1). By means of the vertical track bar (2) value of the chosen parameter can be modified. For the rest of parameters the methodology is analogical.

B.7.5. Defect modelling based on photos

The philosophy of this methodology has been already presented in the section 7.10 (p. 138).

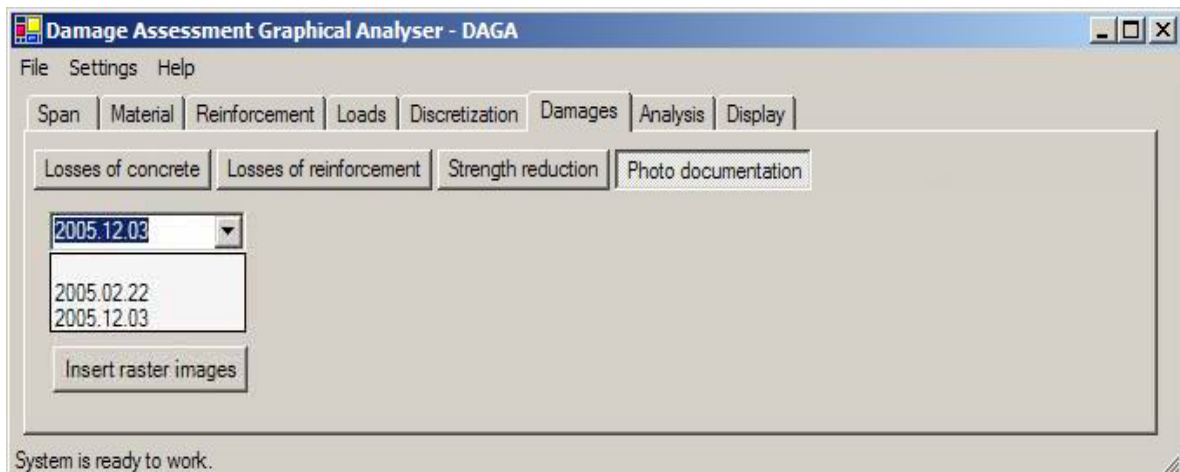


Fig. 10-41 Application of photo documentation collected by bridge inspectors

Using the photographic documentation the user can perform bridge visualisation basing on the results directly from the visual inspections.

B.8. Display

This module is destined for display modifications of the considered structure. The following subtabs are available: Construction parts; Graphs; Reinforcement; Discretization of concrete slab; Shade mode. Using these features it is possible to hide some elements and expose others. For example in order to analyse the results of static-strength analysis the user can hide all reinforcement (tab “*Reinforcement*”) and discretised concrete (tab “*Discretization of concrete slab*”) elements and by means of the “*Graphs*” tab it is possible to analyse the envelopes of bending moment against the load capacity distribution, see example in Fig. 7-15, page 138.

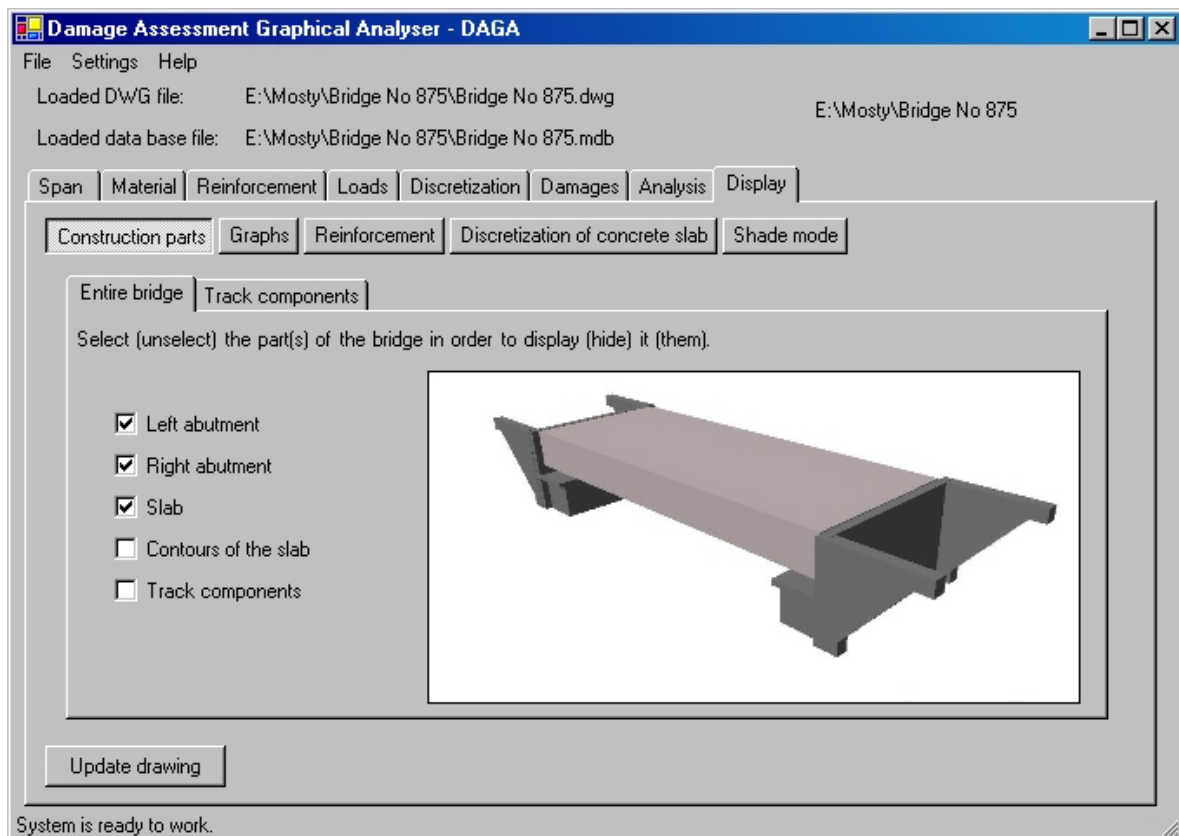


Fig. 10-42 Displaying procedure of the main elements of the structure

In Fig. 10-42 only the abutments and the slab have been set to display. The procedure of the track component defining has been presented in Fig. 10-43. The railway and the sleepers have been set to display only.

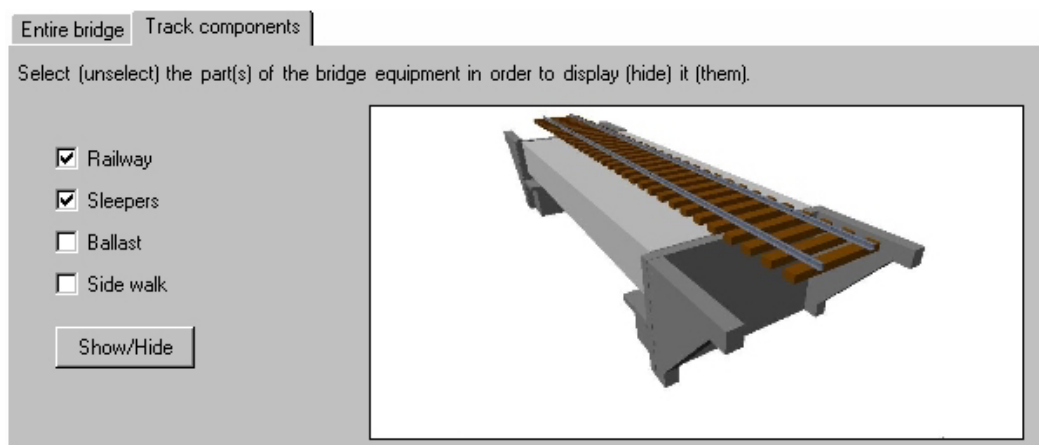


Fig. 10-43 Displaying procedure of the main elements of the track components

In order to work with the reinforcement only, the user can hide everything and by means of the “*Reinforcement*” tab expose only rebar, see Fig. 10-32.

Appendix C

User's manual of ANACONDA program

The program ANACONDA (ANALysis of CONcrete spans with DAMages) is another computer tool developed by the Author for load capacity assessment of railway RC damaged slab spans. This program is actually in the modelling phase and continuous development progress. The main interface of this program is presented in Fig. 10-44. This tool consists of the following four modules situated in separated tab pages:

- Geometry;
- Moving load;
- Damages;
- Results.

In the next sections of this appendix all these modules will be presented and explained.

C.1. Geometry

At the first step in operation of this system the span geometry (theoretical span length and dimensions of the cross-section) have to be specified, see Fig. 10-44. Concerning the model validation presented in the chapter 6 (section 6.7) and performed training of the neural components (see section 8.3) the analysis of the bridge spans can be performed taking into account the span lengths defined for the range 6.0 m and 19.0 m.

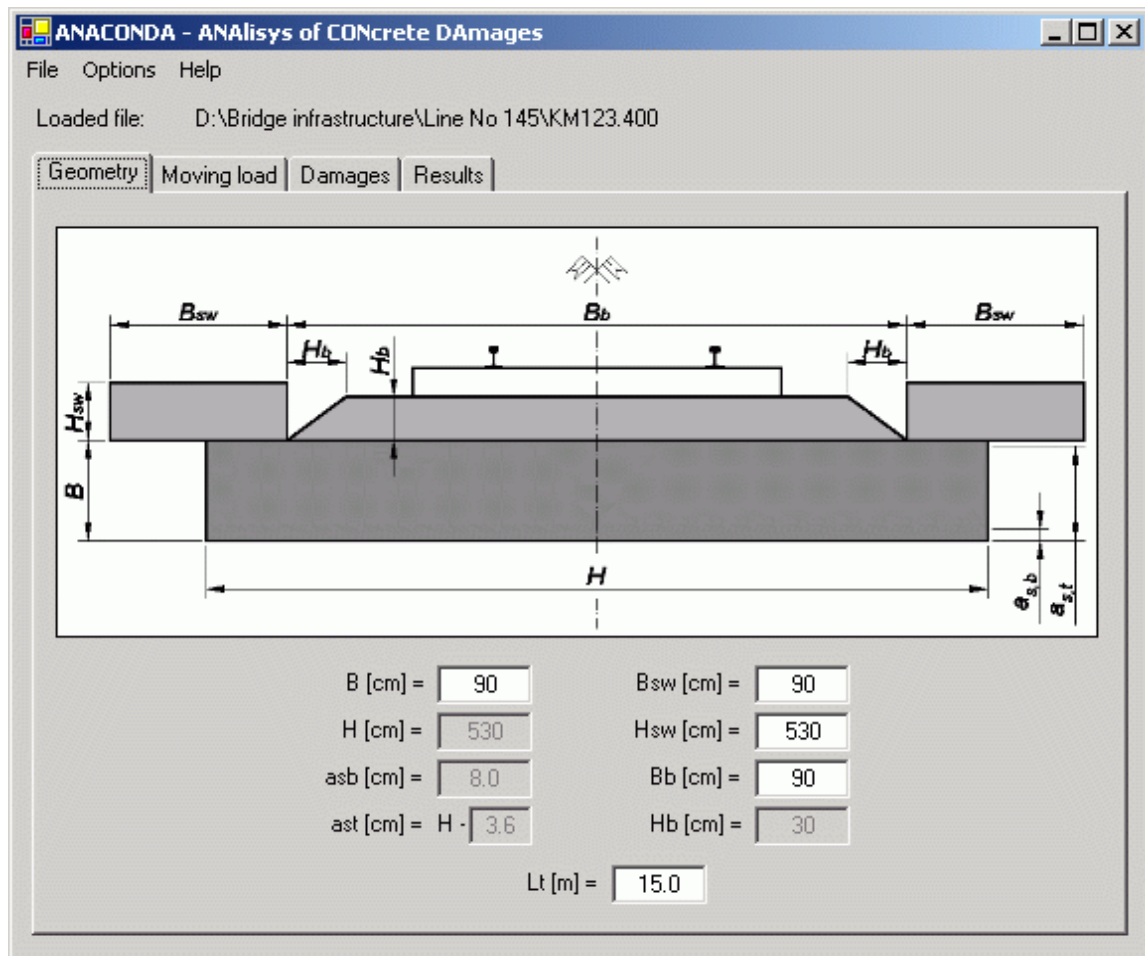


Fig. 10-44 The main interface of ANACONDA and defining procedure of geometry

C.2. Loads

The next step is the moving load class selection according to the PN-85/S-10030 (Fig. 10-45).

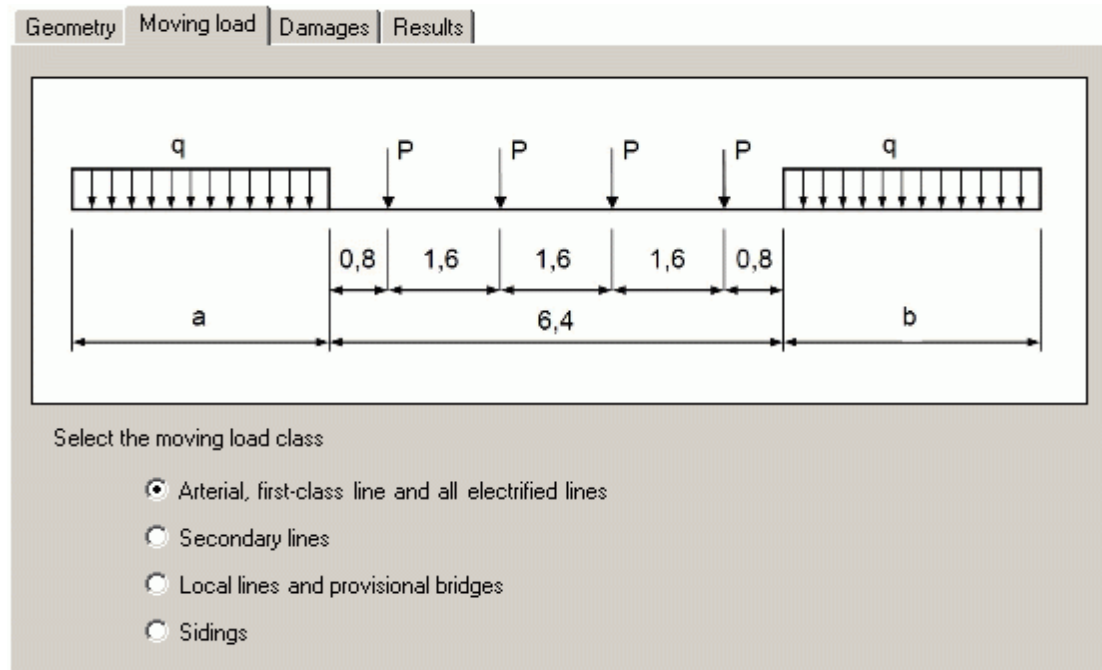


Fig. 10-45 Defining procedure of moving load

The bridge loads are composed of the moving and dead parts. The dead load is determined in the phase of the geometry definition and for this reason in this tab page only moving load is considered. Intensities of these loads are related to values presented in B.5 (Appendix B, page 209).

C.3. Defects

An example of interface created for defect modelling (in this case – modification of area of cross section of the bottom reinforcement, called in the chapter 3.4 *loss of reinforcement*) has been presented in Fig. 10-46.

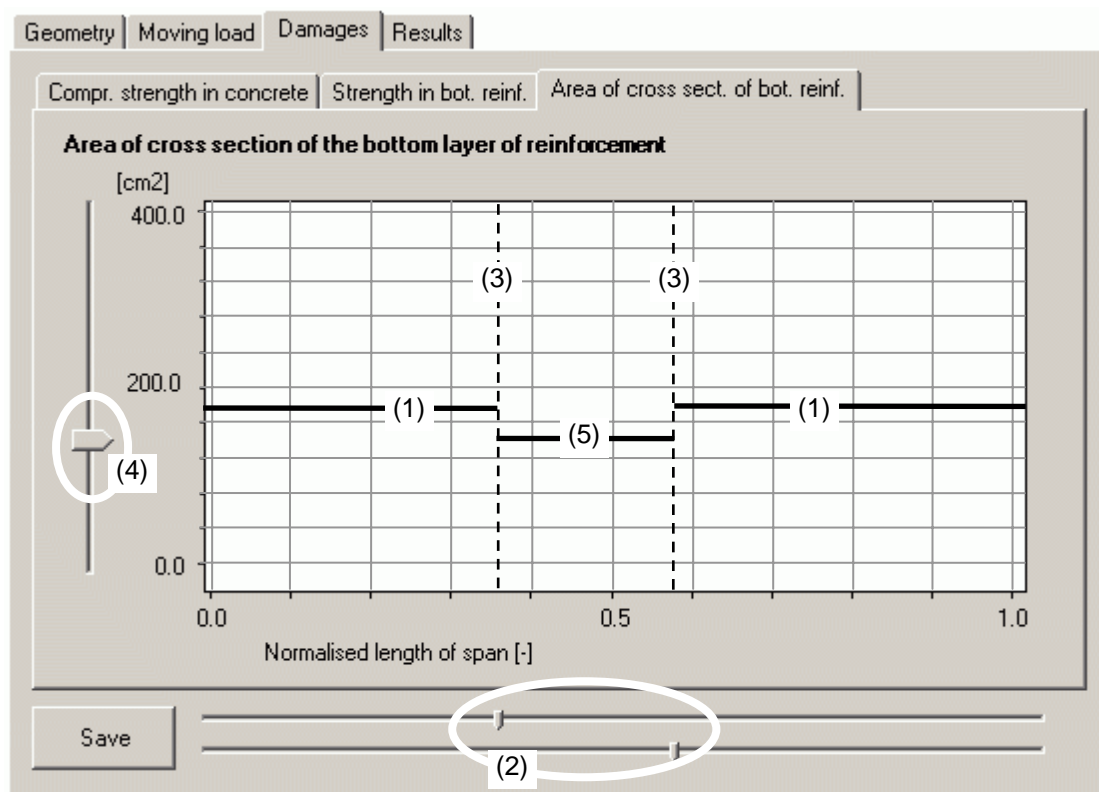


Fig. 10-46 Defect modeling interface of ANACONDA

In this graph distribution of area of reinforcement (1) has been plotted. By means of the horizontal track bars (2) the user specifies a zone (3) of modifications. The vertical track bar (4) is destined for area of reinforcement cross section modification. Actual value of reinforcement area of cross section at this zone has been updated (5). The button “save” allows saving this value distribution in data base.

In case of other defects (properties) user performs analogical actions. User can perform this operation using other tabs like *compressive strength in concrete* or *strength in bottom reinforcement*. The first is to specify a zone of modifications and then to set an actual value, then to save in the data base.

C.4. Analysis and results

The specified geometry, loads, code and defects allow performing the analysis of load capacity of RC railway slab span and to see its results. Entire span is divided into the 1000 virtual cross sections of constant parameters like: material properties, amount of reinforcement, dimensions etc. For each of them program ANACONDA assesses the maximal bending moment at each cross section and evaluates the load capacity of each cross section. After this operation program ANACONDA plots these graphs in its interface and user can observe them. In Fig. 10-47 an example of the results of analysis is presented.

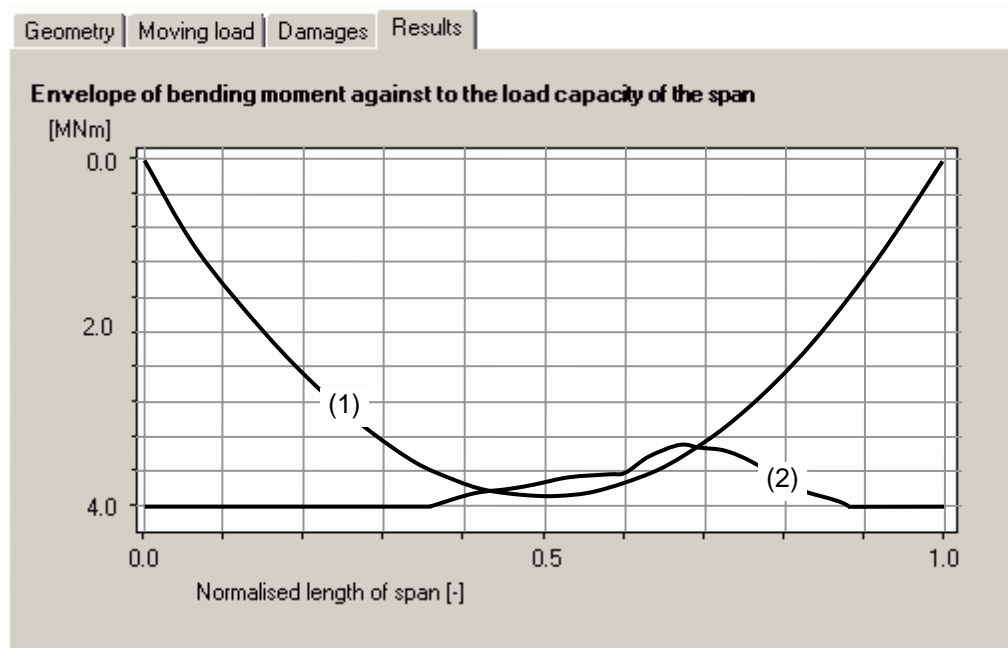


Fig. 10-47 Results of analysis

The image consists of two graphs: envelope of bending moment (1) for analysed span and envelope of load capacity (2). In this situation an example of a damaged railway slab span has been presented. In the middle of the span values of bending moment exceed the values of the load capacity. It means that the bridge does not meet the prescribed safety standards. This result can be used as a basis for making decisions by railway bridge administration regarding the further operation of the analysed construction. In this case user can consider reduction the class of the moving load or introduce repair actions for restoring previous load capacity of the span.